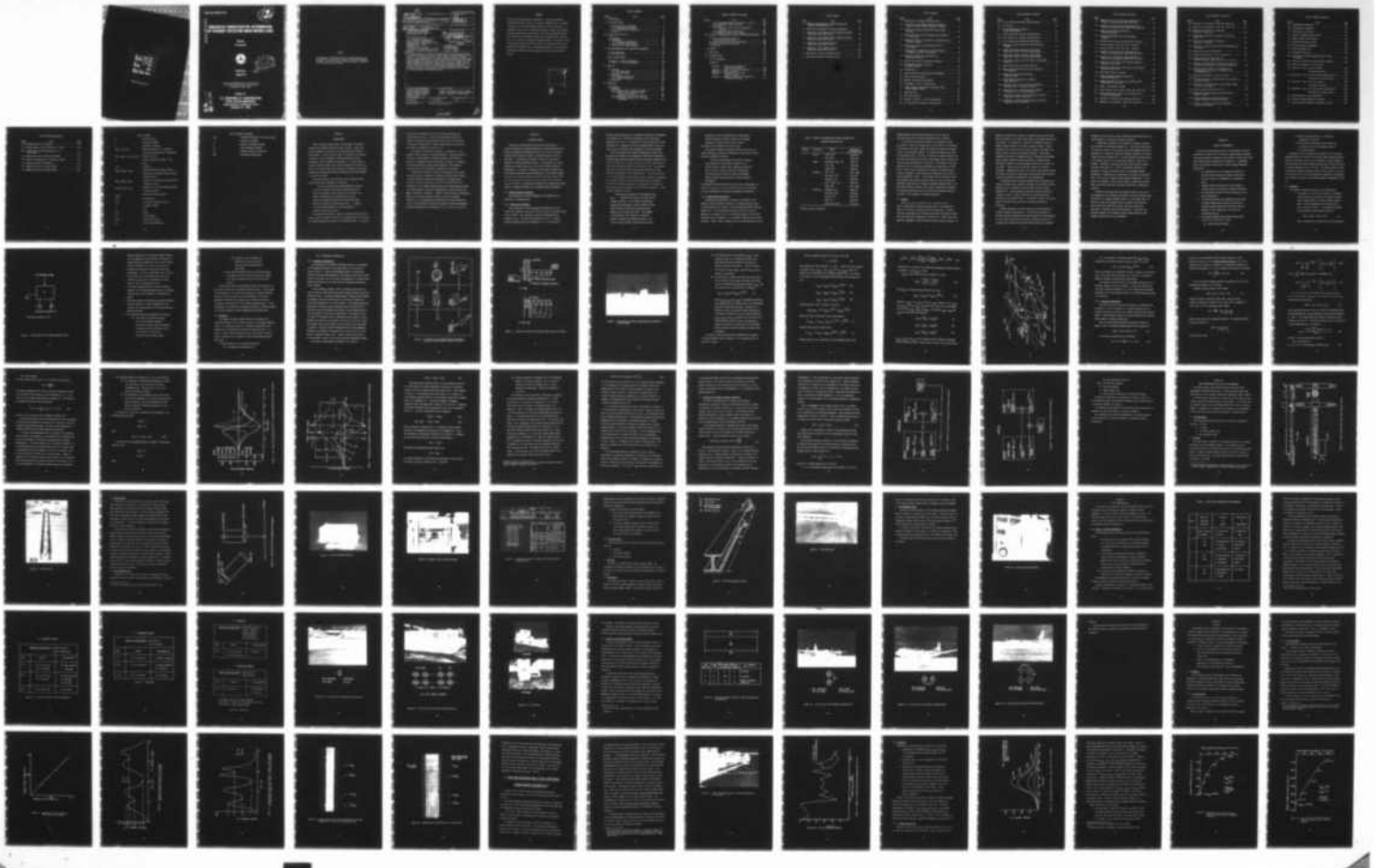
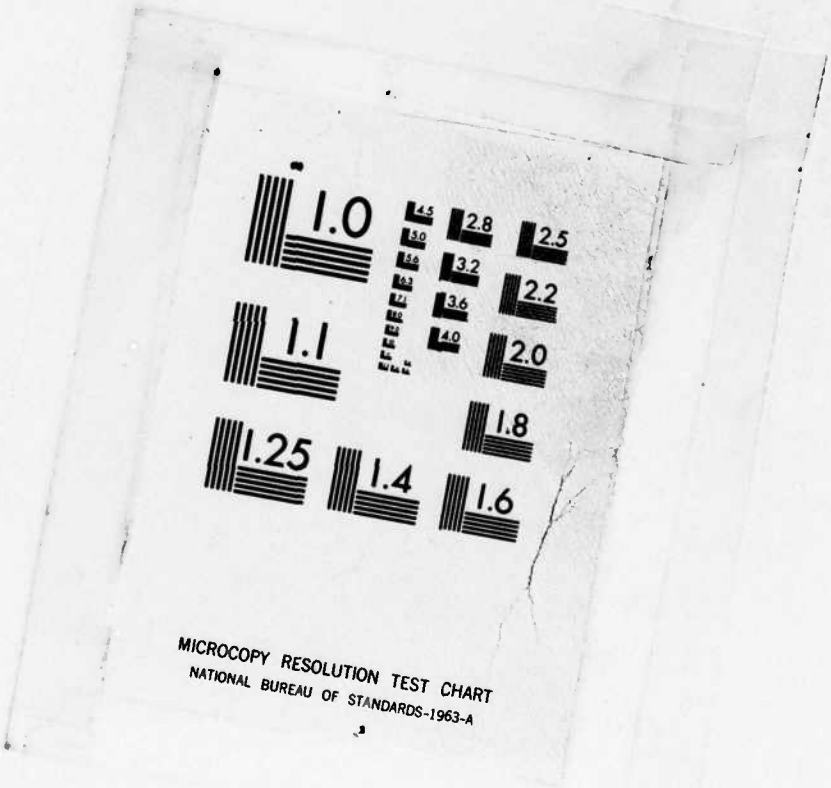
AD-A047 161 NONCONTACT NONDESTRUCTIVE DETERMINATION OF PAVEMENT DEFLECTION UNDER MOVING LOADS(U) PURDUE RESEARCH FOUNDATION LAFAYETTE IN M E HARR ET AL. AUG 77

UNCLASSIFIED FAA-RD-77-127 DOT-FA73WAI-361 F/G 13/2 NL




1.0
1.1
1.25
1.4
1.6
1.8
2.0
2.2
2.5
2.8
3.2
3.6
4.0
4.5
5.0
5.6
6.3
7.1
8.0
MICROCOPY RESOLUTION TEST CHART
NATIONAL BUREAU OF STANDARDS-1963-A

Report No. FAA-RD-77-127

AD A047161

# NONCONTACT NONDESTRUCTIVE DETERMINATION OF PAVEMENT DEFLECTION UNDER MOVING LOADS

M.E. Harr

N.T. Ng-A-Qui




DDC
RECEIVED
NOV 28 1977
F

Final Report

August 1977

Document is available to the U.S. public through the National Technical Information Service, Springfield, Virginia 22161.

Prepared for

U.S. DEPARTMENT OF TRANSPORTATION
FEDERAL AVIATION ADMINISTRATION
Systems Research & Development Service
Washington, D.C. 20590

AD No. ____
DDC FILE COPY

NOTICE

This document is disseminated under the sponsorship of the Department of Transportation in the interest of information exchange. The United States Government assumes no liability for its contents or use thereof.

Technical Report Documentation Page

| 1. Report No. | 2. Government Accession No. | 3. Recipient's Catalog No. |
|---|---|---|
| FAA-RD-77-127 | | |

4. Title and Subtitle
Noncontact Nondestructive Determination of Pavement Deflection Under Moving Loads

5. Report Date
August 1977

6. Performing Organization Code

7. Author(s)
M. E. Harr N. T. Ng-A-Qui

8. Performing Organization Report No.

9. Performing Organization Name and Address
Purdue Research Foundation
Division of Sponsored Research
West Lafayette, IN 47907

10. Work Unit No. (TRAIS)

11. Contract or Grant No.
DOT-FA73WAI-361

12. Sponsoring Agency Name and Address
U. S. Department of Transportation
Federal Aviation Administration
Systems Research and Development Service
Washington, D.C. 20590

13. Type of Report and Period Covered
Final Report
Dec 1974 - Dec 1976

14. Sponsoring Agency Code
ARD-430

15. Supplementary Notes
Department of the Air Force
Air Force Civil Engineering Center (AFSC)
Tyndall Air Force Base, Florida 32403

16. Abstract

This report presents a procedure for nondestructively evaluating and predicting the deflection response of various flexible pavements to loads imposed by different aircraft. Transfer function theory is used to form the basis of a pavement evaluation and response scheme. Two mobile systems were developed for the measurement of pavement deflections; the Light Emitting Diode (LED) system and the Linear Variable Differential Transformer (LVDT) system. The report concludes that the rapid nondestructive measurement of pavement deflections due to moving prototype loads is feasible and that a total nondestructive evaluation scheme based entirely on the use of prototype loads and measured deflections can be fabricated to evaluate and predict instantaneous response and cumulative effects of loads of various magnitudes and configurations.

| 17. Key Words | 18. Distribution Statement |
|---|---|
| Civil engineering<br>Airfield pavement performance<br>Airfield pavement evaluation<br>Pavement deflection response<br>Transfer function theory<br>Energy concepts | Document is available to the U.S. public through the National Technical Information Service, Springfield, Virginia 22161. |

| 19. Security Classif. (of this report) | 20. Security Classif. (of this page) | 21. No. of Pages | 22. Price |
|---|---|---|---|
| unclassified | unclassified | 327 | |

Form DOT F 1700.7 (8-72) Reproduction of completed page authorized



390 985

## PREFACE

This work was conducted under sponsorship of the Federal Aviation Administration (FAA) as part of the runway roughness study to determine the effect of the loaded pavement profile on aircraft operations. An outgrowth of this study is a noncontact system to measure the pavement deflection basin under a moving load. This report describes the hardware developed and associated transfer function theory which forms the basis for a pavement evaluation and response scheme. (The effect of the loaded pavement profile will be the subject of a separate report to be published in September 1977.) Continued development of the noncontact system reported herein is being sponsored by the FAA under separate contract.

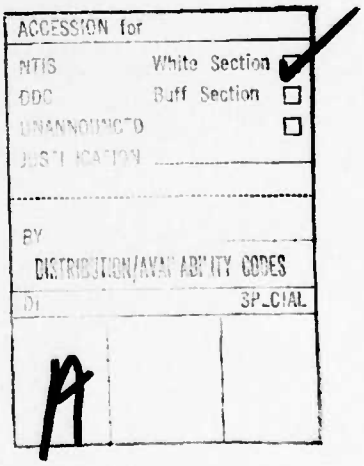


TABLE OF CONTENTS


| Section | Title | Page |
|---|---|---|
| I. | INTRODUCTION | 1 |
| II. | LITERATURE REVIEW | 3 |
| | 2.1 Airfield Pavement Evaluation | 3 |
| | 2.1.1 Destructive Evaluation | 3 |
| | 2.1.2 Nondestructive Evaluation | 5 |
| | 2.2 Analysis | 7 |
| III. | THEORY AND METHODOLOGY | 10 |
| | 3.1 Hypotheses | 11 |
| | 3.2 Evaluation | 14 |
| | 3.2.1 Signature Determination | 15 |
| | 3.2.2 Parameter Determination | 23 |
| | 3.3 Prediction of Pavement Response | 33 |
| IV. | NEW INSTRUMENTATION FOR DEFLECTION MEASUREMENT | 38 |
| | 4.1 The LED System | 38 |
| | 4.2 The LVDT System | 46 |
| V. | FIELD INVESTIGATIONS | 51 |
| | 5.1 Series A - Field Investigation | 51 |
| | 5.2 Series B - Field Investigation | 60 |
| VI. | RESULTS | 66 |
| | 6.1 Equipment | 66 |
| | 6.1.1 The LVDT System | 66 |
| | 6.1.2 The LED System | 67 |
| | 6.2 Evaluation | 77 |
| | 6.2.1 Pavement Deflections | 77 |
| | 6.2.2 Transfer Functions | 89 |
| | 6.3 Prediction | 102 |
| VII. | DISCUSSION | 105 |
| | 7.1 Equipment | 105 |
| | 7.2 Evaluation | 111 |
| | 7.2.1 Concepts Used in Computer Programs | 112 |
| | 7.2.2 Parameter of the Maximum Lateral Deflection Profile | 116 |
| | 7.2.3 Parameters of the Transfer Function | 118 |
| | 7.2.4 Relationship Between the k and $A_{peak}$ Parameters | 128 |

TABLE OF CONTENTS (Continued)


| Section | Title | Page |
|---|---|---|
| | 7.2.5 Approximate Method to Estimate k, c and m | 131 |
| | 7.2.6 Estimating Design Parameters | 136 |
| | 7.3 Prediction | 139 |
| | 7.3.1 Validity of the Concept of Equivalency Function | 140 |
| | 7.3.2 Effects of Gear Configurations | 142 |
| | 7.3.3 Relative Effects of k, c and m | 143 |
| VIII. | EFFECTS OF DISTRIBUTION OF PASSES ON PAVEMENT PERFORMANCE | 144 |
| | 8.1 Pass to Coverage Ratio Based on Tire-Contact Area Width | 144 |
| | 8.2 Deflection Based Pass to Coverage Ratio | 148 |
| | 8.3 Effect of Lateral Distribution | 151 |
| | 8.4 Discussion | 152 |
| IX. | SUMMARY | 160 |
| X. | CONCLUSIONS | 162 |
| XI. | RECOMMENDATIONS | 164 |
| | LIST OF REFERENCES | 166 |
| | APPENDICES | 173 |
| | Appendix A: Research and Development of Measurement Systems | 173 |
| | Appendix B: Series A: Field Investigations | 191 |
| | Appendix C: Computer Programs | 210 |
| | Appendix D: Data Digitized from Light Sensitive Paper | 248 |
| | Appendix E: Example of Simplified Procedure for Estimating k and CBR | 312 |

## LIST OF TABLES


| Table | Title | Page |
|---|---|---|
| 1. | Summary of Nondestructive Testing Equipment and Pertinent Characteristics | 6 |
| 2. | Field Testing Equipment Development Methodology | 52 |
| 3. | Parameters of the Maximum Lateral Deflection Profile: Eglin AFB, March 1976: Site 1 | 82 |
| 4. | Parameters of the Maximum Lateral Deflection Profile: Eglin AFB, March 1976: Site 2 | 83 |
| 5. | Parameters of the Transfer Function: Eglin AFB, March 1976: Site 1 | 99 |
| 6. | Parameters of the Transfer Function: Eglin AFB, March 1976: Site 2 | 100 |
| 7. | Data Used in Lateral Distribution Study | 152 |
| 8. | Data Used in Lateral Distribution Study | 158 |

LIST OF FIGURES


| Figure | Title | Page |
|---|---|---|
| 1. | Kelvin Model of Pavement-Subgrade System | 12 |
| 2. | An Overview of the Transfer Function Concept as Applied to Wheel-Pavement-Subgrade Interaction | 16 |
| 3. | Location of Signature and Relative Gage Location and Setup | 17 |
| 4. | Setup During Stationary Beam-Moving Load Operation: P-2 Fire truck | 18 |
| 5. | Overview of Method of Calculation of Signature Due to Prototype Loading | 22 |
| 6. | Typical Zero, First and Second Derivatives of the Signature | 28 |
| 7. | Determination of Parameter of Transfer-Function - A Graphical Overview of Methodology | 29 |
| 8. | Overview of Scheme for Determining the Equivalency Function | 35 |
| 9. | Overview of Scheme for Predicting Signature | 36 |
| 10. | Light Emitting Diode (LED) Beam: Schematic Details | 39 |
| 11. | LED Beam Setup | 40 |
| 12. | Light Emitting Diode Triangulation Arrangement | 42 |
| 13. | Typical LED Sensor Module | 43 |
| 14. | Magnetic Tape Recording Equipment | 44 |
| 15. | Arrangement of Data of Magnetic Tape | 45 |
| 16. | Linear Variable Differential Transformer (LVDT) Beam: Schematic Details | 47 |
| 17. | LVDT Beam Setup | 48 |
| 18. | Light Beam Recorder | 50 |
| 19. | Synopsis of Series A - Field Investigations | 54 |
| 20. | F-4 Aircraft and Pertinent Characteristics | 57 |

LIST OF FIGURES (Continued)


| Figure | Title | Page |
|---|---|---|
| 21. | P-2 Fire Truck and Pertinent Characteristics . . . . . | 58 |
| 22. | F-4 Load Cart . . . . . | 59 |
| 23. | Site Characteristics: Series B - Field Investigations . . . . . | 61 |
| 24. | C-130 Aircraft and Pertinent Characteristics . . . . . | 62 |
| 25. | C-131 Aircraft and Pertinent Characteristics . . . . . | 63 |
| 26. | C-135 Aircraft and Pertinent Characteristics . . . . . | 64 |
| 27. | Comparison of LVDT on Beam and LVDT Installed in Pavement . . . . . | 68 |
| 28. | Pavement Deflections Measured by LED System: Eglin AFB - Site 1: P-2 Fire Truck Loading . . . . . | 69 |
| 29. | Pavement Deflections Measured by LVDT System: Eglin AFB - Site 1: P-2 Fire Truck Loading . . . . . | 70 |
| 30. | Actual Digital Output From LED System on Light Beam Recorder . . . . . | 71 |
| 31. | Analog Output from LVDT System (Typical) . . . . . | 72 |
| 32. | Setup During Moving Beam-Moving Load Operation: F-4 Load Cart . . . . . | 75 |
| 33. | Summary of Taxiway Deflection Data: Eglin AFB: Site 1 . . . . . | 76 |
| 34. | System Response Functions F-4 Loading: Eglin AFB: Site 1 . . . . . | 78 |
| 35. | Eglin AFB: Site 1: Lateral Profile of Maximum Deflections for F-4 Loading (Typical) . . . . . | 80 |
| 36. | Eglin AFB: Site 2: Lateral Profile of Maximum Deflections for F-4 Loading (Typical) . . . . . | 81 |
| 37. | Variability of Maximum Lateral Deflection Profile: Eglin AFB - Site 1, March 1976 . . . . . | 84 |
| 38. | Variability of Maximum Lateral Deflection Profile: Eglin AFB, Site 2, March 1976 . . . . . | 85 |

LIST OF FIGURES (Continued)


| Figure | | Page |
|---|---|---|
| 39. | Comparison of Local and Site Characteristics as shown by βr Values: Eglin AFB, March 1976 . . . . . | 86 |
| 40. | Comparison of Local and Site Characteristics as shown by A-Parameter Values: Eglin AFB, March 1976 . . . | 87 |
| 41. | Effect of Two Consecutive Passes on Measured Deflection . . . . . | 88 |
| 42. | Calculated Equivalent Force and Components (Typical) . . . . . | 91 |
| 43. | Comparison of Newtonian and Convolution Solutions . . . . . | 92 |
| 44. | Transfer Function: Eglin AFB, Site 1 (Typical) . . . . . | 93 |
| 45. | Transfer Function: Eglin AFB, Site 2 (Typical) . . . . . | 94 |
| 46. | Comparison of Local and Site Characteristics as shown by the k-Parameters: Eglin AFB, March 1976 . . . . | 95 |
| 47. | Comparison of Local and Site Characteristics as shown by the c-Parameters: Eglin AFB, March 1976 . . . . | 96 |
| 48. | Comparison of the Peaks of the Transfer Function: Eglin AFB, March 1976 . . . . . | 97 |
| 49. | Comparison of the Time to First Peak of TDT Function: Eglin AFB, March 1976 . . . . . | 98 |
| 50. | Input-Output Relation (Typical) . . . . . | 101 |
| 51. | Typical Comparison Between Measured and Predicted Signatures . . . . . | 103 |
| 52. | Summary Comparison of Measured and Predicted Peak Deflections for Two Sites . . . . . | 104 |
| 53. | Summary of Measurement Systems . . . . . | 107 |
| 54. | Runway Overrun Tests: Eglin Air Force Base, March 1976 . . | 110 |
| 55. | Sketch showing the Concept of the Criteria Used in Parameter Determination . . . . . | 114 |
| 56. | Comparison of Calculated and Measured Signatures . . . . . | 117 |
| 57. | Comparison of A-Parameters: Eglin AFB, March 1976 . . . . . | 119 |

LIST OF FIGURES (Continued)


| Figure | Title | Page |
|---|---|---|
| 58. | Comparison of β-Parameters: Eglin AFB, March 1976 . . . . | 120 |
| 59. | Comparison of r-Parameters: Eglin AFB, March 1976 . . . . | 121 |
| 60. | Comparison of Equivalent k-Parameters: Eglin AFB, March 1976 . . . . . | 123 |
| 61. | Comparison of Equivalent c-Parameters: Eglin AFB, March 1976 . . . . . | 124 |
| 62. | Comparison of Equivalent m-Parameters: Eglin AFB, March 1976 . . . . . | 125 |
| 63. | Locations of Stations where Relative Stiffnesses were Determined . . . . . | 126 |
| 64. | Histogram of Relative Stiffnesses . . . . . | 127 |
| 65. | Relationship Between the A and k Parameters . . . . . | 129 |
| 66. | Nondestructive Evaluation Curves for Flexible Pavement, Single Wheel Load, 100 sq. in. . . . | 130 |
| 67. | Frequency Characteristics of Forces at the Points of Inflection, Crossing Point and Maximum Deflection . . . | 132 |
| 68. | Frequency Characteristics of Normalized Time Corresponding to the Point of Inflection and the Crossing Point . . . . . | 134 |
| 69. | Approximate Correlation of CBR and k-Value . . . . . | 138 |
| 70. | Lateral Distribution of Aircraft Used in the Design of Airfield Pavements . . . . . | 146 |
| 71. | Overview of the Concept Used in the Deflection Based p/c Ratio Calculations . . . . . | 149 |
| 72. | Discrete Distributions Used in Study . . . . . | 153 |
| 73. | Relationship Between Cumulative Deflections and Number of Passes . . . . . | 154 |
| 74. | Effects of Frequency and Characteristics of Lateral Deflection Profile of p/c Ratio . . . . . | 155 |
| 75. | Overview of Evaluation Scheme Using Deflection Frequency Relationship . . . . . | 157 |

LIST OF FIGURES (Continued)


| Figure | Title | Page |
|---|---|---|
| A-1 | Triangulation Arrangement | 175 |
| A-2 | Triangulation Paprameters | 176 |
| A-3 | Laser Setup in Laboratory | 179 |
| A-4 | Typical Triangulation Displacement | 180 |
| A-5 | Normal Incidence Displacement | 181 |
| A-6 | Normalized Deflection Curves | 182 |
| A-7 | LED Triangulation Arrangement | 184 |
| A-8 | LED Displacement Curve | 185 |
| A-9 | Repackaged Electronics | 186 |
| A-10 | Test Setup for Moving Beam-Moving Load--Purdue University | 188 |
| A-11 | Flow Chart of LED System Data Reduction Software | 189 |
| A-12 | Details of Components of LVDT System | |
| B-1 | Eglin AFB - Site 1 (A) Site location | 192 |
| | (B) Station locations | 192 |
| B-2 | Eglin AFB - Site 1 (A) Site profile characteristics | 193 |
| | (B) Details of boring location | 193 |
| B-3 | Eglin AFB - Site 2 (A) Site location | 194 |
| | (B) Station locations | 194 |
| B-4 | Eglin AFB - Site 2 (A) Site profile characteristics | 195 |
| | (B) Details of boring location | 195 |
| B-5 | Photo Sequence of Gage Installation | 196 |
| B-6 | Details of Gages Installed in Pavement | 204 |
| B-7 | Gage Calibration Equipment (Micrometer on Mount) | 205 |

LIST OF FIGURES (Concluded)


| Figure | Title | Page |
|---|---|---|
| B-8 | Typical Pass by P-2 Fire Truck | 206 |
| B-9 | Typical Results of Peak Deflections - KC135A | 208 |
| B-10 | Typical Results of Peak Deflections - P-2 Fire Truck | 209 |
| C-1 | Summary Flow Chart of Subroutine EXACFIT | 211 |
| C-2 | Details of Interpolation in Subroutine EXACFIT | 212 |
| C-3 | Definition Sketch for Signature | 215 |
| C-4 | Summary Flow Chart of Program FNDPRM | 216 |
| C-5 | Summary Flow Chart of Program PREDCT | 222 |

## LIST OF SYMBOLS

| | |
|---|---|
| $m$ | - equivalent mass |
| $c$ | - equivalent damping |
| $k$ | - equivalent stiffness |
| $z(t)$, $\dot{z}(t)$, $\ddot{z}(t)$ | - pavement deflection (or signature), velocity and acceleration, respectively |
| $F(t)$, $F_{sn}(t)$, $F_x(t)$, $F_{ln}(t)$ | - loading function |
| $x$ | - lateral distance from edge of tire print |
| $A(t)$ | - signature |
| $A'_{peak}$, $A''_{peak}$, $A_{peak}$ | - maximum deflection at edge of wheel, parameter of the maximum lateral dynamic deflection basin |
| $\beta'_{peak}$, $\beta''_{peak}$, $\beta_{peak}$ | - parameter of the maximum lateral dynamic deflection profile |
| $r'_{peak}$, $r''_{peak}$, $r_{peak}$ | - parameter of the maximum lateral dynamic deflection profile |
| $z_{max_j}$ | - maximum deflection at gage j |
| $I(t)$ | - modified input |
| $G(t)$ | - the reduced transfer function |
| $s$ | - a complex variable |
| $t$ | - time |
| $O(t)$ | - output |
| $\Delta T$ | - time increment |
| $EF(t)$ | - equivalency function |
| $T_p$ | - time to peak deflection |

## LIST OF SYMBOLS (Concluded)

| | |
|---|---|
| W(X) | - subgrade deflection at x from tire print |
| p | - pressure on subgrade |
| $\bar{k}$ | - modulus of subgrade reaction |
| CH | - shear stiffness parameter |
| $E_s$ | - subgrade modulus of elasticity |
| CBR | - California Bearing Ratio |

# SECTION I

## INTRODUCTION

Today, personnel concerned with the evaluation of airfield pavements are confronted with three major problems. First, many primary pavements are old and/or are approaching early stages of deterioration. Second, the gross weight of aircraft is increasing continually, thus the demands on airfield pavements are also increasing. Third, procedures (References 1, 2, 3 and 4) used to evaluate airfield pavements are; either, destructive in nature, or, apply to only small areas of the pavement: in addition, they require considerable performance time and are therefore costly with respect to the flow of traffic.

The problem faced by the Air Force in this context has been stated by one author (Reference 5) who wrote,

> "The Air Force alone owns enough pavement to be able to provide a 200-foot wide runway stretching from the state of Washington to the Southern tip of Florida. The problem of maintenance and rehabilitation of this inventory becomes more complex and critical each year. Most of the systems are over 20 years old . . . coupled with these aging pavements is the rapid growth of aircraft traffic and weights."

The need exists today for a method of pavement evaluation which would be able to quantify the stage of the aging process of a pavement and provide guidance with respect to its rehabilitation. It should be

able to do so considering the action of varying magnitudes and configurations of loads, and under varying ambient conditions. Ideally, it should be nondestructive, rapid, permit the evaluation of the entire pavement with a minimum interruption to air traffic, and should be inexpensive and easy to use.

The problem of evaluating a pavement is a complex one. The pavement section consists of various materials. These materials are far from the ideal models of classical mechanics; and they vary diurnally, seasonally and with repetitions of loading. In addition, both vehicular and non-vehicular loads applied to the pavement-subgrade system vary in magnitude, intensity, and frequency.

Recognizing the nature and scope of the problem, and the need that exists today to overcome it, research activities were initiated at Purdue University toward the development of a nondestructive pavement evaluation capability to account for the complexity and variability of the pavement-subgrade system, and simultaneously satisfy the demands imposed by practical considerations; such as mobility and ease of operation of equipment. Research in this endeavor is predicated on the use of transfer function theory as the key to pavement evaluation. This methodology has evolved over a 15 year period from concept, through theory and laboratory studies to field investigations using fixed installations (References 6, 7, 8, 9, 10, 11, 12 and 13).

## SECTION II

## LITERATURE REVIEW

The need for improving methods and developing theories to quantify adequately the complex mechanism of pavement-subgrade interaction has generated considerable activity in the area of pavement analysis and evaluation in general, and nondestructive testing in particular. In evaluation procedures, efforts are being made to eliminate or reduce destructive testing. In nondestructive testing emphasis is currently being put on the use of surface deflection measurements. In analysis, attempts are being made to deviate from the classical approaches and use probabilistic and stochastic models. Because in the recently published literature several excellent state of the art papers and literature reviews already exist (References 14, 15, 16 and 17), no attempt will be made here to repeat these works, however, a synoptic overview of the principal works is presented.

### 2.1 Airfield Pavement Evaluation

The evaluation of airfield pavements can be categorized as destructive or nondestructive.

#### 2.1.1 Destructive Evaluation

These procedures, as the name implies, destroy parts of the system; and, generally, involve the use of test pits, laboratory and/or in situ testing. Five procedures, with minor modifications are currently in use. These are the procedures of the U. S. Federal Aviation Administration (FAA) (Reference 1); U. S. Navy Bureau of

Yards and Docks (Reference 2); the Canadian Department of Transportation (Reference 3); the British Department of the Environment (Reference 4) and the U. S. Department of the Army and the Air Force (Reference 18). Basically, the five procedures involve the use of field tests in conjunction with sampling and laboratory testing.

The FAA procedure uses California Bearing Ratio (CBR) tests conducted in accordance with procedures in MIL-STD 621A Method 101. The Navy method uses non-repetitive plate load tests conducted according to specifications of American Society for Testing and Materials (ASTM) Test Method-Designation D-1196 (Reference 19). The Canadian practice uses repetitive plate bearing tests specified in ASTM Test Method Designation D-1195 (Reference 20). The British procedure also uses repetitive plate bearing tests but these are conducted in a slightly different manner from the ASTM D-1195 Test Method. The Air Force evaluation procedure is summarized in the report of the testing program conducted in a recent (1975) evaluation. It was reported (Reference 21) that,

> "Field testing consisted of 28 exploratory test pits . . . Thickness measurements were made on each pavement component, in situ density and moisture contents were determined, values of Modulus of Subgrade Reaction and CBRs were obtained and bulk samples of soil layers were taken. Core samples were extracted at 184 locations to ascertain pavement thickness and subsurface profile. Laboratory testing included classification of soils;

development of soil moisture-density relationships; Marshall testing of asphaltic concrete; and tensile splitting of Portland cement concrete cores."

The period of the evaluation was about 8 days.

The prevalent feeling concerning the use of test pits, and current destructive evaluation procedures was quite aptly put when one author (Reference 22) wrote,

> "Yet most civil engineers still cannot scientifically evaluate the load carrying capacity of an airport pavement without first rendering it unserviceable in a way no aircraft could have accomplished. The resulting test pits when filled and resurfaced remain as abrupt discontinuities to uniform pavement performance."

This general feeling coupled with the many other disadvantages of destructive testing has directed research towards the development of rapid, nondestructive evaluation equipment and procedures.

### 2.1.2 Nondestructive Evaluation

Nondestructive procedures are based on the analysis of the measured surface deflection response of a pavement-subgrade system to loads applied at the surface. The main differences among existing methods are: (1) the magnitude and manner in which the load is applied to the surface, and (2) the particular aspect of the surface disturbance that is measured, i.e., deflection magnitude, wave length, frequency. Table 1 shows a summary of the major load classes and their

TABLE 1 SUMMARY OF NONDESTRUCTIVE TESTING EQUIPMENT AND PERTINENT CHARACTERISTICS

| Category | Load Class | Device | Deflection Measurement Made |
|---|---|---|---|
| 1 | Static | Plate (19)[a] | Magnitude |
| | | Plate (20) | Magnitude |
| 2 | Impact | Washington State (58) | Magnitude |
| | | Paris (58) | Magnitude |
| | | German (58) | Magnitude |
| 3 | Vibratory | Shell (23) | Wave Length |
| | | Road Rater (25) | Magnitude |
| | | Dynaflect (23) | Magnitude |
| | | Corp of Engr. (25) | Magnitude |
| | | AFCEL (68) | Wave Length |
| 4 | Vehicular | Benkleman (69) | Magnitude |
| | | California (55) | Magnitude |
| | | Lacroix (70) | Magnitude |
| | | TRRL (71) | Magnitude |
| | | South Africa (23) | Curvature |

[a]Numbers refer to references

characteristics, devices being developed and in use, and the particular aspect of the surface disturbance that is measured.

In the static load class repetitive or non-repetitive loads are applied to plates of varying sizes on the surface of the pavement. In the impact load class, weights are allowed to free-fall and impact a plate on the pavement surface. The weights may range in size from 20 lbs (Reference 23) to 500 lbs, as was used by Isaada (Reference 24). The vibratory procedures also show a considerable range in magnitude of vibratory loads and frequency of vibration. Peak vibratory loads may range from 0.75 to 25 kips and frequencies may range from 1 to 5000 hertz. Green and Hall (Reference 25) conducted a thorough study of vibratory equipment. Their work and the references cited in Table 1 provide additional details. Of the devices that use vehicular loads, the Benkleman beam measures rebound deflection, and the LaCroix and California deflectometer are somewhat automated Benkleman beams. The TRRL device employs an optical (non contact) displacement transducer for measuring deflections, and the South African apparatus measures curvature of the pavement as the wheel approaches.

## 2.2 Analysis

Numerous analytical solutions exist, employing various models, representing a pavement-subgrade system. These models are based on the theories of elasticity and viscoelasticity. Numerous equations representing their behavior under static and dynamic loading have also been solved (References 26 through 40). In 1972, Boyer (Reference 11) presented a rather definitive review of these solutions. In

addition, he employed the concept of transfer function theory along with the results of full scale field testing, using gages installed in the pavement. He proposed an "a posteriori" modelling concept to develop transfer functions and predict pavement response. Highter (Reference 13) reviewed the use of energy concepts and methods, and failure criteria relative to pavement evaluation. Using energy concepts he was able to substantiate that "a functional relationship exists between cumulative energy as measured by cumulative peak deflections imparted to a given pavement system and the condition of the system". Three sources of data were studied to verify his hypothesis. AASHO Road Test data, the Air Force base traffic records from Pease and Castle Air Force Bases, and data from field testing of overlays specifically constructed for his investigation.

A theoretical study of dynamic stiffness and its application to vibratory nondestructive testing of pavements was conducted by Weiss (Reference 41) in conjunction with the study by Green and Hall (Reference 25). Weiss developed a nonlinear vibration theory for pavements and gave a method of obtaining the shear modulus and thickness of each pavement layer. In this work a vibrator is used to generate the deflections from which the dynamic stiffness is calculated.

Wiseman (Reference 42) used the Hogg and the Hertz models to estimate pavement characteristics. The Hogg model provided the required pavement stiffness for full-depth asphalt airfield pavements. He then related the computed stiffness to projected traffic and a characteristic length using published Asphalt Institute procedures.

Wiseman also used the Hertz model to compute the single wheel load on a rigid pavement as a function of measured stiffness.

A probabilistic analysis of the response of pavement structures was undertaken by McCullough (Reference 17). He cited the application of stochastic process, in this regard by the Texas Highway Department (Reference 43), California Division of Highways (Reference 44) and the Asphalt Institute (Reference 45). He also illustrated the application of the Markov process and its theoretical relation to states of a pavement. Reliability techniques have also been reported by Darter and Hudson (Reference 46). In 1976, Moavenzadeh (Reference 47) presented a stochastic simulation model for predicting pavement performance. Recognizing the limitations of his model, he concluded that it can be used to compare various design alternatives. It also accounts for geometry, load area and intensity, random inter-arrival times, statistical variation in material properties and temperature histories.

Inherent in all analytical and stochastic models is the notion that parameters can be obtained that reflect the actual vehicular load experienced by a pavement subgrade system. At the present time, the literature shows that parameters used in analysis are obtained by static field test, laboratory testing, vibrations, impact and measurement of pavement rebound characteristics. The actual time dependent response of the pavement-subgrade system subject to one complete vehicular pass is not considered.

## SECTION III

## THEORY AND METHODOLOGY

There exist today numerous elastic and viscoelastic solutions (References 26 through 40) to the overall vehicle-pavement-subgrade interaction problem, in addition to the results of several full scale field testing programs (References 48 through 50). Accumulated theory and prototype testing point to the following fundamental observations:

1. The characteristics of the component materials of a pavement-subgrade system vary locally, even within the small volume of a representative "homogeneous" sample.
2. Pavement-subgrade characteristics and response to loadings change with seasonal and ambient conditions.
3. Load repetitions affect the various components of the system differently.
4. A nondestructive field test conducted in situ using prototype loading better reflects the action of a pavement-subgrade system than destructive tests on samples, or tests conducted in situ using non-representative loads.
5. The pavement subgrade system exhibits three basic behavioral characteristics; namely,
   (a) inertial characteristics,

(b) elastic characteristics, i.e. linear and independent of time, and

(c) viscoelastic characteristics that account for the memory and the time dependent nature of the system response.

Recognition of the complexity and variability of the pavement-subgrade system and the nature of the wheel loading-pavement-subgrade interaction problem, has led to the development of global methods of characterizing the pavement-subgrade system under prototype conditions of loadings (References 38, 51, and 52). The global concept provides a quantitative spatial evaluation rather than one limited to the very near vicinity of a point and the subsequent assumptions of homogeneity and isotropy in the case of the classical theories (References 11 and 12).

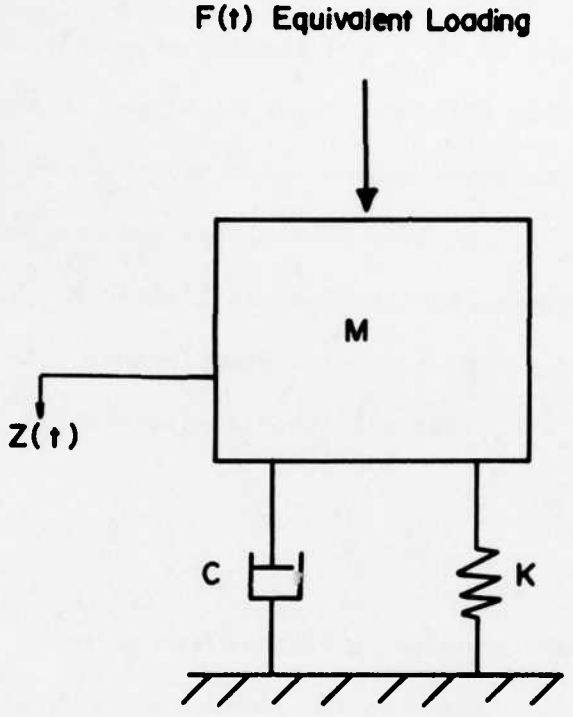
## 3.1 Hypotheses

The principal hypotheses embodied in this research are:

1. The response of a point on the surface of a pavement-subgrade system when subjected to vehicular loadings can be characterized by a (Kelvin) lumped parameter model. The three parameters of the model are m, c, and k, as shown in Figure 1. The equation describing the hypothesized lumped parameter system is

$$m\ddot{z}(t) + c\dot{z}(t) + kz(t) = F(t) \qquad (1)$$

where m represents the equivalent mass (the interacting




$$m\ddot{z}(t) + c\dot{z}(t) + kz(t) = F(t)$$

Figure 1. Kelvin Model of the Pavement Subgrade System

inertial components of the pavement-subgrade system), c is the damping (the time dependent viscoelastic or energy dissipating component), and k is the stiffness (elastic component); z(t), z(t) and z(t) are the equivalent acceleration, velocity and deflection, respectively. F(t) is the equivalent input force due to the wheel load, (its maximum value for the F-4 aircraft, for example, is approximately 25 kips). Figure 1 shows the hypothesized model.

2. The salient characteristics of the time dependent response of the pavement-subgrade system to a complete vehicular pass can be obtained in a nondestructive manner.
3. Equivalent parameters describing the pavement-subgrade system stiffness (k), energy dissipation (c) and inertial (m) characteristics can be extracted from the measured response.
4. The extracted parameters accomplish the following:
    (a) they reflect the global structural state of the pavement-subgrade system and; whereas, they are responsive to seasonal and local variations, they can be used as the basis of a nondestructive evaluation scheme.

(b) they can be used to predict the deflection response to varying magnitudes and configurations of wheel loads.

5. Many current parameters used in conventional design and analysis can be obtained from the noted response of a pavement-subgrade system to actual vehicular loading.

The developed theory and methodology provide the following: (1) the theoretical basis of a pavement evaluation scheme. This includes the determination of the deflection response of a pavement-subgrade system to prototype loading, and the methodology of extracting parameters describing the equivalent mass, stiffness and energy dissipation characteristics of the pavement-subgrade system. (2) The methodology for predicting the deflection response of flexible pavements to prototype loadings of varying magnitudes and configurations.

## 3.2 Evaluation

The pavement evaluation scheme consists of determining the parameters inherent in the transfer function of the pavement-subgrade system. The transfer function is a mathematical expression which represents the mechanism that converts the equivalent input to an output. Figure 2 shows an overview of the input-transfer function-output interrelation as it applies to wheel load-pavement-subgrade interaction.

The basic elements of the evaluation scheme are:

(a) the signature determination, and

(b) the parameter determination.

### 3.2.1 Signature Determination

The signature is the pavement deflection-time plot corresponding to the pavement deflection at the outer edge of the tire print as shown in Figure 3. Because the mechanical setup of the measuring equipment precludes the measurement of deflections closer than 3 inches from the outer edge of the tire print, the signature is calculated from deflections measured in the field using the "stationary beam-moving load" procedure.

In this procedure (Figures 3 and 4) a cantilever beam with its pivot outside the deflection basin supports sensing elements within the deflection basin. The sensing elements measure relative motion between the pavement surface and the beam as the load vehicle travels in a direction perpendicular to the beam position. The sensing elements are positioned at different lateral distances from the load wheel and therefore record the deflection time history for one complete pass of the load vehicle at the points of measurement. The location of the tire print is determined from the impression the tire makes on silver adhesive tape placed on the pavement in its path in front of the beam. The distance from the outer edge of the tire print to the first gage is measured. From this initial measurement and the fixed intergage distances, the distance of each gage from the outer edge of the tire print is calculated [Figure 3(b)]. Figure 4 shows an Air Force P-2 fire truck about to make a pass by two stationary measurement systems.

The method of calculating the signature is as follows:

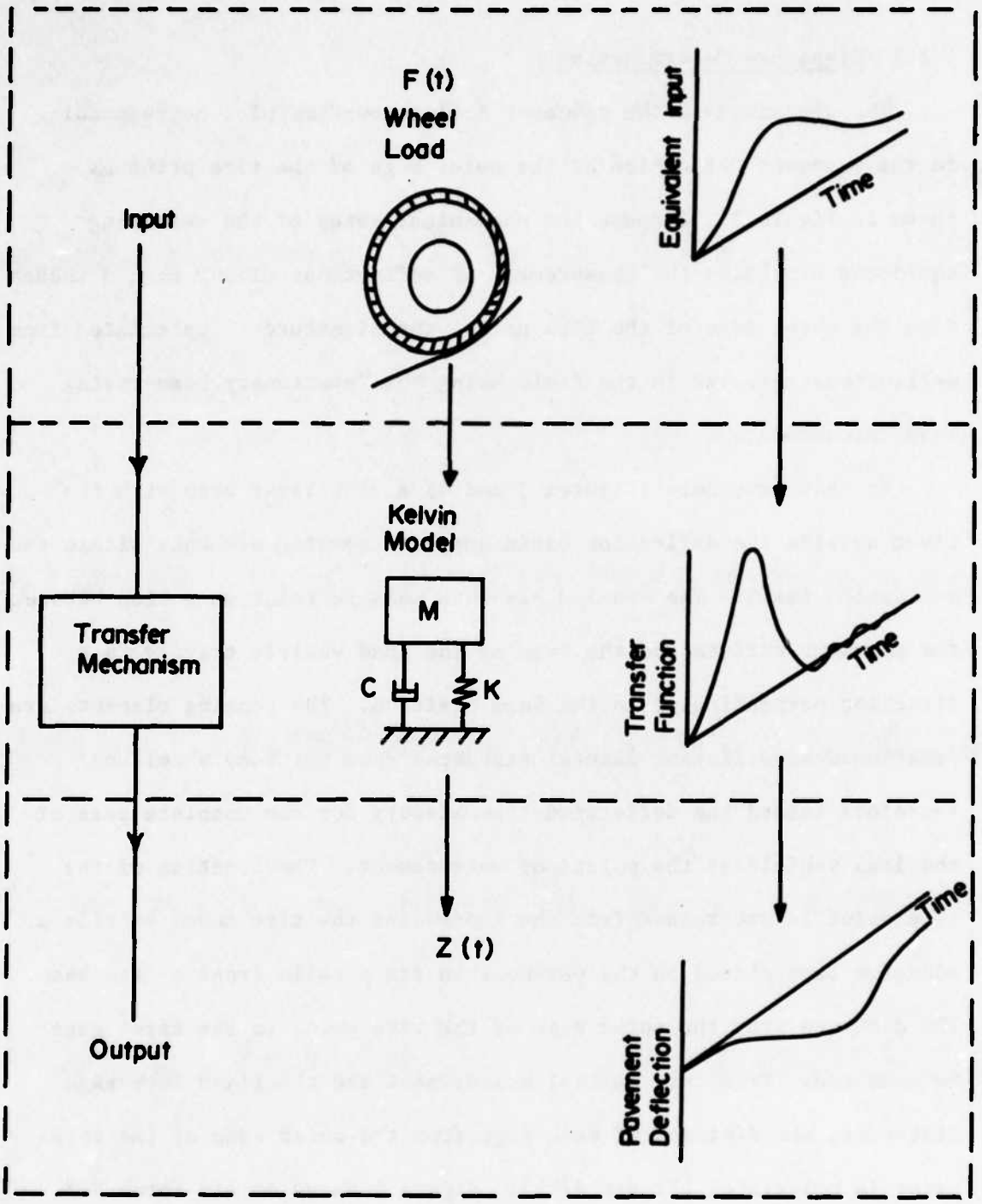
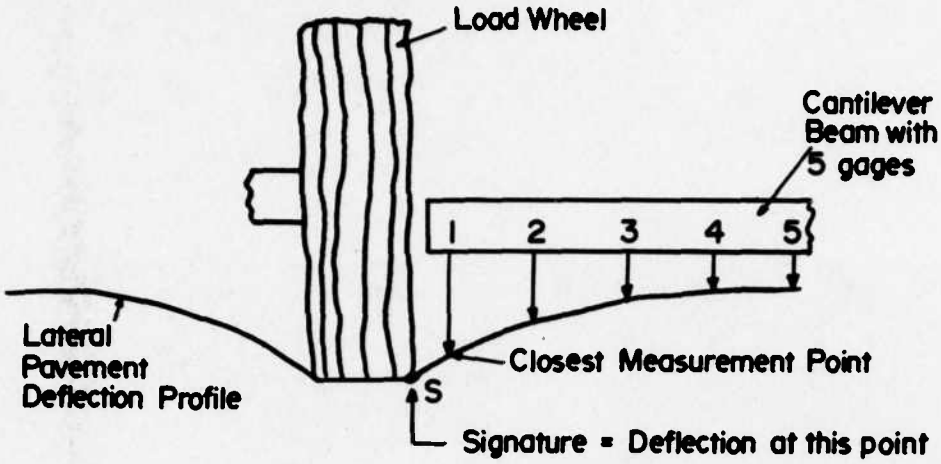
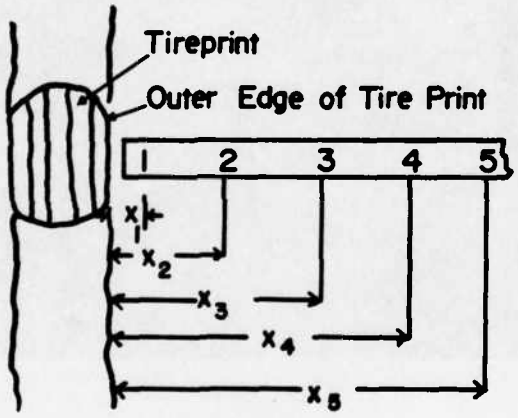



Figure 2. An Overview of the Transfer Function Concept as Applied to Wheel-Pavement Subgrade Interaction




(a) Profile




(b) Plan View

Figure 3. Location of Signature and Relative Gage Location and Setup

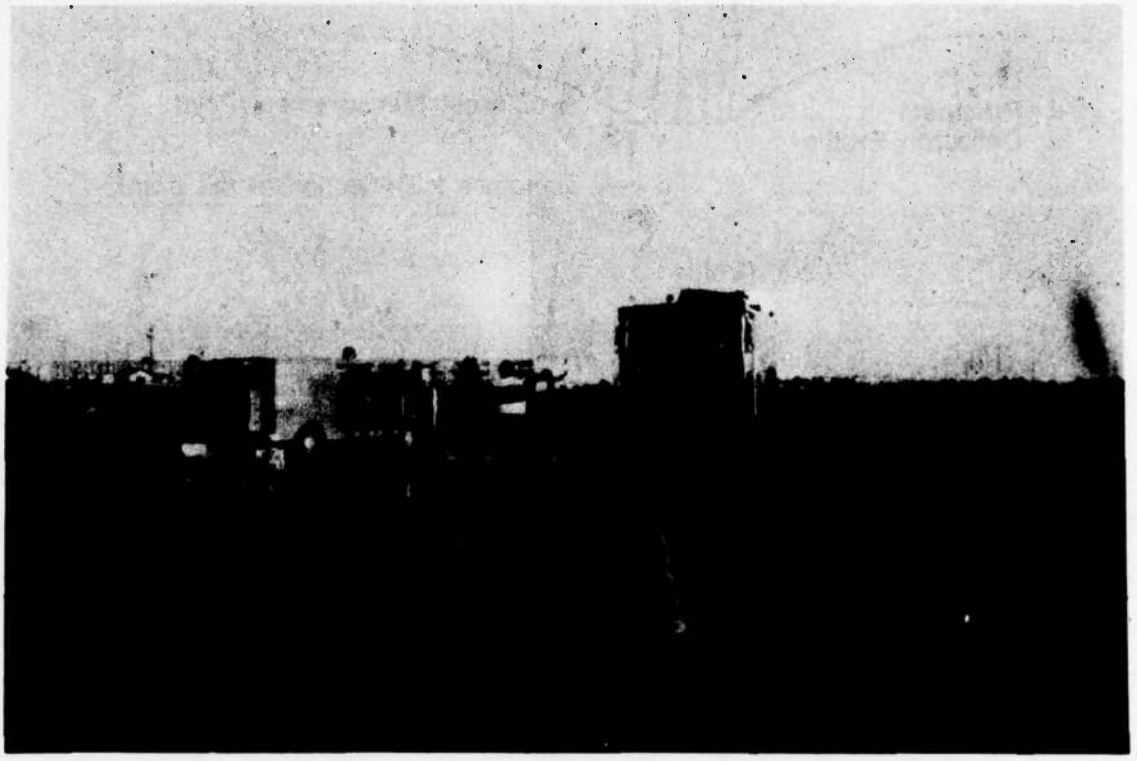


Figure 4. Setup During Stationary Beam-Moving Load Operation - P-2 Fire Truck

(a) The maximum value of the deflection, $z_{max}$, at each particular gage (j) is obtained from each of the deflection-time plots recorded at said gage (j) during one pass of the vehicle. V and W of Figure 5 show $z_{max_1}$ and $z_{max_2}$ ($z_{max_3}$, $z_{max_4}$ and $z_{max_5}$ are not shown), in perspective.

(b) The distances $x_j$ [Figure 3(b)] from the outer edge of the tire print to each gage as recorded in the field, and the corresponding maximum gage readings, $z_{max_j}$, are then fitted with a curve given by the equation

$$z_{max_j} = A_{peak} \exp (\beta_{peak} x_j^{r_{peak}}) \qquad (2)$$

where $A_{peak}$, $\beta_{peak}$ and $r_{peak}$ are parameters describing the attenuation of the maximum values of the deflection-time plots recorded on each gage. Equation (2) is similar in form to those used by Boyer (Reference 11) and Highter (Reference 12), but has three parameters, $A_{peak}$, $\beta_{peak}$ and $r_{peak}$, instead of two that they used. Baladi (Reference 52) also uses a three-parameter equation to describe the attenuation of the maximum lateral deflection profile caused by vehicular loads on highways.

The curve fitting calculations are performed by the computer subroutine EXACFIT listed in Appendix C. The equations used are derived as follows:

Given the general equation of the curve in the form

$$z = A \exp(\beta x^r) \qquad (2a)$$

This equation has three unknowns, A, $\beta$ and r. Using this basic equation and values of $(x_1, z_{max_1})$, $(x_2, z_{max_2})$ and $(x_3, z_{max_3})$, (where the numbers in the subscripts refer to gages numbered from 1, the closest to the wheel, to 5 the farthermost from the wheel), the following are had:

$$z_{max_1} = A'_{peak} \exp(\beta'_{peak} x_1^{r_{peak}}) \qquad (3a)$$

$$z_{max_2} = A'_{peak} \exp(\beta'_{peak} x_2^{r_{peak}}) \qquad (3b)$$

$$z_{max_3} = A'_{peak} \exp(\beta'_{peak} x_3^{r_{peak}}) \qquad (3c)$$

Dividing equation (3a) by equation (3b) gives

$$z_{max_1}/z_{max_2} = \exp(\beta'_{peak} x_1^{r'_{peak}} - \beta'_{peak} x_2^{r'_{peak}})$$

Taking the natural logarithm of both sides produces

$$\ln z_{max_1} - \ln z_{max_2} = \beta'_{peak} (x_1^{r'_{peak}} - x_2^{r'_{peak}}) \qquad (4)$$

Similarly from equation (3a) and (3c)

$$\ln z_{max_1} - \ln z_{max_3} = \beta'_{peak} (x_1^{r'_{peak}} - x_3^{r'_{peak}}) \qquad (5)$$

Dividing equation (4) by equation (5) and rearranging terms gives

$$(x_1^{r'_{peak}} - x_3^{r'_{peak}}) \left(\frac{\ln z_{max_1} - \ln z_{max_2}}{\ln z_{max_1} - \ln z_{max_3}}\right) = x_1^{r'_{peak}} - x_2^{r'_{peak}} \qquad (6a)$$

Equation (6a) is solved by an iteration-interpolation procedure detailed in Appendix C, and $r'_{peak}$ is found.

$\beta'_{peak}$ is then calculated using equation (5), where

$$\beta'_{peak} = \frac{\ln z_{max_1} - \ln z_{max_3}}{x_1^{r'_{peak}} - x_3^{r'_{peak}}} \qquad (5a)$$

Then $A'_{peak}$ is calculated using equation (3a) where

$$A'_{peak} = z_{max_1} / \exp\left(\beta'_{peak}\, x_1^{r'_{peak}}\right) . \qquad (3a)$$

Using $(x_1, z_{max_1})$, $(x_3, z_{max_3})$ and $(x_5, z_{max_5})$ instead of $(x_1, z_{max_1})$, $(x_2, z_{max_2})$ and $(x_3, z_{max_3})$, equations (3a), (3b) and (3c) are again solved to find $r''_{peak}$, $\beta''_{peak}$ and $A''_{peak}$. The desired $r_{peak}$, $\beta_{peak}$ and $A_{peak}$ are found using the equations

$$r_{peak} = \left(r'_{peak} + r''_{peak}\right)/2 \qquad (7)$$

$$\beta_{peak} = \left(\beta'_{peak} + \beta''_{peak}\right)/2 \qquad (8)$$

$$A_{peak} = \left(A'_{peak} + A''_{peak}\right)/2 \qquad (9)$$

$r_{peak}$, $\beta_{peak}$ and $A_{peak}$ are the parameters which describe the maximum lateral deflection profile, partly shown in Figure 5 as the curve V'VW.

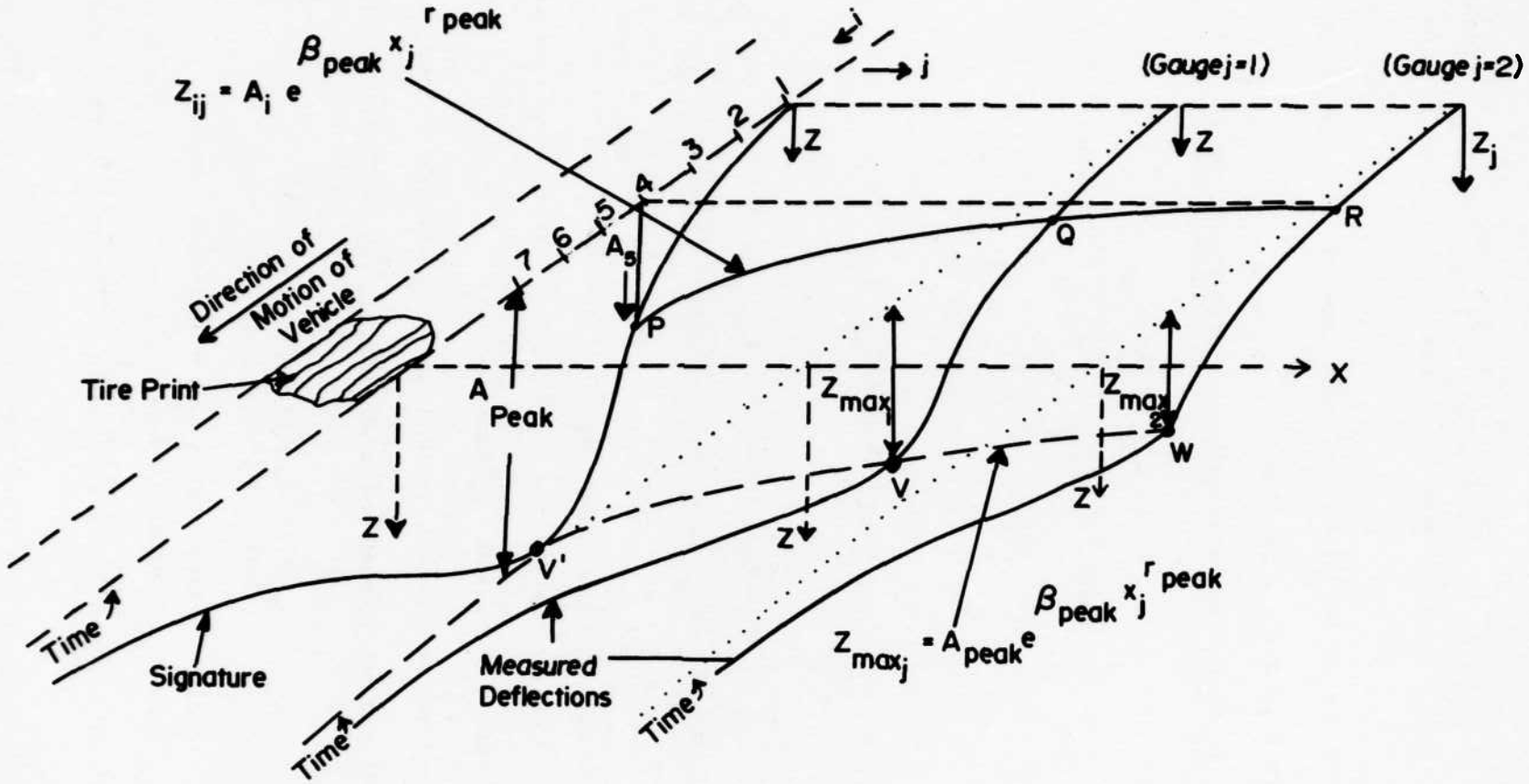



Figure 5. Overview of Method of Calculation of Signature Due to Prototype Loading

(c) The signature is calculated using the $r_{peak}$ and $\beta_{peak}$ parameters and the basic equation, equation (2a), in the form

$$A(t) = z_1(t)/\exp\ (\beta_{peak}\ x^{r_{peak}}) \qquad (10)$$

where $z_1(t)$ refers to the deflection at gage 1 (closest to the wheel), and t is the time shown discretized as i in Figure 5. Subroutine SIGNTR in Appendix C performs these computations.

The signature thus calculated is the pavement deflection due to prototype loading at point S in Figure 3. Using this signature as the output (Figure 2), parameters k, c, and m describing the transfer mechanism of the three-parameter model of the pavement-subgrade system, are calculated.

### 3.2.2 Parameter Determination

The objective of the theoretical procedure is to determine the equivalent m, c and k parameters of a pavement-subgrade from the signature obtained from actual field loadings using transfer function theory. These parameters define the transfer mechanism that converts wheel loadings to pavement deflections.

The wheel load-pavement-subgrade interaction, as shown in Figure 2, can be represented mathematically by the equation (1):

$$m\ddot{z}(t) + c\dot{z}(t) + kz(t) = F(t) \qquad (1)$$

It can also be represented by the equation

$$I(t) * G(t) = \frac{F(t)}{m} * G(t) = z(t) \qquad (11)$$

where F(t) is the equivalent loading (input) function, m is the equivalent mass, G(t) is the reduced transfer function, z(t) is the response and the symbol (*) represents the mathematical operation of convolution (Reference 53). In its integral form equation (11) becomes

$$z(t) = \int_0^t \frac{F(t)}{m} \cdot G(t-\tau)\, d\tau \qquad (12)$$

G(t), the reduced transfer function in equations (11) and (12) is obtained from equation (1) as follows:

Consider the basic equation of the model:

$$m\ddot{z}(t) + c\dot{z}(t) + kz(t) = F(t) \qquad (1)$$

taking the Laplace transform of both sides, imposing initial conditions (pavement is assumed to be at rest prior to loading) of $z(0) = \dot{z}(0) = 0$, and transposing terms, yields:

$$\bar{z}(s) = \frac{\bar{f}(s)}{m} \cdot \left( \frac{1}{s^2 + \frac{c}{m} s + \frac{k}{m}} \right)$$

where the bars denote the transformed function. The reduced transfer function is defined as

$$\bar{G}(s) = \frac{1}{s^2 + \frac{c}{m} s + \frac{k}{m}}$$

Inverting $\bar{G}(s)$ gives,

$$G(t) = \left[ \frac{1}{\frac{k}{m} - \frac{c^2}{4m^2}} e^{-\frac{c}{2m} \cdot t} \right] \left[ \sin \sqrt{\frac{k}{m} - \frac{c^2}{4m^2}}\, t \right] \qquad (13a)$$

if $k/m < \frac{c^2}{4m^2}$, namely, the system is overdamped, then

$$G(t) = \left[ \frac{1}{\frac{c^2}{4m^2} - \frac{k}{m}} e^{-\frac{c}{2m} \cdot t} \right] \left[ \sinh \sqrt{\frac{c^2}{4m^2} - \frac{k}{m}}\, t \right] \qquad (13b)$$

Two ways to obtain the equivalent input (loading function) F(t) will be pursued in this work. The first way is by the direct substitution in the equation

$$m\ddot{z}(t) + c\dot{z}(t) + kz(t) = F(t) \qquad (1)$$

of the calculated values of z(t), $\dot{z}(t)$ and $\ddot{z}(t)$ obtained from the measured deflections, and the parameters of the transfer mechanism m, c and k. The second method is by implicit convolution using equations (11) and (12). The implicit discrete form of equation (12) is given (Reference 53) by the equation

$$I(i) = \frac{O(i)/\Delta T - \sum_{m=1}^{k=i-1} I(m) \cdot G(k + 2 - m)}{I(1)} \qquad (14)$$

where G() = the reduced transfer function

O(i) = the output z(i)

m x I(i) = F(i) = the equivalent loading function (15)

$\Delta T$ = time increment

and, the initial value of I(i) = I(1) is given by the equation

$$I(1) = \frac{O(1)}{G(1) \cdot \Delta T}$$

The same two arguments above lead to two ways of finding the output z(t), given the forcing function and the parameters m, c, k. The first is by the closed form solution of equation (1). The second is by explicit convolution using the equation

$$O(i) = z(i) = \sum_{j=1}^{i} G(i) \cdot I(i - j + 1)\ \Delta T \qquad (16)$$

where z(), G(), I() and $\Delta T$ are as defined in equation (14).

During field testing, only the deflections with time are measured, and from these deflections the signature A(t) in equation (10) can be obtained as discussed previously. How then are the parameters of transfer frunction and the loading functions determined?

In concept, the methodology used is as follows: The signature A(t) is taken to be equivalent to the response z(t) in equations (11) to (16) as discussed in the previous section entitled "Signature Determination". The input function F(t) is now known initially. It is assumed however that the maximum value of F(t) is the wheel load, or approximately 25 kips (Reference 54) for the F-4 aircraft, which is the main vehicle of interest in the present study. Using the signature z(t), the maximum assumed value (25 kips) of the equivalent input, and the equations developed previously in this section, the k, c, and m parameters of the pavement-subgrade system are determined.

The detailed procedure for finding k, c, and m is as follows:

(1) The signature is differentiated numerically to yield the time history of the velocity $z(t)$ and the acceleration $z(t)$. Typical plots of $z(t)$, $z(t)$, and $z(t)$ are shown in Figure 6.

(2) The components of the equivalent force, due to each of the three parameters, on the left hand side of the basic equation (1), are then considered for three special conditions, labelled as sections (1), (2), and (3) in Figure 7.

At section (1), the point of inflection of the signature, the following equations hold:

$$\ddot{z}(t_1) = 0$$

$$m\ddot{z}(t_1) = 0$$

hence,

$$c\dot{z}(t_1) + k\, z(t_1) = F(t_1) \qquad (17a)$$

At section (3), the maximum deflection response, the following equations hold:

$$\dot{z}(t_3) = 0$$

$$c\dot{z}(t_3) = 0$$

hence,

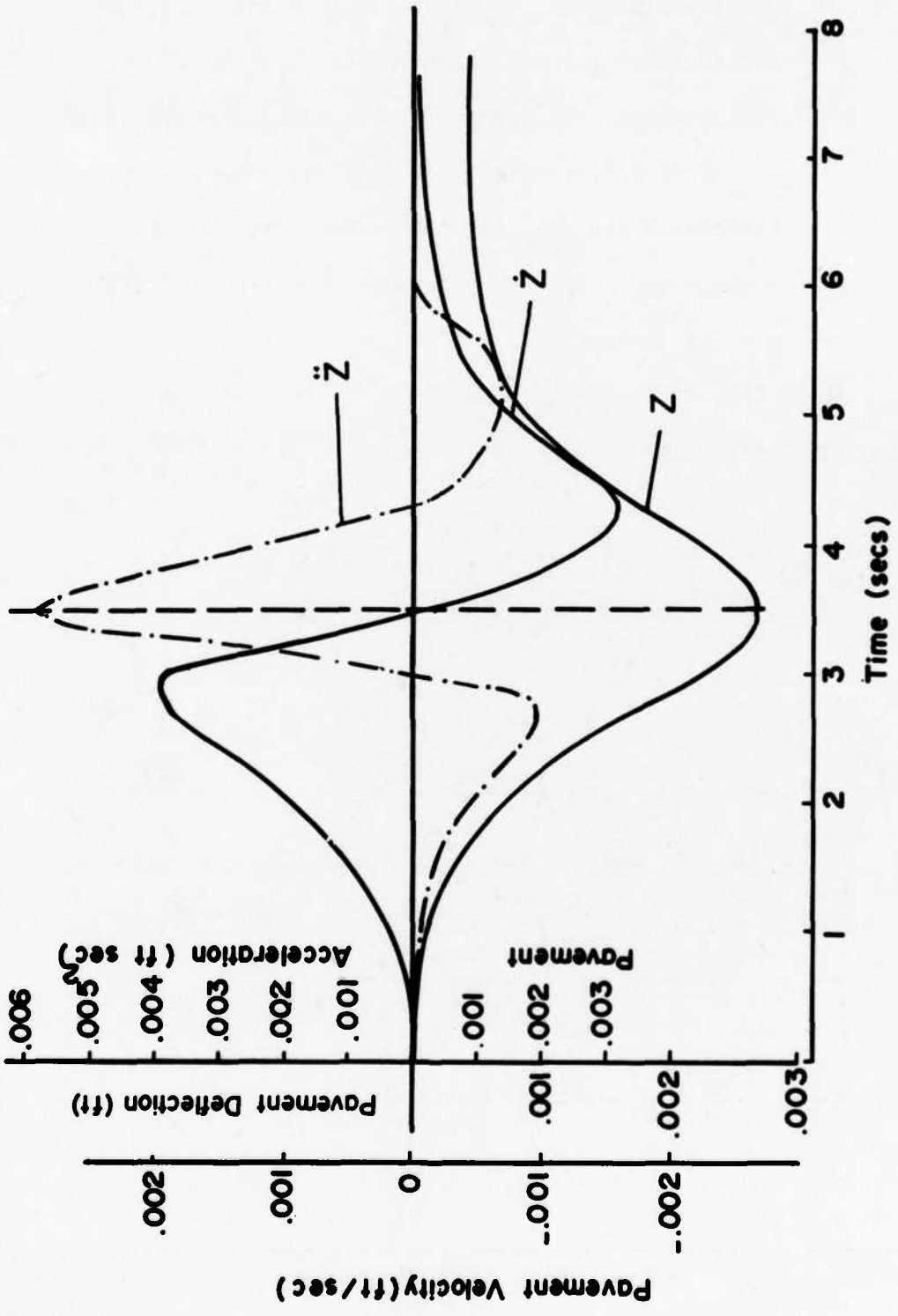



Figure 6. Zero, First and Second Derivatives of the Measured Displacement Function (Typical)

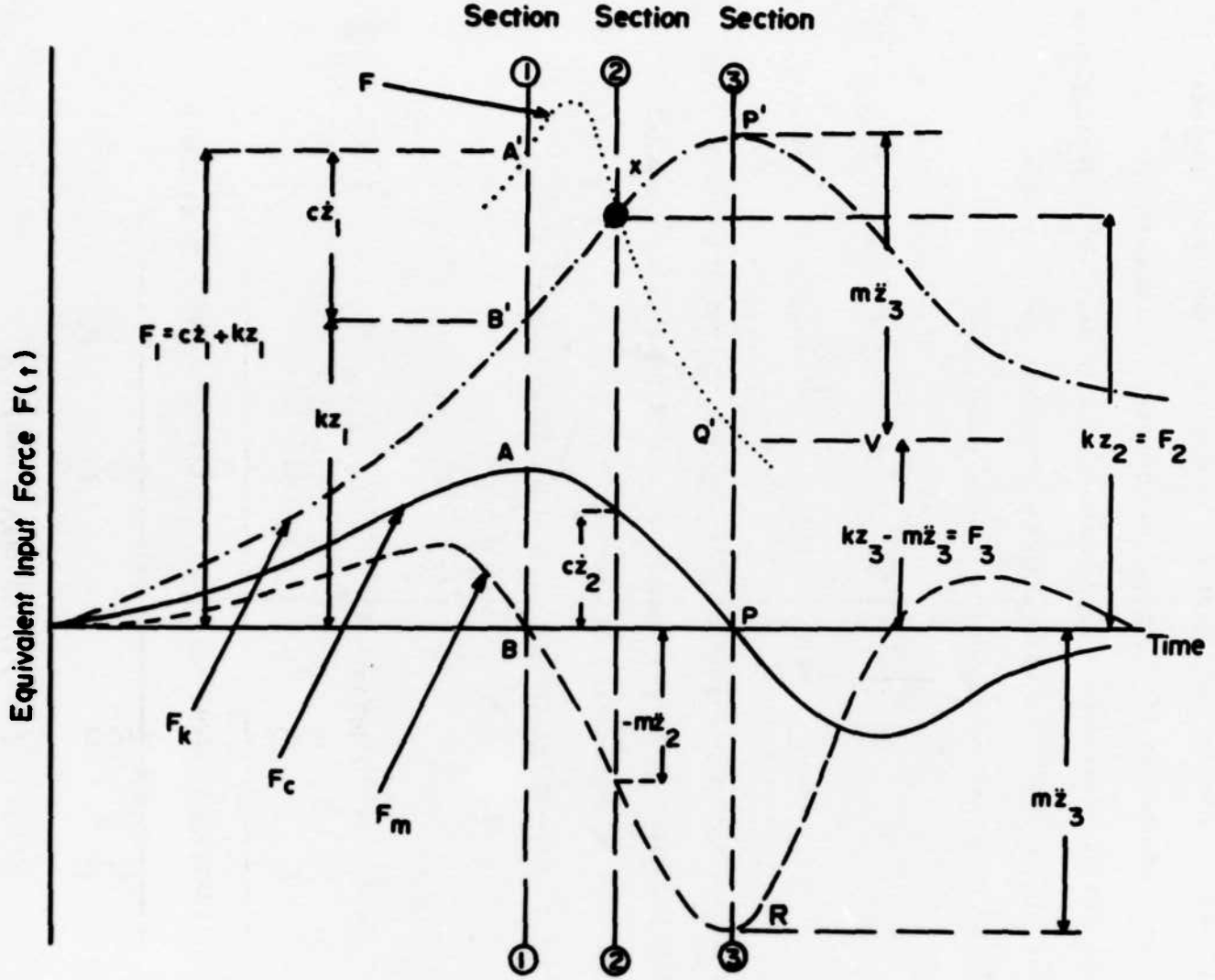



Figure 7. Determination of Parameters of Transfer Function - A Graphical Overview of Methodology

$$m\ddot{z}(t_3) + kz(t_3) = F(t_3) \qquad (17)$$

The third special condition occurs, for each deflection data set, at a time between the time corresponding to the point of inflection [section (1)] and the maximum deflection [section (3)]. With reference to Figure 7, with increasing times from section (1) to section (3), the stiffness component [kz(t)] of the equivalent input force increases from B' to a maximum at P'. During this passage, the damping component [cz(t)] decreases from a maximum of A to zero (P). Similarly, the inertial component [mz(t)] decreases from zero (B) to a negative value of R. The time corresponding to the conditions,

$$c\dot{z}(t_2) = - m\ddot{z}(t_2) \qquad (18)$$

$$\text{and, hence,} \quad kz(t_2) = F(t_2) \qquad (19)$$

will be called the crossing point. It provides the final special condition for determining the measure of the parameters m, c and k. This condition is represented as section (2) of Figure 7. It should be noted that between section (1) and the crossing point,

$$kz(t) \leq F(t_2)$$

and between the crossing point and section (3)

$$kz(t) > F(t_2)$$

In concept, therefore, the crossing point represents the time at which the Winkler hypothesis (Reference 55) is satisfied.

(3) Using the equation in paragraph (2) and the developed method, an iterative procedure, given in detail in Appendix C was used to determine the k, c and m parameters in this study. Briefly the procedure is as follows:

The signature of the load vehicle is obtained as described in the section entitled "Signature Determination". A first trial value of k is taken as a fraction (AA1 < 1.0)[1] of the wheel load (25 kips) divided by the maximum value of the signature. Then it is assumed that another fraction (AA2 < 1) of the wheel load acts at the time corresponding to section (3) Figure 7. The first trial value of m is calculated for the conditions at section (3) using equation (17). The initial trial value of the c parameters is then computed using equation (18) at the first estimated crossing point in the data set, i.e., at the first discrete interval of time after section (1). Using these first estimates of k, c and m the transfer function G(t) [equation (13)] is had [EXACT 1][1]. Next the loading function F(t) is obtained by implicit convolution [equations (14) and (15) and NWCONV] in the time domain using the signature deflection z(t) is output and G(t). The maximum value of F(t) is then found. A check is made to see if this (maximum) value of F(t) satisfies the necessary (500 pound) criterion that,

[1]Capital letters in parentheses refer to computer programs or symbols used in computer programs in Appendix C.

$$24{,}500 \text{ lb} \leq F(t) \text{ maximum} < 25{,}500 \text{ lb} \qquad (20)$$

If this criterion is not satisfied, the next crossing point is selected, c is recalculated and the same procedure is followed to obtain the maximum value of F(t), which is again examined with respect to the previously stated criterion. This process is repeated until the possible crossing points are exhausted i.e. section (3) Figure 7 is reached, or the maximum value F(t) satisfies the previously stated criterion, whichever occurs first.

If all possible crossing point times are exhausted a new value of m is calculated by incrementing the value of AA2. Using the first trial value of k and the second trial value of m a new c is calculated for the first estimated crossing point. The procedure is repeated, checking the maximum value of F(t) against the 500 pound criterion. If this criterion is not satisfied the sequence of crossing points is again stepped through. If these are exhausted a next trial value of m is assumed and the entire process is repeated. If the incremented value of AA2 reaches unity, a second trial value of k is calculated by incrementing AA1, and the entire procedure, including a new sequence of m and c values, is examined at all possible crossing points. This process is repeated until the 500 pound criterion (equation 20) is satisfied.

If the 500 pound criterion is satisfied, a new c value is calculated for conditions corresponding to the time at the inflection point of the signature (section (1), Figure 7, equation 17a); using the current k value and the force obtained by convolution, corresponding to the time of inflection. If this new c value does not correspond to the

c value which satisfied conditions at the crossing point and the 500 pound criterion, the iteration process is continued by selecting another crossing point and repeating the entire procedure. If the c values do correspond then the corresponding k, c, and m values are the desired parameters.

### 3.3 Prediction of Pavement Response (Signature)

The theory and methodology for signature and parameter determination developed in the previous sections were used to predict the signature of a vehicle (vehicle A) at a site prior to the actual passage of the vehicle at that location. This was done by first obtaining signatures of both a standard vehicle and vehicle A at another site, and the signature of the standard vehicle at the new site. This is accomplished by using an equivalency function.

The equivalency function is defined as the ratio of the loading (input) function of a vehicle, $F_1(t)$, and the loading function of the standard vehicle, $F_2(t)$, both obtained at the same location (at a standard site). This relationship is given by the equation.

$$\text{Equivalency Function} = EF(t) = \frac{F_1(t)}{F_2(t)} \tag{21}$$

The procedure for determining the equivalency function is as follows: with reference to Figure 8, Block I, at a standard site the signature due to a standard vehicle is obtained as discussed in the section entitled "Signature Determination". Using this signature as output, the transfer function, $G_2(t)$, of the standard site and the loading $F_2(t)$ of the standard vehicle at the standard site are determined as previously discussed in the section entitled "Parameter

Determination". Next the signature of A (the vehicle whose response is to be predicted) is obtained at the standard site. Using the transfer function of the standard site as determined by the standard vehicle and the signature of vehicle A at the standard site, the loading function $F_1(t)$ of vehicle A is obtained by implicit convolution using equation 14 and 15, and subroutine NWCONV (Appendix C). Once the equivalency function is had from equation 21, the predicted signature is obtained as follows:

First, the signature of the standard vehicle, $z(t)$, its loading function $F_{sA}(t)$ and the transfer function $G_A(t)$ are obtained at the new site as discussed in the preceding paragraph. These functions are shown schematically in Block III Figure 9. Next the loading function $F_{1A}(t)$, of vehicle A at the new site is calculated using the equation

$$EF(t) \times F_{sA}(t) = F_{1A}(t) \tag{22}$$

Equation 22 is represented in Figure 9 as the connection between the loading function of Block III and the equivalency function at the point labelled $\beta$.

The predicted signature of vehicle A at the new site is computed by the explicit convolution of the loading function of vehicle A at the new site and the transfer function of the new site as determined by the standard vehicle, using equation (16),

$$z(i) = \sum_{j=1}^{i} G(i) \cdot I\ (i - j + 1)\ \Delta T$$

where $G(i)$ = transfer function of the new site

$I(\ )$ = the equivalent loading function of vehicle A at the new

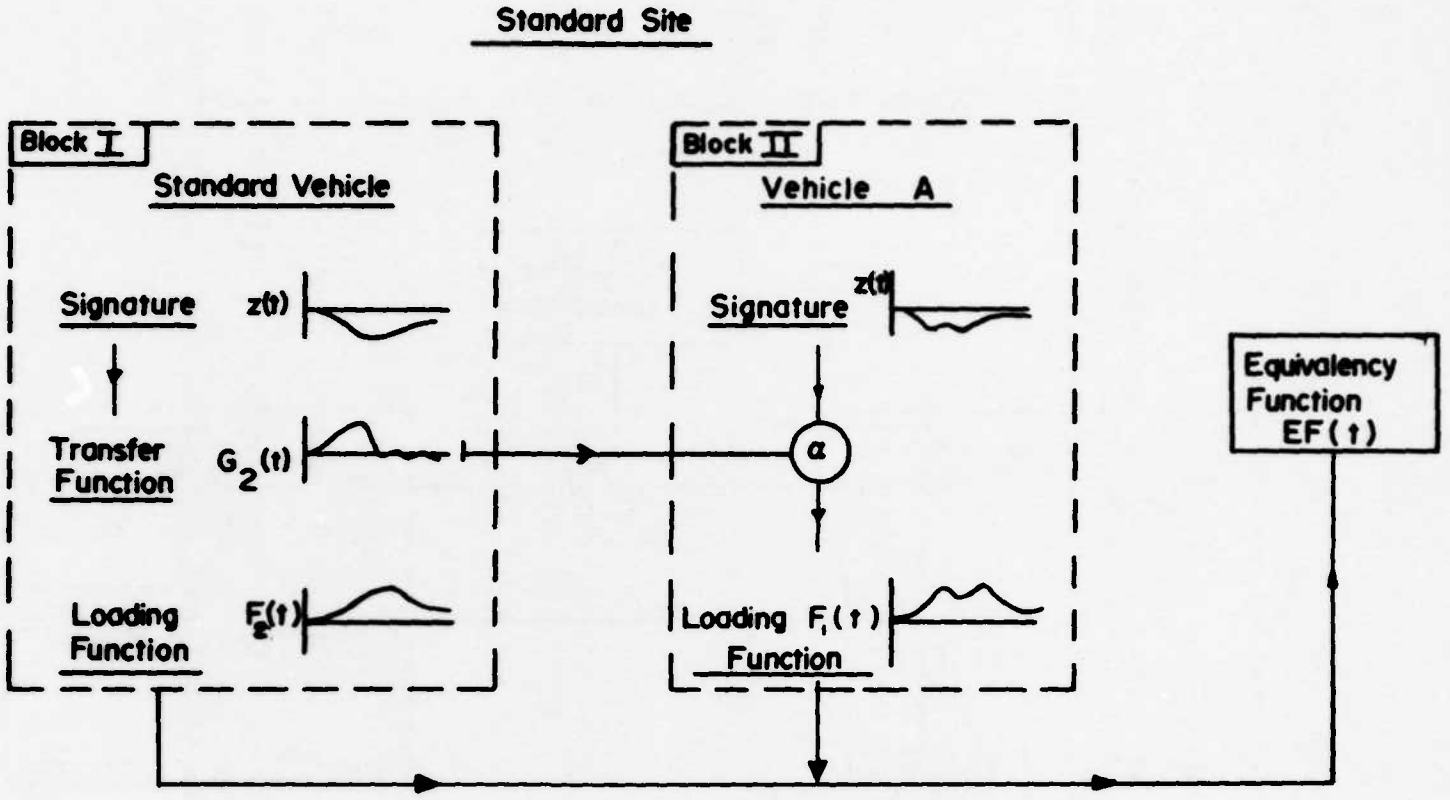



Figure 8. Overview of Scheme for Determining the Equivalency Function

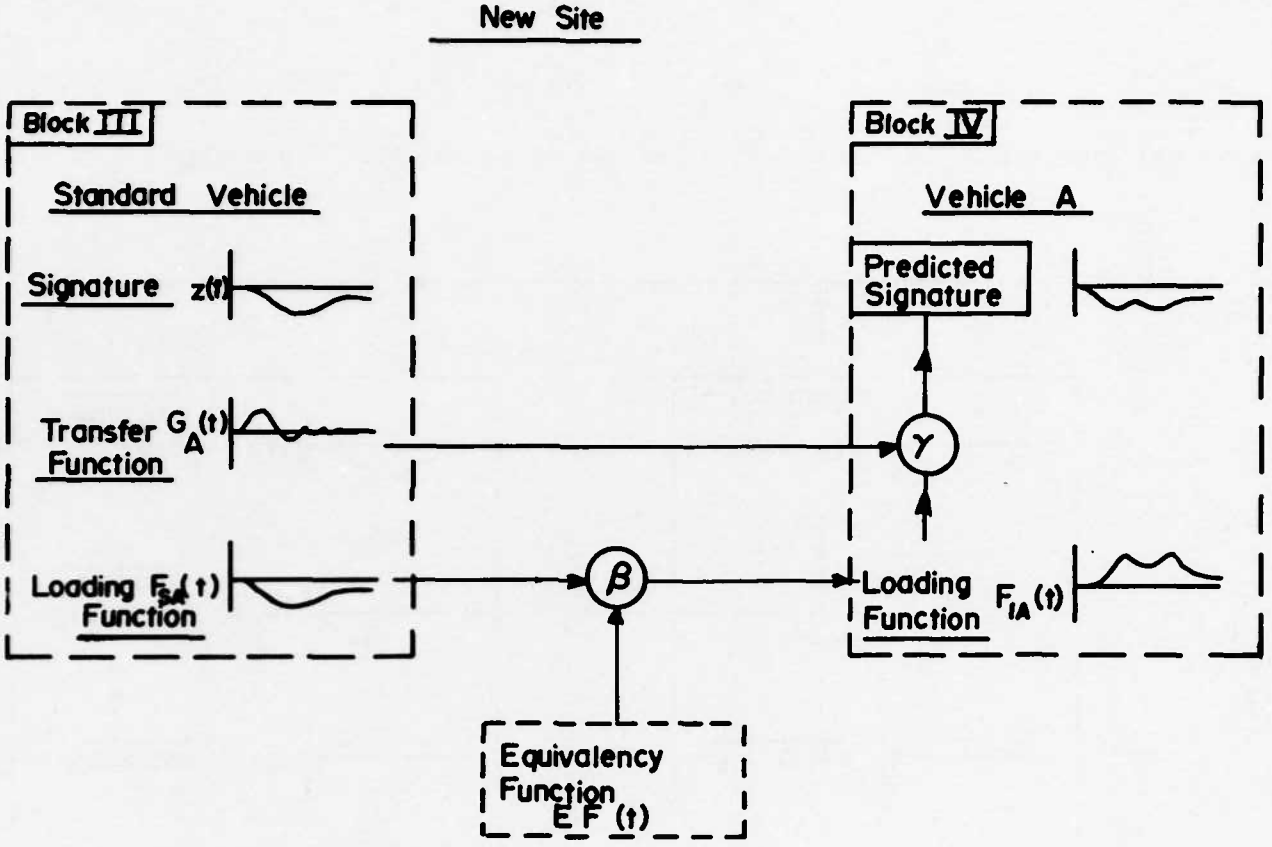



Figure 9. Overview of Scheme for Predicting the Signature

site (see equations 11 and 15)

$z(i)$ = the predicted signature

$\Delta T$ = the time increment

$j$ = dummy variable, and

$i$ = dummy variable indicating the time interval number

The explicit convolution is represented in Figure 9, Block IV as the connection between the equivalent loading and the transfer function at the point labelled $\gamma$ of Figure 9.

The computer program PREDCT that performs the noted calculations to generate the predicted signature is given in Appendix C.

The evaluation and prediction methodologies are clearly dependent on the availability of reliable equipment for measuring pavement deflections.

## SECTION IV

## NEW INSTRUMENTATION FOR DEFLECTION MEASUREMENT

Two mobile systems were developed during this study for the measurement of pavement deflections: the Light Emitting Diode (LED) system and the Linear Variable Differential Transformer (LVDT) system.[3]

The LED system is essentially an optical system which does not make contact within the deflection basin of the pavement. On the other hand the sensing elements of the LVDT system make contact with the pavement surface. A summary of the research effort expended in the development of these systems and their basic developments is presented below.

### 4.1 The LED System

The LED measurement system consists of three major operational sections: they are,

a. the beam

b. the sensor modules, and

c. the recording system

#### a. The Beam

The beam is made of aluminum. Its principal function is to support the sensors above the pavement surface. It is designed so that a 20-mile-per-hour gust of wind will deflect the end of the beam less than 0.004 in. Figure 10 shows schematic details of the beam. Figure 11 shows the LED beam setup. Seven LED sensor modules are shown between the channel of the beam.

---

[3] The LVDT system was developed by Baladi (Reference 52) as part of his research effort, sponsored by the Federal Highway Administration.

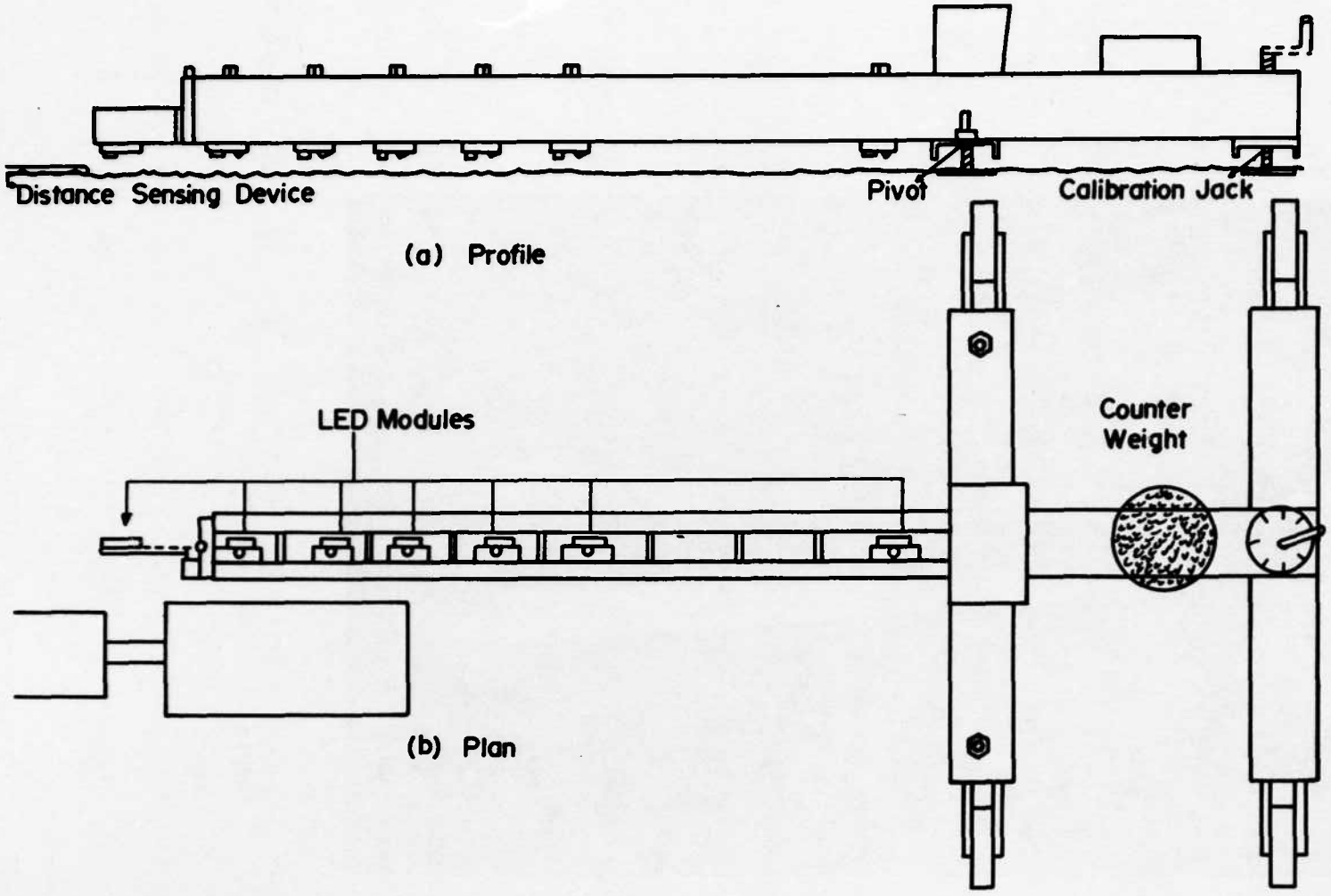



Figure 10. Light Emitting Diode (LED) Beam Schematic Details

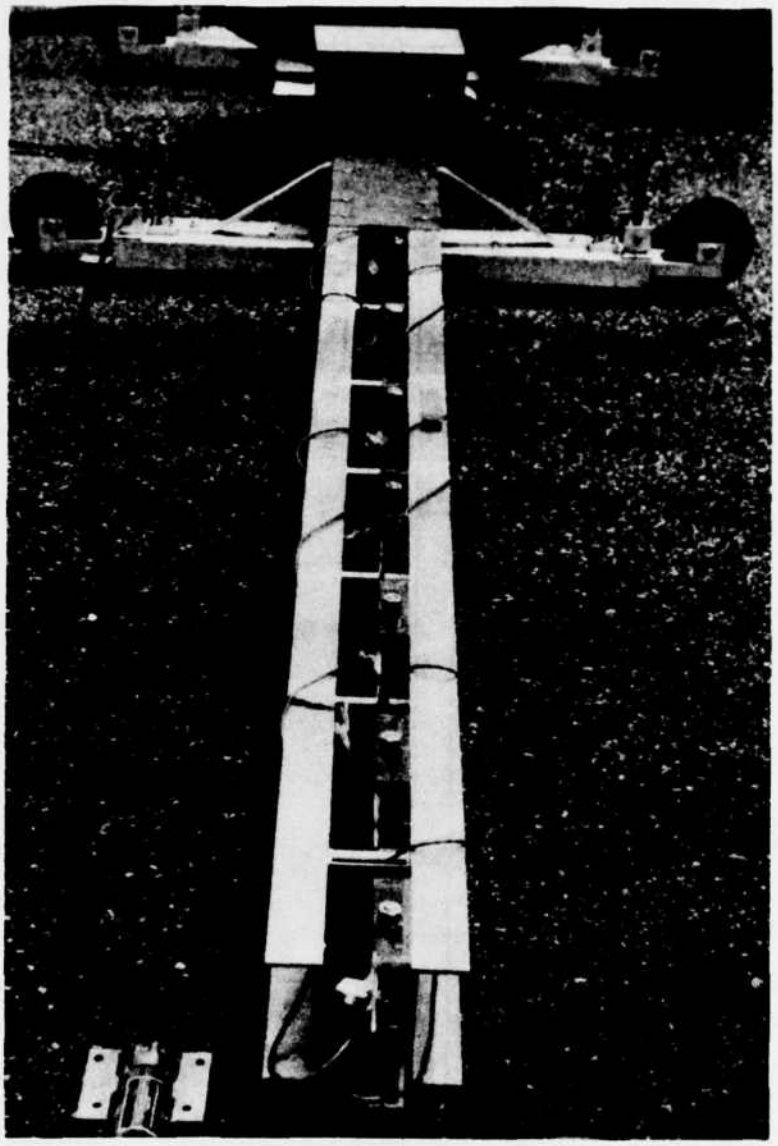


**Figure 11. LED Beam Setup**

b. Sensor Modules

Several ways of obtaining deflections using optical, non-contact techniques were considered prior to selection of the final sensor. These methods can be categorized under two general classes; namely, point methods and global methods. The point methods considered were focal point displacement, beam triangulation, retro-reflector beam displacement methods, diffraction gages, interferometers, Moire gages and grating gages. The global techniques considered were holography and Moire contour techniques.

The technique selected for development was the beam triangulation method, using a light emitting diode as the coherent light source. Figure 12 shows the basic geometrical optics of the beam triangulation method. Basically, pavement deflection is measured by the amount of displacement of the reflected light impinging on the collector lens. Research has established that a line of light impinging on the surface of small chips of various materials, asphalt, concrete, and sand paper, produces a reflected signal that can be normalized to produce a linear position measurement independent of surface reflectivity. The sensors have a range of 0.2 in and an accuracy of 0.0005 in. Figure 13 shows a complete sensor module ready for mounting on the beam. Additional details are given in Appendix A.

c. The Recording System

Signals from the sensors are collected on a magnetic tape unit. Figure 14 shows the recorder[4] used during this investigation. Figure 15

[4]A light beam recorder was also used in some special tests.

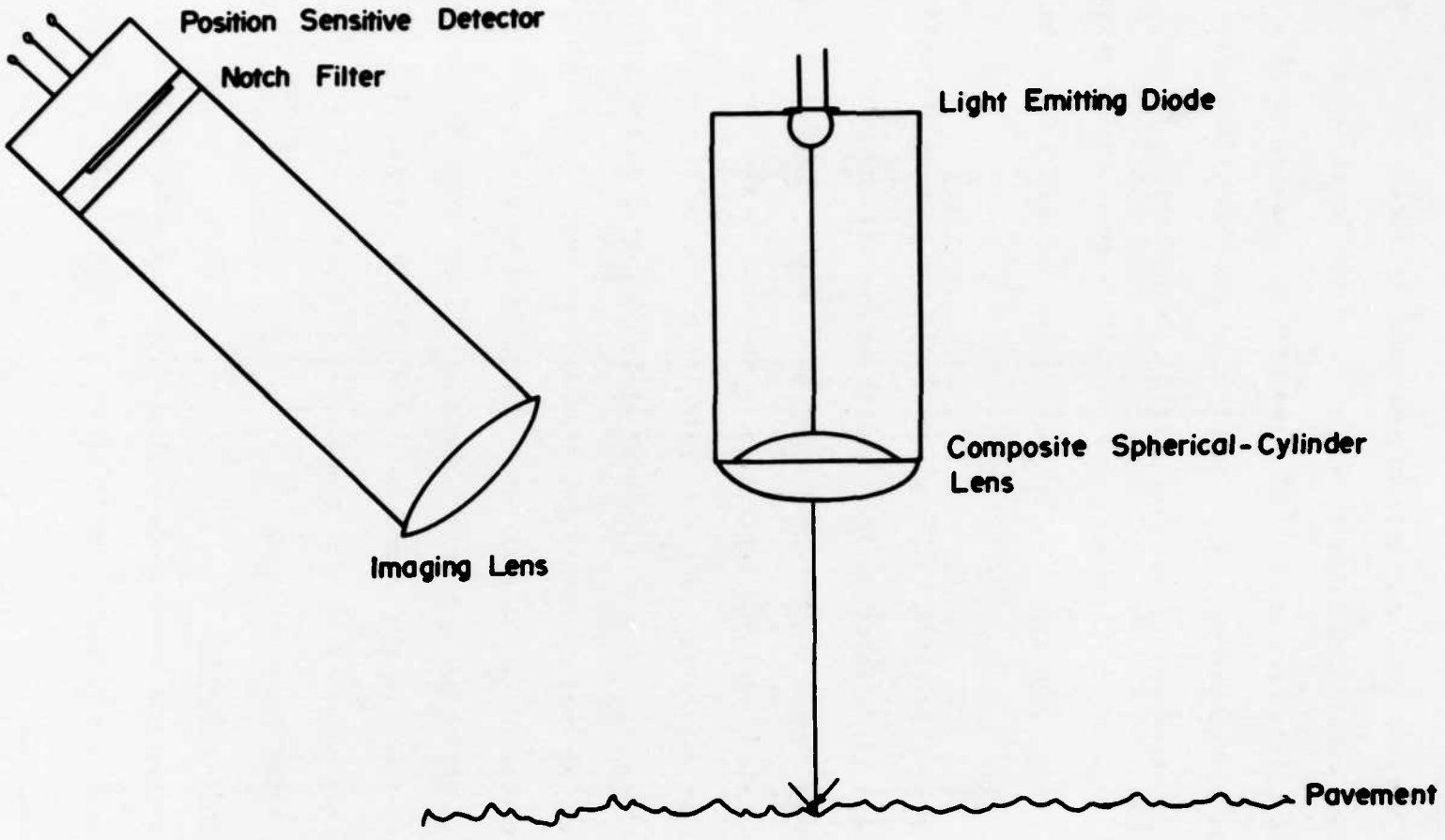



Figure 12. Light Emitting Diode Triangulation Arrangement

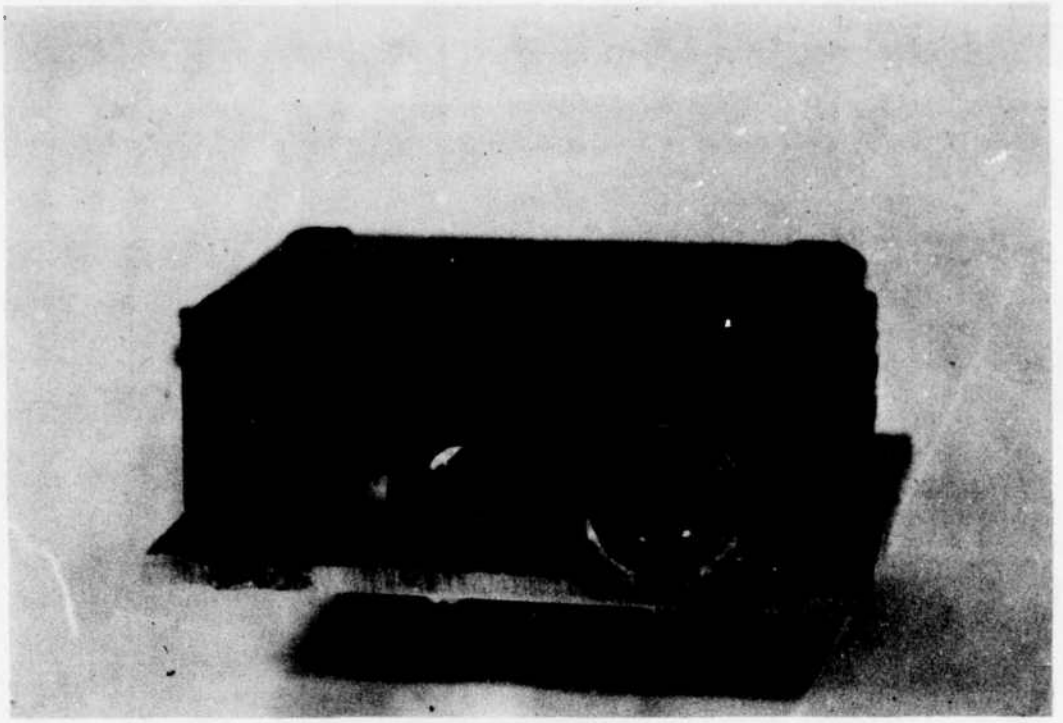


Figure 13. Typical LED Sensor Module

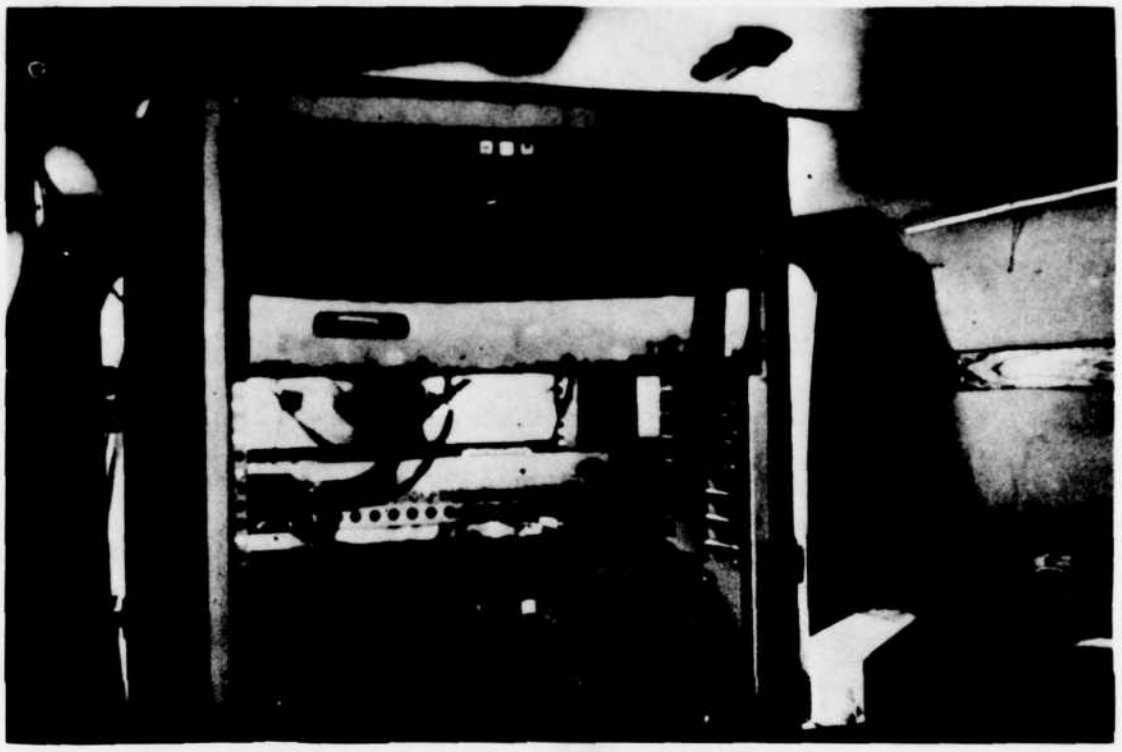


Figure 14. Magnetic Tape Recording Equipment

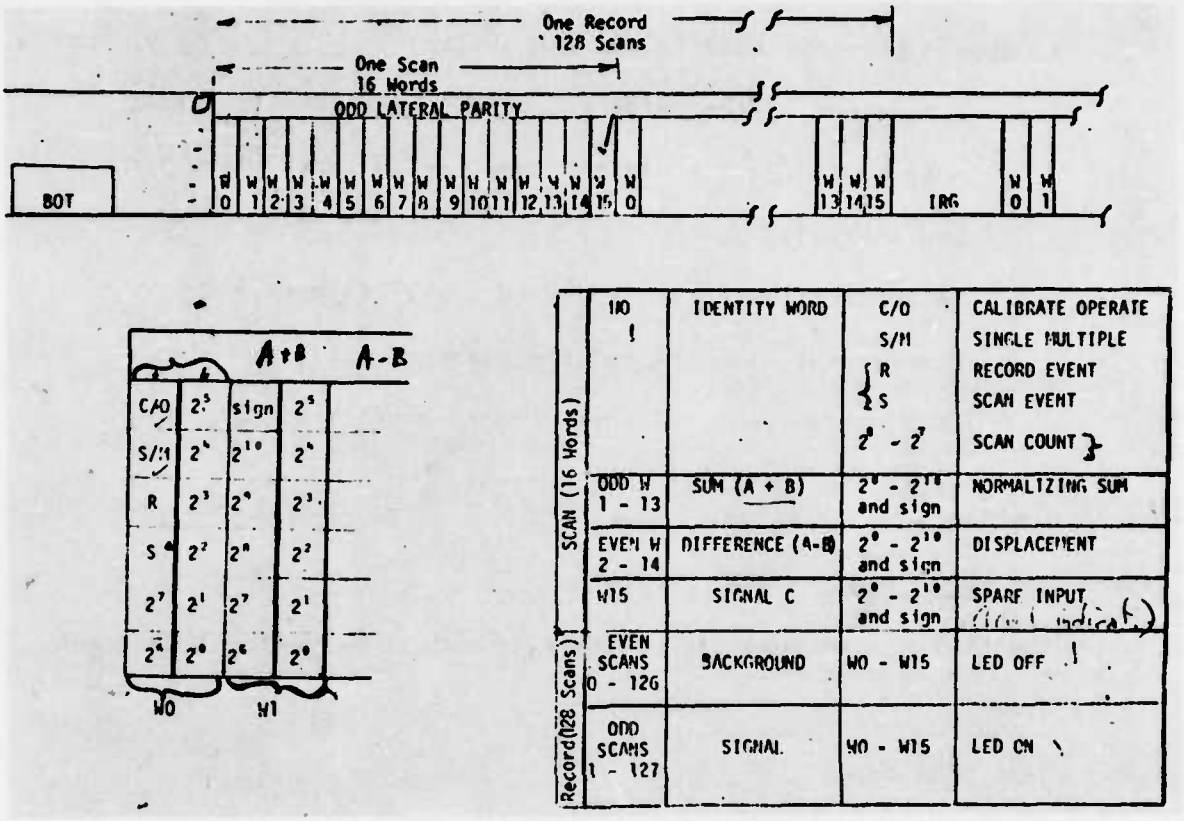



Figure 15. Arrangement of Data on Magnetic Tape (After Murphy [Reference 56])

demonstrates the basic arrangement of the data on the tape. Additional details on the tape decoding and data reduction computer programs are presented in Appendix C.

It should be noted that in the LED system:

1. The output, after being recorded on the magnetic tape, must be fed into a digital computer for data reduction and analysis, and
2. No contact (excepting infrared light) is made between the sensing elements and the pavement surface. The LVDT system required some (minor) contact within the deflection basin of the pavement.

## 4.2 The LVDT System

The LVDT system consists of three principal operational sections. They are:

a. the beam
b. the sensor elements
c. the recording system

### a. The Beam

The beam is a modified wide flange aluminum I-beam. Its dimensions and principal features are shown schematically in Figure 16. A picture of the beam, set up in position for measurements, is shown in Figure 17.

### b. The Sensors

The sensors are LVDT's. These are fixed on the beam as shown in Figure 17, with the sensing elements in contact, through adjustable jacks, with the pavement surface. The relative movement between the

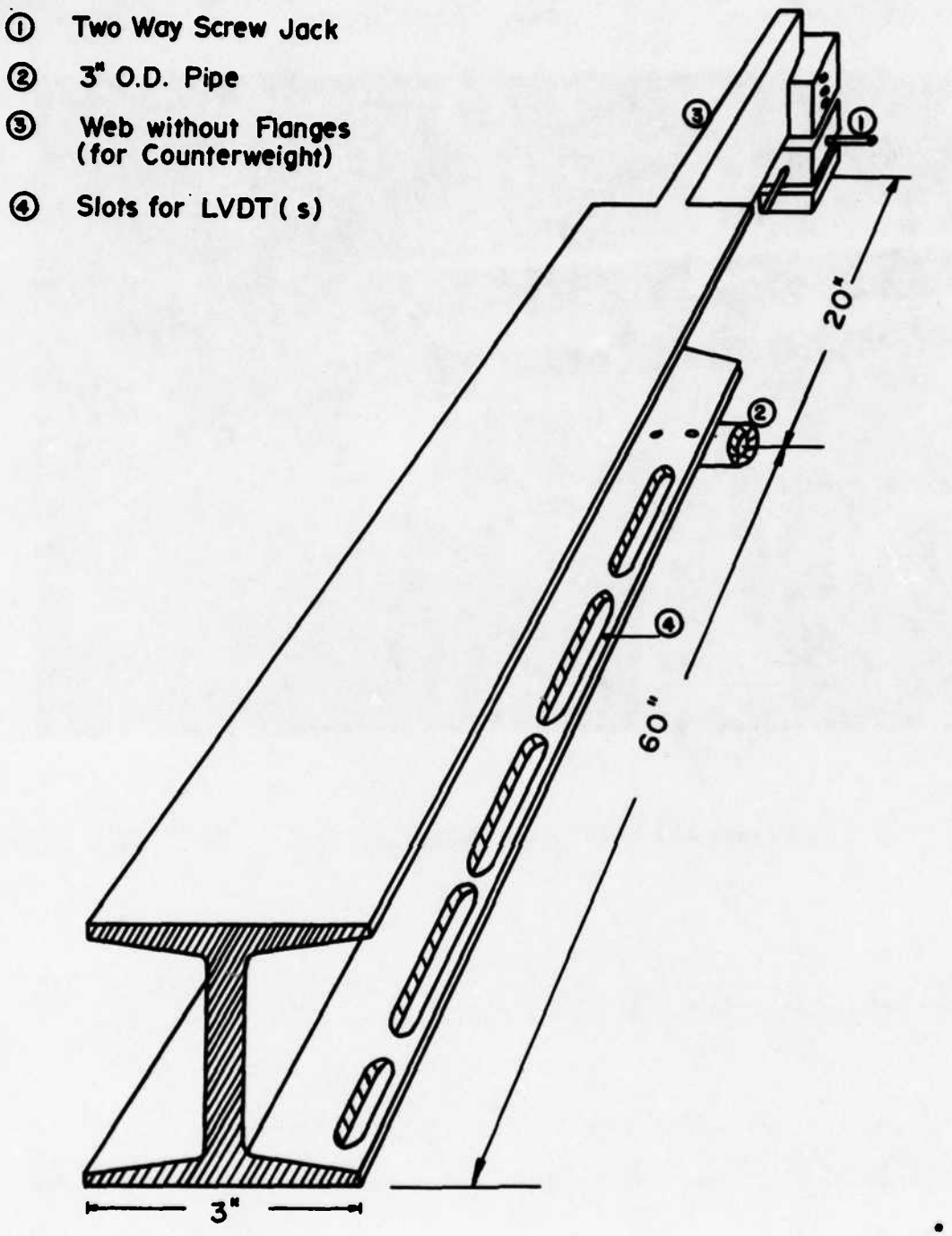



Figure 16. LVDT Beam Schematic Details

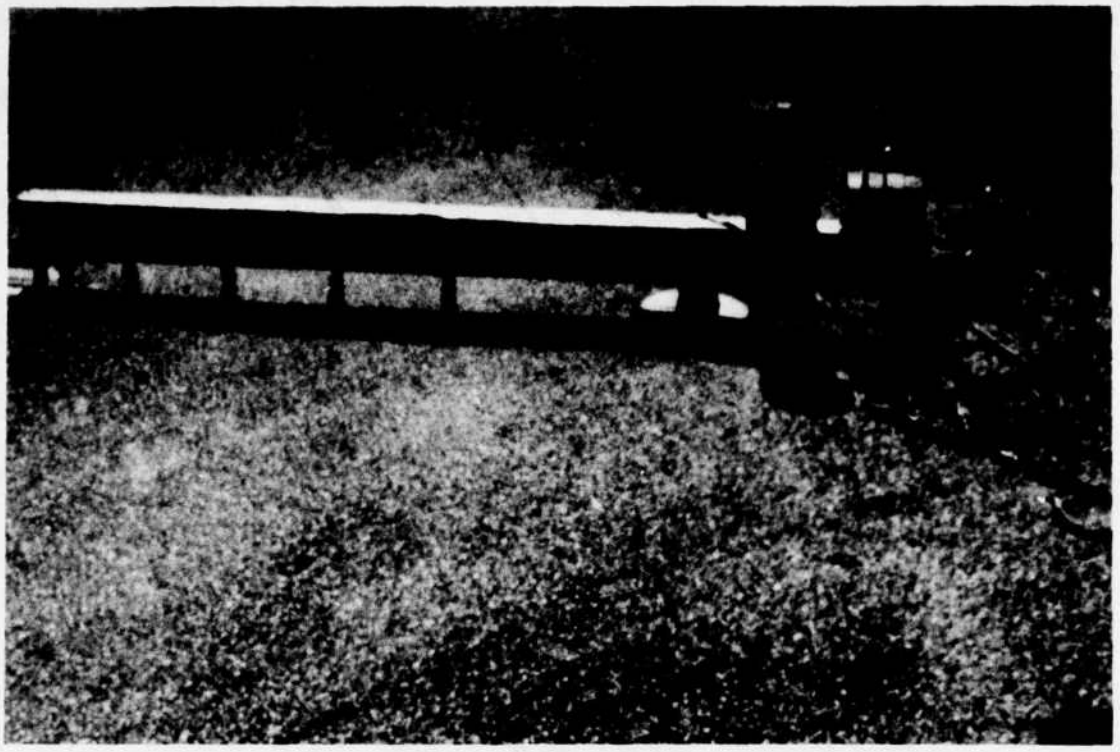


Figure 17. LVDT Beam Setup

core of the sensing element and the induction coil of the LVDT, fixed on the beam, produces a signal which is a measure of the displacement.

c. The Recording System

The LVDT recording system is a six channelled light beam recorder. Figure 18 shows the recorder used in this study. An analogue signal is recorded on light sensitive paper tape. The paper tape output can be converted to digital data by using a digitizing system (Reference 57) which automatically provides punch data cards.

It should be noted that, although the LVDT system requires contact between the pavement and the sensor, its simplicity, directness of data collection and ease of operation make it very adaptable for general use.

The LVDT and the LED systems were both used at various stages of this study.

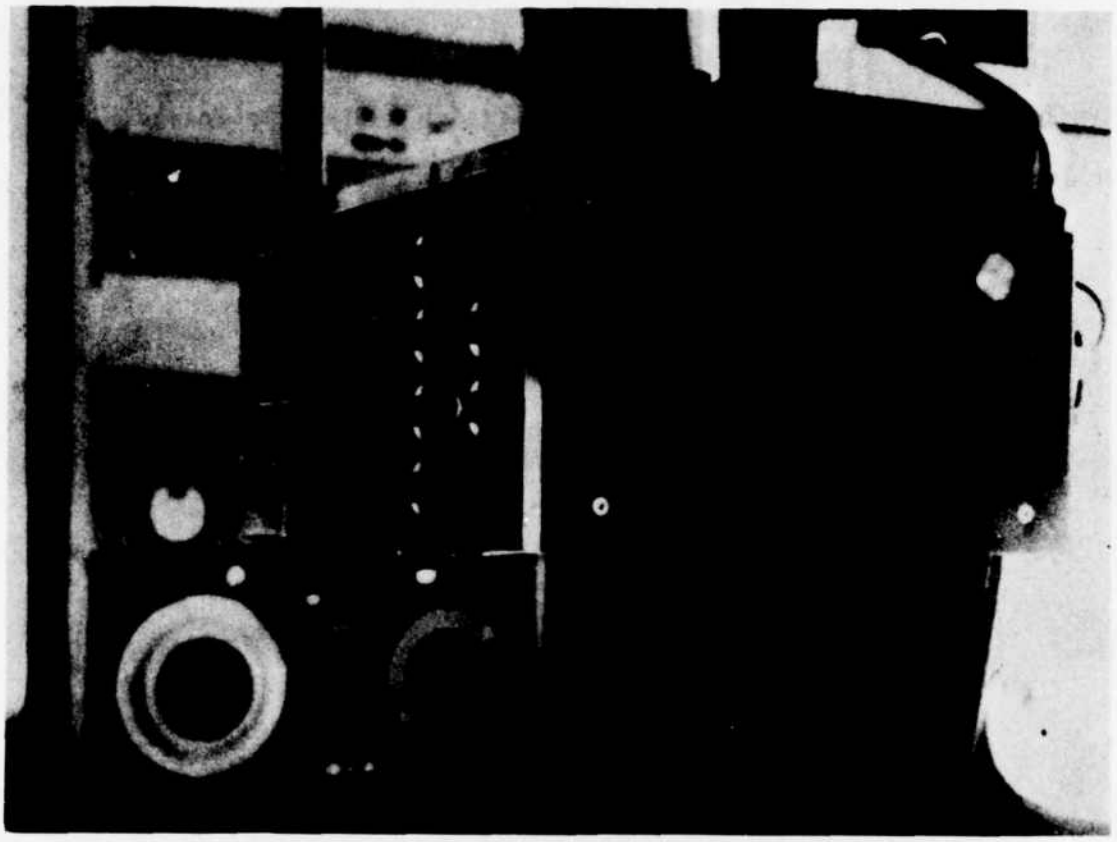


Figure 18. Project Light Beam Recorder

SECTION V

# FIELD INVESTIGATIONS

The results of two series of field investigations were used in the validation of the evaluation and prediction schemes discussed previously. The first series of field investigations, Series A, was conducted during the course of this project. The second series, Series B, had been conducted in 1972 at Kirtland AFB and the basic data were reported by Boyer (Reference 11).

## 5.1 Series A Field Investigations

The principal objectives of this series of field investigations were:

1. To verify that the new nondestructive testing equipment, i.e., LED beam (and LVDT beam), can provide measurements of pavement deflection consistent with destructive test measurements.
2. To use the NDT (nondestructive testing) equipment to obtain deflection measurements for several different vehicles at different sites, for the purposes of providing initial input into the evaluation scheme developed in conjunction with the NDT equipment.
3. To show that the evaluation and prediction schemes are consistent with the factual information currently available.

The methodology evolved over the period of this study therefore reflects the need to satisfy the principal objectives.

The basic methodology with respect to equipment development, shown in Table 2, evolved over the period of this study. As can be seen from

TABLE 2. FIELD TESTING METHODOLOGY OF DEVELOPMENT

| Stage | Method of Measuring Deflections | Features of Method | Distribution of Measurements |
|---|---|---|---|
| 1. | Gages Installed in Pavement | (a) Destructive<br>(b) Fixed | (a) Along one line |
| 2. | LVDT Beam | (a) Nondestructive<br>(b) Contact<br>(c) Stationary | (a) Along one line and/or Global |
| 3. | LED Beam | (a) Nondestructive<br>(b) Noncontact<br>(c) Stationary | (a) Along one line and/or Global |
| 4. | LED Beam | (a) Nondestructive<br>(b) Noncontact<br>(c) Moving | (a) Global |

Table 2 the method of measurement of deflections progressed in four steps from destructive fixed instrumentation, namely gages installed in the pavement, to noncontact, nondestructive instrumentation. Details of the gage installations, LVDT beam and the LED measurement systems are presented in Appendices A and B.

Deflection measurements were obtained during each step using different vehicles at different sites. The developed instrumentation was used as available for measurement purposes as shown in Figure 19. Figure 19 also shows a synopsis of the observed characteristics of the test sites, instrumentation and loading vehicles used in the Series A field investigation. Details of the sites and testing program conducted at each site during each phase are presented in Appendix B.

It should be recognized that the sites selected reflect reasonably well the extremes of the range of the airfield pavement conditions. Site 1 at Eglin AFB is a functionally failed flexible pavement and Site 2 is an in-service taxiway. The loading vehicles used also reflect a range of tire pressures using airfield pavements. The F-4 aircraft and the P-2 fire truck have tire pressures of 255 psi and 55 psi, respectively. The contrast in gross static wheel load also spans a reasonable range. The F-4 aircraft and the P-2 fire truck have gross single wheel[5] loads of approximately 25 kips and 8 kips, respectively. Figures 20 and 21 show the F-4 aircraft and the P-2 fire truck, respectively, and their pertinent characteristics. Figure 22 shows the F-4 load-cart loaded and unloaded. When loaded the central load wheel exerts a load on the pavement equivalent to a single main gear of the

[5]For the F-4, this refers to the main gear.

(a) EGLIN AFB: SITE 1

| General Site Description: Severely Cracked: used as parking area. | | |
|---|---|---|
| Date | Loading | Instrumentation |
| 5-75 | (a) P-2 Fire truck<br>(b) F-4 Aircraft | (a) Gages installed in pavement |
| 11-75 | (a) P-2 Fire truck<br>(b) F-4 Aircraft | (a) Gages installed<br>(b) LVDT Beam<br>(c) LED Beam[a] |
| 3-76 | (a) F-4 Load Cart | (a) LVDT Beam |

Figure 19. Synopsis of Series A Field Investigation

(b) EGLIN AFB: SITE 2

| General Site Description: Few cracks: in use as a taxiway | | |
|---|---|---|
| Date | Loading | Instrumentation |
| 5-75 | (a) P-2 Fire truck | (a) Gages installed |
| 11-75 | (a) P-2 Fire truck | (a) Gages installed<br>(b) LVDT Beam |
| 3-76 | (a) F-4 Load Cart | (a) LVDT Beam |

Figure 19. (Continued)

(c) PEASE AFB

| General Site Description: Uncracked in-service runway: Rutted by several passes of KC-135A Aircraft and P-2 Fire truck | | |
|---|---|---|
| Date | Loading | Instrumentation |
| 7-75 | (a) P-2 Fire truck<br>(b) KC-135A Aircraft | LVDT Beam |

(d) EGLIN AFB: TAXIWAY

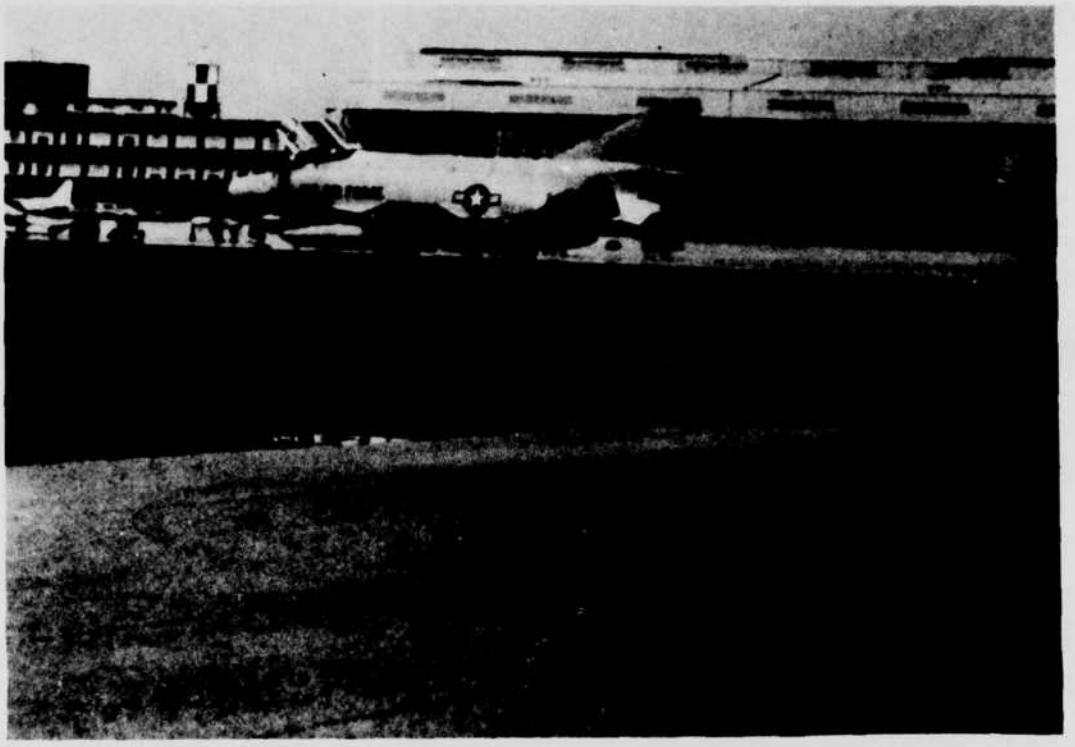
| General Site Description: Cracked not-in service taxiway | | |
|---|---|---|
| Date | Loading | Instrumentation |
| 6-76[b] | F-4 Load Cart | (a) LED Beam[c]<br>(b) LVDT Beam |

a Stationary Beam - Moving Load operation

b 6000 feet of runway were also tested on this date.

c Moving Beam - Moving Load operation

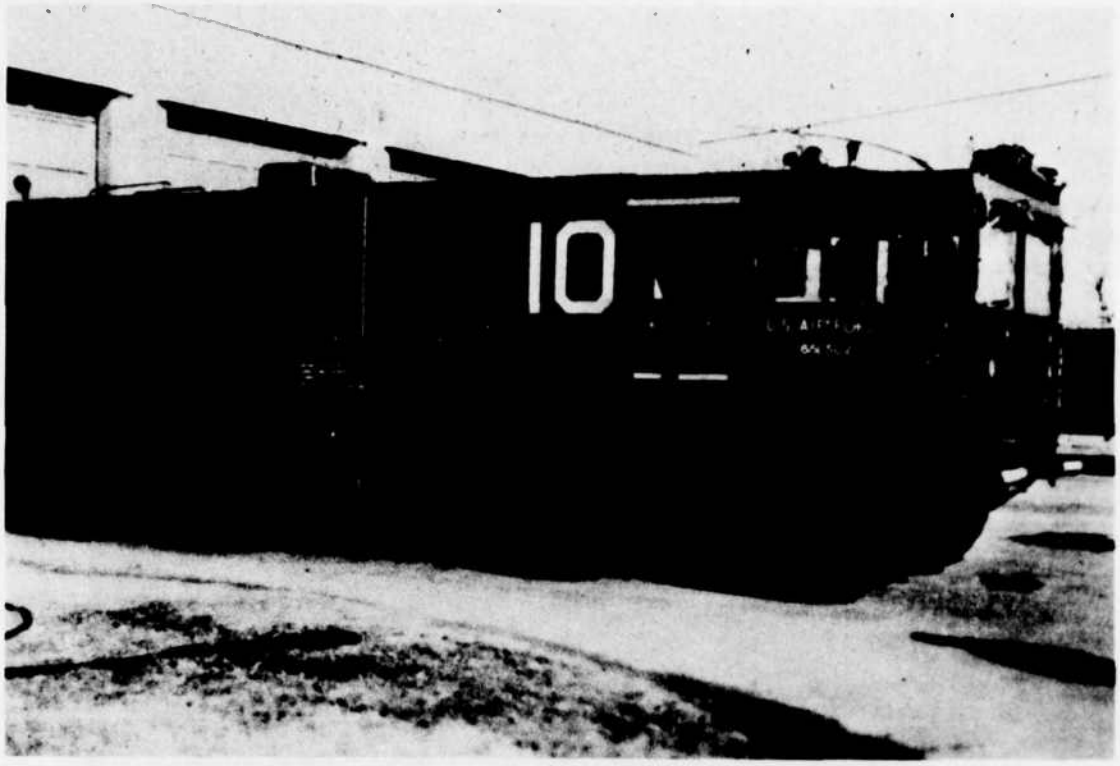
Figure 19. (Concluded)

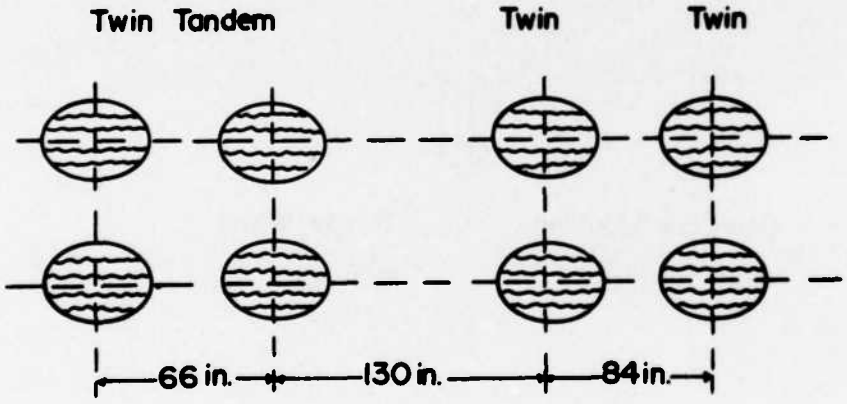




| | |
|---|---|
| Gear Configuration | Single Wheel |
| Test Weight | 25 Kips |

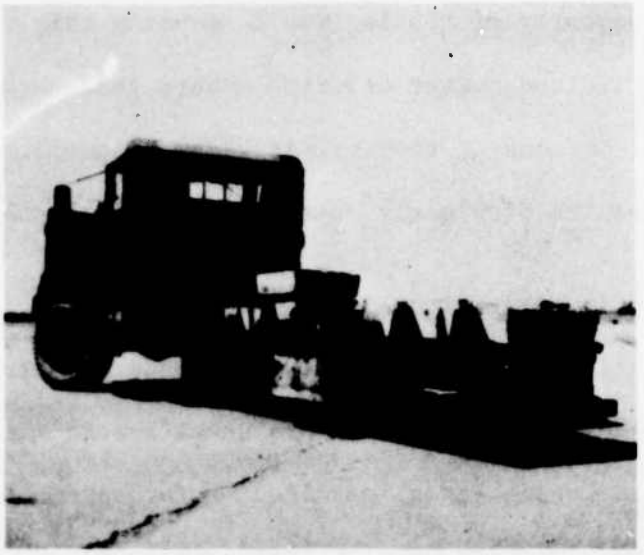
Figure 20. F-4 Aircraft and Pertinent Characteristics




STD. TEST WEIGHT 66,000 lb

Figure 21. P-2 Fire Truck and Pertinent Characteristics



(a) Loaded



(b) Unloaded

Figure 22. F-4 Load Cart

F-4 aircraft. The majority of testing was done using this vehicle.

Because of the limited number of prime movers that were made available during the periods of testing, it became necessary to utilize some test results previously reported by Boyer (Reference 11).

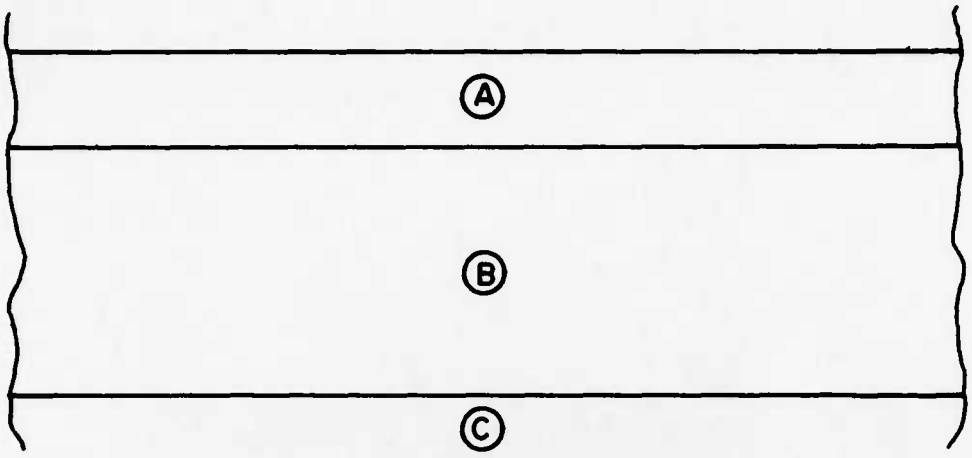
## 5.2 Series B Field Investigations

The field investigations in Series B were conducted by Boyer at Kirtland AFB in New Mexico in 1972. In his investigation deflection measurements were made using gages installed in the pavement in a manner similar to the procedure used in the Series A field investigations. For details on his instrumentation and methodology the reader should refer to the original reference (Reference 11). The pavement characteristics at the three sites reported are shown in Figure 23. The prime movers and their characteristics are shown in Figures 24 through 26.

As previously stated the series B data provide additional information required to test the evaluation and prediction schemes. The gear configuration of the C-130, C-135 and C-131 provide, in addition to a variation in gross load and tire pressures, a loading function due to multiple and sequential wheel loads, and combinations thereof. The C-131 (single-twin) is an example of a multiple but not sequential loading function. The C-130 (single-tandem) is an example of a sequential[6] but partially multiple, loading function. The C-135 (twin-tandem) is an example of sequential and a multiple loading

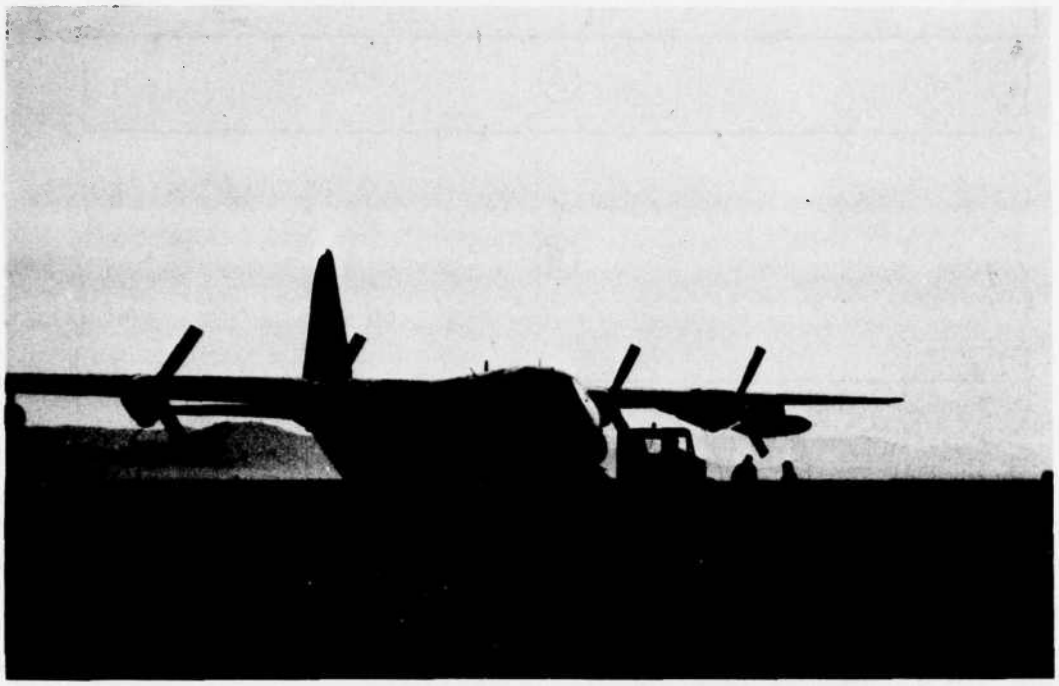
---

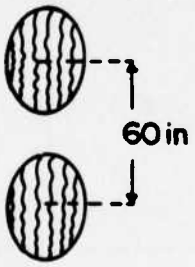
[6] The P-2 fire truck is an example of a purely sequential loading function.




| Test Site No. | Taxiway No. | (A) Asphaltic Concrete (in) | (B) Base Course (in) | (C) Subgrade |
|---|---|---|---|---|
| 1 | 6 | 3 | 9 | Silt / Sand |
| 2 | 2 | 6.5 | 8 | Silt / Sand |
| 3 | 8 | 10 | 6 | Highly Compacted Silt / Sand |

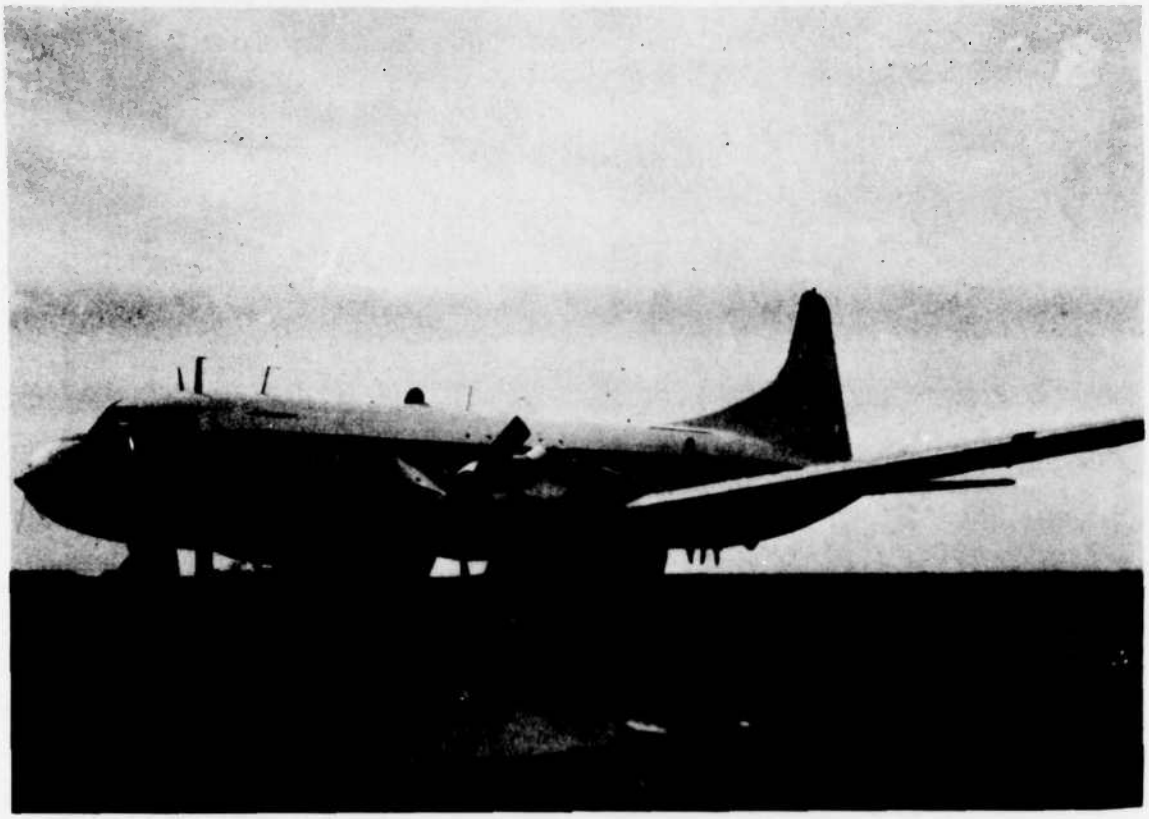
Figure 23. Site Characteristics Series B Field Investigations (Reference 11)

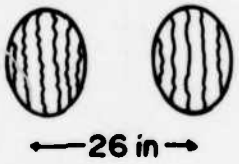





| | |
|---|---|
| Gear Configuration | Single Tandem |
| STD. Test Weight | 90 Kips (Gear load) |

Figure 24. C-130 Aircraft and Pertinent Characteristics

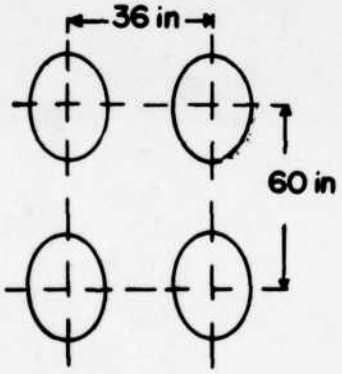





Gear Configuration — Single Twin
STD. Test Weight — 20 Kips (Gear load)

Figure 25. C-131 Aircraft and Pertinent Characteristics






Gear Configuration — Twin-Tandem
STD. Test Weight — 210 Kips (Gear load)

Figure 26. C-135 Aircraft and Pertinent Characteristics

function.

The data from the Series A and the Series B Field investigations were analyzed using the evaluation and prediction schemes previously presented.

# SECTION VI

# RESULTS

This research effort encompasses a broad spectrum of engineering activity ranging from the development of NDT equipment and a procedure for nondestructively evaluating flexible pavements, to the development of a methodology for predicting the deflection response of various pavements to different aircraft. This section presents the following:

1. typical results of equipment field verification tests,
2. results of the evaluation of the two sites (Series A: Field Investigations) using the developed evaluation scheme, and,
3. results of the application of the prediction methodology to three different aircrafts at three different sites (Series B: Field Investigations).

## 6.1 Equipment

It is necessary during the development of new equipment for measurement of pavement deflections to show that the new equipment provides measurements which are consistent with those obtained using established measurement systems. It is assumed that the LVDTs installed in the pavement comprise the absolute measurement system.

### 6.1.1 The LVDT System

The verification check of the LVDT system consisted of a comparison between pavement deflections measured by an LVDT mounted on the beam and an LVDT installed in the pavement as shown in Appendix B of this report.

Figure 27 shows a comparison of the pavement deflection measured

by an LVDT installed in the pavement and an LVDT mounted on the beam, and produced by the same pass of a P-2 fire truck during the testing sequence conducted at Eglin AFB, at Site 1 on November 17, 1975.

The results show that the installed LVDT and the LVDT mounted on the beam give basically the same measurements.

### 6.1.2 The LED System

The verification checking of the LED system consisted of two phases: a laboratory and a field testing phase.

The laboratory phase was conducted by Science Applications Incorporated, and is summarized in Appendix A of this report. The principal field checkout consisted of a comparison between the output[7] from an LED on the LED beam and the output from an LVDT mounted on the LVDT beam.

Figures 28 and 29 show the pavement deflections measured by the LED system and the LVDT system, respectively, and produced by one pass of a P-2 fire truck (Figure 21), during the testing sequence at Eglin AFB, Site 1, on November 19, 1975. Figures 30 and 31 show the actual digital output from the LED system and the analog output from the LVDT system as recorded by the light beam recorder. Since the deflections shown were measured for two separate passes of the P-2 fire truck, a direct comparison of measured deflections can not be made.

As stated previously a direct comparison of the measurements made by the two beams (LED and LVDT) could not be made since it is

---

[7] Due to persistent problems of compatibility between the LED modules and the magnetic tape recording unit, the LED output was recorded on a light beam recorder.

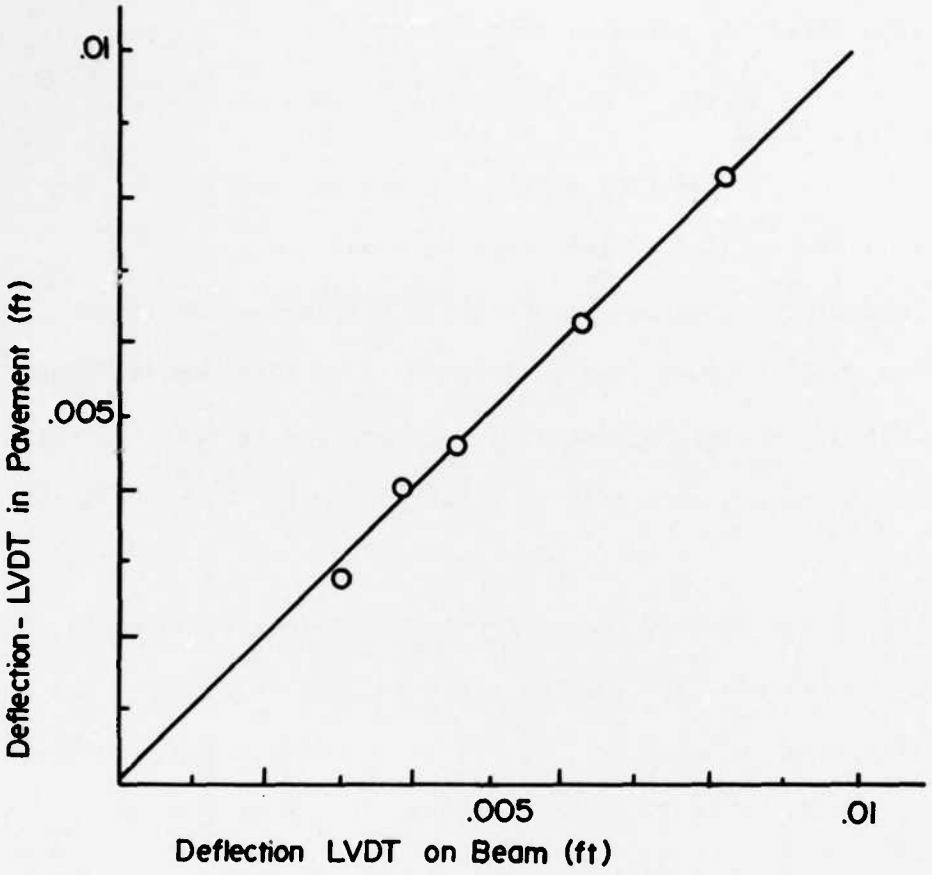



Figure 27. Comparison of LVDT on Beam and LVDT Installed in Pavement

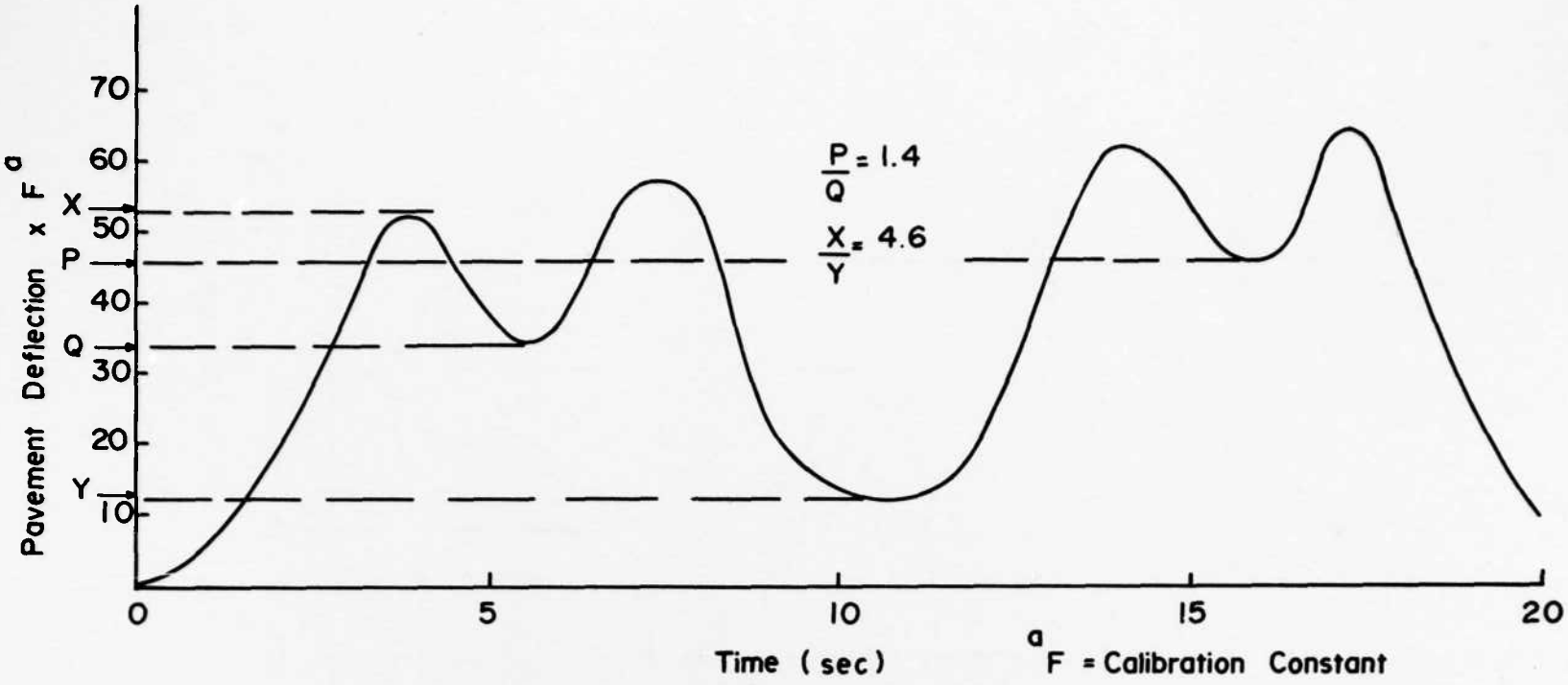



Figure 28. Pavement Deflections Measured by LED System: Eglin AFB - Site 1: P-2 Fire Truck Loading

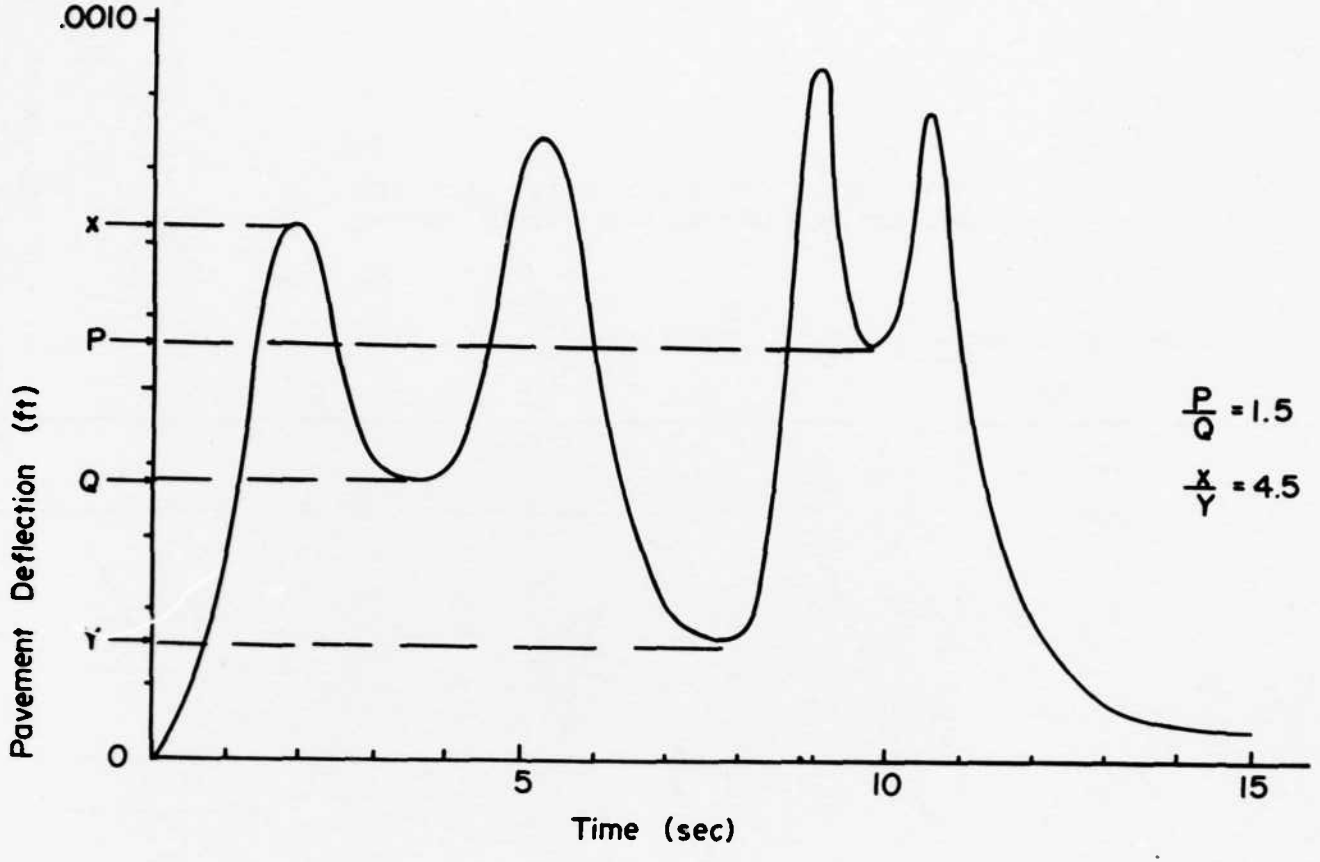



Figure 29. Pavement Deflection of Gage Closest to Edge of Wheel Measured by LVDT System: Eglin AFB - Site 1: P-2 Fire Truck Loading

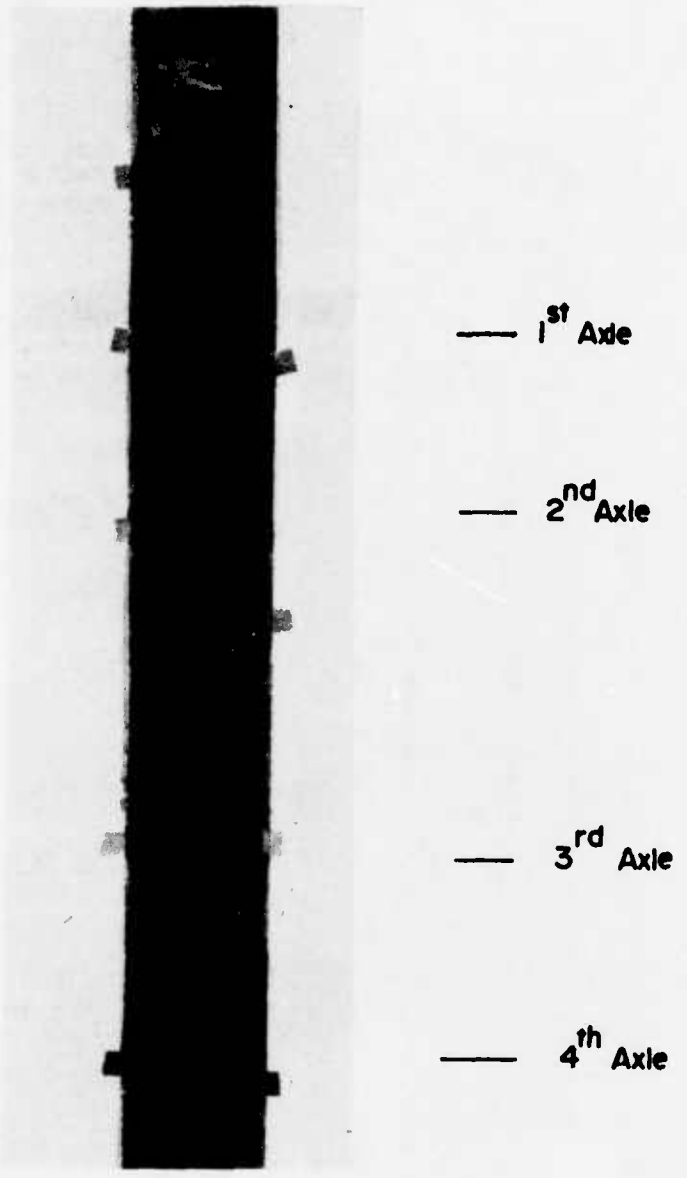



Figure 30. Actual Digital Output From LED System On Light Beam Recorder: P-2 Fire Truck Is Loading Vehicle

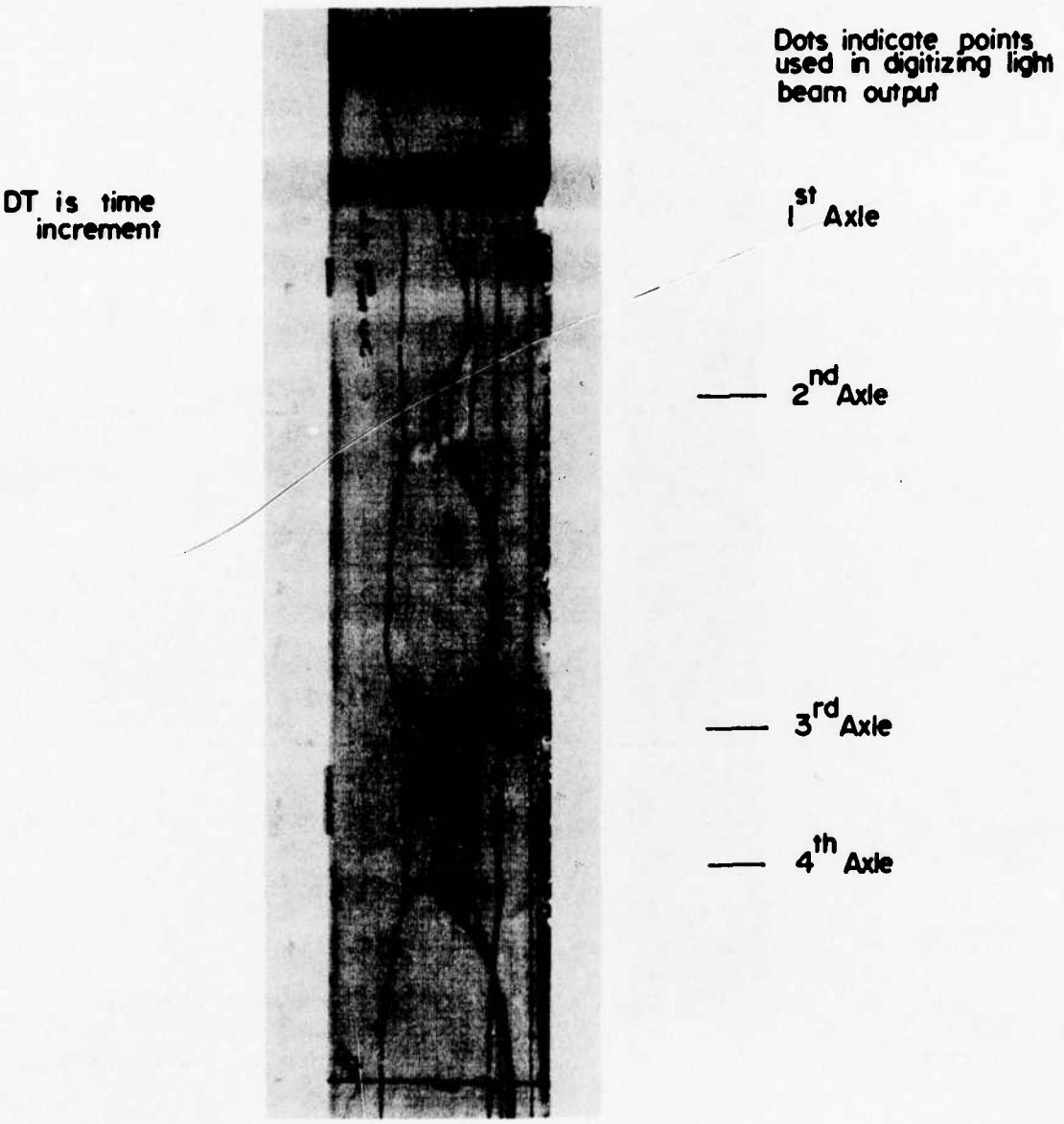



Figure 31. Analog Output From LVDT System: P-2 Fire Truck

impossible to get the two beams over the same point at the same time. Thus, a comparison was made of significant points on the measured deflection plots; e.g., peaks and troughs. The points P, Q, X and Y were selected, where P is the minimum deflection between the second two peaks of the deflection time plot; Q is the minimum deflection between the first two peaks; X is the first peak and Y is the minimum between the first two peaks and the last two peaks. The ratios P/Q and X/Y are thus dimensionless, and are independent of the system (dependent) calibration constants. That is,

$$\frac{X}{Y} = \frac{\text{Actual Light Beam Recorder Output at point X times Constant}}{\text{Actual Light Beam Recorder Output at point Y times Constant}}$$

$$= \frac{\text{Pavement Deflection corresponding to X}}{\text{Pavement Deflection corresponding to Y}}$$

Figures 28 and 29 show that the corresponding ratios have essentially the same values. Both the P/Q and the X/Y ratios differ by only 0.1.

From the discernable deflection observable at point Y in Figure 28 and Figure 29, it can be seen that measurements of less than 0.0001 feet are obtainable by both the LED and LVDT systems.

In June 1976, both the LVDT and the LED systems were used in connection with a study to investigate the difference in the dynamic response of aircraft.

A mechanical system was designed to allow the LED beam to be rigidly mounted on the F-4 load cart. The system was fabricated at Tyndall Air Force Base by Air Force personnel and was then transported to Eglin AFB. At Eglin, 2000 feet of taxiway and 1 1/4 miles of runway

were tested using the LED system attached to the F-4 load cart as shown in Figure 32. The LED measured deflections due to the load wheel of the F-4 load cart as the load cart moved at creep speeds over the pavement. LED measurements were made continuously. The LVDT system was used to make deflection measurements at stations 100 feet apart as the load cart passed in front of the stationary beam. The continuous measurements made by the LED were synchronized with the LVDT stations by the use of an electronic event marker of the LED system. The synchronization allowed the time at which the load wheel passed the LVDT stations to be recorded on the magnetic tape to within 0.25 sec as follows. At the instant the load wheel passed the LVDT station marked on the taxiway, a button was depressed on the control panel of the LED system. This caused a digital record to be made on magnetic tape. Since the scan rate was four scans per second, an event marker could be recorded to within 0.25 seconds, which constituted one scan. Figure 33 shows a summary of the taxiway deflection data. The deflections on the dashed line in Figure 33 were measured at locations offset by about 20 feet from the previous measurement locations. Listing of typical measurements[8] made by the LED system is given in Appendix D.

The results shown on Figures 28 and 29 indicate that the pavement deflection measurements with the LED system are consistent with those of the LVDT system, in form; and the LED can measure deflections with the desired accuracy in a field environment.

---

[8] The LED system data reduction software, a complete listing of all the taxiway data, and a copy of the data (on magnetic tape) has previously been supplied to the Civil Engineering Center, Tyndall AFB, Florida.

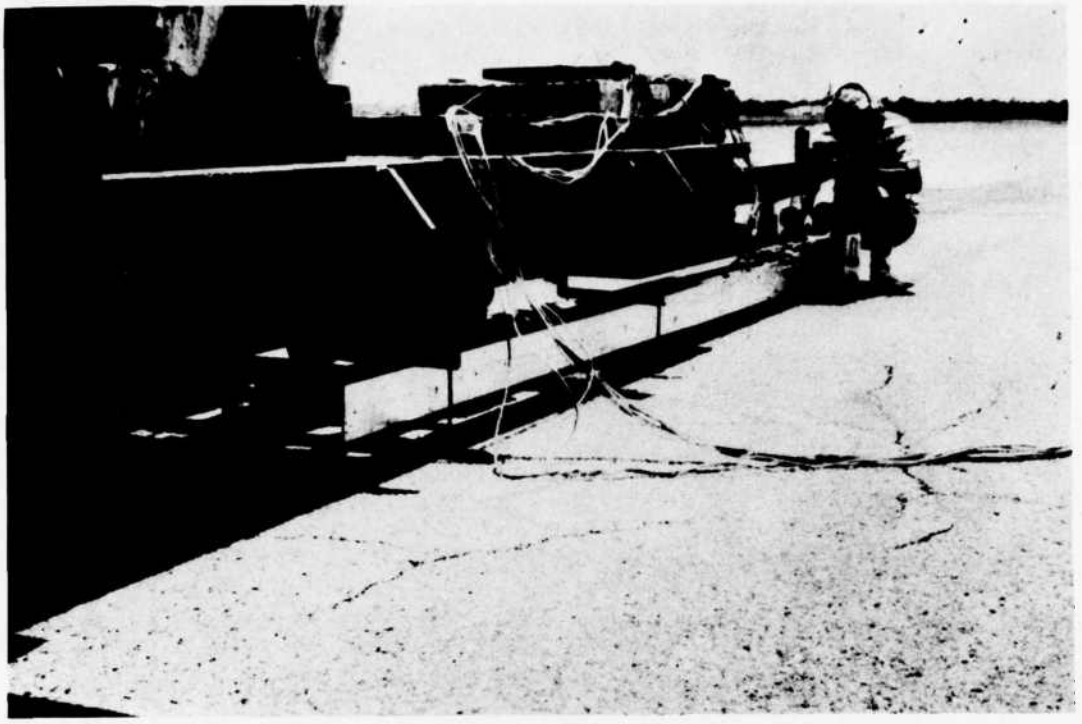


Figure 32. Setup During Moving Beam - Moving Load Operation: F-4 Load Cart

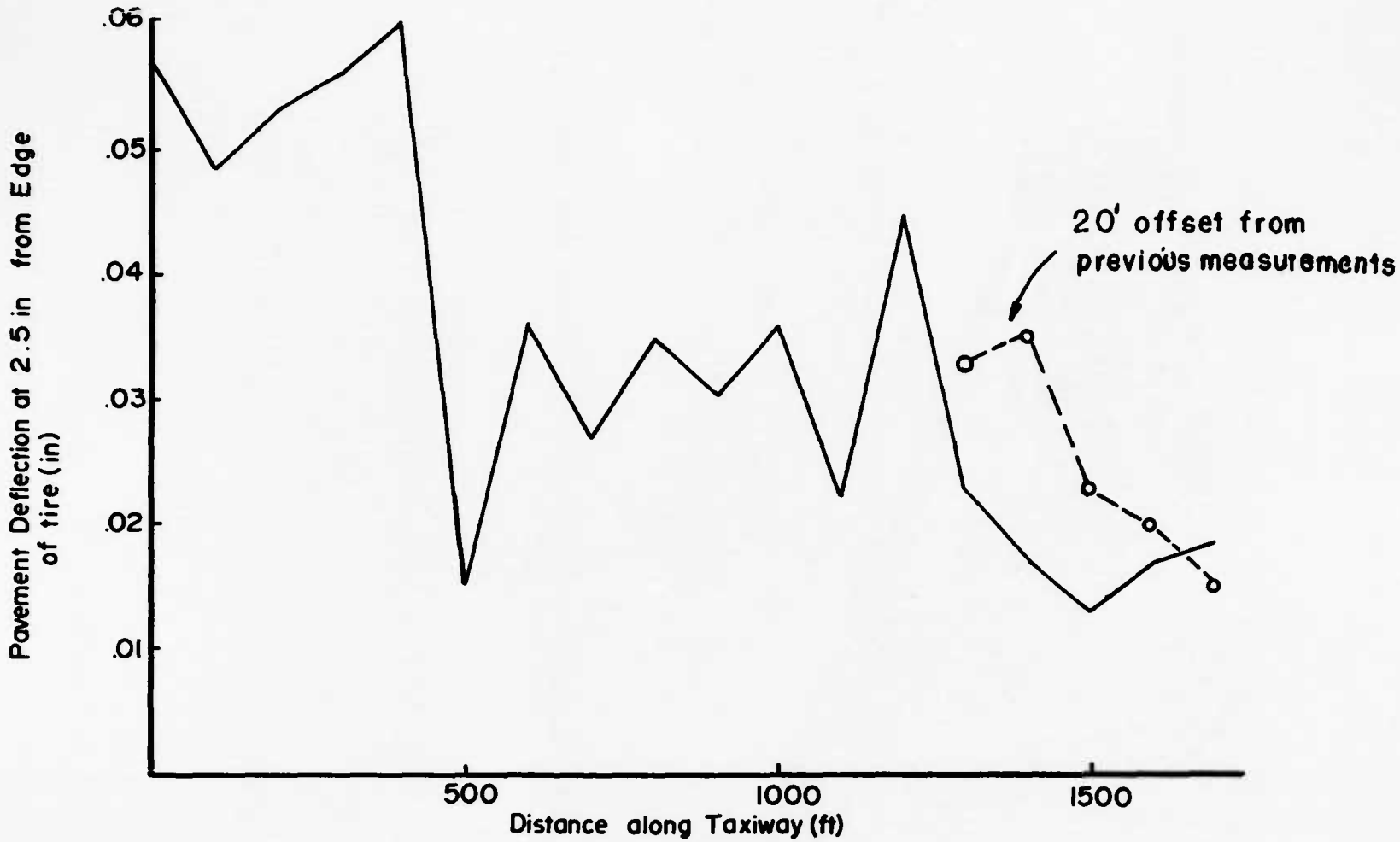



Figure 33. Summary of Taxiway Deflection Measurements-Eglin AFB 1976

## 6.2 Evaluation

Evaluation, as presented here, consists of the following:

1. determining the parameters $A_{peak}$, $\beta_{peak}$, and $r_{peak}$ of the maximum lateral deflection profile due to F-4 loadings,
2. obtaining the k, c, and m parameters of the transfer function, and
3. relating the determined parameters to performance. The two sites in Series A field investigation are compared using the data obtained during the field testing program conducted at Eglin AFB in March 1976. As the F-4 aircraft is the vehicle of primary interest in this study only the results obtained using the F-4 load cart are presented in this section. A more complete listing of the data base and results is given in Appendix D.

Briefly, the evaluation procedure consisted of measuring pavement deflections using the LVDT beam as the F-4 load cart passed in a direction perpendicular to the stationary LVDT beam. From these deflections, the parameters $A_{peak}$, $\beta_{peak}$, and $r_{peak}$ of the maximum lateral deflection profile, and the signature were determined as discussed in detail in paragraph 3.2.1. The k, c, and m parameters at each site were then obtained using the methodology of paragraph 3.2.2.

### 6.2.1 Pavement Deflections

Figure 34 shows a typical set of deflection functions due to the F-4 load cart as measured by the LVDT beam. Gage 1, which recorded

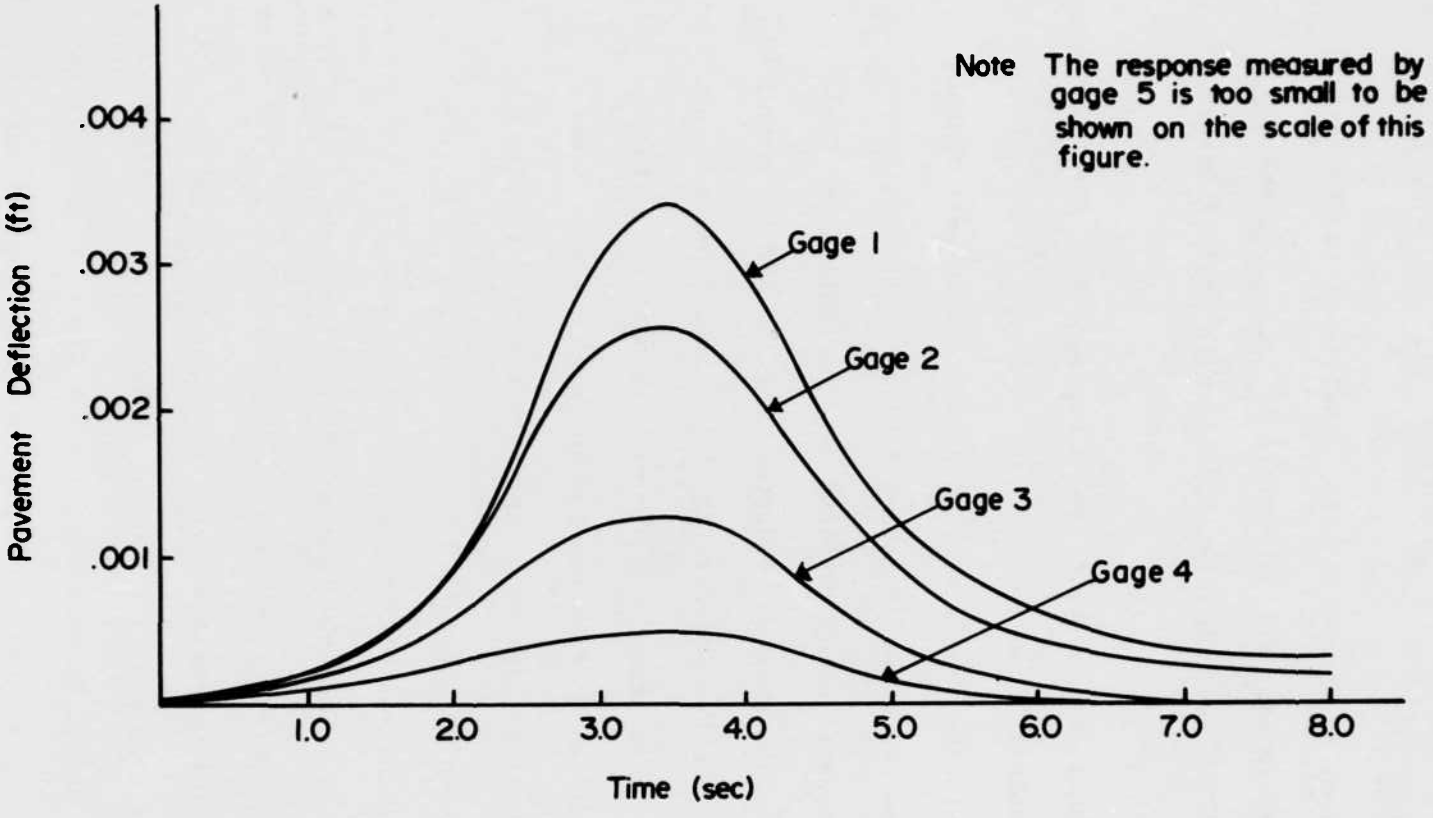



Figure 34. System Response Functions F-4 Loading: Eglin Site 1 (Typical)

the largest deflection is located closest to the wheel. Figure 35 shows the maximum deflection of each gage plotted against the distance of the gage from the edge of the tire print. The dashed line through the points G-1 through G-5 is the lateral profile of maximum deflections at Site[9] 1 for one pass of the F-4 load cart. Figure 35 also shows the $A_{peak}$, $\beta_{peak}$, and $r_{peak}$ parameters determined as discussed in paragraph 3.2.1 and the maximum deflections at each gage calculated by equation 2. Figure 36 shows a similar plot for one pass of the F-4 load cart at Site 2. Tables 3 and 4 give the stations[10] and values of the $A_{peak}$, $\beta_{peak}$, and $r_{peak}$ value for Sites 1 and 2, respectively. Figures 37 and 38 show the variability in the measured maximum lateral deflection values for Sites 1 and 2, respectively. Figures 39 and 40 show a comparison of the local and site characteristics at the two sites as given by the $A_{peak}$, $\beta_{peak}$, and $r_{peak}$ values. "Local" refers to a station or location at a "site". The lines in these figures are drawn for convenience and do not represent continuity of parameter values. Figure 41 shows the typical effects of two consecutive passes on the maximum lateral pavement deflection profiles.

These results show the following:

1. The gage (Gage 1, Figure 34) closest to the wheel records the maximum deflection and retains the most permanent set after the wheel load has passed. The gage (Gage 4, Figure 34) farthest from the wheel does the opposite; namely,

---

[9] Sites are indicated in Figures B-1(a) and B-3(a).

[10] Stations are given in Appendix B, Figures B-1(b) and B-3(b).

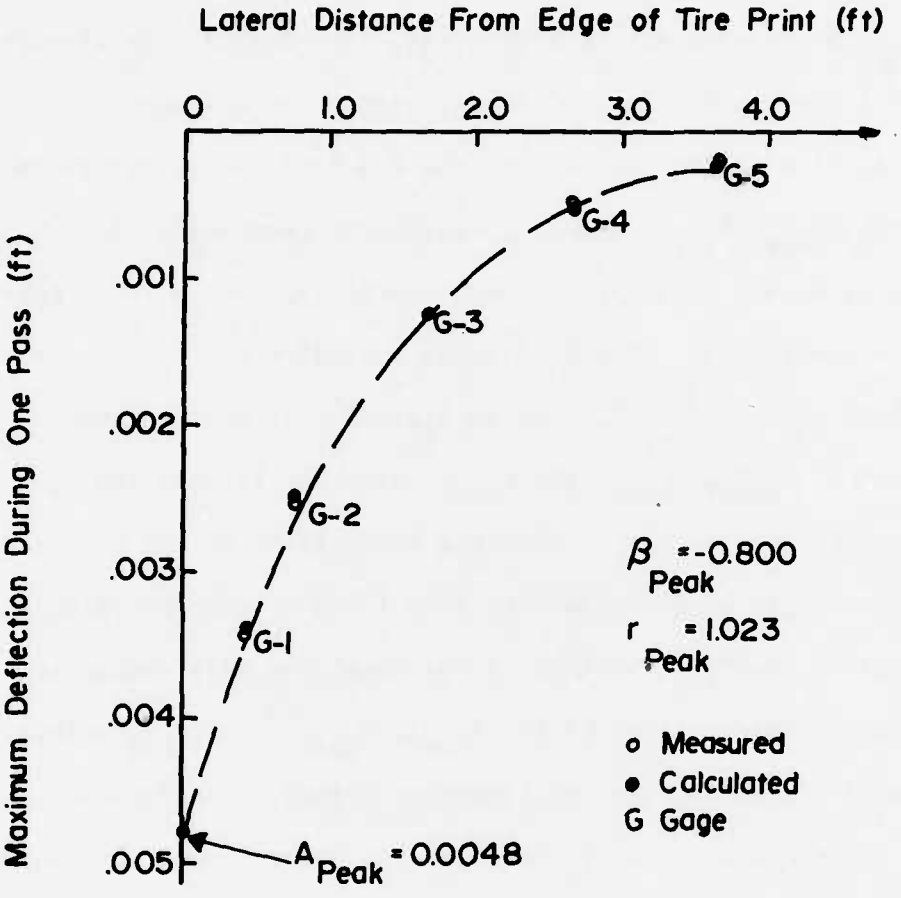



Figure 35. Eglin AFB: Site 1 Lateral Profile of Maximum Deflections for F-4 Loading (Typical)

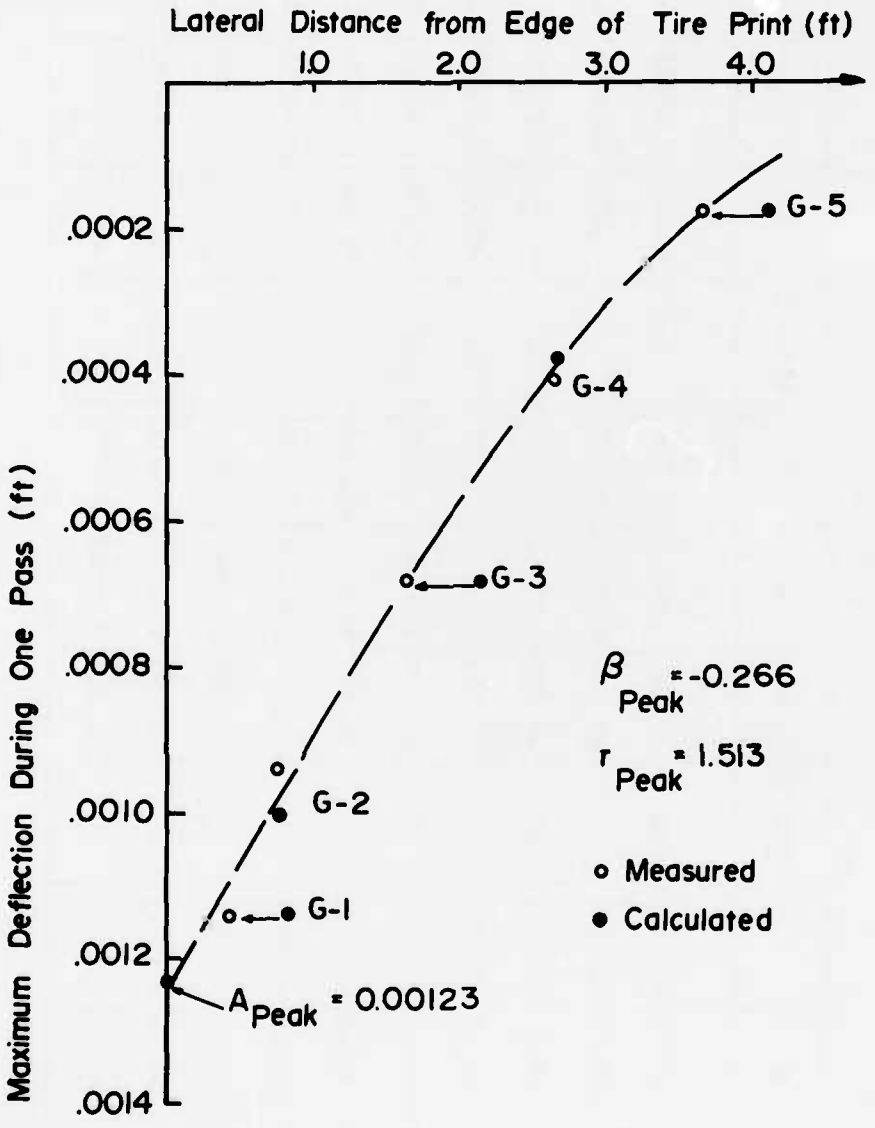



Figure 36. Eglin AFB: Site 2 Lateral Profile of Maximum Deflection for F-4 Loading (Typical)

AD-A047 161 NONCONTACT NONDESTRUCTIVE DETERMINATION OF PAVEMENT DEFLECTION UNDER MOVING LOADS(U) PURDUE RESEARCH FOUNDATION LAFAYETTE IN M E HARR ET AL AUG 77

UNCLASSIFIED FAA-RD-77-127 DOT-FA73WAI-361 F/G 13/2 NL

2/4

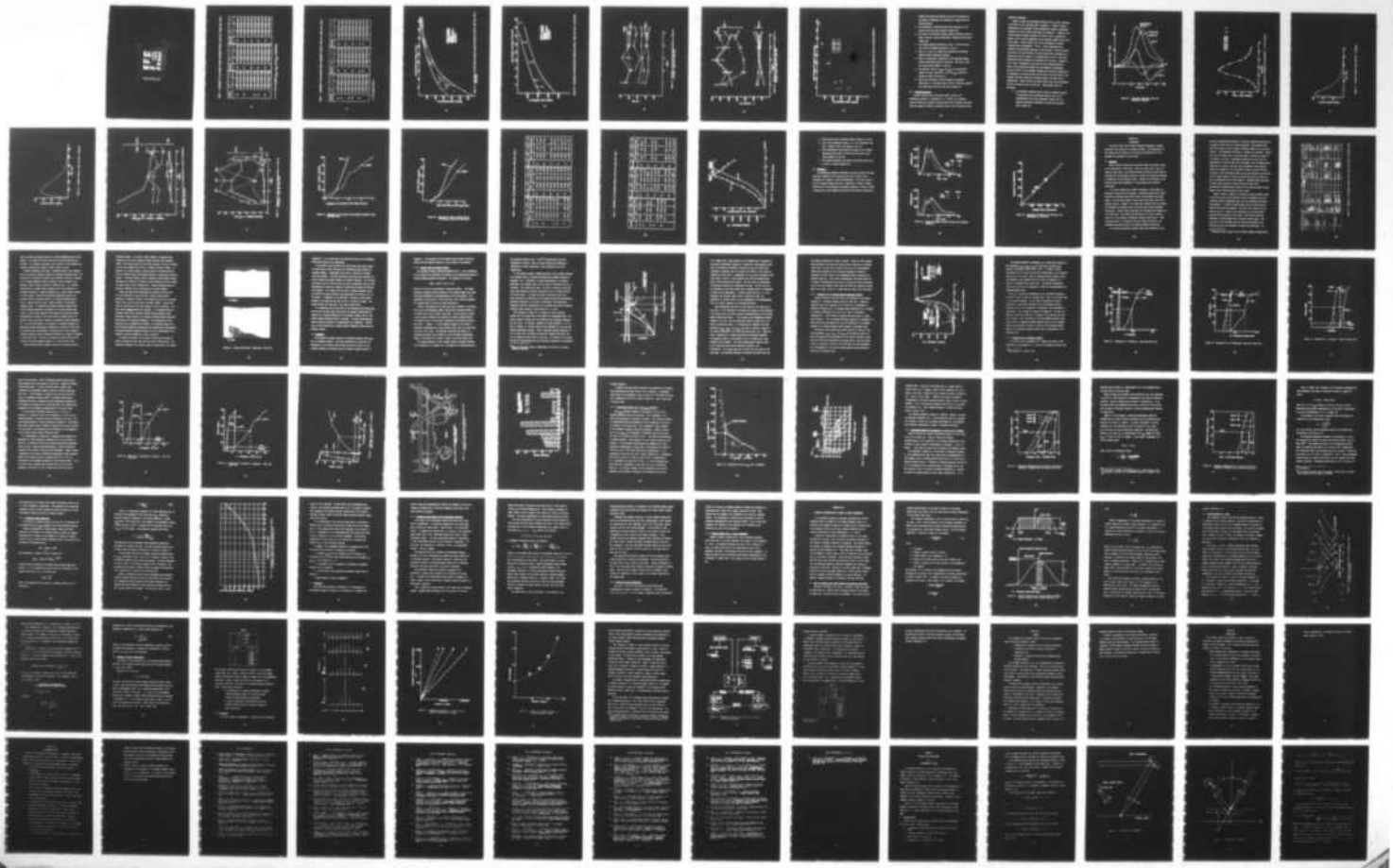
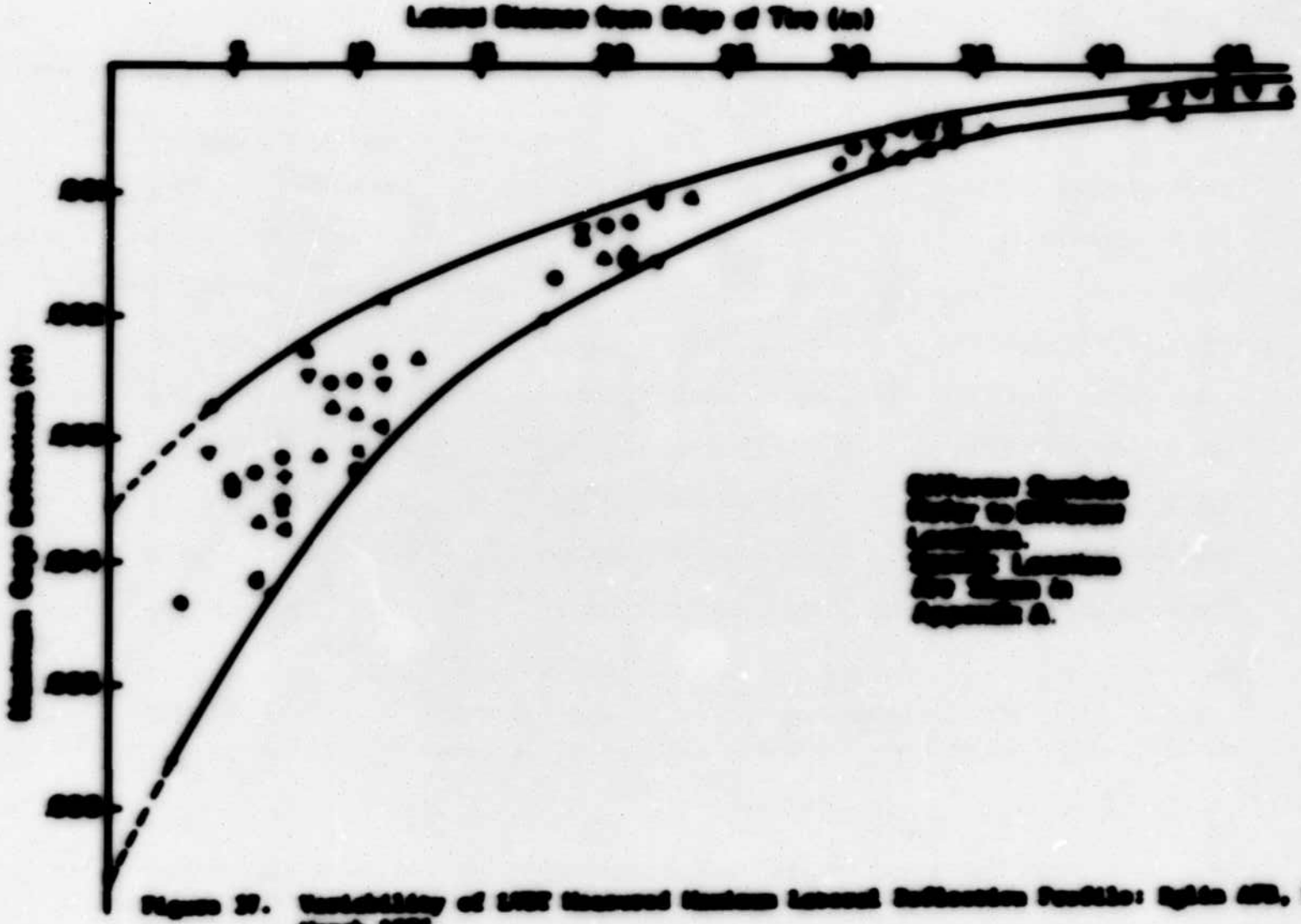


TABLE 4. PARAMETERS[a] OF THE MAXIMUM LIKELIHOOD REPLACEMENT PROFILE, EELAM AFB, WINTER 1976, STEP 2

| Position | Br | A | B | Position | Br | A | B | Position | Br | A | B |
|---|---|---|---|---|---|---|---|---|---|---|---|
| A1 | -0.440 | 0.00000 | -0.445 | B1 | -0.472 | 0.00153 | -0.265 | C1 | -0.581 | 0.00172 | -0.401 |
| A2 | -0.342 | 0.00000 | -0.224 | | -0.470 | 0.00159 | -0.270 | | -0.998 | 0.00335 | -1.109 |
| | -0.343 | 0.00001 | -0.236 | B2 | -0.477 | 0.00110 | -0.402 | C2 | -0.431 | 0.00040 | -0.201 |
| A3 | -0.341 | 0.00133 | -0.215 | | -0.519 | 0.00150 | -0.476 | | -0.582 | 0.00139 | -0.375 |
| A4 | -0.374 | 0.00140 | -0.244 | B3 | -0.568 | 0.00150 | -0.473 | C3 | -0.488 | 0.00125 | -0.296 |
| | -0.370 | 0.00126 | -0.235 | | -0.475 | 0.00104 | -0.327 | | -0.582 | 0.00135 | -0.350 |
| A5 | -0.379 | 0.00143 | -0.241 | B4 | -0.393 | 0.00114 | -0.232 | C4 | -0.550 | 0.00155 | -0.350 |
| | -0.508 | 0.00179 | -0.402 | B5 | -0.449 | 0.00150 | -0.230 | C5 | -0.727 | 0.00197 | -0.704 |
| | 0.777 | 0.00169 | -0.670 | | -0.402 | 0.00150 | -0.286 | | -0.596 | 0.00144 | -0.340 |

a) See footnote Table 3.



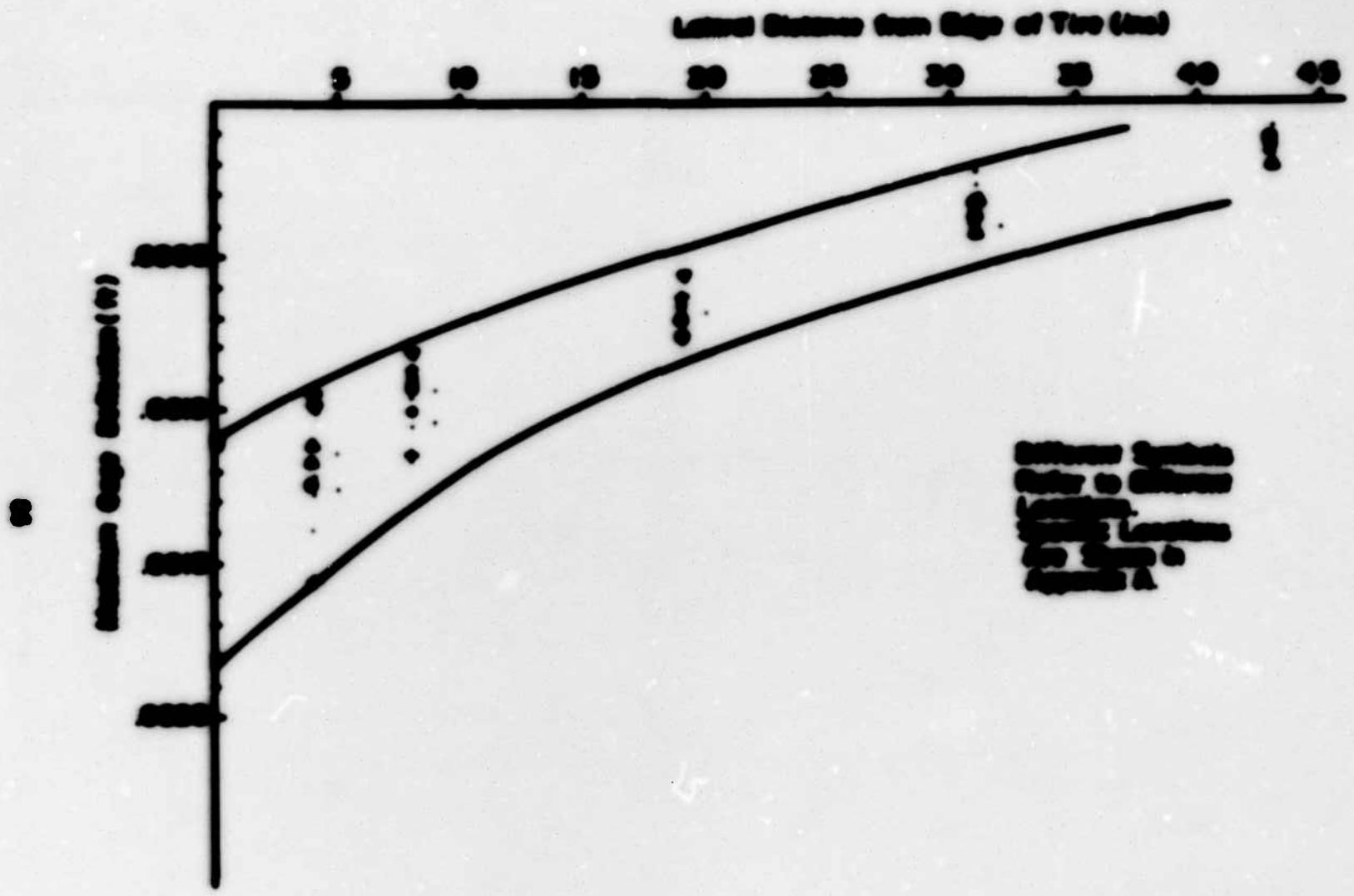



Figure 28. [illegible]

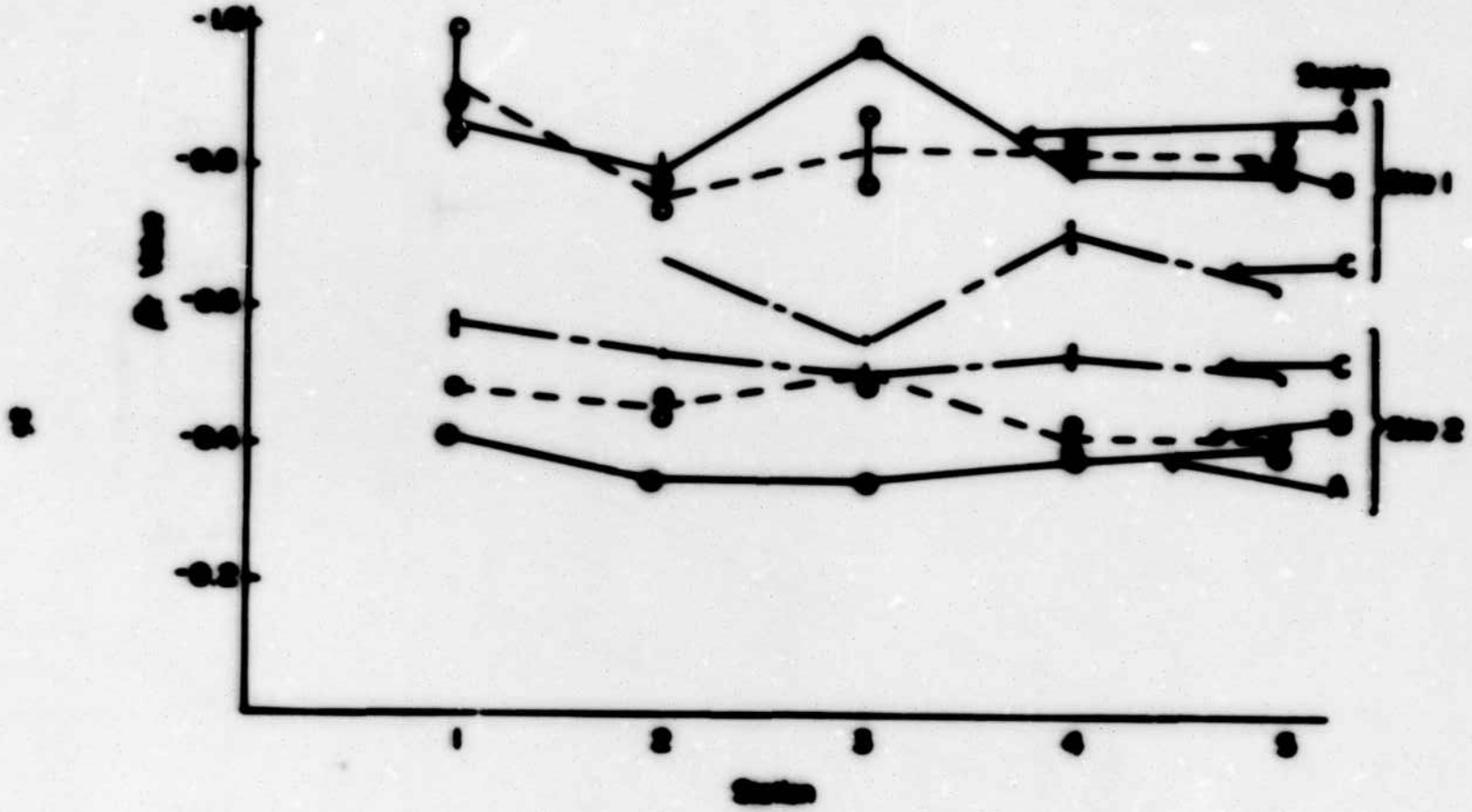


Figure 39. Comparison of Local and Site Characteristics as Shown by Sr values: Eglin AFB, March 1976

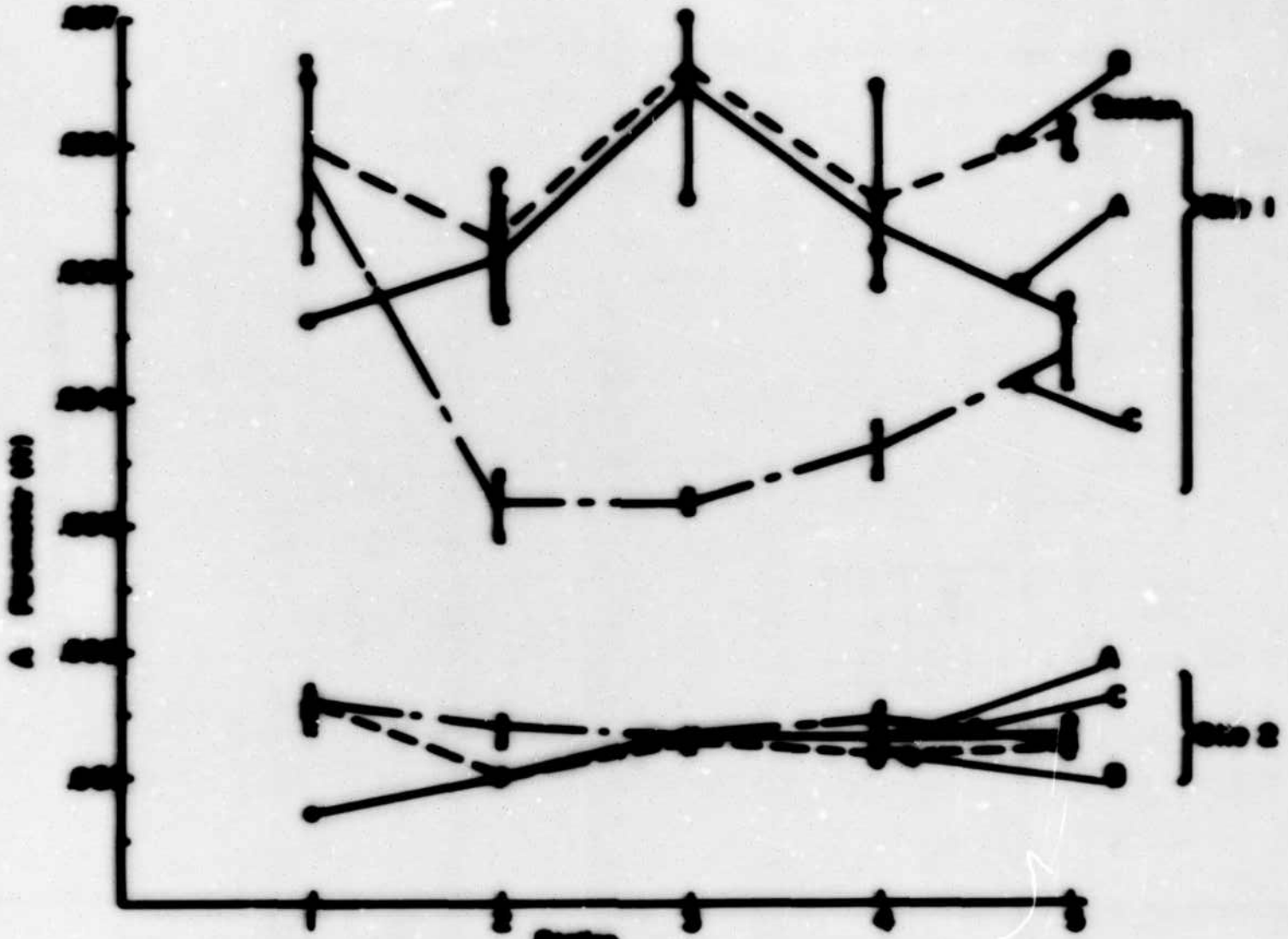




Figure 46. Effect of Tie Connection Forces on Diagonal Deflection

records the smallest deflection and shows no permanent set. The amount of permanent set increases as distance from the shoal decreases.

2. The peakedness of deflection-time plots decreases as the distance from the shoal increases (Figure 36).
3. The width of the measured maximum lateral deflection basin is about 4 feet to 5 feet for both Site 1 (Figure 35) and Site 2 (Figure 36).
4. The maximum measured deflection at Site 1 is about three to four times the maximum deflection at Site 2.
5. There is a close fit between the calculated and measured maximum lateral deflection profiles.
6. There is considerable variability in the measured maximum lateral deflection profile at both Site 1 and Site 2, over the areas tested (Figures 37 and 38).
7. The absolute values of $\tau_{peak}$ and $\delta_{peak}$ are consistently larger for Site 2 than Site 1, and the $A_{peak}$ values are smaller for Site 2 than Site 1.
8. Short term repetition of load decreases the measured deflection i.e. the second pass of the F-4 load cart produced less deflections than the first pass (Figure 41).

### 6.2.2 Transfer Functions

Transfer functions were calculated using the theory and methodology presented in paragraph 3.2.2. Briefly, the procedure involved finding the transfer function which, when convoluted implicitly with the signature yielded an equivalent input, which satisfied certain

specified conditions.

Figure 42 shows the calculated equivalent force and the components of the force on the left hand side of equation 1. Figure 43 shows a comparison of the equivalent force calculated by implicit convolution (equation 15) and by direct substitution in equation 1. Figures 44 and 45 show typical transfer functions for Sites 1 and 2, respectively. Tables 5 and 6 list the parameters of the transfer function for the two sites tested. Station labels (A1, A2 etc) correspond to section locations shown in Appendix B. The k, c, and m parameters were obtained from deflections measured at each location. Where two values are given at the same section, the first listed value corresponds to a forward pass and the second, to a backward pass of the F-4 load cart. Additional entries designate the repetition of the cycle. Figures 46 and 47 show a comparison of the local and site characteristics as given by the equivalent stiffness (k) and damping (c) parameters. Figures 48 (TDT is time dependent transfer) and 49 show a comparison of the magnitude of the first peaks and the time to the first peak of the transfer functions having the parameters listed in Tables 5 and 6, respectively. Figure 50 shows the input force, F(t), and the signature s(t) for one pass of the F-4 load cart. These results show the following:

1. the numerical procedure used to find the transfer function is consistent with the developed theory, both in the determination of the force components (Figure 42), and implicit convolution techniques to obtain the equivalent force (Figure 43).

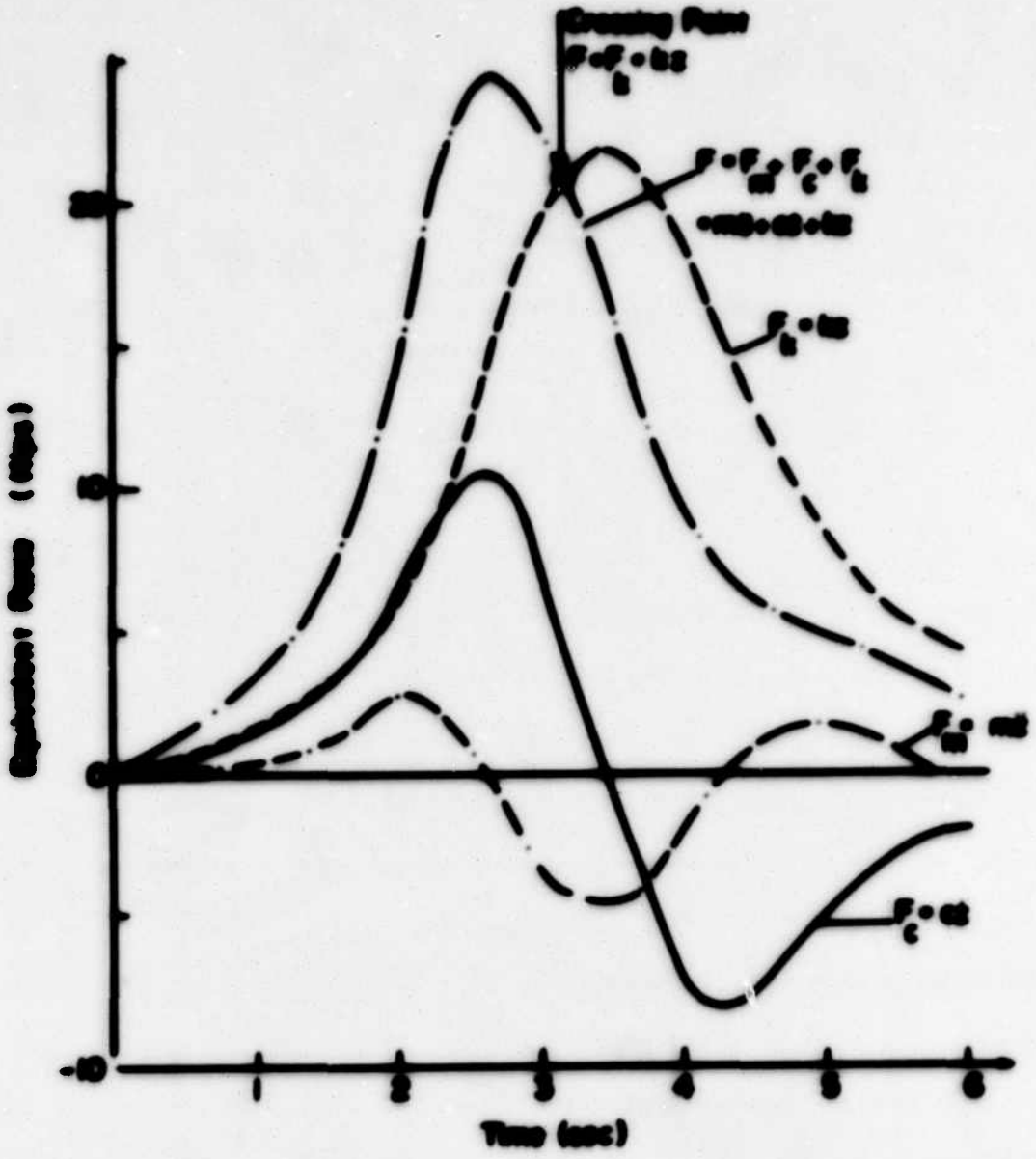



Figure 42. Calculated Equivalent Force and Components (Typical)

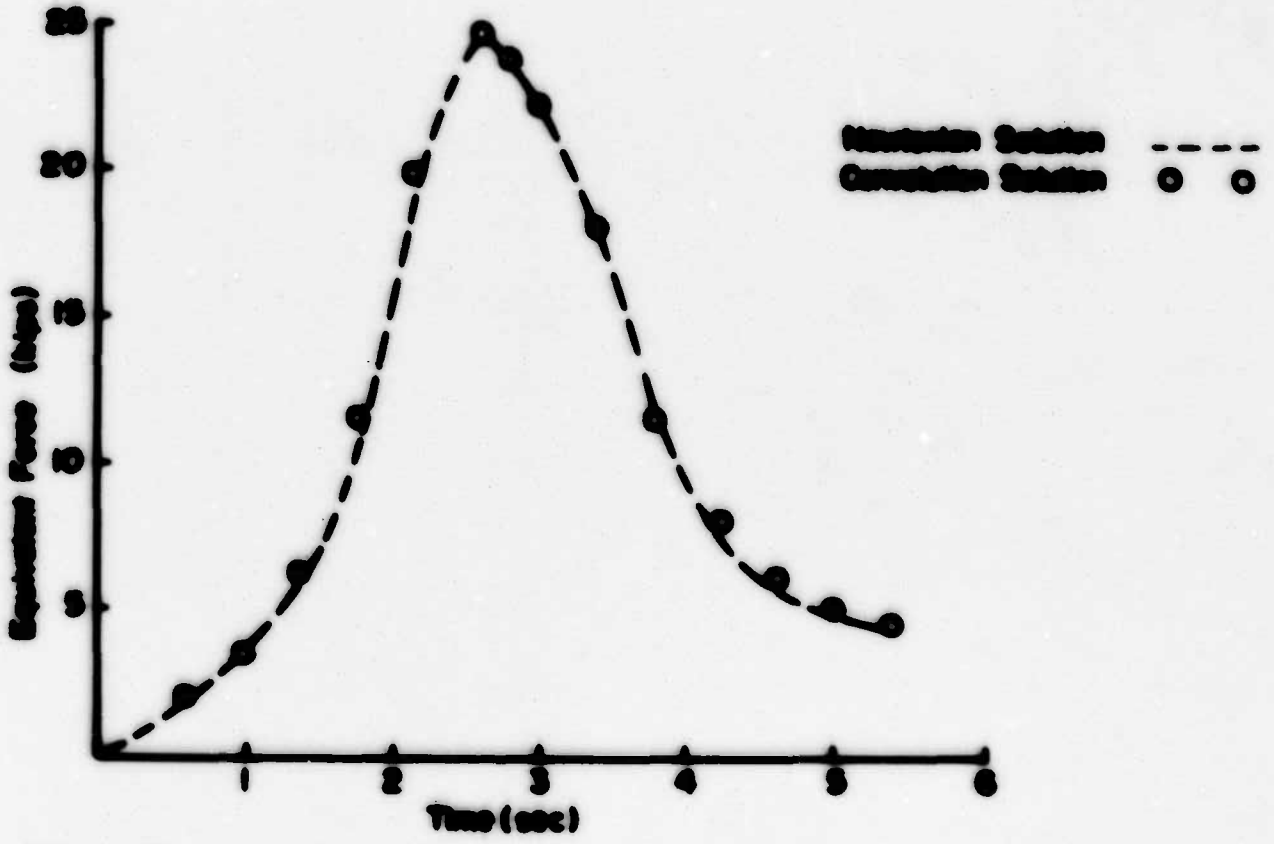



Figure 43. Comparison of Newtonian and Convolution [illegible] (Typical)

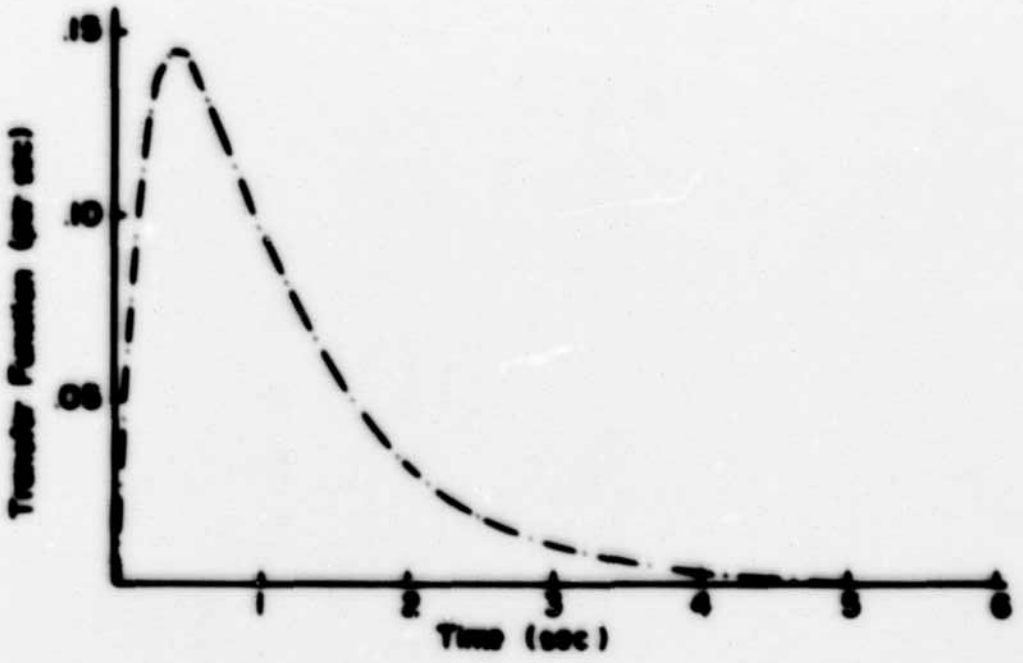



Figure 44. Transfer Function: Eglin AFB Site 1 (Typical)

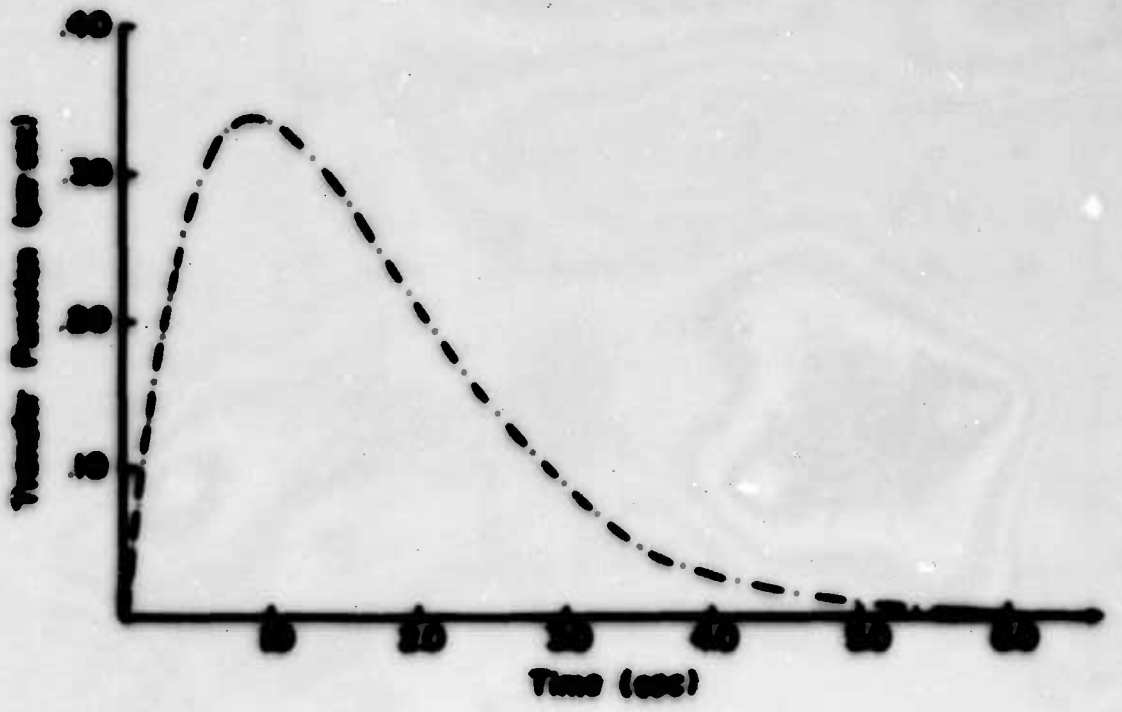



Figure 46. Transfer Function: Spin ATS Disc 2 (Typical)

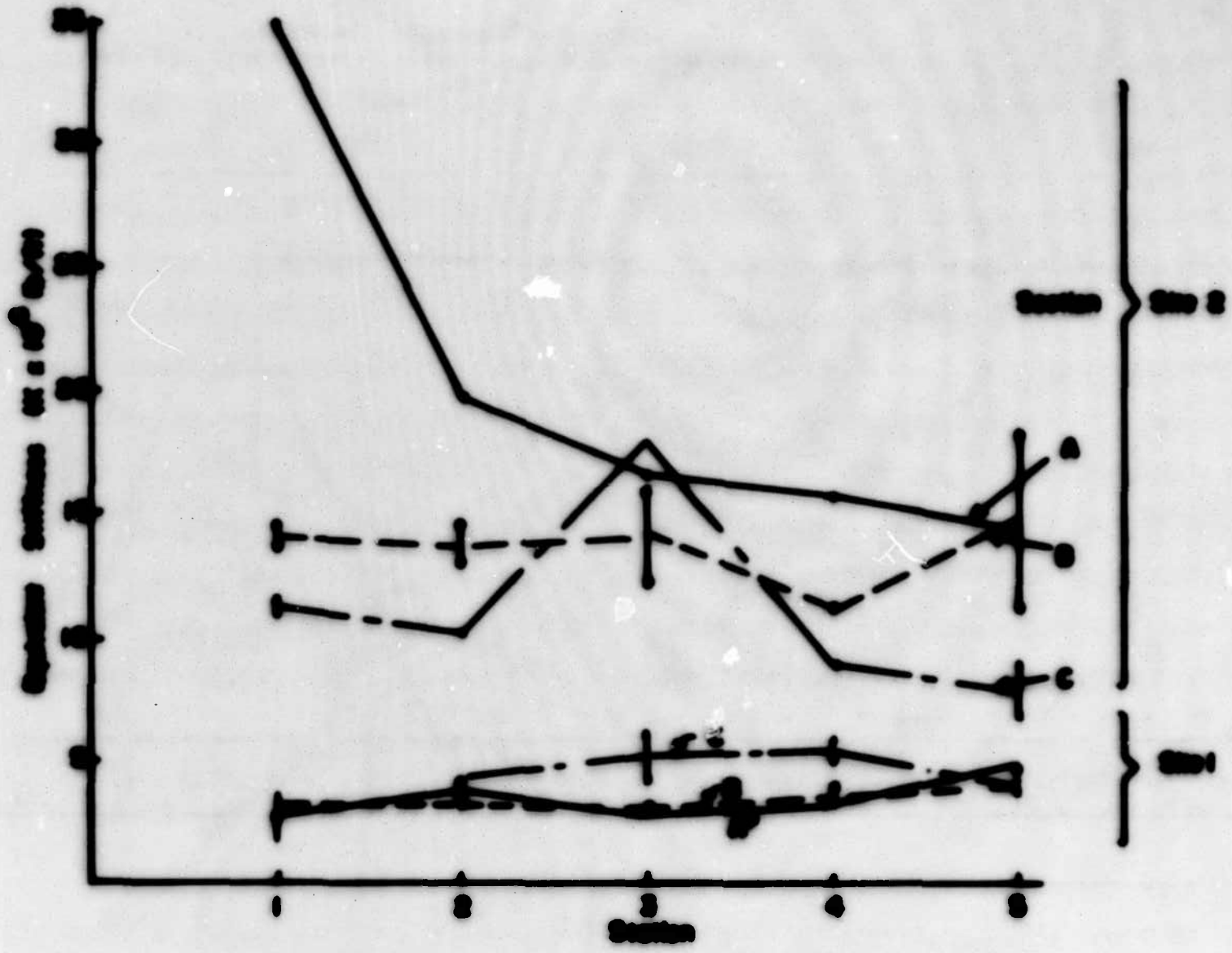



Figure 46. Comparison of Local and Site Characteristics as Shown by S-Parameter: Eglin AFB, March 1976

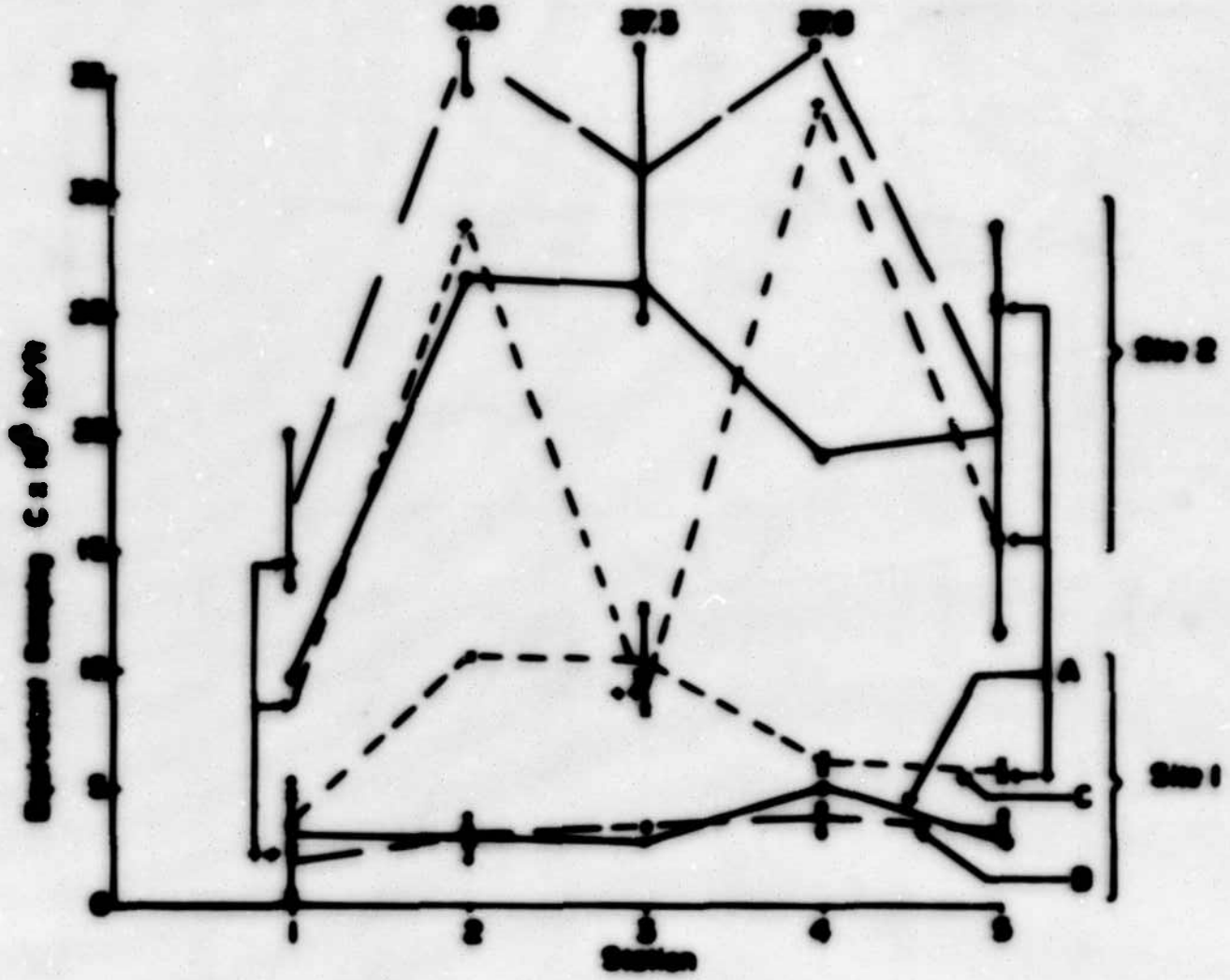


Figure 47. Comparison of Local and Site Characteristics as shown by C-Chromatogram: Eglin AFB, March 1976

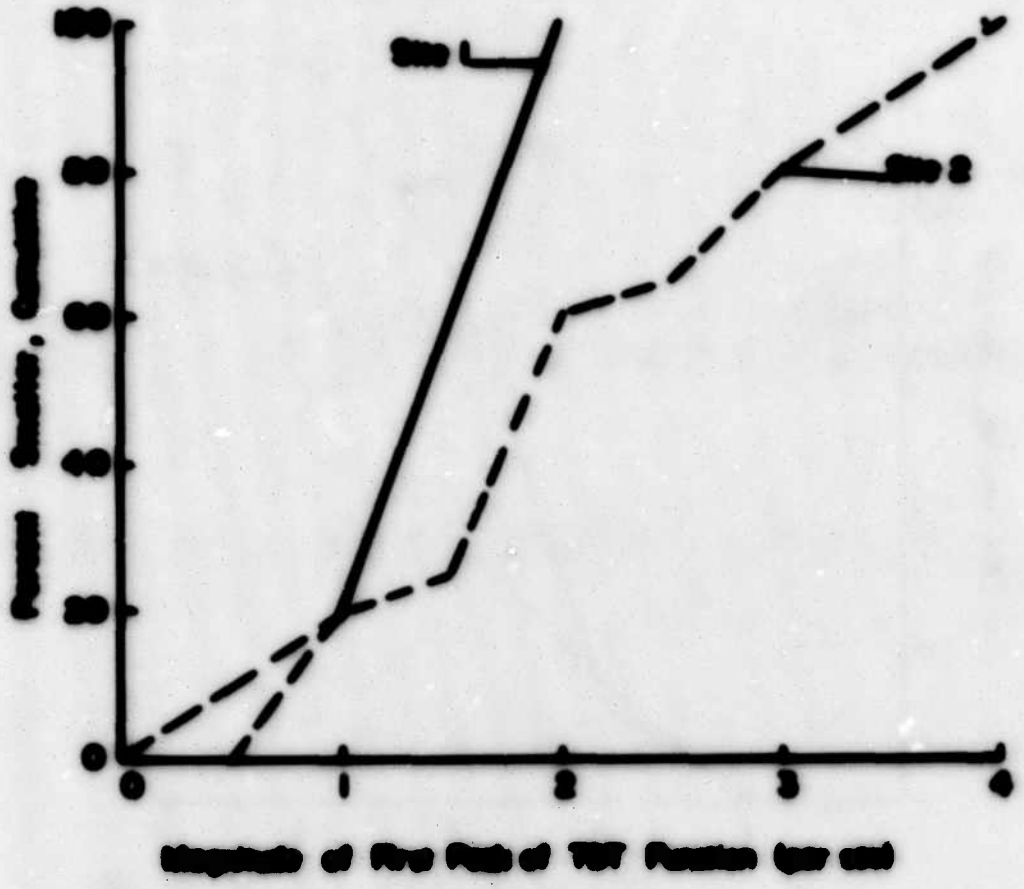


Figure 49. Comparison of The Peaks of The Transfer Functions: Sphinx ASV March 1976

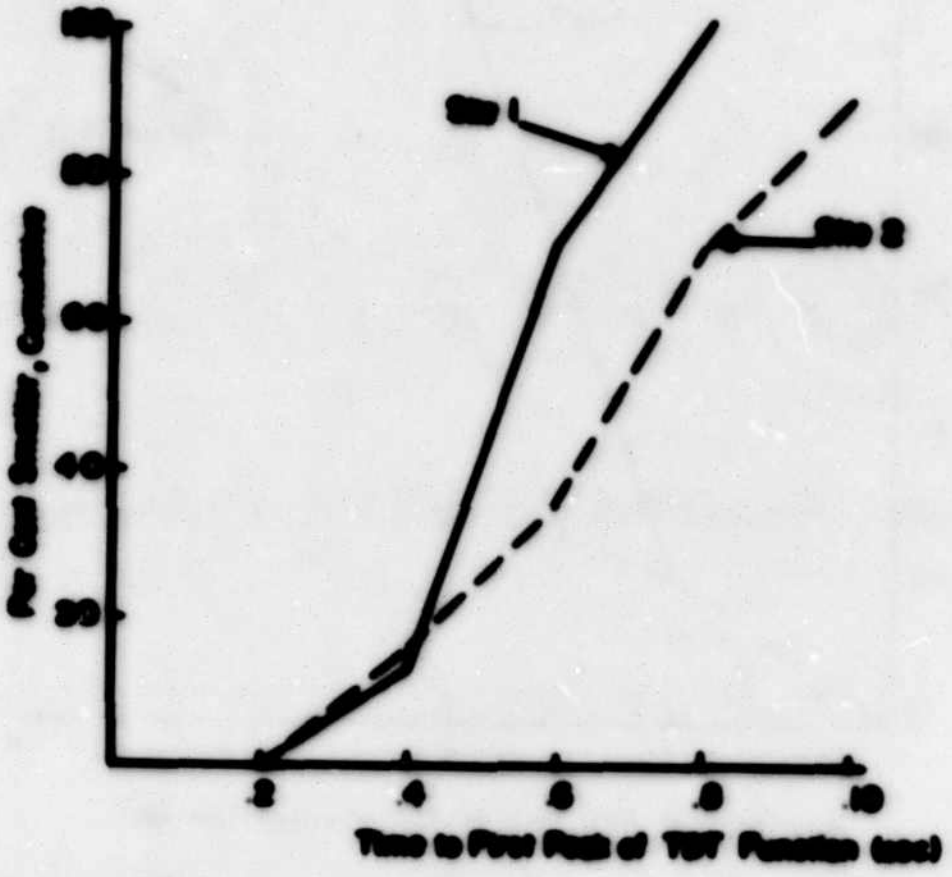


Figure 40. Comparison of Time to First Peak of TDF Function: Eglin AFB, March 1976

TABLE 5. [illegible]

| Position | k x $10^6$ lb/ft | c x $10^6$ lb-sec/ft | n x $10^5$ slugs | Position | k x $10^6$ lb/ft | c x $10^6$ lb-sec/ft | n x $10^5$ slugs | Position | k x $10^6$ lb/ft | c x $10^6$ lb-sec/ft | n x $10^5$ slugs |
|---|---|---|---|---|---|---|---|---|---|---|---|
| A1 | 3.405 | 5.290 | 9.343 | B1 | 3.251 | 0.209 | 2.473 | C1 | 3.925 | 2.298 | 1.954 |
| | 2.744 | 0.468 | 139.0 | | 2.689 | 3.597 | 7.295 | | 2.654 | 4.707 | 5.882 |
| A2 | 4.366 | 2.220 | 4.597 | B2 | 3.997 | 2.827 | 2.978 | C2 | 4.246 | 20.488 | 8.390 |
| | 3.299 | 3.460 | 8.592 | | 4.654 | 3.457 | 8.988 | | - | - | - |
| | 4.092 | 3.954 | 6.496 | B3 | 2.982 | 3.292 | 2.978 | C3 | 4.697 | 22.972 | 22.790 |
| A3 | 2.732 | 2.798 | 3.858 | | 2.365 | 3.564 | 4.854 | | 6.889 | 8.889 | 29.896 |
| A4 | 3.954 | 5.682 | 20.720 | B4 | 3.726 | 4.699 | 5.329 | C4 | 4.828 | 6.373 | 7.553 |
| | - | - | - | | 2.986 | 3.897 | 5.889 | | 5.635 | 5.669 | 22.790 |
| A5 | 4.636 | 3.282 | 9.284 | B5 | 3.595 | 2.686 | 4.539 | C5 | 3.982 | 5.966 | 22.770 |
| | 4.670 | 2.688 | 8.282 | | 3.728 | 3.824 | 7.627 | | 3.962 | 5.875 | 7.247 |

TABLE 6. PARAMETERS OF THE TRANSFER FUNCTION, BELLE AFB, MARCH 1976, RUN 2

| Position | k x $10^6$ lb/ft | c x $10^6$ lb-sec/ft | m x $10^6$ slugs | Position | k x $10^6$ lb/ft | c x $10^6$ lb-sec/ft | m x $10^6$ slugs | Position | k x $10^6$ lb/ft | c x $10^6$ lb-sec/ft | m x $10^6$ slugs |
|---|---|---|---|---|---|---|---|---|---|---|---|
| A1 | 32.89 | 9.885 | 146.0 | B1 | 13.16 | 89.89 | 42.68 | C1 | 20.95 | 2.81 | 693.8 |
| A2 | - | - | - | | 24.54 | 13.85 | 35.95 | | 7.85 | 24.68 | 32.85 |
| | 19.73 | 25.59 | 159.1 | B2 | 11.5 | 54.85 | 226.0 | C2 | - | - | - |
| A3 | 25.59 | 25.25 | 159.1 | | 13.1 | 41.59 | 87.9 | | 20.25 | 28.75 | 97.91 |
| A4 | - | - | - | B3 | 25.92 | 24.85 | 65.25 | C3 | 27.97 | 9.257 | 24.57 |
| | 25.68 | 29.03 | 28.85 | | 22.69 | 57.33 | 29.91 | | - | - | - |
| A5 | 8.88 | 28.91 | 49.63 | B4 | - | - | - | C4 | - | - | - |
| | 13.1 | 23.45 | 24.27 | | 23.81 | 57.85 | 65.89 | | 8.889 | 23.81 | 79.54 |
| | | | | B5 | 27.29 | 25.49 | 63.97 | C5 | 25.78 | 5.44 | 22.27 |
| | | | | | 20.99 | 25.54 | 226.4 | | 8.244 | 25.21 | 20.95 |

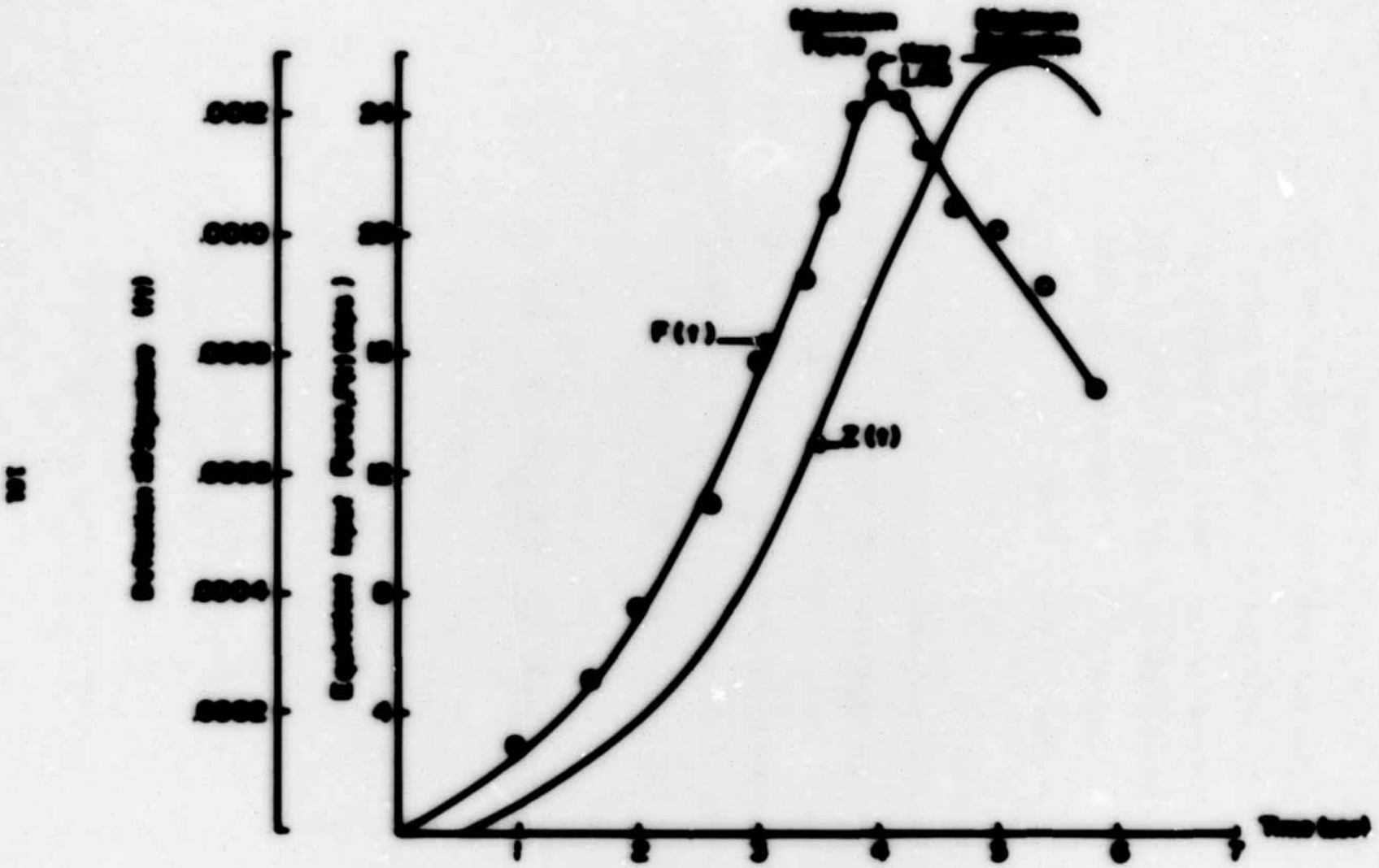
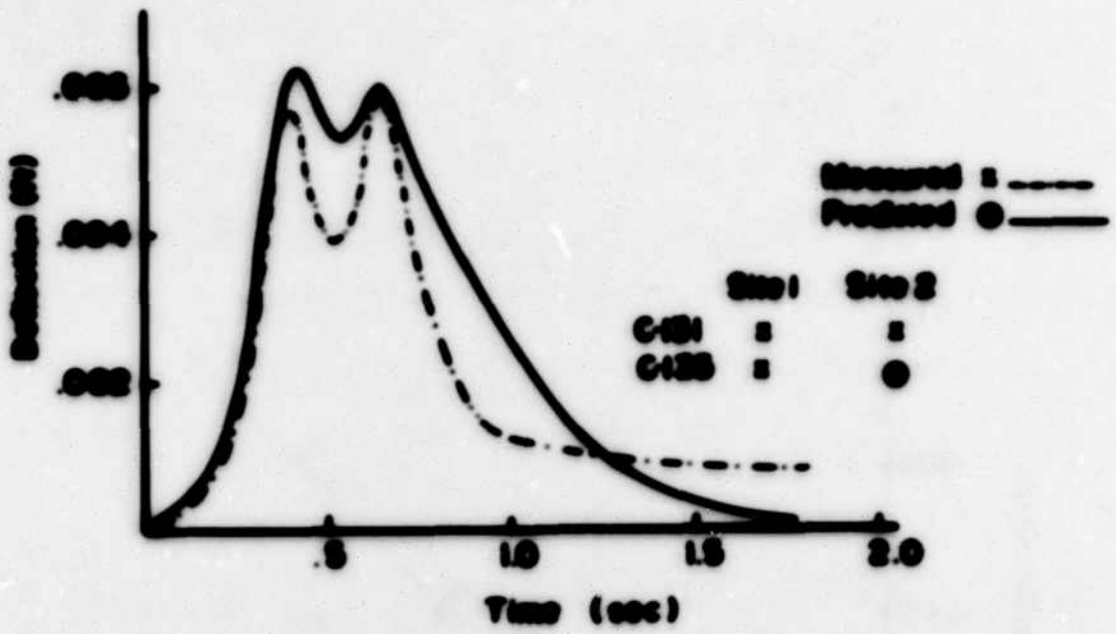



Figure 30. Input-Output Relation (Typical)

2. Both sites are over critically damped (Figures 44 and 45).
3. Site 2 has consistently larger k, c, and n parameters than Site 1 (Tables 5 and 6 and Figures 46 and 47).
4. Minor differences occur between the peaks of the transfer functions and the time to first peak for the two sites tested (Figures 48 and 49).
5. The maximum deflection lags behind the maximum input force by about 1.0 second (Figure 50).

## 6.3 Prediction

The methodology developed previously was used to predict the peak deflection response of the C-130 and the C-135 at Sites 2 and 3 (paragraph 5.2, Series B Field Investigation). The C-131 and Site 1 were the standard vehicle and site, respectively. Figure 51 shows a typical plot of the predicted and measured signature. Figure 52 shows a summary plot of the measured and predicted peak dynamic deflections.



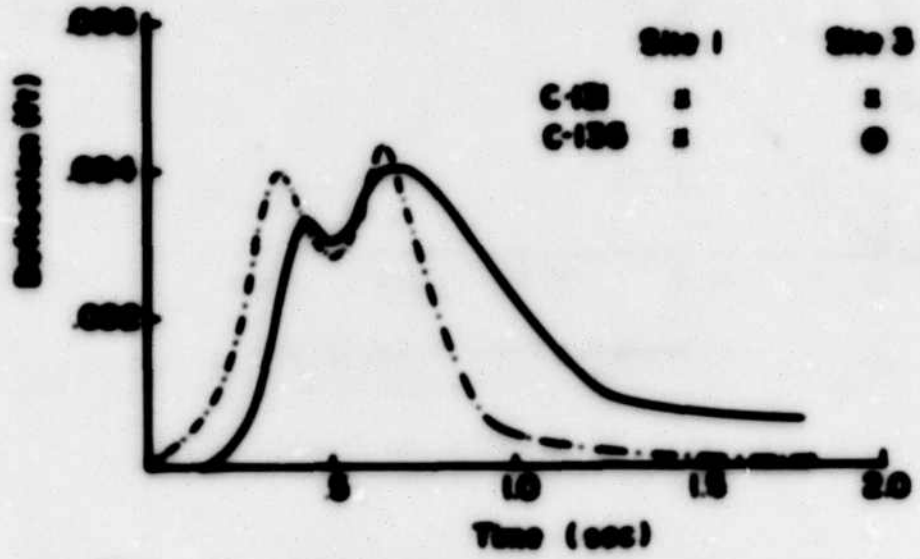


Figure 51. Typical Comparison Between Measured and Predicted Signatures

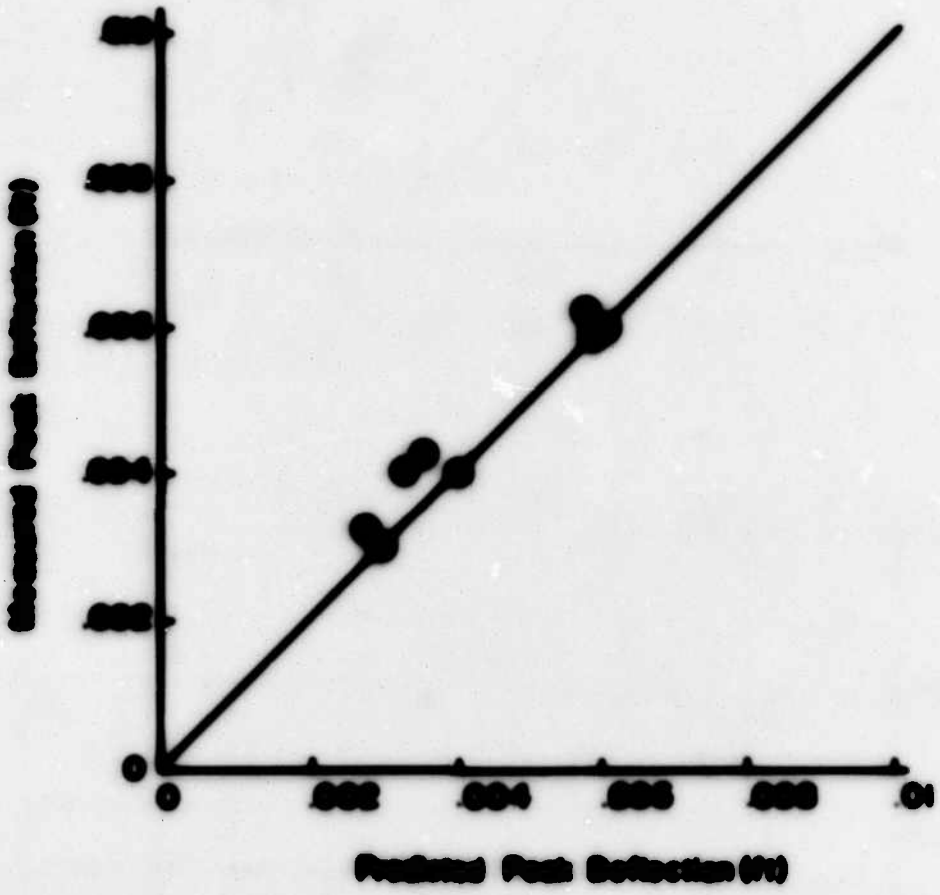



Figure 32. Comparison of Measured and Predicted Peak Deflections for Test Sites

# SECTION VII

# DISCUSSION

The scope of this work includes equipment development, pavement evaluation, and prediction of pavement response. The significance of the results and the reliability and practical applicability of the equipment are discussed in this section.

## 7.1 Equipment

Several optical systems were considered during the initial stages of the development of this study. The first system used a laser as a coherent light source. The initial concept was that the laser would be positioned off the pavement and shoot at either the moving load vehicles or reflectors on the pavement surface. Changes in the position of the reflected light beam impinging on a fixed surface would indicate deflections.

It was next thought that, rather than having a laser fixed at a particular location off the pavement, a cantilever beam with its pivot outside the deflection basin would yield a more versatile and mobile system. The beam would support lasers which would shoot down on the pavement surface. Changes in the light beam reflected from the surface and impinging on collector lens on the beam would indicate pavement deflections. Several lasers would have to be purchased and mounted on a cantilever beam. The expense and bulkiness of the lasers prompted a search for a more compact, inexpensive coherent light source. Light emitting diodes on a cantilever beam were finally selected as the breadboard noncontact system for measuring pavement deflections.

The deflection measuring equipment (LED beam) developed in this

work has a demonstrated capability of measuring pavement deflections on the order of 0.001 inch in a field environment. The companion LVDT beam[11] was found to be more rugged, reasonably simple to use, and very reliable. The breadboard LED system is somewhat more delicate. Special care had to be taken when in the moving mode, to ensure the safety of the lenses of the LEDs. Considerable problems also arose with the compatibility of the LED module and the magnetic tape recording system. These may be a result of the fact that the magnetic tape recording system was designed for use with another system, and thus the finer variations in the electronics which may not have effected the operation of the original design, may have been amplified when the system was used in conjunction with the LED modules. Although efforts were made to reduce these problems at Purdue University other still undiscovered incompatibilities between the LED sensor modules and the magnetic tape recording system may still exist.

Figure 53 shows a summary of measurement systems available today. It can be seen that actual vehicular loads are applied only in the procedures using the Benkleman beam, and the California and LaCroix deflectometer. It should be noted however that for these only the rebound deflections are measured. The total time response for one complete pass of a vehicle is not measured by any current device excepting those reported in this study. Under normal operating conditions a vehicle passes over a pavement without pause. This situation is very different from the conditions modelled by the Benkleman beam or the California or LaCroix deflectometers. For

---

[11] Developed under contract with the Federal Highway Administration.

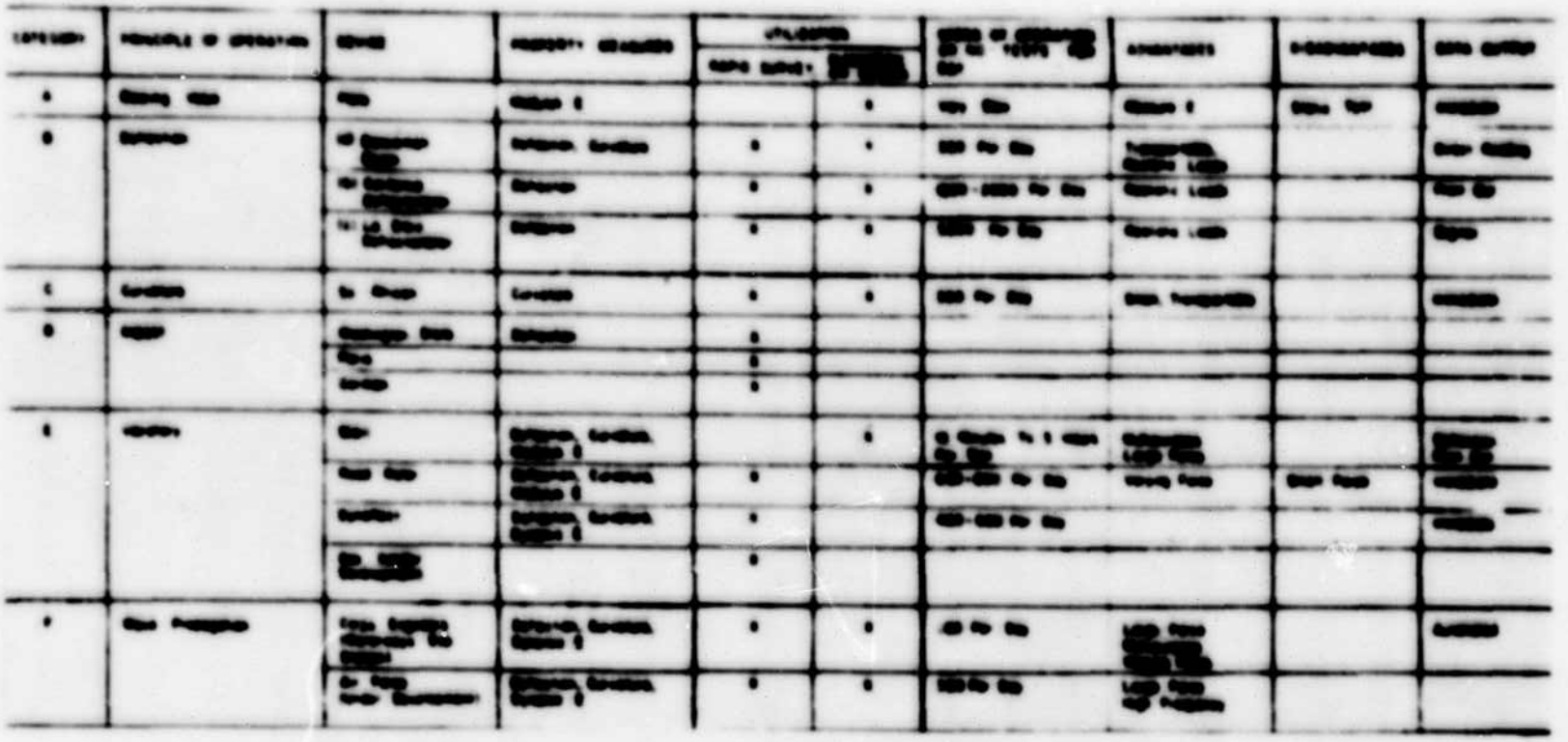


Figure 53. Summary of Measurement Systems (After Yoder and Cramling [Reference 58])

then the testing procedure stops at a maximum deflection under static loading. The vehicle then moves away and the residual deflection is recorded. The complete load cycle is not recorded by this stopping and starting procedure even though an actual vehicle is used.

Vibratory techniques also model a situation which is not representative of prototype vehicular loading on a pavement-subgrade system. The procedure for conducting vibratory tests generally consists of preloading a pavement-subgrade system by applying a static preload to the pavement surface through a plate of a specified size. At a certain preload level the steady state vibratory load is then applied at a designated frequency. Pavement deflection or a certain aspect thereof is then measured. There are significant differences between this procedure and the prototype loading of a pavement-subgrade system. First, a vehicle does not apply a static preload to the pavement-subgrade system. As previously mentioned, vehicular loading under normal operating conditions is applied to the system without pause. Second, a steady state vibratory force applied vertically dissipates approximately 67 percent of its total energy as Rayleigh waves, 26 percent as shear waves and 7 percent as compression waves (Reference 39). The bulk (67 percent) of the energy is therefore dissipated by generating surface disturbances at distances in excess of 20 feet from the vibratory load as evidenced by ground motion at these distances. Prototype loading, however, generally dissipates its energy at distances of less than 5 feet. For the F-4 aircraft the surface effect of the prototype load only extended between 4 to 5 feet from the wheel.

Impact and quasi-static loading likewise do not model prototype

vehicular loading. The time of impact loading is extremely small compared with the time a pavement section actually feels vehicular loads. On the other hand for quasi-static loading, the time of loading is very large compared with that of prototype vehicular loading. In addition, for impact loading, a major portion of the input energy is used to generate surface disturbances similar to steady state vibratory loading. Prototype loading, however, generates little lateral surface disturbance but effects of prototype surface loading are felt at depths of greater than 10 feet (Reference 60). Another important aspect of prototype loadings will be illustrated by an actual example.

During the Marsh field investigation a request was made by the Air Force officials at Eglin AFB that a runway overrun area be evaluated to determine whether it was adequate for use by F-4 aircraft. Figure 34(a) shows the area before prototype loading. Figure 34(b) shows the section after the first passage of the F-4 load cart. The cart vehicle punched through the pavement. It is doubtful that any available steady state vibratory loading testing apparatus (that dissipates a large amount of its energy on Raleigh waves) would have demonstrated the discovered inadequacy. The significance of this experience may be summarized as follows: An evaluation scheme that uses prototype loading in conjunction with nondestructive measurements of pavement-subgrade response provides, not only measurements of its response, but more importantly a test of adequacy.

The speed of operation or the number of tests per day shown in Figure 33 indicate results vary from very slow to 2000 per day. The literature (Reference 23), however, shows the upper limit to be overly



(a) [illegible]



(b) After

Figure 36. [illegible] Overrun Test - Eglin AFB: March 1976

optimistic. On the other hand, the operational speed of the lowspeed USDT and LSD systems are indisputable.

In June 1976, both the USDT and the LSD systems were used at Eglin Air Force Base to help investigate the difference between loaded and unloaded profiles. Measurements were made on 2,000 feet of taxiway using both systems. The USDT stationary beam-moving load operation was used to measure the system response at 100-foot intervals. The LSD beam was fixed to the P-4 load cart and was used in conjunction with the USDT measurements to provide an estimate of deflections between the 100-foot USDT stations. The average time for setup, including manually moving the USDT beam between locations and positioning the load cart, was 7 to 10 minutes. In addition to the 2000 feet of taxiway, the LSD system mounted on the load cart was used to test 1 1/4 miles of runway. The runway testing took less than 1 hour after initial setup.

It is important to note also that in the stationary beam-moving load mode the LSD and USDT beams both provide the complete deflection-time response of a pavement-subgrade due to prototype loading, that is, the entire dynamic deflection basin is obtained. No other instrumentation system currently available has demonstrated this capability. Furthermore, the LSD system does it without making mechanical contact with the pavement surface.

## 7.2 Evaluation

The evaluation procedure consists of measuring pavement deflections due to prototype loadings. From these deflections the signature and parameters of the maximum lateral dynamic deflection profile and the transfer function are obtained using the computer program detailed in

Appendix C. The parameters of the maximum lateral dynamic deflection profile and the transfer function are then related to performance.

7.2.1 Computer Input to Computer Program

The developed computer program determines the m, c, and k parameters of the equation that describes the behavior of the hypothesized model of vehicle-pavement-subgrade interaction. The equation of the model,

$$m\ddot{s}(t) + c\dot{s}(t) + ks(t) = F(t)$$

describes at best an approximation to physical reality. The lumped parameters represent average measures of the actual inertial (m), damping (c), and stiffness (k) characteristics of the real system. F(t) represents an input force at time $t_0$ and s(t), $\dot{s}(t)$, and $\ddot{s}(t)$ represent the signature and its first and second derivatives.

Yoder (Reference 61) has shown that when a vehicle is in motion, F(t) may have instantaneous values varying from 50 percent greater to 50 percent less than the static wheel load. The wide range is caused by many factors including both pavement and vehicle characteristics. The maximum F(t) of 25 kips used to establish the 500-pound criterion (see pages through ) in the computer program is then simply a convenient approximation to actual maximum values which may range from 12.5 kips to 37.5 kips. The 500-pound criterion then serves as a normalizing function and in effect has little physical significance, except in the sense that 25 kips is close to the static wheel load.

The lumped parameters of the transfer function represent measures of the inertial (m), stiffness (k), and damping (c) characteristics of

the pavement-subgrade system. Local[12] characteristics may vary significantly; however, when the overall interaction mechanism is correlated to surface deflections, local variations lose their significance.

In the computer program, FWDPRM parameters of the transfer function were obtained using an iteration-interpolation procedure detailed in paragraph 3.2.2. Conditions at times corresponding to the maximum deflection, the crossing point, and the point of inflection had to be satisfied. Two criteria were used. The first criterion was that the input load obtained by implicit convolution had to be between 24,500 and 25,500 pounds. The second and final criterion was that the c value satisfied the conditions at the crossing point and simultaneously satisfied conditions at the point of inflection. All forces were obtained by implicit convolution of the signature s(t) and the transfer function using a series of trial values of h, c, and m.

With reference to Figure 55, in concept the first criterion ensures that the maximum force lies within the cross-hatched zone. The second criterion ensures that the convolution and Newtonian solutions are very close. For example, consider the curves labelled A, B, D, C, and N in Figure 55. Suppose that the curve labelled N is the true but unknown (Newtonian) solution. Curve B satisfies neither criterion as (1) its peak value is outside the specified (shaded) band width, and (2) the computed c-value would be too large. The failure of the latter criterion is demonstrated when the force $F(t_1)$ (obtained by convolution)

---

[12] Local, as used here refers to dimensions of the size of a typical laboratory specimen.

of Z' (Figure 33) is used instead of R to calculate the c parameter at the point of inflection (section (1), Figure 35), using equation (17a). Curve A satisfies the 300-pound criterion but does not satisfy the c-parameter criterion, since the value of the force Z at the point of inflection is less than R. Substitution of Z for F(c) in equation (17a) would yield a value of c which would be less than the desired value. Curve C would satisfy both criteria. For this curve the convolution and Hertzian solutions are essentially the same. The fact that the two solutions are the same ensures that a standard point of convergence is used for all calculations. It does not mean that the k, c, and n parameters are absolute values since as previously cited, the parameters are average values, and are influenced by the approximation [F(c)] to reality inherent in the hypothesized model.

Since measurements could not be made exactly at the edge of the tire print, it was necessary to calculate the signature (the deflection at the edge of the tire print) using the characteristics of the lateral dynamic deflection profile. It was assumed, and subsequently verified (Figures 35 and 36), that the deflections under the wheel and at the edge are essentially equal. In calculating the signature the three parameters $A_{peak}$, $B_{peak}$, and $C_{peak}$ were used to provide a scaling of the lateral attenuation of the peak deflections with time. Figure 36 shows a comparison of a typical measured and calculated signature. The signature (curve A) was measured as the F-4 passed over a gage embedded in the pavement. The other embedded gages measured points on the deflection basin which provided the inputs to the calculations. The closest gage was 18 inches from the center of the load wheel. The difference between the maximum calculated curve (B)

and measured deflections is about 5 percent. Since all field measurements analyzed in this work were made with the LVDT beam at distances closer than 18 inches from the edge of the tire, the correspondence between the calculated and the measured signatures in Figure 56 indicates the upper bound of the difference between calculated and measured signature. Using linear interpolation, the dotted curve (C) in Figure 56 corresponds more closely to typical calculated signatures used in the data analyzed herein since the LVDT beam permitted measurements to be made as close as 3 inches from the edge of the tire print.

7.2.2 Parameters of the Maximum Lateral Deflection Profile

Pavement deflection has been used as an indicator of the support condition of a pavement-subgrade system for some time. Methods of evaluation have been developed that are based on (a) magnitude of deflection (Reference 62), (b) bending index (Reference 63), (c) radius of curvature (Reference 23), and (d) the "slope of deflection" (Reference 64). These methods in general have used static or quasi-static loadings. For the reasons discussed previously in paragraph 7.1, these deflection measurements are not true indicators of the dynamic response of a pavement-subgrade system subject to vehicular loads.

The dynamic lateral deflection profile defined by equation 2 has three parameters $A_{peak}$, $\beta_{peak}$, and $\tau_{peak}$ which together account for both the magnitude and the curvature of the lateral deflection basin. Since the deflection measurements were made during a nonstop passage of the F-4 load cart in front of the LVDT beam, the three parameters are representative of the actual maximum dynamic lateral deflection basin due to prototype loads.

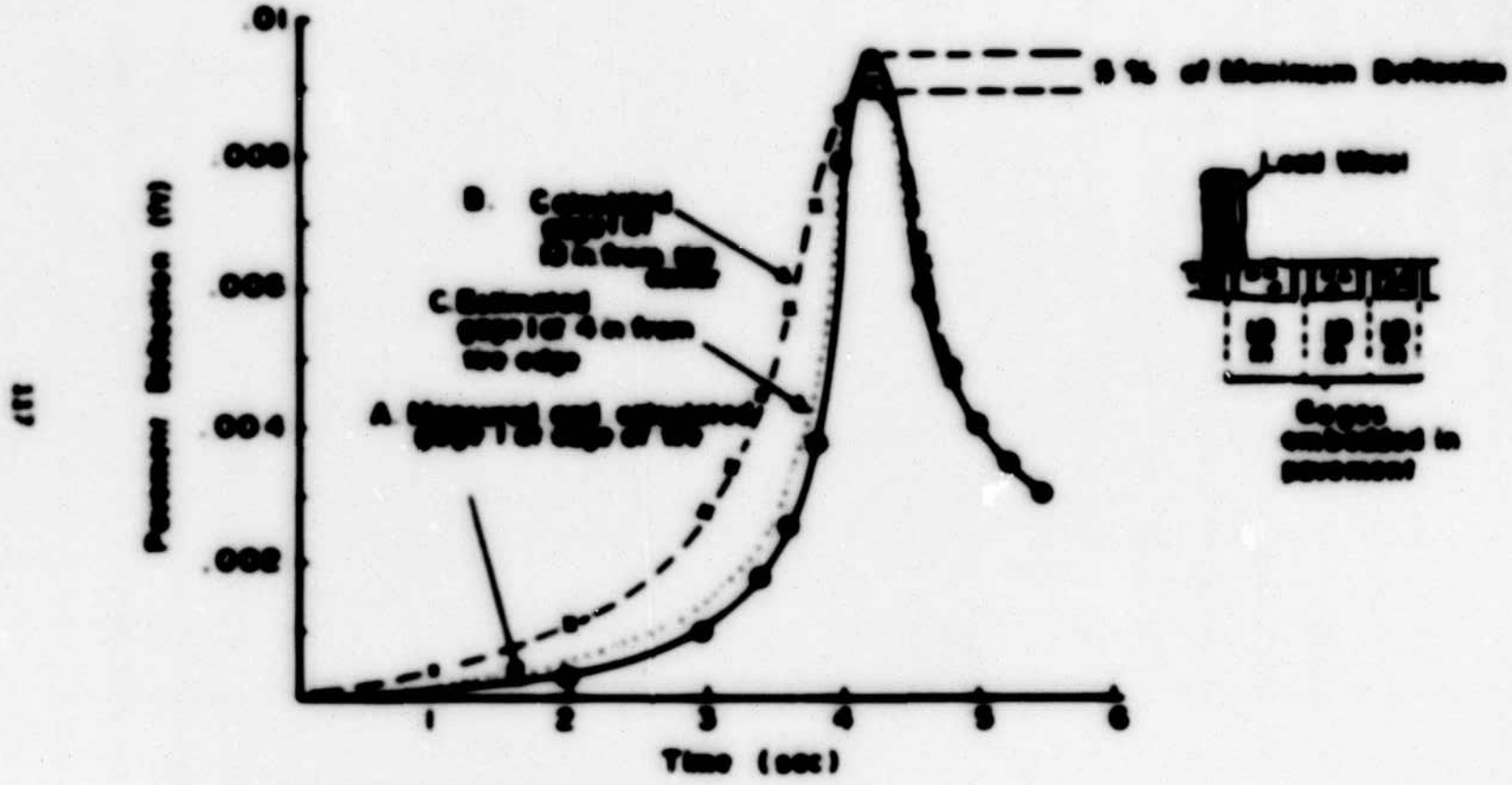



Figure 35. Comparison of Signatures

The results presented in paragraph 6.2.1 showed some variation in the parameters $A_{peak}$, $\delta_{peak}$, $\varepsilon_{peak}$ at each site, and there were distinct differences between Sites 1 and 2. In order to better characterize the two sites and give due consideration to the parameter variability at the sites, plots of cumulative percent smaller versus each parameter were prepared from the results in paragraph 6.2.1. Figures 57 through 59 show these plots. The distinct differences between the two sites are displayed as a shift of the individual site characterization plots.

The U. S. Air Force in recognition of the structural inadequacy of Site 1[13] uses the area as a parking area. Site 2 on the other hand is an in-service taxiway. If the lower 10 percent of the Site 2 parameters is arbitrarily selected as the line denoting failure, criterion based on the correlation of parameters with performance is established. This is shown in Figures 57 through 59. The lower 10 percent as used here means that 10 percent of the values do not meet the criterion. Thus, in Figure 59, the line denoting failure intersects the Site 2 cumulative percent smaller curve at the 10 percent smaller value whereas in Figures 57 and 58, the 90 percent smaller value of the cumulative percent smaller plot is intersected by the criterion line.

7.2.3 Parameters of the Transfer Function

The results given in paragraph 6.2.2 showed that there is some variation in the parameters k, c, and n of the transfer function over

---

[13] See Appendix B, Figure B-1(a)

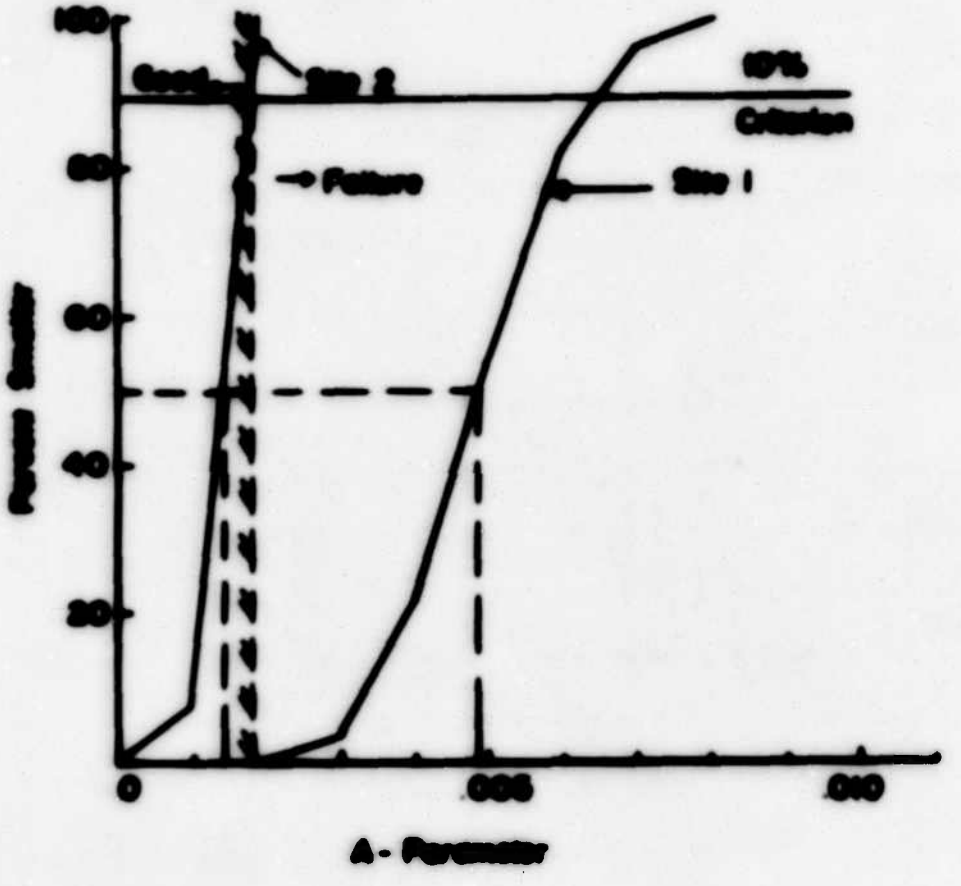



Figure 37. Comparison of A Parameters: Eglin AFB March 1976

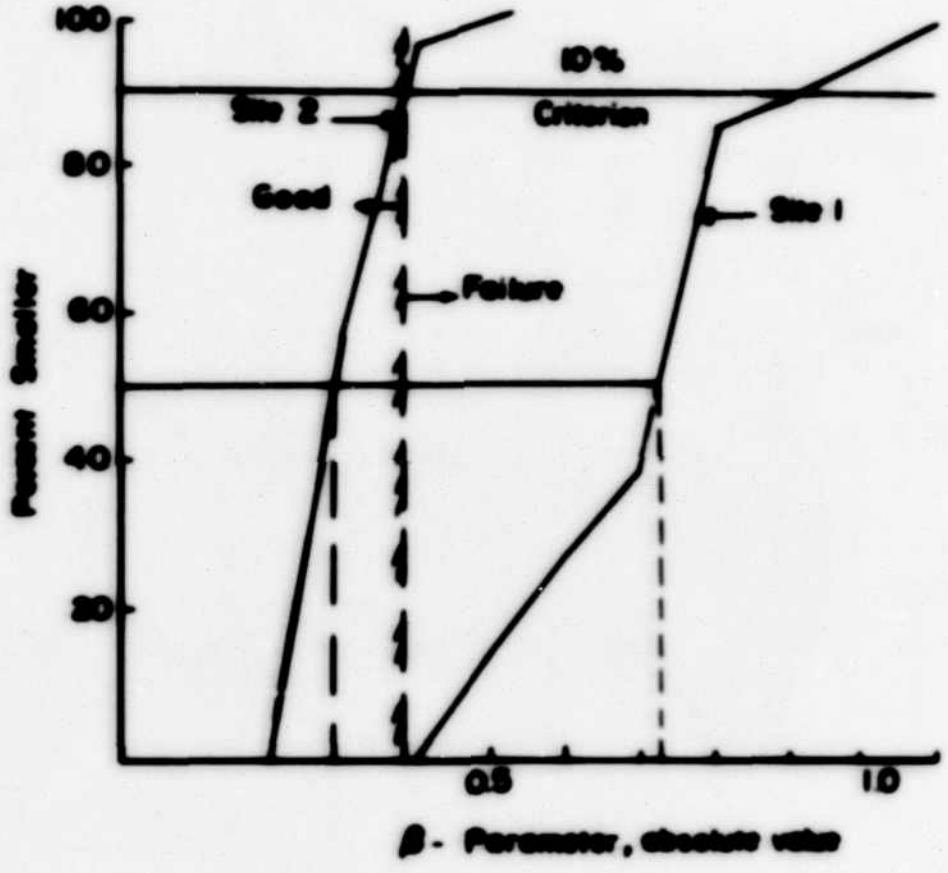



Figure 56. Comparison of the β-Parameters: Eglin AFB, March 1976

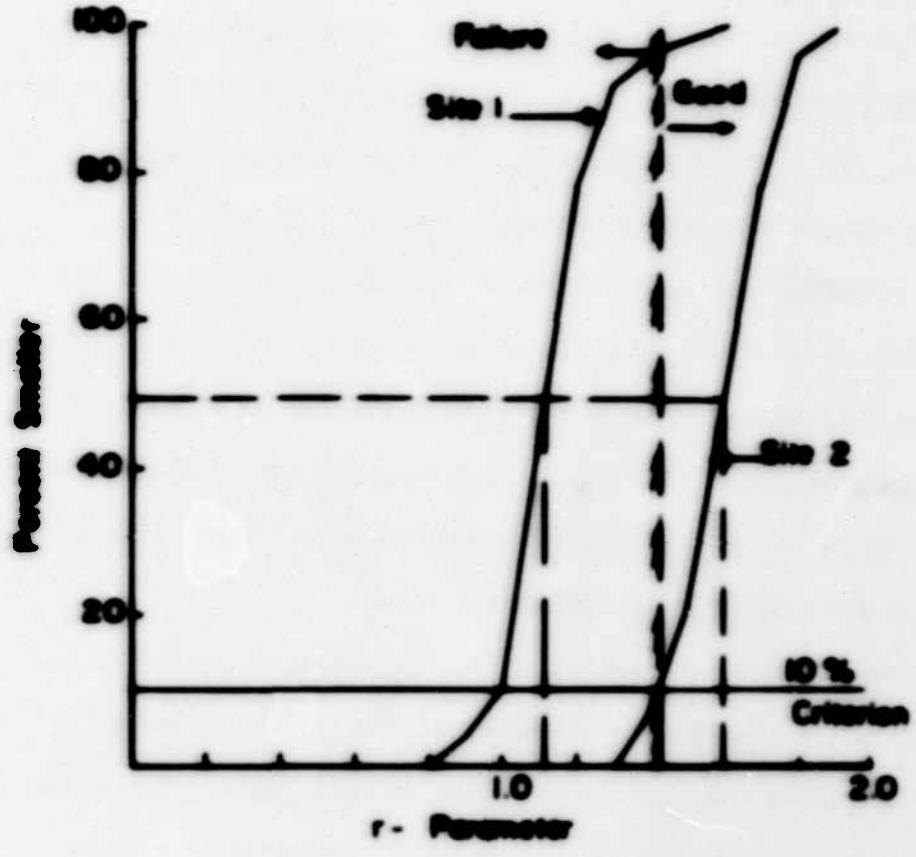



Figure 59. Comparison of r Parameters: Eglin AFB March 1976

each of the two sites. Plots of cumulative percent smaller versus each parameter have been prepared for each site. Figures 60 through 62 show these plots. It can be seen that Site 1 exhibits more uniformity and considerably smaller values of all three parameters than Site 2. With reference to Figure 60 the fact that the entire curve of "cumulative percent smaller" is shifted towards higher stiffnesses for Site 2 indicates that the stiffnesses determined in the evaluation procedure are not local hard spots, but represent the variability in the stiffness characteristics of the area tested.

If the arbitrary 10 percent criterion shown in Figures 57 through 59, is applied to each of the parameters k, c, and n of the exponential function, a criterion based on performance can be had. The line denoting failure is shown on Figures 60 through 62. The performance based criteria shown in Figures 60 through 62 can then be used in the same manner as was presented in the discussion of the parameters of the maximum lateral dynamic deflection basin.

It is interesting to compare the k parameters with stiffness as determined in a 1973 evaluation (Reference 28) by the Air Force, in which an F-4 aircraft was used as the load vehicle and the Benkelman beam was used to measure rebound deflections. Figure 63 shows the locations where relative stiffnesses were determined. Figure 64 shows a histogram on the relative stiffnesses calculated by their procedure. Figure 64 also shows the mean k parameters for Sites 1 and 2 as calculated by the procedures developed in this research effort. Site 1 is shown to have a smaller mean stiffness than all the sections evaluated, while Site 2 is in the range that occurs with about 9

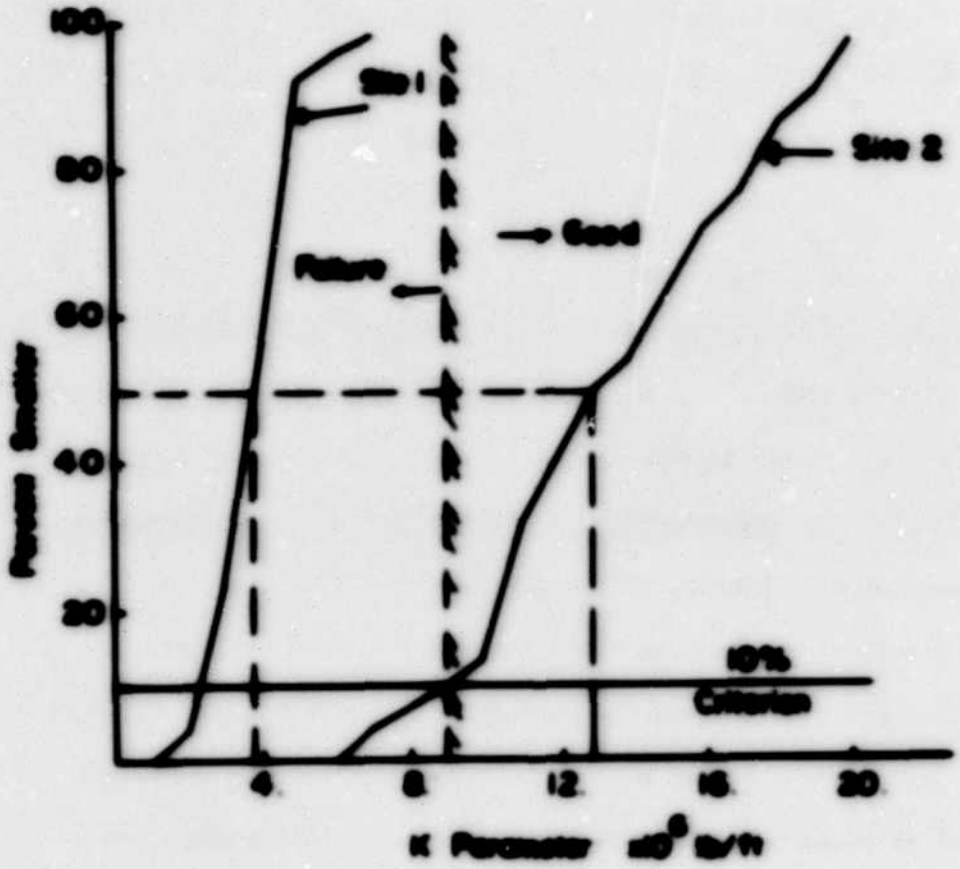



Figure 60. Comparison of Equivalent k Parameters: Eglin AFB March 1976

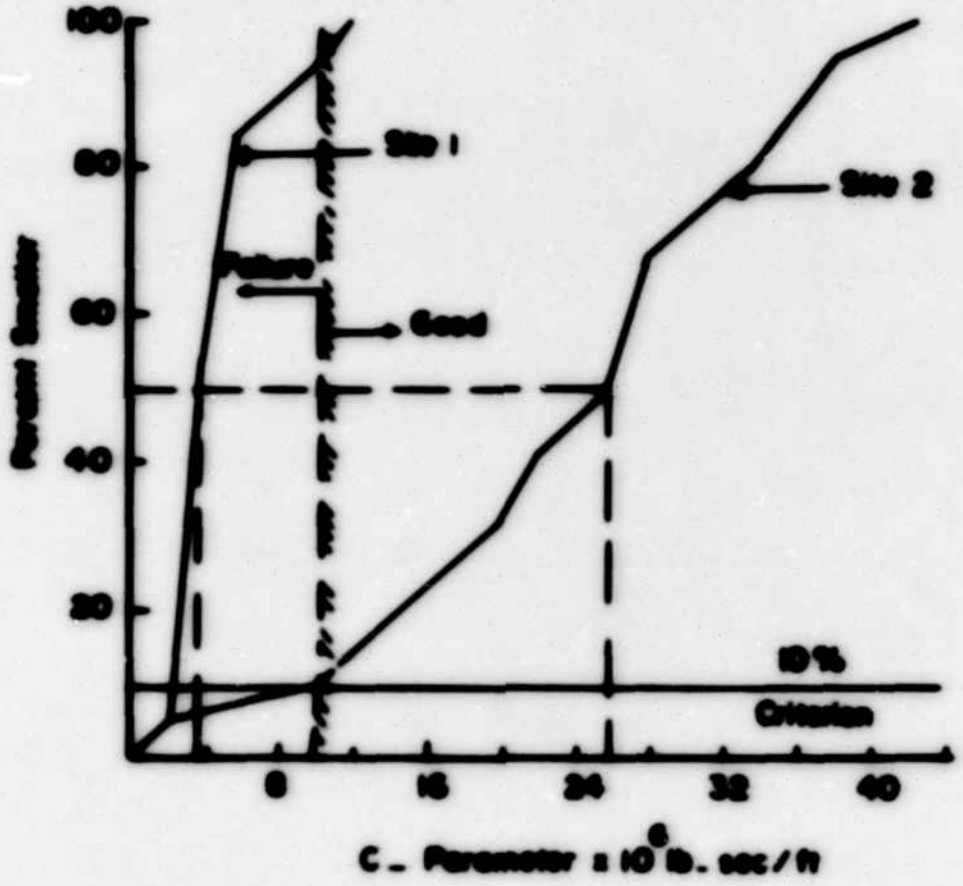



Figure 61. Comparison of Equivalent c Parameters: Eglin AFB March 1976

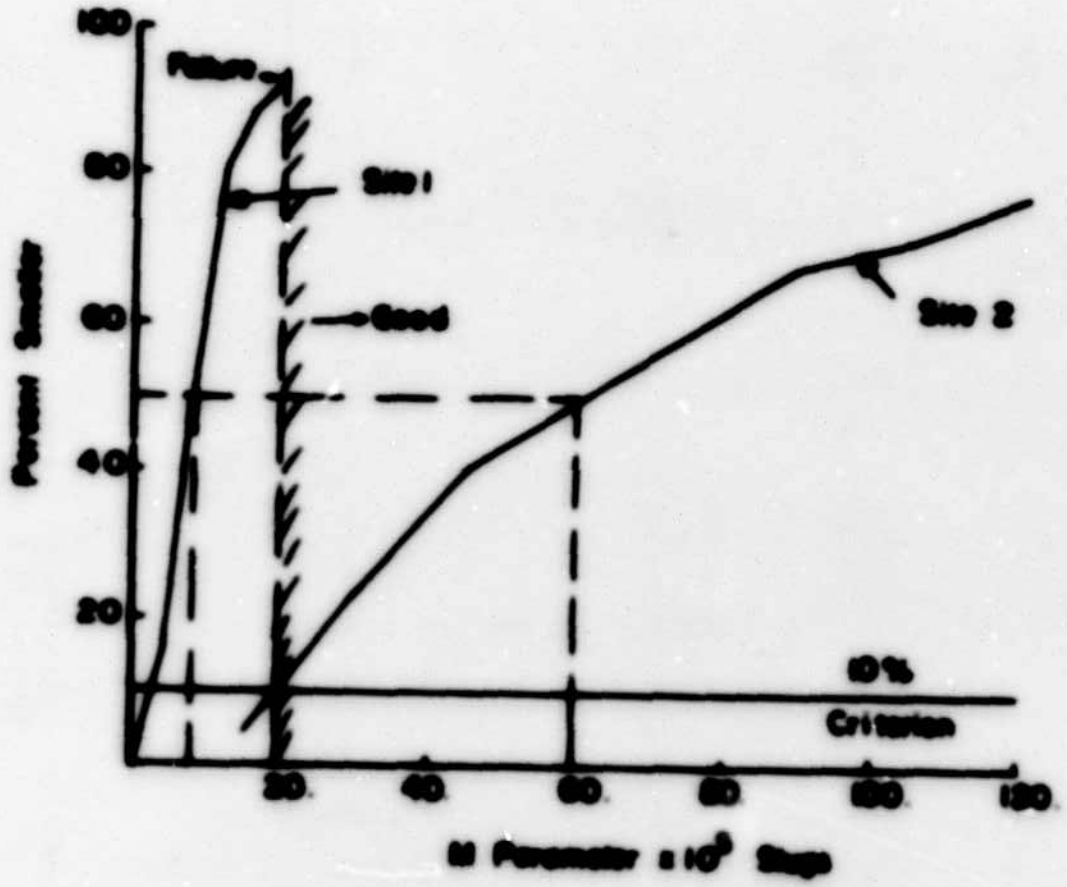



Figure 62. Comparison of the Equivalent n Parameters: Eglin AFB, March 1976

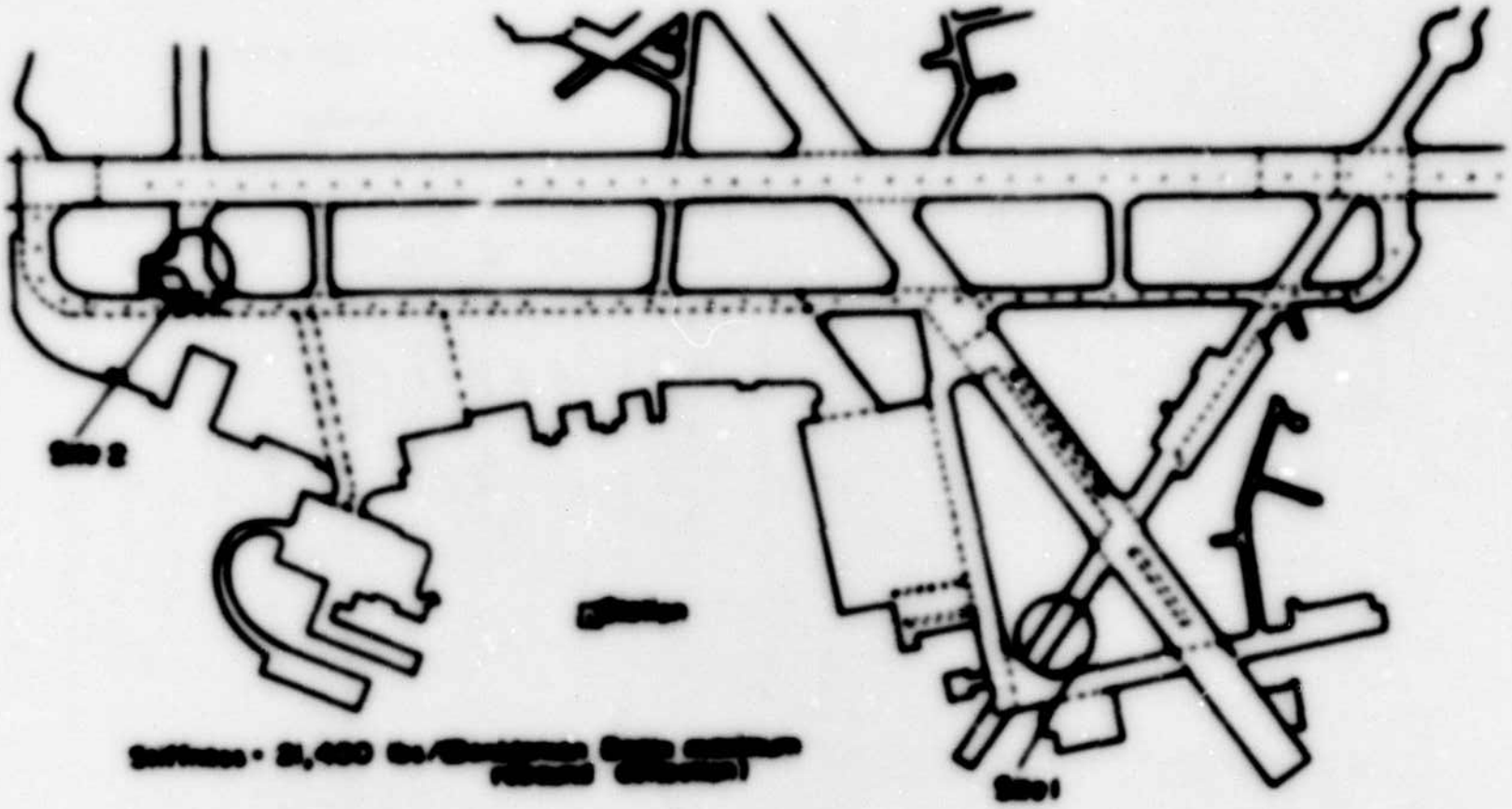


Figure 61. Locations of Stations Where Relative Stiffnesses Were Determined (after AFCEC, Tyndall AFB)

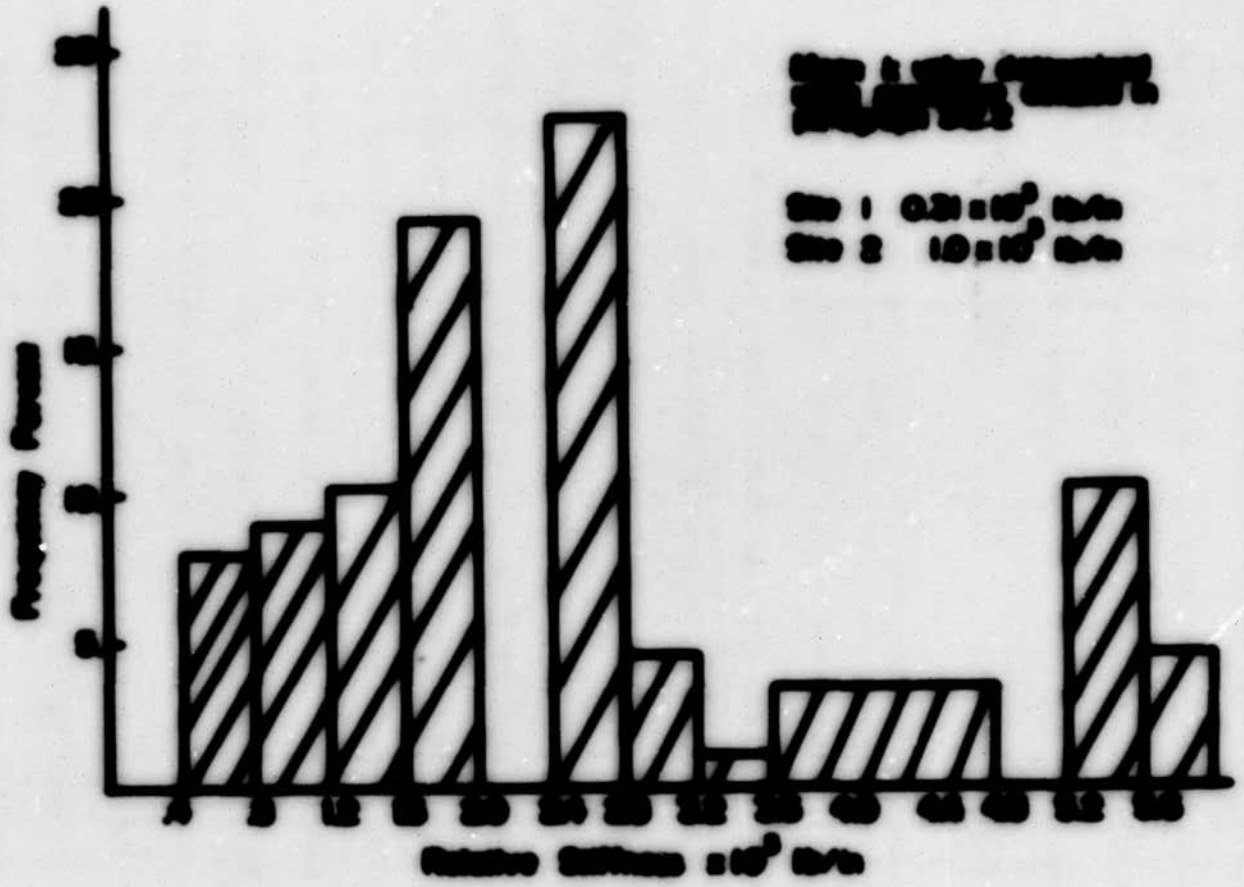


Figure 64. Histogram of Salaries Collected (Based on 47[illegible] Inputs)

percent frequency.

It appears then that field performance and comparison of stiffness both substantiate the lower limit of the k parameter. A reasonable lower bound of an acceptable k value of about $9.0 \times 10^6$ lb/ft (750 kips/in) is suggested by the Site 2 curve in Figure 60. This is the lower 10 percent value.

### 7.2.4 Relationship between the k and $A_{peak}$ parameters

The $A_{peak}$ parameter defined in this study is basically the maximum deflection under the load wheel. The k parameter, on the other hand, represents an equivalent stiffness. This stiffness reflects the complicated unknown interaction of all the materials in the zone of influence of the wheel load. The k parameter is thus a measure of the stiffness resulting from this interaction. Figure 65 shows a plot of the $A_{peak}$ and corresponding k parameters from the two sites as given in the results in Tables 5 and 6. The dashed line represents a limiting envelope. There appears to be two linear sections to this envelope. If the straight line portions are extended, the A and k parameters corresponding to their point of intersection are 0.0026 ft (0.0312 in) and $6 \times 10^6$ lb/ft (500 kips/in) respectively. It is interesting to note that the Site 2 (active taxiway) (k, A) parameters fall below the line P(I) (0.0312 in) and the Site 1 (pushing area) (k, A) parameters lie above the P(I) line. It is also interesting to note where the k coordinate of this point (I) lies, if plotted on Figure 66. The curves in Figure 66 were developed by the Corps of Engineers using vibratory techniques and correlations with actual

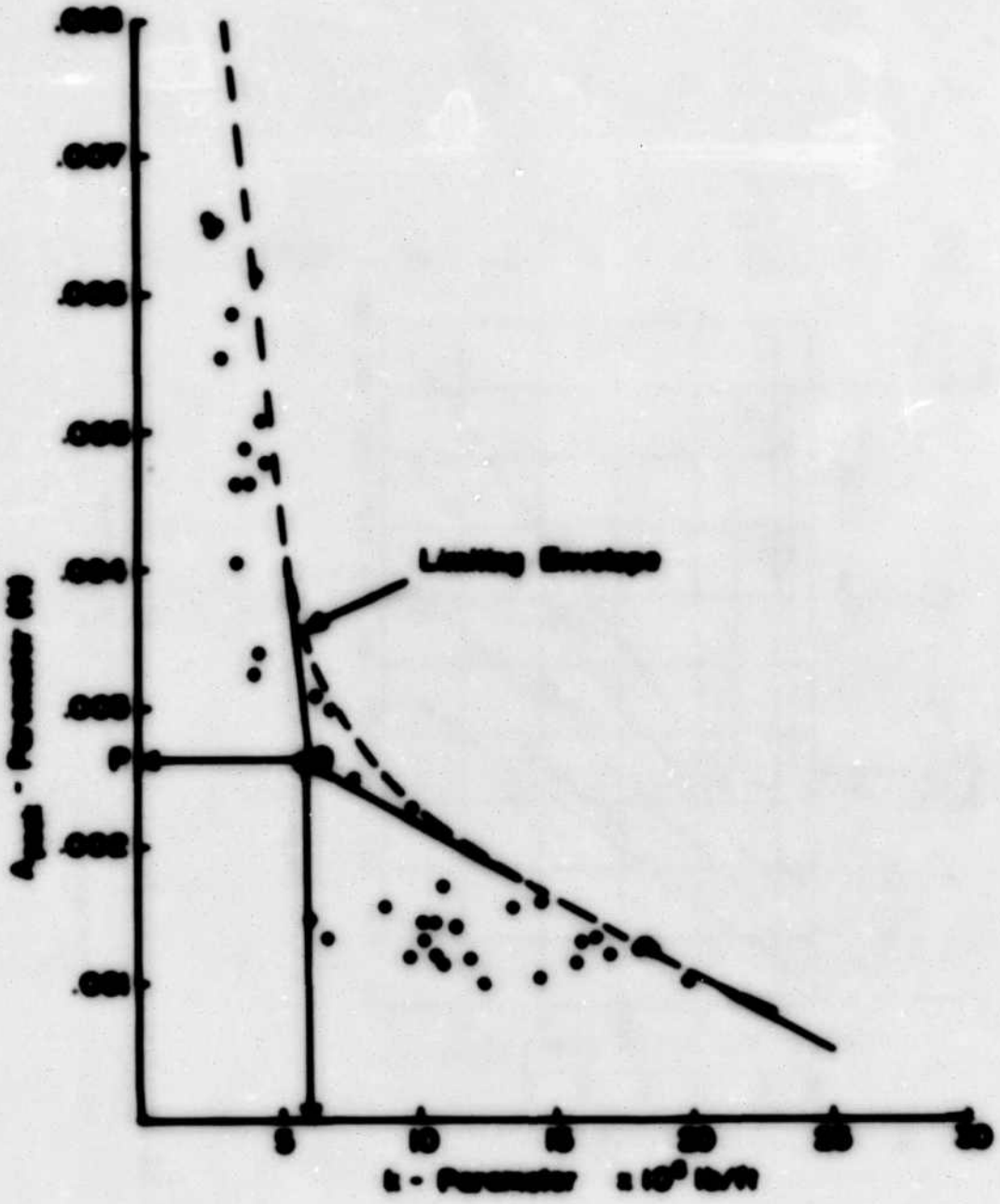



Figure 65. Relationship Between $A_{peak}$ and k Parameters

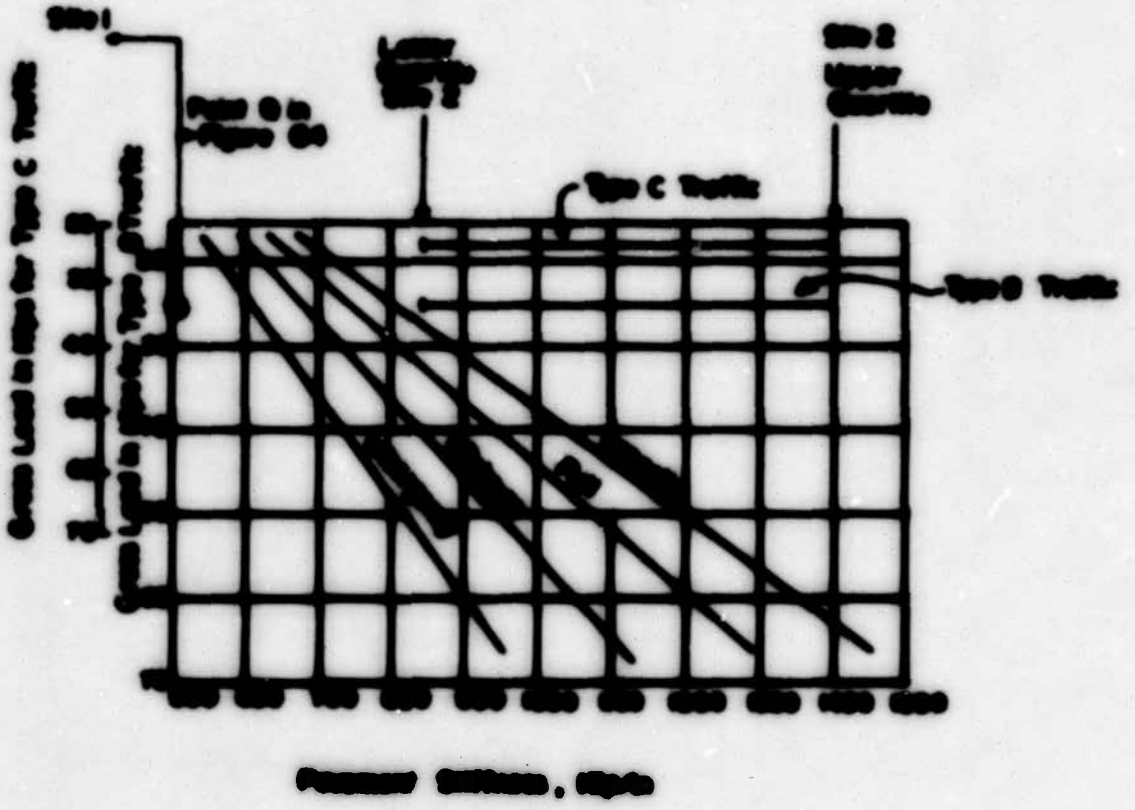


Figure 66. [illegible] Deformation Curves for Flexible Pavement, Single Wheel Load, 100 lb. (after Dimmick (Reference 16))

aircraft loads. Since the F-4 aircraft gear is a single wheel of contact area 102 in.$^2$ loaded to about 25 kips (Reference 56), the h value of the point q (Figure 65) can be plotted directly on Figure 66 for C type or D type traffic. Figure 66 also shows h-parameters corresponding to the lower and upper quartile values at Site 2 (active tendency). Site 2 lies above the equality line and Site 1 lies below the emergency line. This estimation appears to confirm the known status of Sites 1 and 2.

The limiting envelope to Figure 65, therefore, appears to provide an additional evaluation tool. Since deflections alone are measured, the limiting h value can be estimated from Figure 65, and compared with available correlations as shown, to estimate load rating.

7.2.3 Approximate Method for Estimating h, s and n for F-4 Loading

Figure 59 showed the typical relationship between the input force P(t) and the output s(t). Figure 67 shows the frequency characteristics of P(t) normalized by the maximum assumed wheel load (25 kips) at three sections corresponding to sections 1, 2 and 3 of Figure 7. Sixty data sets were used to develope the frequency curves.

With reference to Figure 67, at the point of inflection (section 1), the normalized force ratio has a max value of approximately 0.9. This suggests that the maximum applied force occurs at a time close to maximum pavement velocity. Similarly at maximum deflection (section 3), 0.5 of the maximum force is the max value of normalized force ratio. This indicates that at the time the measured deflection is a maximum the wheel has already passed the point under consideration. At the

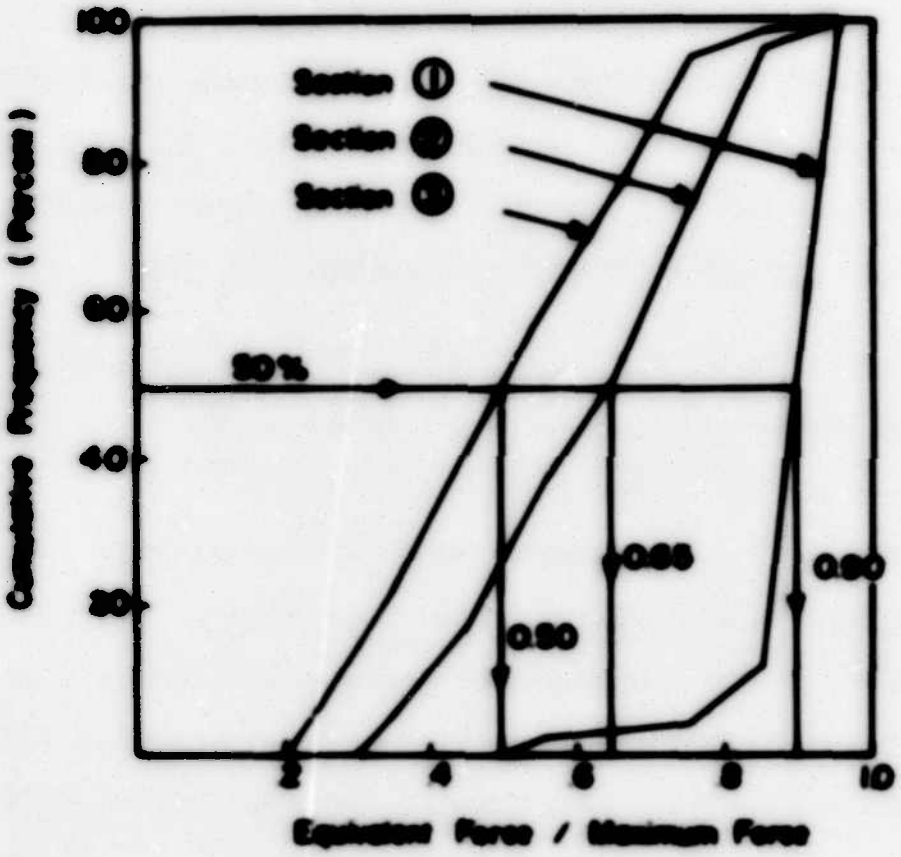



Figure 67. Frequency Characteristics of Forces at the Point of Inflection, Crossing Point and Maximum Deflection

crossing point (section 2), approximately 0.65 of the maximum load is the mean value of the force ratio.

Figure 66 shows the frequency characteristics of the time normalized by the time to peak deflection corresponding to the point of inflection (section 1) and the crossing point (section 2) respectively. At the 90 percent level the normalized time ratio is seen to be 0.72 and 0.90 for the point of inflection (section 1) and the crossing point (section 2) respectively.

Figures 67 and 68 suggest a simplified approximate method for determining the transfer function parameters from the deflection-time history of one pass of a vehicle. In order to determine k from the signature s(t), the deflection $s(t_2)$[14] is found at 0.9 $T_p$, where $T_p$ is the time to the peak deflection (Figure 68). The force $F(t_2)$ applied at the time ($t_2$) is approximately 0.65 $P_{max}$ (Figure 67) where $P_{max}$ is 25 kips for the F-4 loading. As was noted in paragraph 3.2.2 at the crossing point.

$$F(t_2) = k \cdot s(t_2)$$

hence, using the approximate values,

$$k = \frac{F(t_2)}{s(t_2)} = \frac{(0.65)(25000)}{s_{0.9\,T_p}}$$

[14] For the sake of clarity, the subscript of "t", such as in $t_2$, will be retained to describe the corresponding section in Figures 67 and 68.

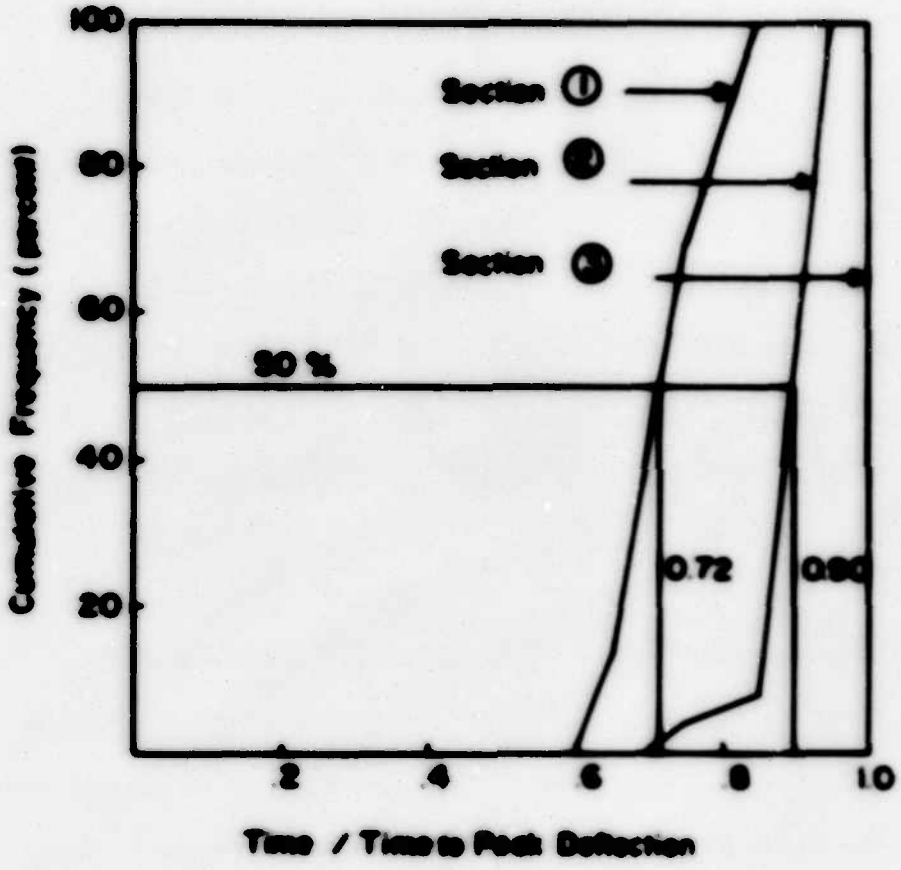



Figure 68. Frequency Characteristics of Times at the Point of Inflection, Crossing Point and Maximum Deflection

Once k is known, the c parameter can be obtained by applying the same reasoning to the point of inflection (section 1, Figure 67); namely,

$$c = [F(t_1) - ks(t_1)]/\dot{s}(t_1)$$

where $F(t_1)$ is 0.9 $P_{max}$ (Figure 67) and $s(t_1)$ and $\dot{s}(t_1)$ are the deflection and numerical approximation of the velocity, respectively, at the time corresponding to 0.72 $T_p$ (Figure 68).

The parameters m can then be estimated using the equation for conditions at the crossing point, where

$$m = -\frac{c \times \dot{s}(t_2)}{\ddot{s}(t_2)}$$

and $\dot{s}(t_2)$ and $\ddot{s}(t_2)$ are the numerical values for the velocity and acceleration at the time 0.9 $T_p$.

The developed approximate procedure for estimating k, c and m was examined with respect to 38 data sets from both Sites 1 and 2 at Eglin AFB[15]. The normalized forces at the crossing point and the point of inflection were taken to be 0.65 and 0.85[16], respectively. The normalized times at the crossing point and the point of inflection were taken to be 0.72 and 0.9, respectively. The k, c and m parameters obtained using the simplified procedure were then compared with their computer solutions. Correlation coefficients of 0.93, 0.93 and 0.90

---

[15] See Appendix B

[16] 0.9 was tried initially but 0.85 yielded c values which correlated more closely with the computer solutions.

were obtained from the linear least squares correlation study for the b, c and n parameters, respectively. The advantage of the simplified procedure is that it allows reasonably reliable estimates to be made of parameters without the need of a digital computer.

7.2.6 Estimating Design Parameters

The modulus of subgrade reaction ($\bar{k}$) and CBR of the subgrade can be estimated from the $A_{peak}$ parameter of the peak deflection profile.

Using the assumption of a Winkler model, Pister and William (References 26) developed the following relation between the subgrade deflection W(x), pressure on the subgrade (p), modulus of subgrade reaction ($\bar{k}$) and a shear stiffness parameter (CH) as the distance from the edge of the loaded area (x):

$$W(x) = \frac{p}{2\bar{k}} \exp(-x/CH)$$

This expression is similar in form to equation (2),

$$\varepsilon_{max_j} = A_{peak} \exp(\beta_{peak} x_j^{r_{peak}})$$

which was found to describe the maximum lateral dynamic deflection profile. If it is assumed that the two relations correspond at their maximum values (for x = 0), it follows that

$$A_{peak} = \frac{p}{2\bar{k}}$$

Hence, this suggests that the modulus of subgrade reaction can be obtained as,

$$\bar{k} = \frac{p}{\Delta_{peak}} \qquad (23a)$$

Using a 1:1 simplifying assumption [cf. Yoder (Reference 35)] to calculate the attenuation of the wheel load, $P_{max}$, through the pavement section of thickness D, the contact pressure, p, equals $P_{max}/(5.64 + D)^2\pi$; where 5.64 is the radius of the equivalent circular contact area due to the F-4 aircraft with tire pressure 250 psi and a $P_{max}$ of 25,000 pounds. Substituting in equation (23a) gives

$$\bar{k} = \frac{P_{max}}{2.0(5.64 + D)^2\pi\Delta_{peak}} \qquad (23b)$$

CBR values can then be estimated using established correlations (Reference 65) between $\bar{k}$ and CBR. One such correlation given by the Portland Cement Association (Reference 65) is shown in Figure 69.

Using equation (23b) and the maximum, median and minimum values of $\Delta_{peak}$ calculated at site 2, and a D of 17 inches, $\bar{k}$ values of 323, 462 and 646 pounds per cubic inch were obtained. The same calculation for site 1 (with D = 9 in) gave $\bar{k}$ values of 257, 316 and 515. The correlation chart shown in Figure 69 gave the range of CBR value for site 2 from 28 to 73, and for site 1 from 18 to 52.

Moduli of subgrade reaction were not determined under asphaltic concrete pavement sections at Eglin Air Force Base by the Air Force Civil Engineering Center during the 1974 Survey (Reference 21): subgrade CBRs were obtained for these sections and these only at a few locations (about 10 in number). In the area of site 2, a CBR

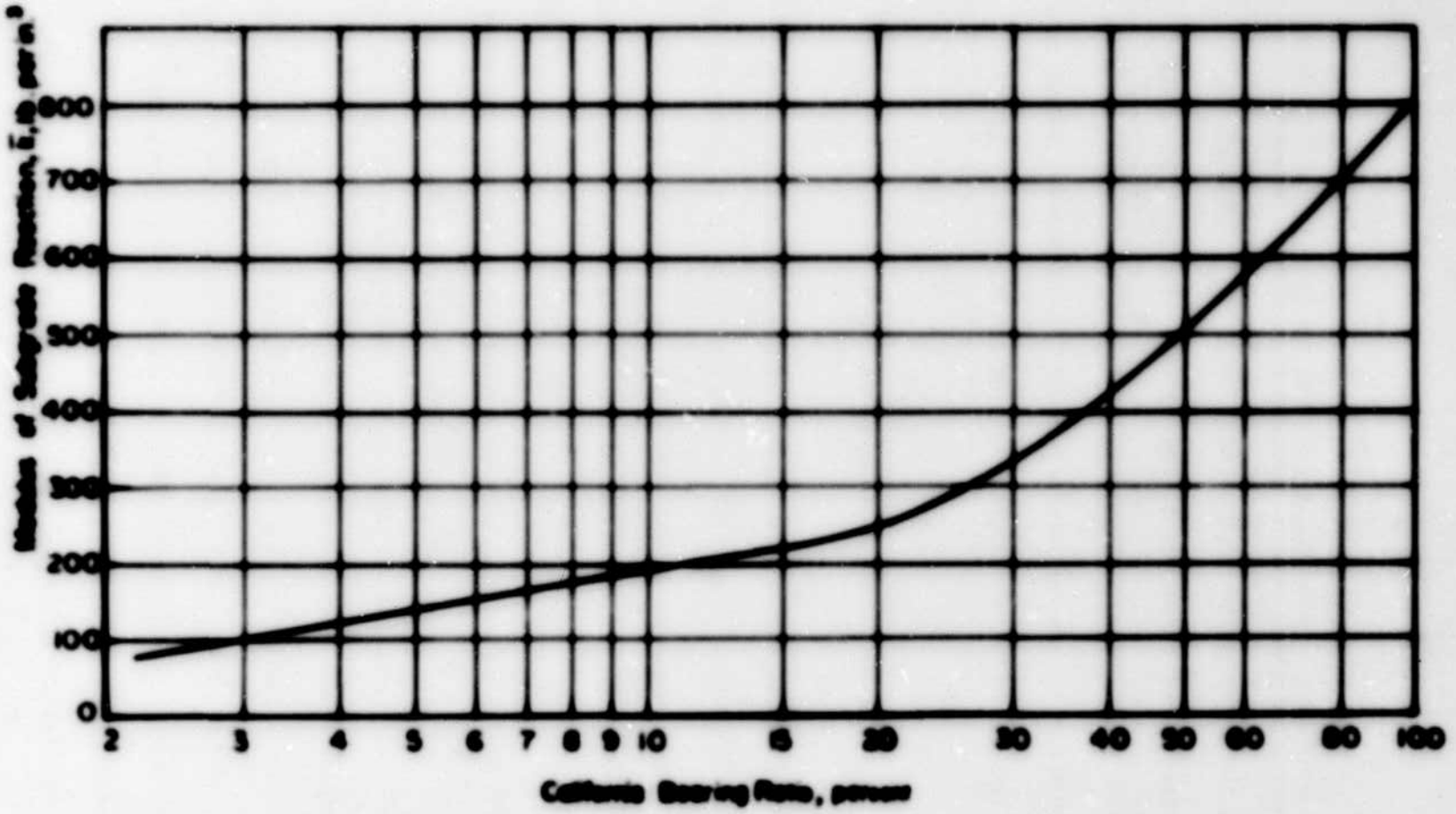



Figure 69. Relationship Between California Bearing Ratio and Modulus of Subgrade Reaction (after PCA [Reference 65])

value of 75 was reported. As noted above, this corresponds quite closely to the minimum calculated value of 73. The range of subgrade CBRs throughout the pavement sections varied from 10 to 85 percent. Reported $\bar{k}$ values, under the Portland Cement concrete sections, ranged from 220 to 520 psi.

It is interesting to note that the lower value of the range of CBRs for site 1 was about 18 while the low value for all the results was 10. Even though no CBR values were available in the vicinity of site 1, a comparison of its corresponding CBR and $\bar{k}$ values with those at site 2 indicate it to be an inferior pavement. This had been recognized by the Air Force as it is used only as a parking area; whereas, site 2 is an in-service taxiway.

In summary, the recommended procedure for estimating the $\bar{k}$ and CBR values from prototype F-4 loadings is as follows:

1. Estimate $A_{peak}$ from an arithmetic plot of distance ($x_j$) from edge of the tire print versus peak deflections at each gage ($z_j$). $A_{peak}$ is the intercept at $x = 0$.

2. Use equation (23b) to estimate $\bar{k}$, the modulus of subgrade reaction, and, if desired,

3. Find CBR value from established correlation charts such as Figure 69.

A worked example is shown in Appendix E.

## 7.3 Prediction

The prediction methodology consisted of (1) determining the relationship between the inputs of two vehicles at a standard site,

and (2) using this relationship to predict the response of one of the vehicles at another site, if only the response of that site to the other vehicle is measured.

### 7.3.1 Validity of the Concept of the "Equivalency Function"

The concept of the equivalency function has been used in many areas of engineering. In foundation engineering it has many names, some of which are "shape factor", "depth factor", and "inclination factor". In highway and airfield work it is known as "the equivalent single wheel load" or the "equivalent single axle load" or "layer equivalency factor". The basic underlying concept of "equivalency" is that two different entities can be related by a multiplier. In this work, the multiplier is a function of time - the equivalency function - and not a number.

The question arises as to whether the equivalency function defined at one site is applicable at another site where another set of conditions prevails. The results, Figure 32, showed that the equivalency function is indeed applicable under sets of conditions different from those under which it was first determined.

The equivalency function as defined in equation 21 is essentially a linear ratio of inputs of two vehicles at the same site. In reality the relationship between inputs is probably not linear; however, three factors seem to combine to make the effects of nonlinearity negligible.

First, consider the strain induced in the system due to prototype loading. Measured peak deflections are of the order of 0.05 inch,

whereas the depth of influence of the wheel load is of the order of 12 feet or 144 inches (Reference 60). Small strains, in general of about 0.0003, are thus induced in the system as a result of prototype loading. The linear approximation is valid because strains are small.

The linear approximation to actual nonlinear material behavior at small strains has been used in mechanics for years. Herr (Reference 66) has shown that if the functional relationship ($F_1$) between stress ($\sigma$) and strain ($\epsilon_x$, $\epsilon_y$, $\epsilon_z$, $\cdots$ $\gamma_{xy}$), given by the equation

$$\sigma_x = F_1 (\epsilon_x, \epsilon_y, \epsilon_z, \gamma_{yz}, \gamma_{xz}, \gamma_{xy})$$

is expanded in Maclaurin series, the equation

$$\sigma_x = (F_1)_o + \left(\frac{\partial F_1}{\partial \epsilon_x}\right)_o \epsilon_x + \left(\frac{\partial F_1}{\partial \epsilon_y}\right)_o \epsilon_y + \cdots + \left(\frac{\partial F_1}{\partial \gamma_{xy}}\right)_o \gamma_{xy}$$

results, if the higher order terms in the Maclaurin series are eliminated. The zero subscripts denote the value of the function $F_1$ relationship and its derivatives at zero strain. From this relation it can be seen that if strains are small a linear relationship exists between $\sigma_x$ and $\epsilon_x$, $\epsilon_y$, $\epsilon_z$, etc. Applying this same reasoning to the equivalency functions, the linear approximation between equivalent inputs works, because of the strains induced in pavement-subgrade systems due to prototype loads are, in general, small at all sites. The equivalency function at one site is thus the same equivalency function at another site where strains are small and of the same order of magnitude.

The second factor, which contributes to the validity of the

linear equivalency function, is inherent in the flexible pavement design procedures, that have evolved, and supports the "small strain" concept previously cited.

Pavements are designed, basically, to limit subgrade deflections. This can be inferred from the fact that conventionally, thick sections are constructed over weak subgrades, while on the other hand, thinner sections are built over strong subgrades. The net effect is that deflections and thus strains are forced to stay within the same order of magnitude of small strains by the design procedures. Since pavement sections are generally designed using conventional procedures, the "small strain" concept previously discussed should be valid for most pavements. Thus, the equivalency function between two such sites would be valid if strains at the two sites are of the same order of magnitude and small.

The third and final factor concerns the time the maximum load is actually applied at a point on the pavements. The time period that the wheel load is over a point is very small. Authors (References 40 and 47) have used Dirac Delta (impulse) functions to represent vehicular loads. Since the time is small, factors such as settlement, which normally are amplified in static cases, are of minimal importance in the dynamic mode.

### 7.3.2 Effects of Gear Configuration

The C-135, C-131 and C-130 aircraft have different gear configurations as shown in Figures 24 through 26. The prediction methodology permitted a vehicle having a single-twin gear configuration

(C-121) to be used as a standard vehicle to predict the response of a tri-tandem gear (C-135) and a single tandem gear (C-130). This implies that any vehicle in the inventory can be used as a standard vehicle. The combination of evaluation and prediction can thus be performed simultaneously by the selected vehicle. Thus, at each site evaluated, the response of all vehicles in the inventory can be predicted as a part of the evaluation.

### 7.3.3 Relative Effects of k, c and n Parameters

Figure 42 showed a typical plot of the calculated equivalent total force and of its force components with respect to the parameters k, c and n. The maximum resisting force due to the k parameter is seen to be about twice that of the resisting force due to the c parameter, and about 7 times greater than that of the n parameter. If design procedures could be directed toward greater utilization of the k parameter it appears that a more logical basis for design could be had.

## SECTION VIII

## EFFECTS OF DISTRIBUTION OF PASSES ON PAVEMENT PERFORMANCE

It is generally accepted by personnel concerned with airfield pavements that the response of the pavement-subgrade system is a function of the number of wheels on an aircraft gear, its gross load, tire pressures, width of tire print, ambient conditions and the lateral distribution of passes (References 1, 2, 3 and 4).

A method for quantifying the cumulative effect of the lateral distribution of passes, type of aircraft and ambient conditions in the content of pavement evaluation is presented. This method expands the concept of cumulative total pavement deflection presented by Highter and Horr (Reference 12). They found that a pavement could only accomodate a certain number of feet of cumulative total deflection prior to the onset of distress. Their data base consisted of AASHO Road Test data, data collected from Ponce and Castle Air Force Bases and from prototype testing on specially designed test sections at Kirtland Air Force Base. Analysis of the data showed that a threshold cumulative total peak pavement deflection, at which severe distress occurs in asphaltic airfield pavements, was about 2000 feet. For asphaltic highway pavements the threshold, was about 1200 feet.

### 8.1 Pass to Coverage (p/c) Ratio Based on Tire-Contact Area Width

The pass to coverage (p/c) ratio, in concept, relates the number of passes made by a vehicle across a pavement-section to the number of passes over a selected point on the pavement. This ratio has been

related conventionally to the number of wheels on an aircraft landing gear, the width of the tire print and the lateral distribution of the aircraft wheel paths.

Two procedures (References 1 and 57) have been used to define the p/c ratio. Both of these procedures use as principal parameters the width of the tire print and the lateral distribution characteristics of the passes over a particular pavement section. The FAA procedure (Reference 1) defines p/c using the relationship

$$c = \frac{0.75\ D\ N\ W}{12T} \qquad (24)$$

where

c = coverages

N = Number of wheels of gear of aircraft

T = Traffic width in feet (generally, 7.5)

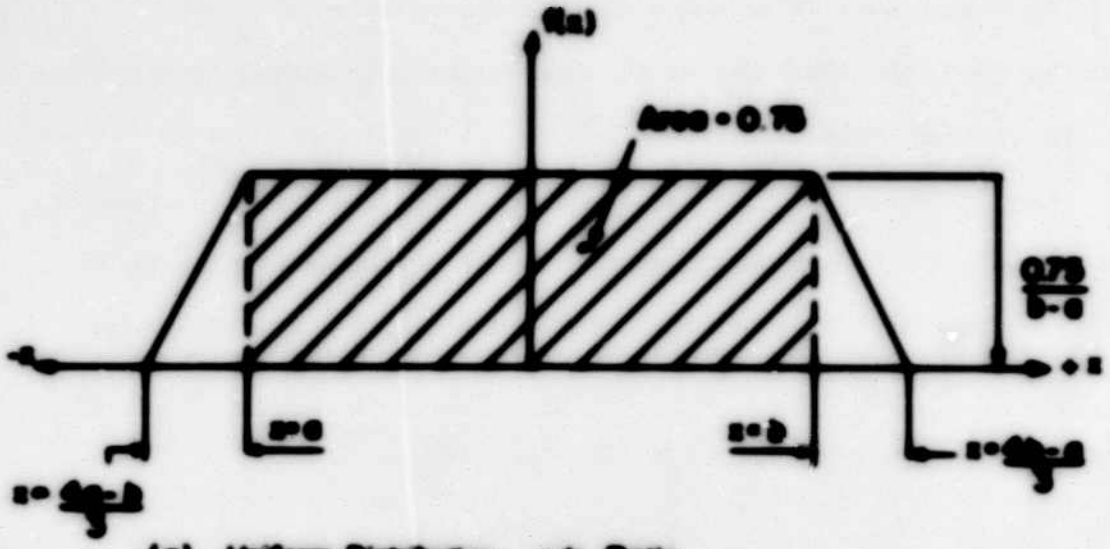
W = Width of tire contact area of one tire in inches, and

D = Cycles of operation (one cycle consists of one landing and one takeoff)

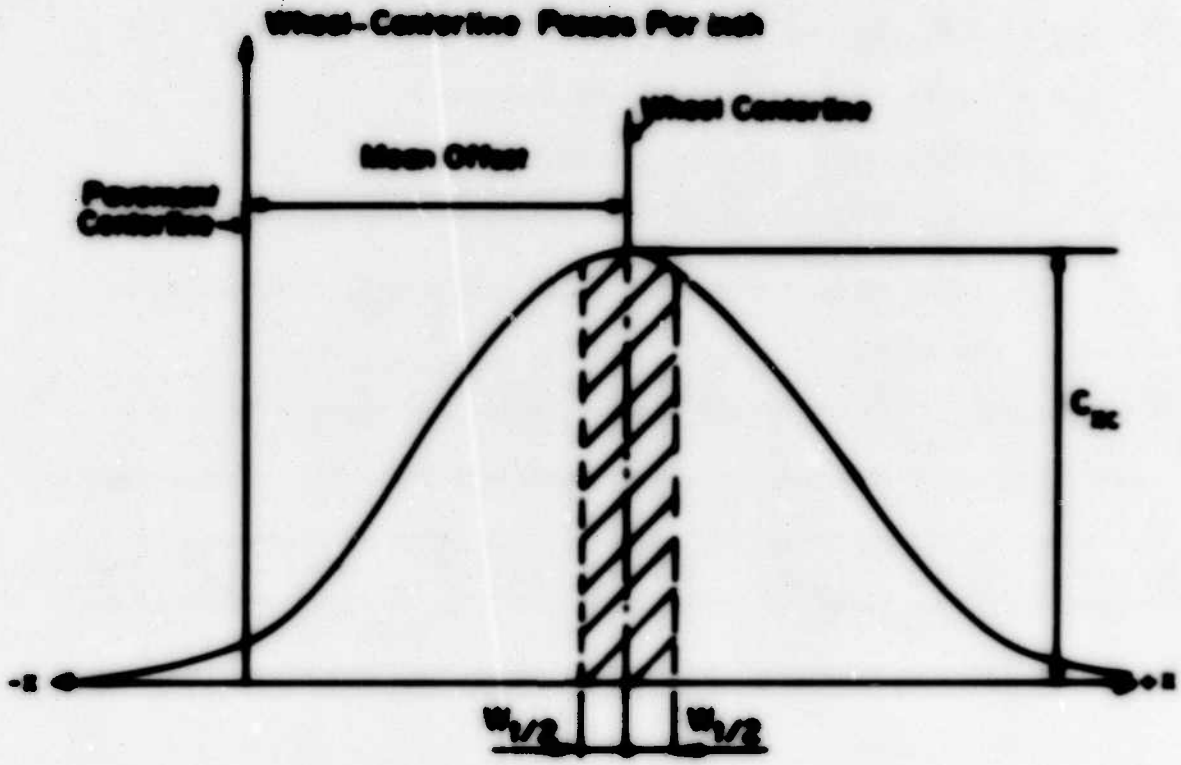
The constant, 0.75, is based on the assumption that the lateral distribution of aircraft can be approximated by a uniform distribution as shown in Figure 70(a). In concept, one cycle of operation is essentially two passes. Hence using D = p/2, equation (24) becomes,

$$c = \frac{(p/2)\ (0.75\ N\ W)}{12T}$$

$$= \frac{0.75\ p\ N\ W}{24T}$$



(a) Uniform Distribution p/c Ratio




(b) Theoretical Normal Distribution

Figure 70. Lateral Distribution of Aircraft Used in Design of Airfield Pavement (after Hoang [Reference 57])

Then

$$\frac{p}{c} = \frac{3T}{N W}$$

Based on measurements of the lateral distribution of aircraft on various runways and taxiways, Hofstad (Reference 57), proposed the use of a normal distribution instead of the uniform distribution, to describe the lateral distribution of aircraft. He gave the following expression for the p/c ratio:

$$p/c = \frac{1}{C_{nc} W_t}$$

where $W_t$ is the width of the tire contact area, "$C_{nc}$ represents the number of wheel-centerline passes per inch of width, per aircraft pass, which accumulate at the point where maximum accumulation occurs". Coverage c is defined as the maximum number of wheel passes at the point of maximum accumulation. Figure 70(b) illustrates the p/c ratio concept as applied to a single wheel. In concept, with reference to Figure 70(b), only the effects of tire prints or partial tire prints applied to the surface within the width $W_t$ are considered in this method.

The current FAA procedure and Hofstad's proposed method both use the tire print (contact area width) as a key parameter in the definition of the p/c ratio. The method developed here uses the measured dynamic lateral deflection profile, due to the prototype load, to define pass to coverage; and relates this ratio to performance extending the peak cumulative deflection concept introduced by Highter

and Marr (Reference 12).

## 8.2 Deflection-Based p/c Ratio

The fundamental concept underlying the deflection-based p/c ratio is founded on the following reasoning. The level of significance of a loaded wheel during one pass over a pavement section is indicated by the measured lateral dynamic deflection basin. As the lateral distance from the load wheel increases, the work done by the load decreases. Hence, immediately under the wheel the influence is greatest; whereas, at a point where the measured deflection is zero, the influence is negligible.

As one pass, in effect, produces deflections from a maximum under the wheel to zero at some distance from the wheel; for a p/c ratio to be meaningful, it should account not only for the induced energy level corresponding to the maximum deflection but for all the levels in the range. The principal reasoning here is that the pavement-subgrade system "remembers" not only the maximum deflection but all load induced deflections. Hence, in general, large load induced deflections at a point result in greater work done and remembrances of it, than do smaller load induced deflections.

With reference to Figure 71, each of the curves labelled P, Q, R, S represents a series of peak lateral deflections. If one pass of a load wheel is applied at a point corresponding to x = 0, the maximum deflection (at x = 0) would be $A = \Delta_0$. If the same load had been applied at x = 1, a maximum deflection of $\Delta_1$ would have been measured at x = 0. If the load had been applied at x = 2, then $\Delta_2$

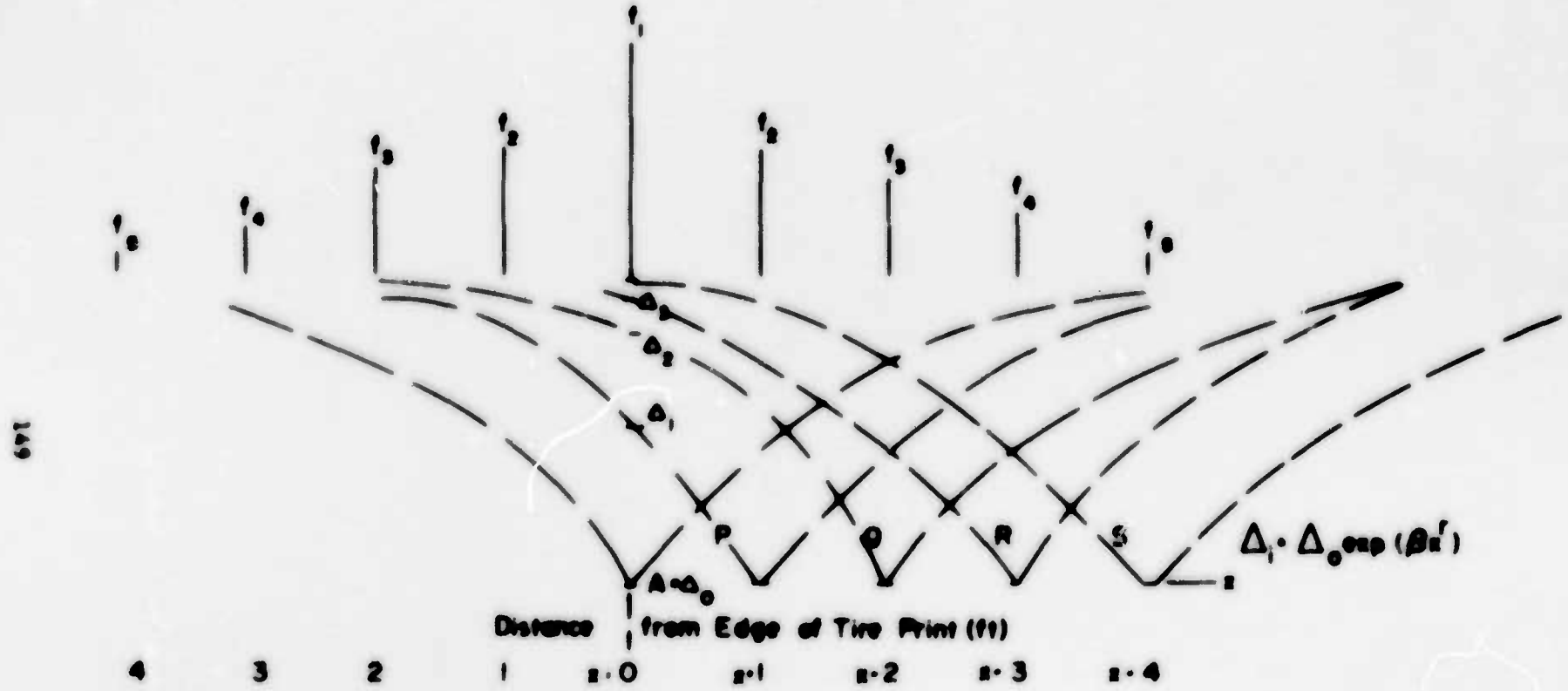



Figure 71. Overview of the Concept Used in the Deflection Based p/c Ratio Calculations

would have been measured at x = 0; similarly for a load at x = 1, etc.

One coverage then, in concept, is the cumulative peak deflection at the point in question that corresponds to maximum deflection A under the wheel. For example, if one pass of a load wheel is made at x = 0, then one coverage results at that point. On the other hand, one pass made at x = 1 corresponds to the fractional coverage $\Delta_1/A$ at x = 0.

Suppose that $f_o$ through $f_n$ are the discrete frequencies at x = 0, 1, 2, 3, ....., n, of the distribution of passes of aircraft laterally about x = 0. Then the cumulative peak deflection at x = 0 due to this frequency distribution becomes

$$\text{Cumulative Peak Deflection} = N_p \sum_{i=0}^{n} \Delta_i f_i$$

where $N_p$ is the number of passes and $\Delta_i$ are the peak deflections corresponding to the points in question. The coverages $N_c$ due to the $N_p$ passes is then,

$$N_c = \frac{\text{Cumulative Peak Deflection}}{\text{Maximum Deflection under the Wheel}}$$

$$= N_p \sum_{i=0}^{n} \Delta_i f_i / \Delta_o$$

Therefore,

$$\frac{N_p}{N_c} = \frac{P}{C} = \frac{\Delta_o}{\sum_{i=0}^{n} \Delta_i f_i}$$

Equation (24) is seen to have the same form as the expression for the equivalent permeability of a layered system (Reference 67)

$$k_y = \frac{d}{\sum_{n=1}^{n} d_n/k_n} \qquad (25)$$

where $k_y$ is the equivalent vertical permeability, $d_n$ and $k_n$ are the thickness and coefficient of permeability respectively of layer $n$, and $d$ is the sum of all the thicknesses.

## 8.3 Effects of Lateral Distribution

The effects of the frequency and of the lateral distributions of aircraft on the cumulative peak deflection and the deflection-based p/c ratio were studied.

Equation (2) in the form,

$$\Delta_j = \Delta_o \exp(\beta x_j^r)$$

was used to calculate the lateral dynamic deflection profile, where $\Delta_j$ and $x_j$ are the deflections and distances from the edge of the tire print at measurement points $j$ in a direction perpendicular to the direction of motion of the wheel. $\Delta_o$, $\beta$, and $r$ are the parameters describing the maximum dynamic lateral deflection basin as discussed in paragraph 3.2.1. The numerical values, shown in Table 7, will be used to illustrate the procedure. These values were obtained from data collected at Site 1, Eglin AFB, in March 1976.

Table 7

| $\Delta_o$ = 0.00479<br>$\beta$ = -0.801<br>r = 1.021 | |
|---|---|
| $x_j$ (ft) | $\Delta_j$ (ft) |
| 0 | 0.00479 |
| 1 | 0.00215 |
| 2 | 0.00094 |
| 3 | 0.00041 |
| 4 | 0.00018 |

Four discrete distributions are shown in Figure 72 for an assumed single wheel load. Figure 73 shows the effect of the four assumed lateral distributions (keyed by number to Figure 72) on the cumulative deflection. Figure 74 shows the effect of the scatter of the frequency distribution, as given by its standard deviation based p/c ratio. These results show that,

1. the assumption of a uniform distribution of passes (distribution ① on Figure 72) yields the least cumulative peak deflection per pass and,
2. as would be expected, the distribution with the smallest scatter yields the greatest cumulative peak deflections.

8.4 Discussion

The results showed the dependence of cumulative peak deflection

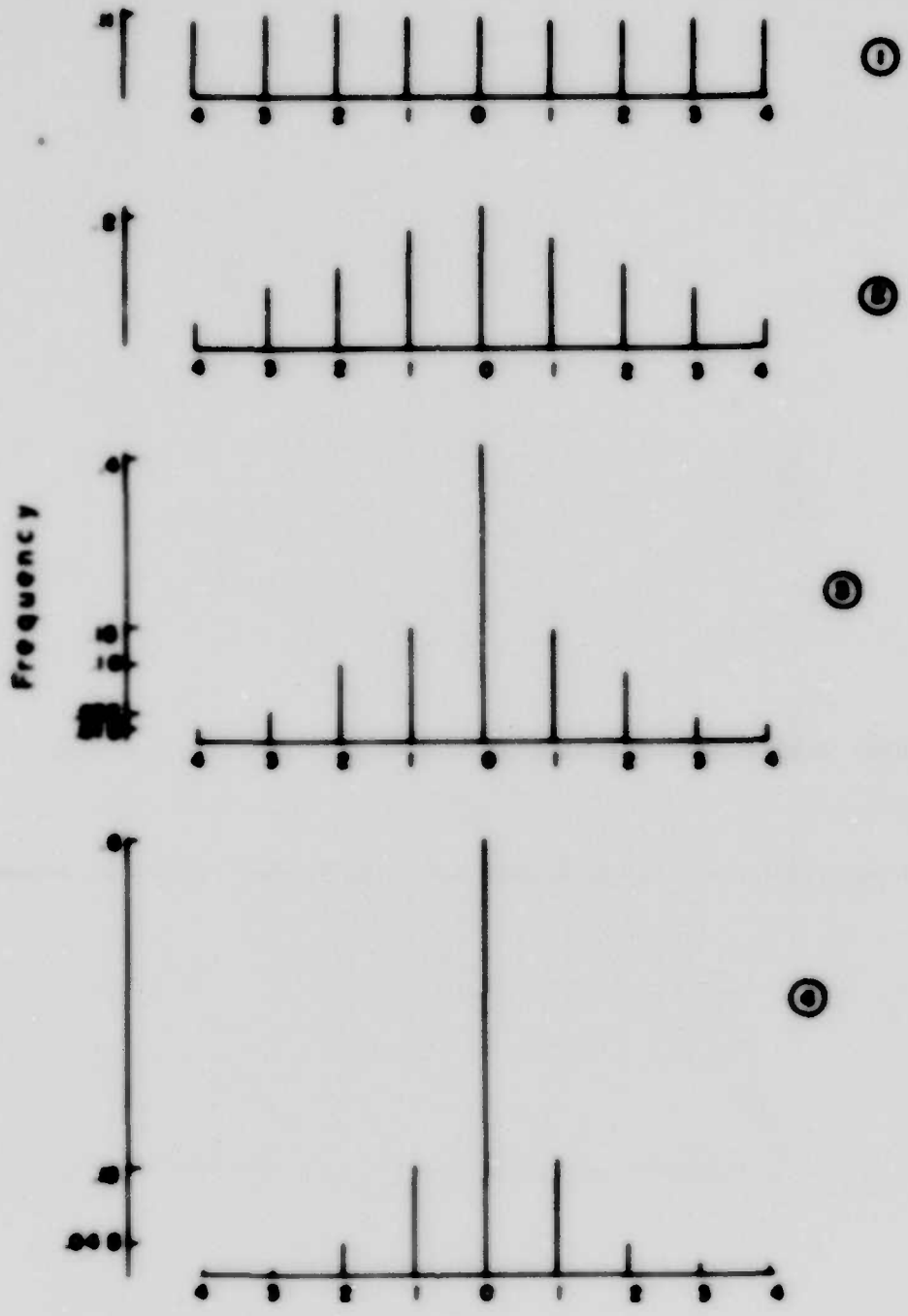



Figure 72. Discrete Distributions Used in Study

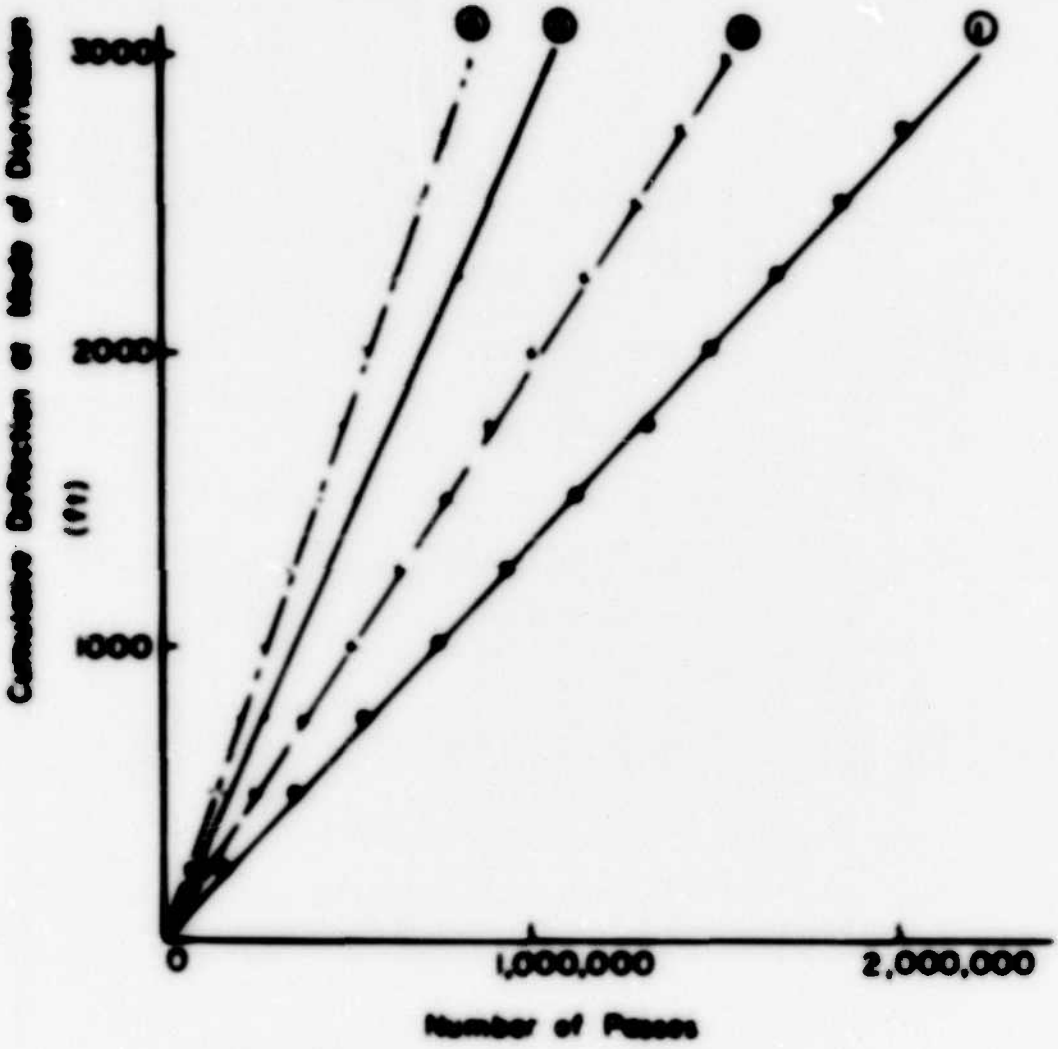



Figure 73. Cumulative Deflection vs. Passes for Four Discrete Distributions of Passes

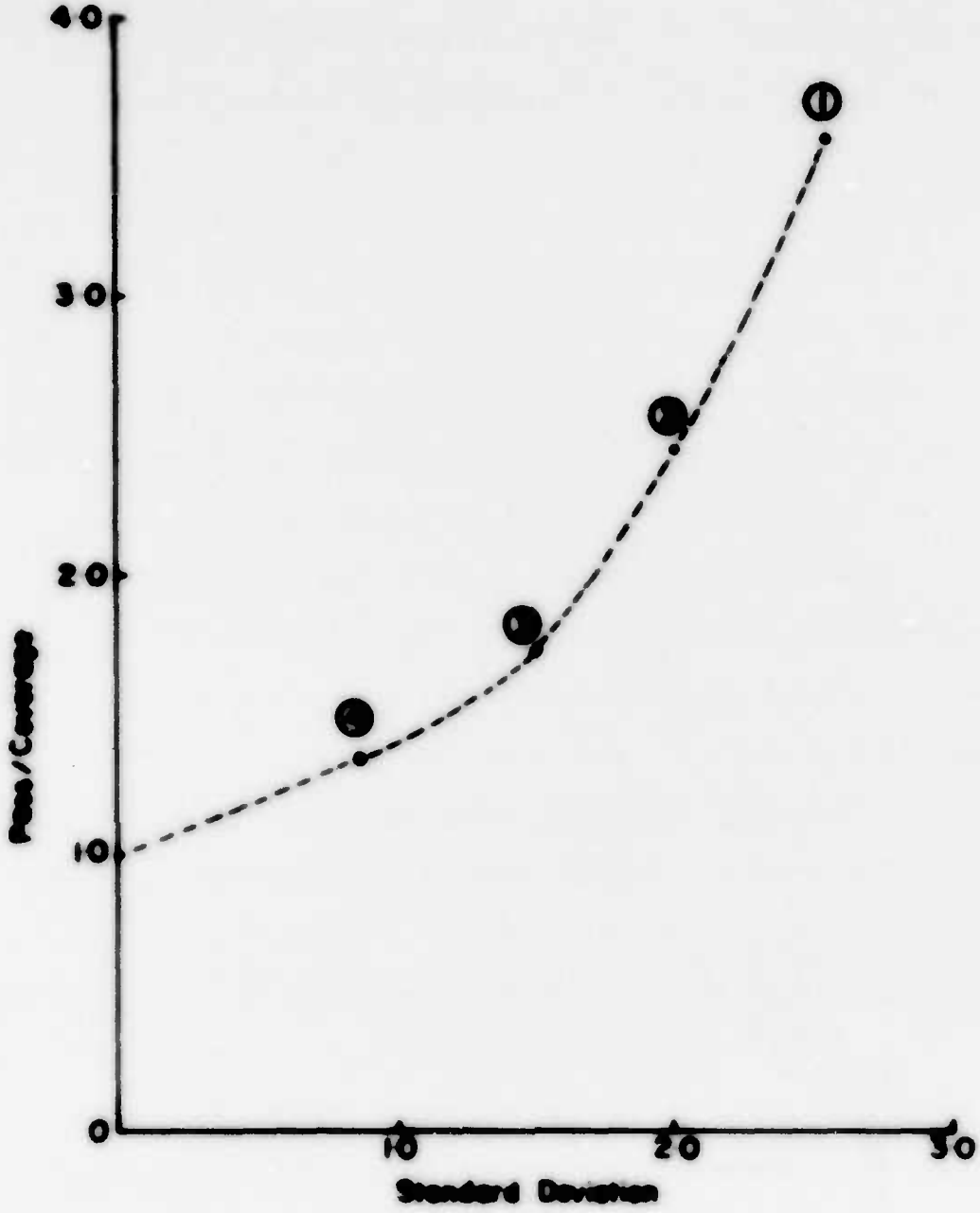



Figure 74. Effects of Standard Deviation on Deflection-Based p/c Ratio

on the lateral distribution of passes and the peak deflection profile. The p/c ratio thus provides a means of quantifying the variability of the input (aircraft loads) characteristics and pavement-subgrade system response (output).

With reference to Figure 75, input variables consist of aircraft loads and lateral distribution characteristics of loads. These can include wind effects, surface condition, type of aircraft, and quantity of fuel aboard. The main output variable is the peak pavement deflection profile. Inherent in this measurement are temperature effects and other ambient conditions. Figure 75 shows how the p/c ratio can be utilized to estimate the amount of energy imparted to a pavement-subgrade system due to variable inputs and also how to estimate the number of passes required to induce a certain energy input as given by the total cumulative peak deflections.

For example, assuming that the lateral distribution of passes has a standard deviation Of 2.0 (distribution ② in Figure 73), the number of passes required to reach the threshold[13] total cumulative peak deflection value of 2200 feet is 1,160,000 passes or 580,000 cycles of operation.

On the other hand, if the assumed lateral distribution of passes has a standard deviation of 2.66, then 580,000 cycles of operation would yield a cumulative peak deflection value of about 1500 feet, which is well below the threshold[13] value for that distribution. For this case 850,000 cycles of operation could be tolerated before severe

[13] The threshold value of 2200 feet was given by Highter (Reference 12) without due regard to the lateral positioning of traffic. Lacking additional information at this time the same value was used in the present study.

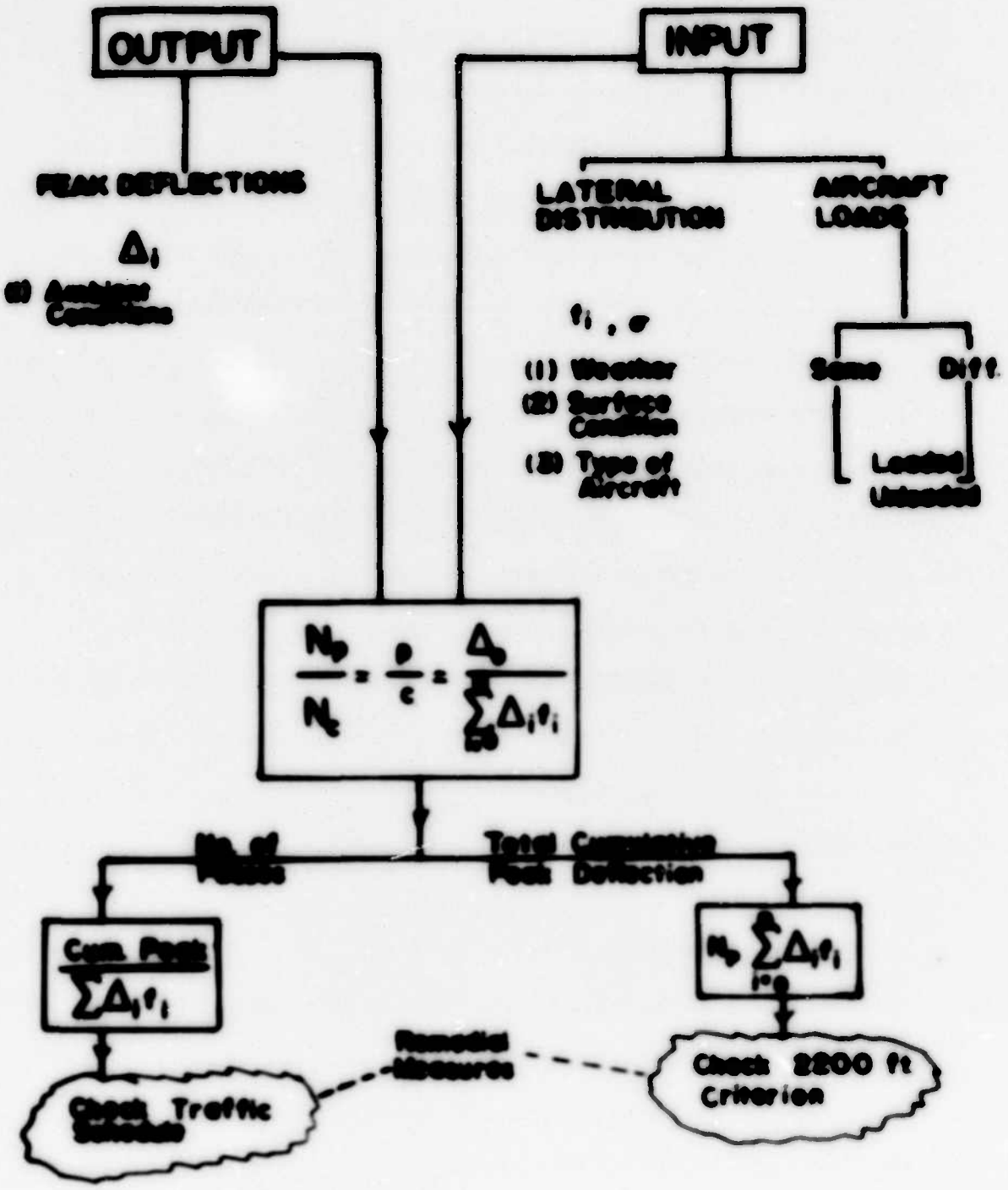



Figure 75. Overview of Evaluation Scheme Using Deflection Frequency Relationship

distress might be expected.

As another example, suppose that due to overlay or resurfacing of pavement, parameters and peak deflections change to those given in Table 8 after 290,000 cycles of operation, then 700,000 cycles of operations (rather than 290,000) would now be required to attain the threshold[14] value of 2200 feet. This assumes that the section "remembers" the loading prior to resurfacing. If resurfacing had not taken place, only 290,000 cycles of operation would have been required to show effects of distress.

The above examples have attempted to show that actual measured distribution data such as that provided by HoSang (Reference 57), and actual measured deflections (which account for ambient seasonal effects) can be combined to estimate the cumulative damage effects due to prototype loads. Once a standard site and standard vehicle have been selected, the damage effects of various magnitudes of loads

Table 8

| | |
|---|---|
| $\Delta_0$ | = 0.0012 |
| $\beta$ | = -0.2256 |
| r | = 1.7770 |
| $x_j$ (ft) | $\Delta_j$ (ft) |
| 0 | 0.00120 |
| 1 | 0.00096 |
| 2 | 0.00055 |
| 3 | 0.00024 |
| 4 | 0.00085 |

[14] See Footnote 13.

and gear configurations and their distributions can be estimated. By monitoring the effects of specific pavement sections, the direction which remedial measures should take could be established [see Highter and Barr (Reference 12)].

## SECTION IX

## SUMMARY

The findings of the present research effort can be summarized under three basic categories, namely:

1. nondestructive pavement testing equipment development,
2. nondestructive pavement evaluation and behavior prediction, and
3. extension of cumulative peak deflection-damage-energy related concepts.

Two equipment systems for use in the nondestructive evaluation of flexible pavements have been developed. They are the LED system and the LVDT system. The feasibility of rapidly measuring pavement deflections caused by moving loads using the developed equipment has been investigated. Field testing of the developed systems using prototype loads was conducted.

A nondestructive pavement evaluation methodology using transfer function theory has been developed. Parameters of the transfer function which reflect site characteristics have been isolated and related to performance of two sites. Parameters of the lateral peak deflection profiles have been investigated. Simplified procedures for estimating the parameters of the transfer function and parameters (CBR, etc.) used in design have been suggested.

A methodology has been presented for predicting the deflection if the response at a standard site to a standard load vehicle and another vehicle, and the response of the other sites to the standard vehicle are known. The same transfer function parameters that are used in the

evaluation phase are used in the prediction scheme.

A method of accounting for the lateral distribution of aircraft on a pavement, and variability of input and output to the pavement-subgrade system has been presented. The interrelationship among the components of NDT pavement evaluation-response prediction-cumulative damage prediction based on deflections caused by prototype loading has been discussed. The deflection based pass to coverage ratio was shown to be a vital link in the scheme.

## SECTION X

## CONCLUSIONS

This research effort has attempted to cover a spectrum of activities that comprise nondestructive testing and evaluation of flexible airfield pavements. The following conclusions have been reached as a result of this study.

1. Rapid nondestructive measurements of pavement deflections due to moving prototype loads can be obtained in the field using the LED system "breadboarded" in this research effort and the companion LVDT system.
2. The parameters of both the transfer function and the peak lateral deflection profile reflect characteristics of the pavement-subgrade systems and can be used as the basis of a nondestructive pavement evaluation scheme. Some common parameters such as CBR and modulus of subgrade reaction can be obtained from those defined in this study.
3. The developed methodology, using the same parameters of the transfer function that are used to evaluate a pavement system, can be used to predict the deflection response function of a site to different magnitudes and configurations of loadings.
4. The concept of cumulative peak deflection (Reference 12) as it relates to energy induced in a pavement-subgrade-system due to load repetition, was extended to account for the lateral distribution of aircraft. The frequency characteristics and the number of passes of aircraft are shown to

effect, significantly, the amount of distress a pavement might evidence in time.

## SECTION XI

## RECOMMENDATIONS

This work has afforded the opportunity to consider in some depth a significant portion of the current state of the art of nondestructive testing theory and methods used on airfield pavements. Based on the findings of this work the following recommendations are forwarded:

1. The use of prototype loadings in evaluation should be encouraged.
2. The development of a scheme, based on the use of nondestructively measured pavement deflections due to prototype loads, similar to that briefly discussed in paragraph 8.4 of this work should be pursued.
3. The prototype of noncontact measuring equipment shown to be feasible in this investigation should be developed. This development should take advantage of the current state of the art in optical design.
4. A thorough study of the lateral distribution of aircraft has recently been made (Reference 57). A similar information gathering study should be initiated to collect data on numbers and types of aircraft using specified pavements at both commercial and military installations. Pavement deflections should be obtained regularly at the sections being monitored. This data base is necessary if the concepts and the preliminary conclusions reached at this time are to be validated and generalized.
5. The speedy development of a prototype device to move over the

pavement sections and simultaneously measure its own dynamic deflection basin without significantly interrupting traffic would greatly facilitate the information gathering phase. This would simultaneously provide a common denominator or standard vehicle.

6. Research should be directed towards determining the influences of the components of a pavement-subgrade system on the k, c, and n parameters. The success of this endeavor would be a step towards optimizing design procedures and the use of paving materials.

## LIST OF REFERENCES


1. Federal Aviation Administration, Advisory Circular AC 150/5320-6A, Airport Paving, U. S. Department of Transportation, May 1967.

2. Design Manual - Airfield Pavements, Department of the Navy, NAVFAC - DM-21, June 1973.

3. Design and Evaluation of Flexible and Rigid Pavements, Department of Transportation, Ottawa, Canada, June 1962.

4. Design and Evaluation of Aircraft Pavements, 1971, Directorate of Civil Engineering Development, Department of the Environment, London, 1971.

5. Hanson, D., I., "Special Problems with Airfield Pavement Maintenance," Proceedings of a Workshop on Pavement Rehabilitation, Transportation Research Board, Report No. FHWA-RD-74-60, Washington, D.C., June 1974.

6. Busching, H. W., Goetz, W. H., and Marr, M. E., "Stress-Deformation Behavior of Anisotropic Bituminous Mixtures," Proceedings, Assn. Asphalt Paving Technology, Vol. 36, 1967.

7. Goetz, W. H., Marr, M. E., and Lal, H. B., "Invarient Properties of a Sheet-Asphalt Mixture," Highway Research Record No. 158, 1967.

8. Swami, S. A., Goetz, W. H., Marr, M. E., "Time and Load Independent Properties of Bituminous Mixtures," Highway Research Board, Record No. 313, 1970.

9. Ali, G. A., "A Laboratory Investigation of the Application of Transfer Functions to Flexible Pavements," Ph.D. Thesis, Purdue University, August 1972.

10. Marr, M. E., Boyer, R. E., "Predicting Pavement Performance Using Time-Dependent Transfer Functions," AFWL-TR-72-204, Kirtland Air Force Base, New Mexico, January 1973.

11. Boyer, R. E., "Predicting Pavement Performance Using Time-Dependent Transfer Functions," Ph.D. Thesis, Purdue University, August 1972.

12. Highter, W. H., and Marr, M. E., "Application of Energy Concepts to the Performance of Airfield Pavements," Tech. Rept. AFWL-TR-72-225, Kirtland Air Force Base, New Mexico, June 1973.

13. Highter, W. H. "The Application of Energy Concepts to Pavements," JHRP Rept. 38, Purdue University.

14. Haas, R., "Surface Evaluation of Pavements: State of the Art," Report No. FHWA-RD-74-60, Transportation Research Board, Washington, D. C., June 1970.

15. McComb, Richard A., and Labra, John J., "Structural Evaluation and Overlay Design for Highway Pavement," A Review Report No. FHWA-RD-74-60, Transportation Research Board, Washington, D.C.,

16. Witczak, M. W., "Structural Evaluation and Overlay Design Methodology for Airfield Pavements: State of the Art," Report No. FHWA-RD-74-60, Transportation Research Board, Washington, D.C., June 1970.

17. McCullough, B. Frank, "State of the Art in Predicting the Probabilistic Response of Pavement Structures." Transportation Research Record No. 575, 1976.

18. "Airfield Flexible Pavements Air Force, Departments of the Army and the Air Force," TM 5-824-2 (AFM 88-6, Chap. 2), Feb. 1969.

19. American Society for Testing and Material "Standard Method for Nonrepetitive Static Plate Load Tests on Soils and Flexible Pavement Components for Use in Evaluation and Design of Airport and Highway Pavements." ASTM Designation D1196 Vol. , 1971.

20. American Society for Testing and Materials, "Standard Method for Repetitive Static Plate Load Tests of Soils and Flexible Pavement Components, for Use in Evaluation and Design of Airport and Highway Pavements." ASTM Designation D1195, Vol. , 1971.

21. AFCEC - Tyndall AFB, "Air Field Evaluation Report - Eglin AFB, Florida," Tyndall AFB, Florida, March 1975.

22. Vittas, George P., "A User Viewpoint on Airport Design Standards Past, Present and Future." Symposium on Nondestructive Tests and Evaluation of Airport Pavements, U. S. Army Engineer Waterways Experiment Station, Vicksburg, Mississippi, November 1975.

23. Scrivner, Frank H., Peohl, Rudell, Moore, W. M., and Phillips, M. B. "Detecting Seasonal Changes in Load-Carrying Capabilities of Flexible Pavements." Highway Research Board, National Cooperative Highway Research Program Report 76, 1969.

24. Isaada, M. M., "Impulsive Load Stiffness of Flexible Pavements," Proceedings of the American Society of Civil Engineers, Journal of Soil Mechanics and Foundation Division, Vol. 96, No. SM2, March 1970.

25. Green, J. L. and Hall, J. W., "Nondestructive Vibratory Testing of Airport Pavements, Experimental Test Results and Development of Evaluation Methodology and Procedure," Vol. 1, Report No. FAA-RD-73-205-1, U. S. D. T. - FAA, Washington, D. C., September 1975.

26. Pister, K. S., and Williams, M. L., "Bending of Plates on a Viscoelastic Foundation," Journal of the Engineering Mechanics Division, Proceedings of the ASCE, Vol. 86, No. EM5, October, 1960.

27. Pister, K. S., and Monismith, C. L., "Analysis of Viscoelastic Flexible Pavements," Flexible Pavement Design Studies 1960, Highway Research Bulletin 269, 1960.

28. Reissner, E., "A Note on Deflections of Plates on a Viscoelastic Foundation," Transactions of the ASME, Vol. 25, No. 1, March 1958.

29. Hoskin, B. C., and Lee, E. H., "Flexible Surfaces on Viscoelastic Subgrades," Journal of the Engineering Mechanics Division, Proceedings of the ASCE, Vol. 85, No. EM4, October, 1959.

30. Barksdale, R. D., and Leonards, G. A., "Predicting Performance of Bituminous Surfaced Pavements," Proceedings, International Conference on the Structural Design of Asphalt Pavements, University of Michigan, 1967.

31. Pister, K. S., and Westmann, R. A., "Analysis of Viscoelastic Pavements Subjected to Moving Loads," Proceedings, International Conference of the Structural Design of Asphalt Pavements, University of Michigan, 1963.

32. Harr, M. E., and Lewis, K. H., "Analysis of Concrete Slabs Subjected to Warping and Moving Loads," Highway Research Board Record No. 291, 1969.

33. Harr, M. E., and Leonards, G. A., "Analysis of Concrete Slabs on Ground Journal of the Soil Mechanics and Foundations Division," Proceedings of the ASCE, Vol. 85, No. SM3, June, 1959.

34. Gesi, D. C., "Analysis of Finite Beams on Elastic Foundations," Journal of the Structural Division, Proceedings of the ASCE, Vol. 84, No. ST4, July 1958.

35. Pister, K. S., "Viscoelastic Plate on a Viscoelastic Foundation," Journal of the Engineering Mechanics Division, Proceedings of the ASCE, Vol. 87 No. EM1, February 1961.

36. Hogg, A. H. A., "Equilibrium of a Thin Plate, Symmetrically Loaded, Resting on an Elastic Foundation of Infinite Depth," Philosophical Magazine, Vol. 25, 1938.

37. Terzaghi, K., "Evaluation of Coefficients of Subgrade Reaction," Geotechnique, Vol. 5, No. 4, December, 1955.

38. Harr, M. E., "Influence of Vehicle Speed on Pavement Deflection," Proceedings, Highway Research Board, Vol. 44, 1962.

39. Freudenthal, A. M., and Lorsch, H. G., "The Infinite Elastic Beam on a Linear Viscoelastic Foundation," Journal of the Engineering Mechanics Division, Proceedings of the ASCE, Vol. 83, No. EM1, January 1957.

40. Perloff, W. H., and Moavenzadeh, F., "Deflection of Viscoelastic Medium due to a Moving Load," Proceedings, International Conference on the Structural Design of Asphalt Pavements, University of Michigan, 1967.

41. Weiss, R. A., "Nondestructive Vibratory Testing of Airport Pavements," Vol. II, Report No. FAA-RD-73-205-II, U. S. D. T.-FAA, Washington, D.C., April 1975.

42. Wiseman, Gdalyah, "The Interpretation of Surface Deflection Measurements Using the Model of an Infinite Plate on an Elastic Foundation," Symposium on Nondestructive Test and Evaluation of Airport Pavements, Vicksburg, Mississippi, November 1975.

43. Orellana, J. E., "FPS-11 Flexible Pavement System Computer Program Documentation," Texas Highway Department; Texas Transportation Institute, Texas A&M University; and Center for Highway Research, University of Texas at Austin, Research Rept. 123-15, April 1972.

44. Zube, E. and R. Forsyth, "Flexible Pavement Maintenance Requirements as Determined by Deflection Measurements," Highway Research Record 129, 1966.

45. "Asphalt Overlays and Pavement Rehabilitation," The Asphalt Institute, Manual Series 17, November 1969.

46. Darter, M. I. and Hudson, W. R., "Probabilistic Design Concepts Applied to Flexible Pavement Design," Center for Highway Research, University of Texas at Austin, Research Rept. 123-18, 1973.

47. Moavenzadeh, Fred, "Stochastic Model for Prediction of Pavement Performance," Transportation Research Record 575, Washington, D.C., 1976.

48. Vignot, J. E. et al., "Aircraft Dynamic Wheel Load Effects on Airport Pavements: Final Report," Report No. FAA-RD-70-19, May 1970, Federal Aviation Administration, Washington, D.C.

49. Horn, W. J. and Ledbetter, R. H., "Pavement Response to Aircraft Dynamic Loads: Instrumentation Systems and Testing Program," Report No. FAA-RD-74-39, Vol. I, June 1975, Federal Aviation Administration, Washington, D.C., and Technical Report S-75-11, Vol. I, June 1975, U. S. Army Engineer Waterways Experiment Station, CE, Vicksburg, Miss.

50. Ledbetter, R. H., "Pavement Response to Aircraft Dynamic Loads; Presentation and Analysis of Data; Appendix B: Data," Report No. FAA-RD-74-32, Vol. II, September 1975, Federal Aviation Administration, Washington, D.C., and Technical Report S-75-11, Vol. II, September 1975, U. S. Army Engineer Waterways Experiment Station, CE, Vicksburg, Miss.

51. Szendrei, S., and Kühn, S. H., "Interpretation of Vibration Tests on Roads by the Impedance Method," Highway Research Board No. 66, 1963.

52. Baladi, G. Y., "Invariant Properties of Highway Material," Ph.D. Thesis submitted to Purdue University December 1976.

53. Harr, M. E., "Analytical and Numerical Methods in Engineering," Class Notes, Purdue University, 1975.

54. AFWL, "Aircraft Characteristics for Airfield Pavement Design and Evaluation," Technical Report No. AFWL-TR-69-54, Kirtland Air Force Base, N. M., October 1969.

55. Yoder, E. J. and Witczak, M. W., "Principles of Pavement Design," 2nd Edition, John Wiley and Sons, Inc., New York, 1975.

56. Murphy, Carl G., "Electro-Optical Pavement Deflection Measuring System," Submitted to Purdue University, W. Lafayette, Indiana, 1976.

57. HoSang, Victor A., "Field Survey and Analysis of Aircraft Distribution on Airport Pavements," Report No. FAA-RD-74-36, Federal Aviation Administration, Washington, D.C., February 1975.

58. Yoder, Eldon J. and Gramling, L. Wade., "Measurement Systems - Report of Group 2," Proceedings of a Workshop on Pavement Rehabilitation, Federal Highway Administration, Report No. FHWA-RD-74-63, Washington, D.C., June 1974.

59. Woods, K. B., "Screening of Surface Waves in Soils," Journal of Soil Mechanics and Foundations Division, Proceedings, American Society of Civil Engineers, Vol. 94, No. SM4, July 1968.

60. Ledbetter, R. H., Ulery, Jr., H. H., and Alvin, R. G., "Traffic Tests on Airfield Pavements for Jumbo Jets," Proceedings of the Third International Conference on the Structural Design of Asphalt Pavements, University of Michigan, Ann Arbor, Michigan, 1972.

61. Whittemore, Allan P., Wiley, John R., Schultz, Phillip C, and Pollock, Donald E., "Dynamic Pavement Loads of Heavy Highway Vehicles," National Cooperative Highway Research Program Report 105, Highway Research Board, 1970.

62. Nichols, Jr. F. P., "Deflections as an Indicator of Flexible Pavement Performance," Special Report, Virginia Council of Highway Investigation and Research, 1963.

63. Ford, Jr. M. C., and Bissolt, J. R., "Flexible Pavement Performance Studies in Arkansas," Highway Research Board Bulletin 321 (1962).

64. Kung, Juang-Yuan, "A New Method in Correlation Study of Pavement Deflection and Cracking," Proceedings of the Second International Conference on the Structural Design of Asphalt Pavement, University of Michigan, Ann Arbor, Michigan 1967.

65. Portland Cement Association, "The Design of Concrete Pavements for City Streets," PCA, Skokie, Illinois, 1963.

66. Harr, M. E., "Foundations of Theoretical Soil Mechanics," McGraw Hill Book Company, New York 1966.

67. Harr, M. E., "Groundwater and Seepage," McGraw Hill Book Company, New York 1962.

68. Nielsen, John P.,"Pavement Evaluation System,"AFCEC-TR-76-28, Tyndall Air Force Base, Florida, December 1976.

69. Benkelman, A. C., "Analysis of Flexible Pavement Deflection and Behaviour Data," Highway Research Board Bulletin 210, 1959.

70. Prandi, E., "LaCroix-LCPC Deflectograph," Proceedings of the Second International Conference on the Structural Design of Flexible Pavements, University of Michigan, Ann Arbor, Michigan, August 1967.

71. Still, P. B., and Winnett, M. A., "Development of Contactless Displacement Transducer," Transport and Road Research Laboratory TRRL Rept. 680, Department of the Environment, Crowthorne, Berkshire 1975.

# APPENDIX A

# RESEARCH AND DEVELOPMENT

# OF

# MEASUREMENT SYSTEMS

The breadboard model of the LED system was subcontracted by Purdue University to Science Applications Incorporated (SAI), New Mexico, during the period May, 1974 to December, 1975. The contents of Section a of this Appendix is based principally on SAI's Final Report (Reference 56).

During the period January 1975 to June 1976, the breadboard model electronics was upgraded at Purdue University and work was done to convert the static measurement system in order to make it more compatible with a moving beam-moving load concept. Section b of this Appendix presents a summary of this work.

Section c of this Appendix presents some details of the Linear Variable Differential Transformer System (LVDT) developed at Purdue University by G. Baladi (Reference 52) for a study sponsored by the FHWA.

a. <u>The LED System</u>

Several optical systems were considered during the development of the LED system. These include:

1. A retroflector module whose motion is detected by a laser beam.
2. A limited version of the global Moire method.
3. Focal point shift detection.
4. Triangulation of a light spot on a surface.

As the triangulation method was finally selected for development, only the summary details concerning this method are presented herein.

The breadboard model employing the triangulation method is shown in Figure A-1. This arrangement has an image shift $\delta_2$ (Figure A-2) perpendicular to the line of view which is related to the pavement deformation by the equation,

$$\delta_2 = m \frac{\sin(\gamma + \beta)}{\sin \gamma} \cdot \frac{\delta}{\tan(90 - \gamma)}$$

where m is the magnification of the deformation. Other symbols are designated in Figure A-2. The pavement "roughness" function is represented by f(x).

The straight line of the input center ray is given by

$$y = (x-b) \tan(90 - \gamma)$$

or

$$y = x \tan(90 - \gamma) + a$$

The intersection of the input ray with f(x) is at $x_o$, giving

$$f(x_o) = x_o \tan(90 - \gamma) + a$$

and the intersection with the displaced f(x) is at $x_1$, giving

$$\delta + f(x_1) = x_1 \tan(90 - \gamma) + a$$

Using a Taylor expansion near $x_o$ to get $f(x_1)$ and dropping higher orders gives

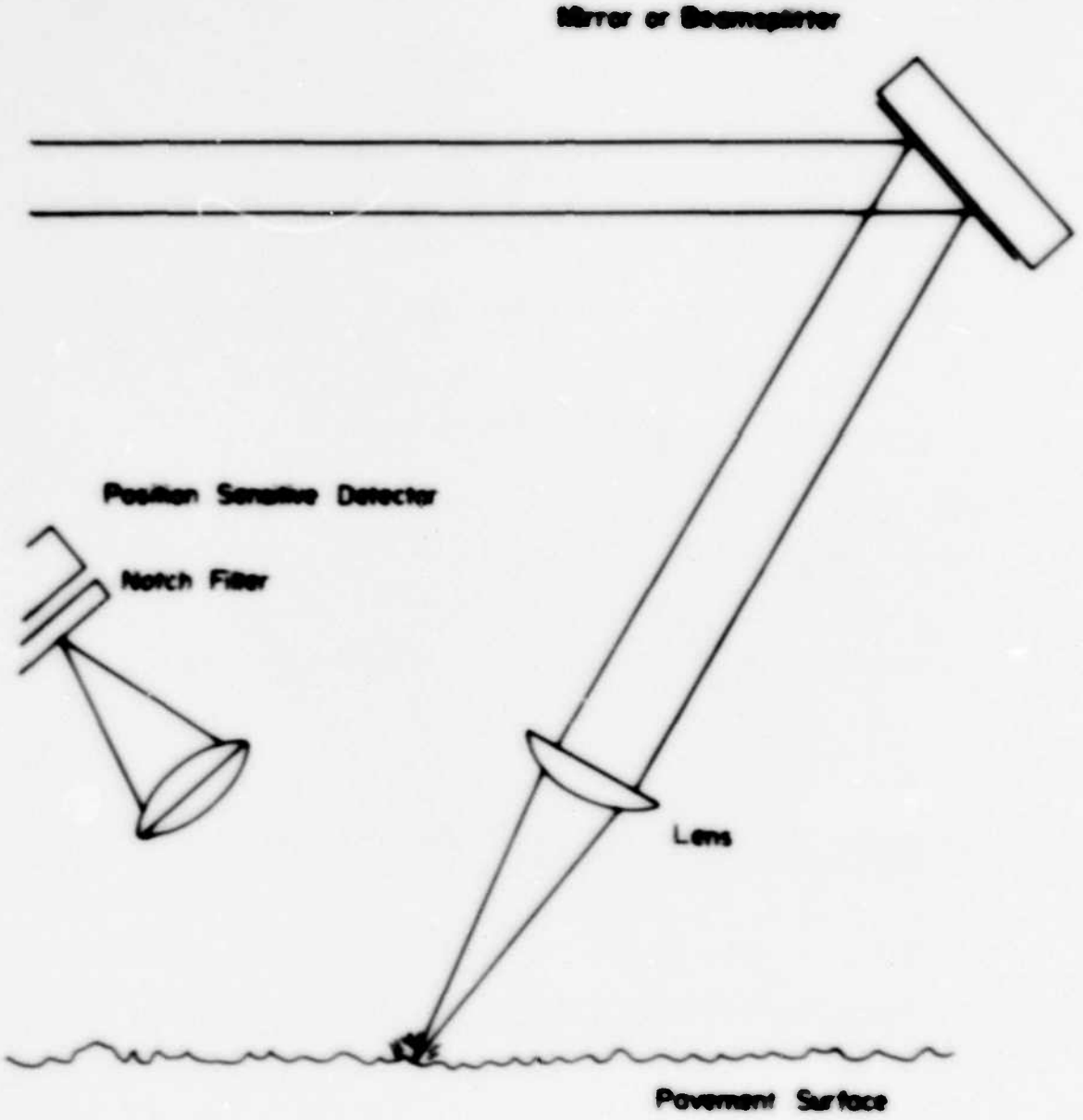



Figure A-1. Triangulation Arrangement

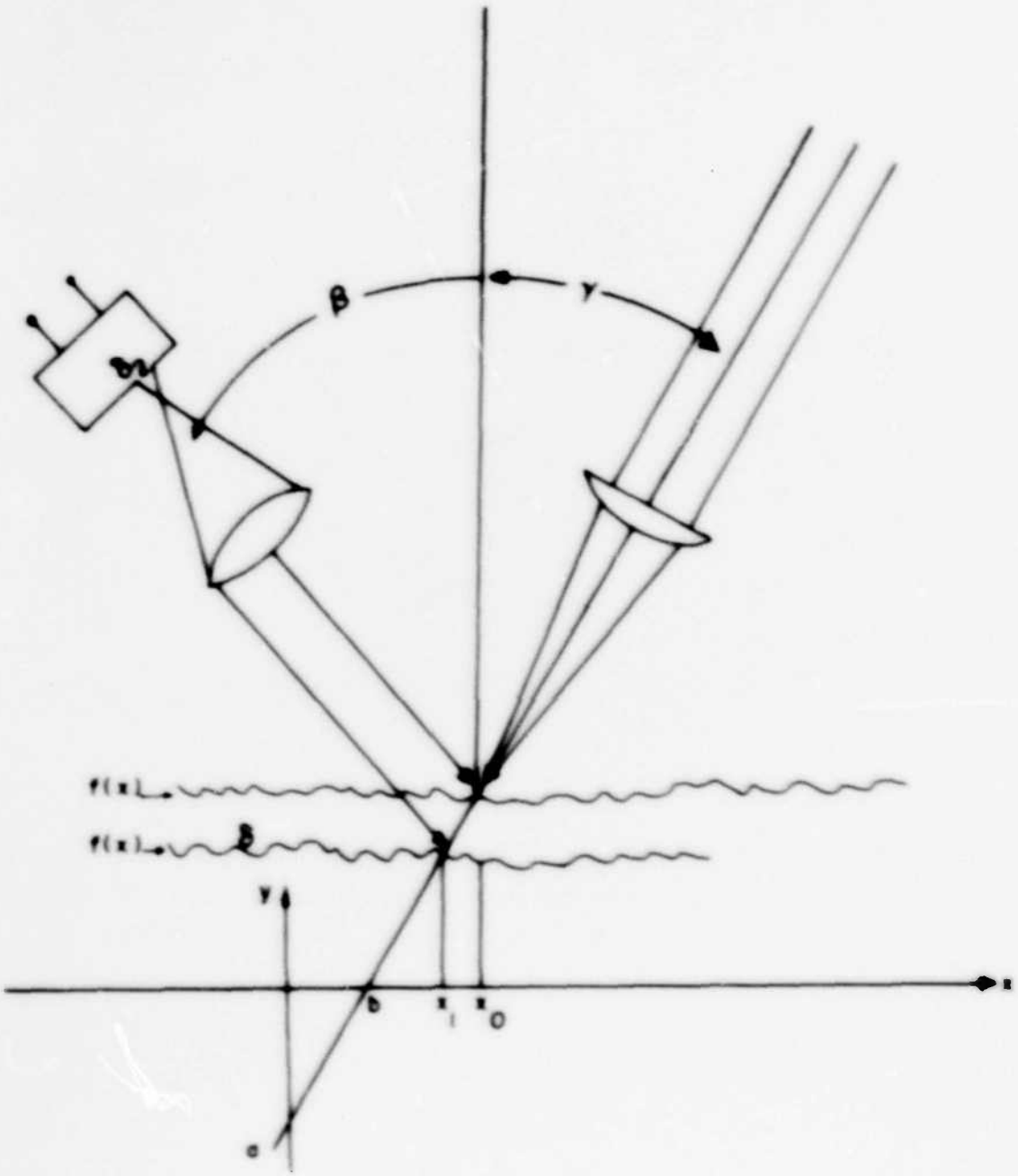



Figure A-2. Triangulation Parameters

$$f(x_1) = f(x_o) + \frac{f'(x_o)}{1}(x_1 - x_o) + \frac{f''(x_o)}{2}(x_1 - x_o)^2$$

Substitute this into the second intersection equation and subtracting the two gives

$$(x_1 - x_o)\tan(90 - \gamma) - \delta = f'(x_o)(x_1 - x_o) + \frac{f''(x_o)}{2}(x_1 - x_o)^2$$

which is solved to obtain,

$$(x_1 - x_o) = \frac{2\delta}{[f'(x_o) - \tan(90-\gamma)] \pm [f'(x_o) - \tan(90-\gamma)]^2 - 2f''(x_o)\delta}$$

The image point is shifted by the component $\delta_2$ normal to the axis of the imaging lens where,

$$\delta_2 = m \frac{\sin(\gamma + \delta)}{\sin\gamma}(x_1 - x_o)$$

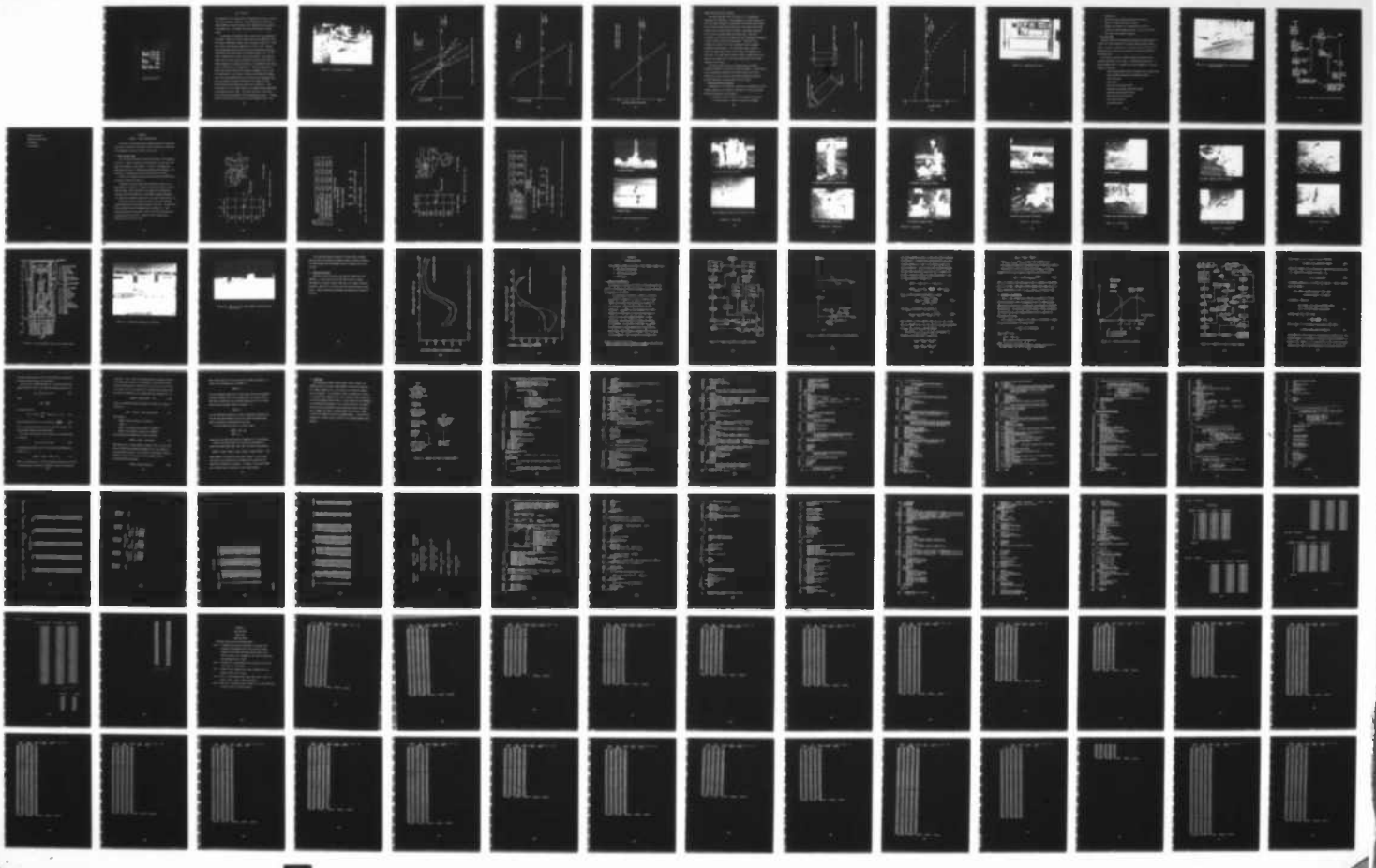
The image motion can then be obtained as a function of the arrangement parameter ($\gamma$), the surface $f(x_o)$ and the surface displacement, ($\delta_1$) by the equation

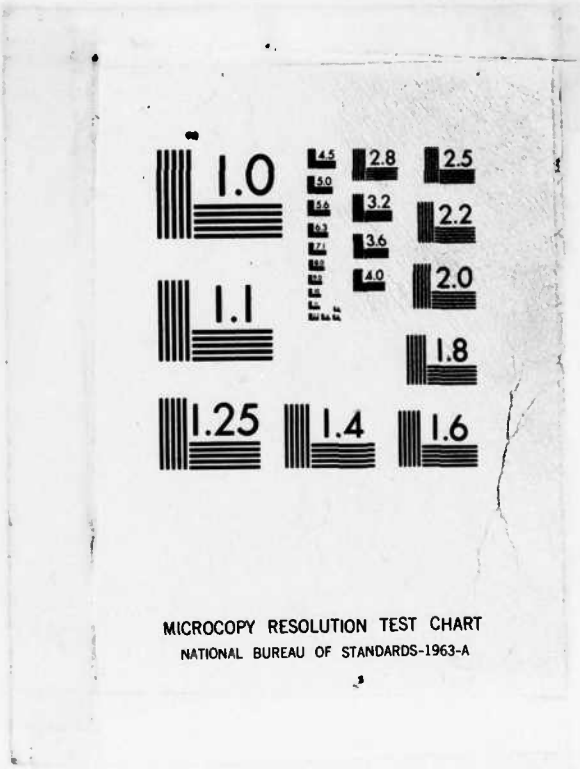
$$\delta_2 = m\,\delta_1 \left[ \frac{\sin(\gamma + \delta)}{\sin\gamma} \cdot \frac{2}{\left(\frac{\cos\gamma}{\sin\gamma} - f'(x_o)\right) \pm \left(\frac{\cos\gamma}{\sin\gamma} - f'(x_o)\right)^2 - 2f''(x_o)\delta} \right]$$

However, the pavement is rough on the scale of the focused spot on the runway. To eliminate the dependency on surface roughness, there are two alternatives. First, make the focused spot a focused line long enough that the effects of roughness are averaged to zero and second, reduce the angle between the pavement normal and input ray, $\gamma$, to zero. The image motion equation when $\gamma = 0$ reduces to

AD-A047 161 NONCONTACT NONDESTRUCTIVE DETERMINATION OF PAVEMENT DEFLECTION UNDER MOVING LOADS(U) PURDUE RESEARCH FOUNDATION LAFAYETTE IN M E HARR ET AL AUG 77 3/4

UNCLASSIFIED FAA-RD-77-127 DOT-FA73WAI-361 F/G 13/2 NL




1.0
1.1
1.25
1.4
1.6
1.8
2.0
2.2
2.5
2.8
3.2
3.6
4.0
4.5
5.0
5.6
6.3
7.1
MICROCOPY RESOLUTION TEST CHART
NATIONAL BUREAU OF STANDARDS-1963-A

$$\delta_2 = m\,\delta \sin \beta$$

The sensitivity of the image motion is maximized when $\beta$ goes to $90^{\circ}$ but that is not physically possible. Also the collection of light for imaging depends on the solid angle of the imaging lens with respect to the pavement spot. The larger $\beta$ forces the solid angle to smaller values.

A triangulation arrangement using a laser input was breadboarded and tested. Figure A-3 shows the laser setup in the laboratory at SAI. Some typical displacement signal curves are given in Figure A-4. These data are for four different samples and $\gamma = 23^{\circ}$, $\beta = 45^{\circ}$. Several other arrangements and the theory given above demonstrated that these calibration curves become smooth and repeatable when $\gamma = 0^{\circ}$, $\beta = 45^{\circ}$ using a cylinder lens to focus a line on the surface. Also shown in Figure A-5 is a curve which was obtained by using the sum of the two position signals as a normalization factor. An extension of the linear range is obtained with the normalization. Using the normalization method also yields a further more important advantage, that is, that the reflectivity of the surface is removed from affecting the signal. Figure A-6 shows normalized data for concrete and gray sandpaper which have the maximum and minimum reflectance of the sample set used. Their reflectance difference was greater than a factor of 2. The differences in the two signals appear in the regions where normalization has extended the linear range. The major contributor to this error was the inaccurate measurement of the normalization constant. If higher precision electronics had been used in this breadboard, most of the

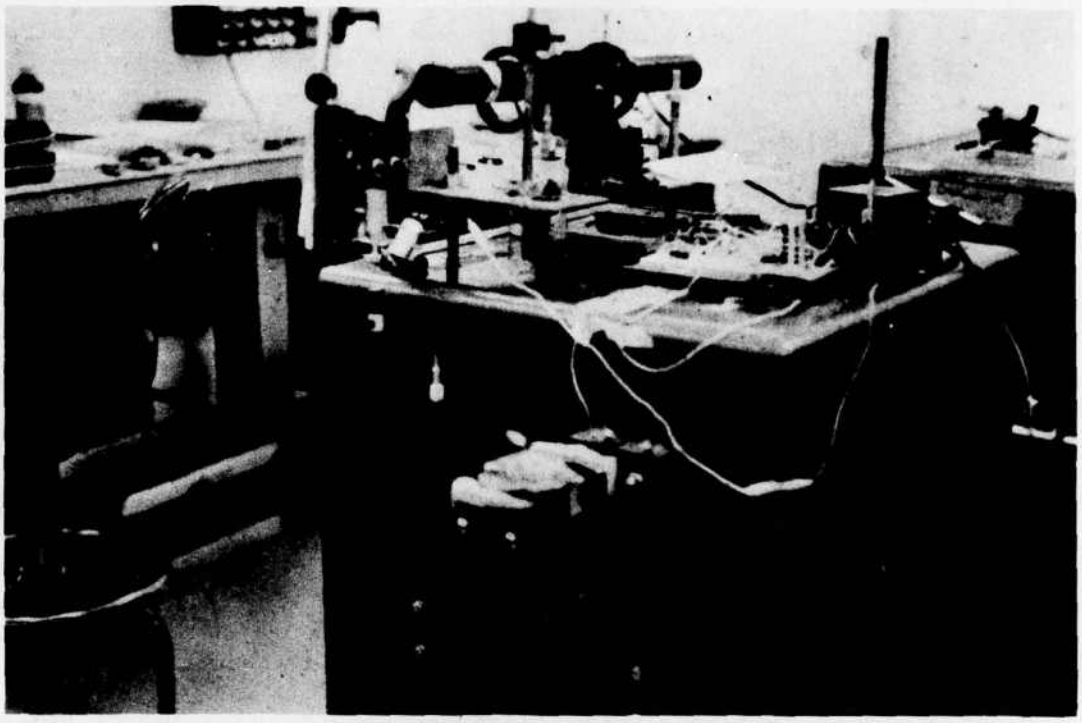


Figure A-3. Laser Setup in Laboratory

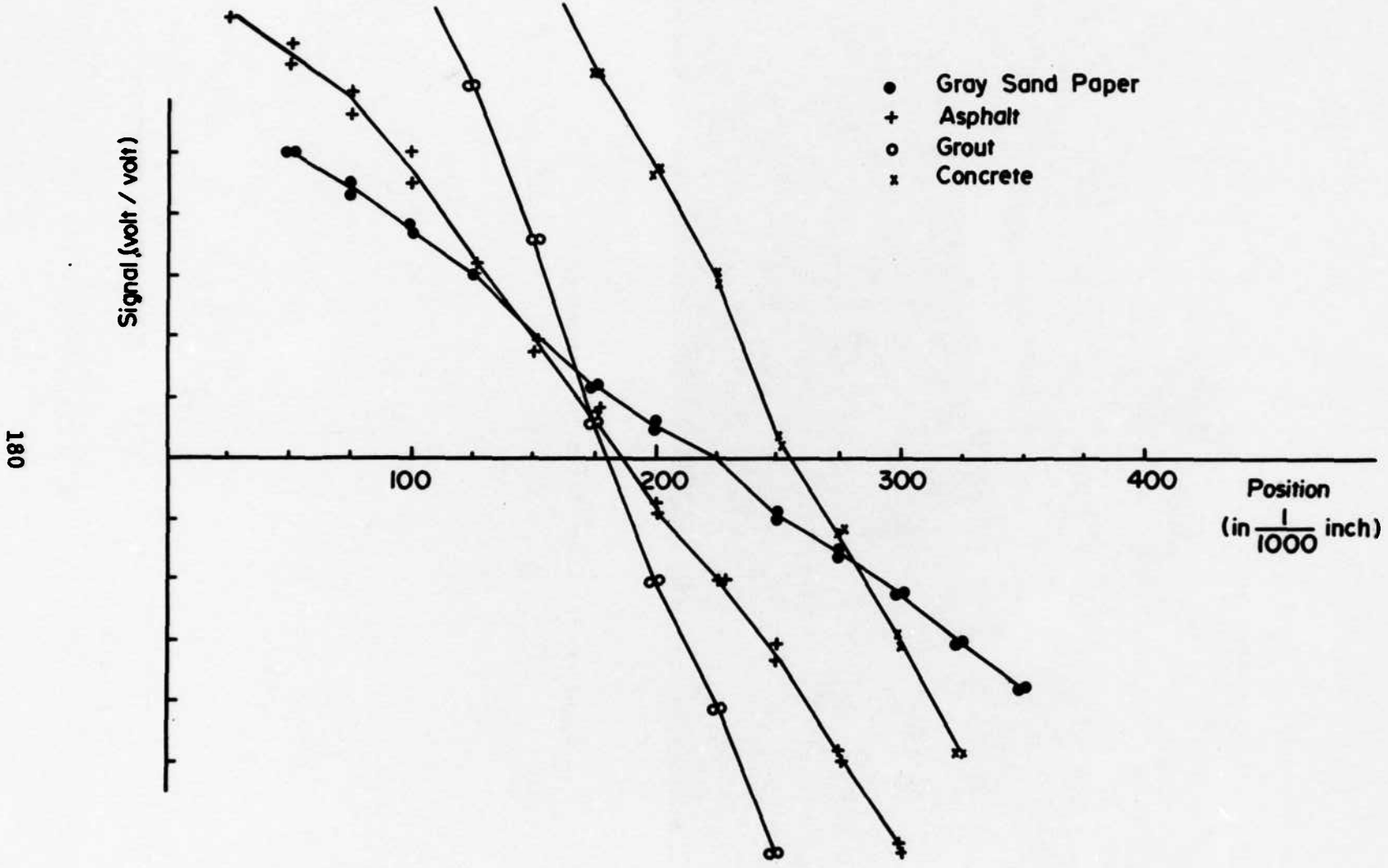



Figure A-4. Typical Triangulation Displacement Curves

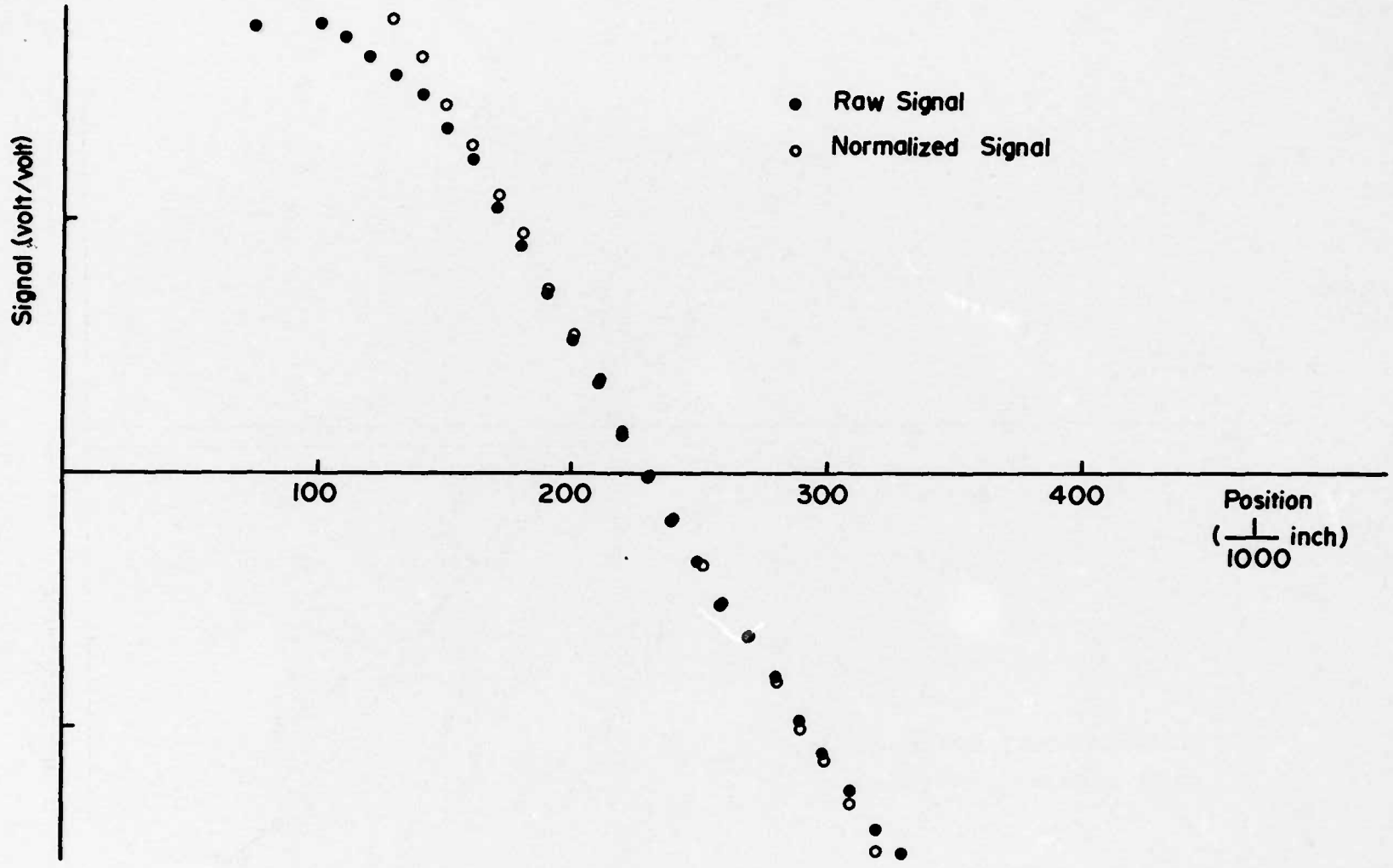



Figure A-5. Normal Incidence Displacement Curve

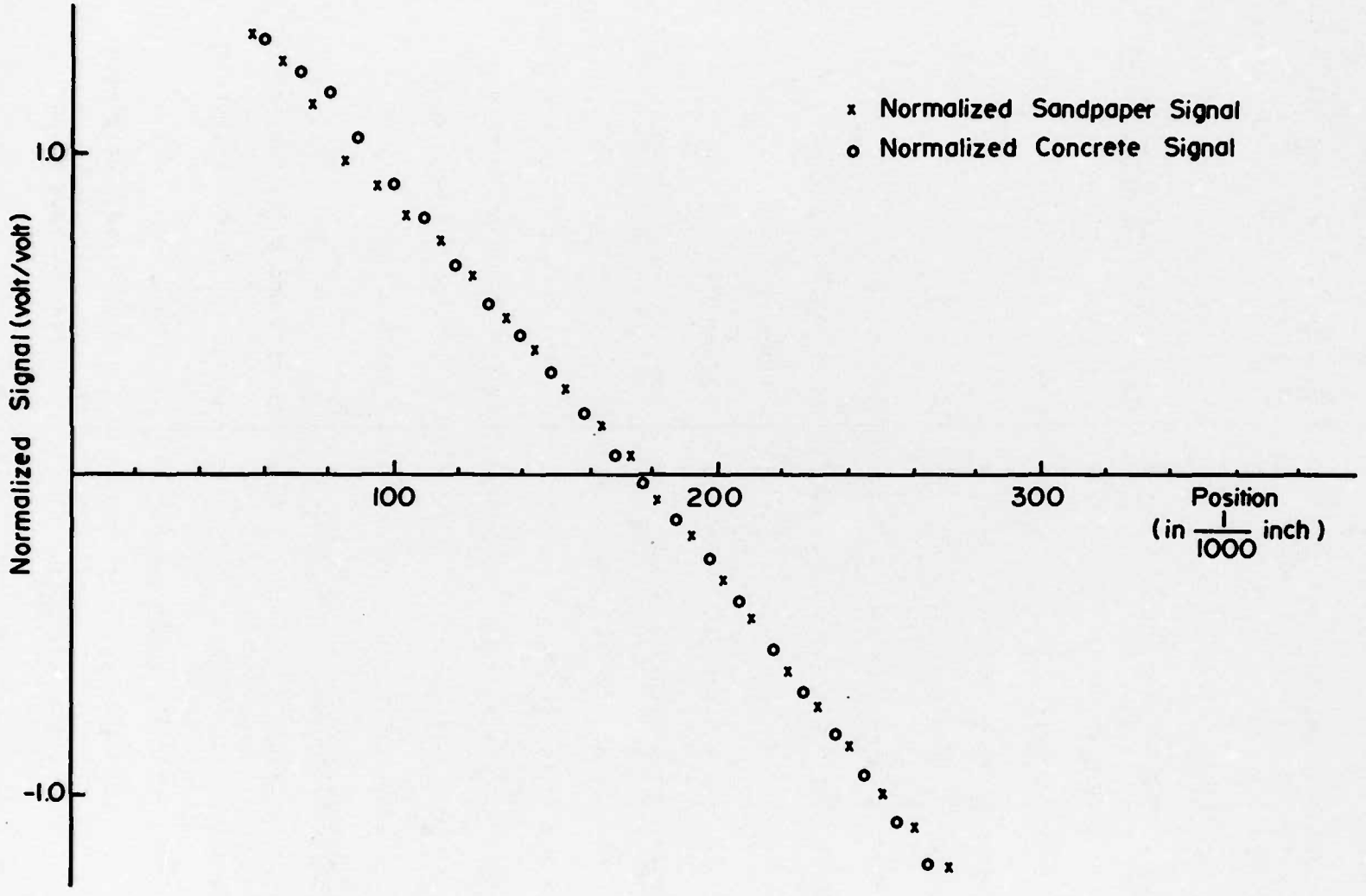



Figure A-6. Normalized Deflection Curves

signal differences would disappear.

The choice was made to use LED sources in a triangulation arrangement to deflections. This arrangement is shown in Figure A-7 and is the same triangulation arrangement as was tested before except that the light emitting diode replaces the input laser beam and the cylinder lens has been modified by adding a convex-plano spherical lens to form a composite spherical-cylinder lens. This lens arrangement was developed by mapping the three dimensional distribution of energy using an aperture and photodiode. The peak of the intensity was found for each lens arrangement until an optimum arrangement was determined. The displacement signal, shown in Figure A-8 demonstrates effects of the change in sharpness of the focal zone. The curve shows a change in slope in either side of the central focus region that is due to the larger area for the "line" focussed on the surface.

The basic optical principle as described herein remained unchanged throughout the course of system development. The electronics and the mechanical attachments were however modified to be more consistent with the concepts of the moving load-moving beam which evolved subsequent to the conclusions of SAI's effort.

b. Additional Work on LED System

Repackaging of the breadboard electronics and modification of the software supplied by SAI was done by personnel at Purdue University. This work consisted of the following:

1. Converting the basic wiring of the breadboard electronics to printed circuits. Figure A-9 shows the repackaged

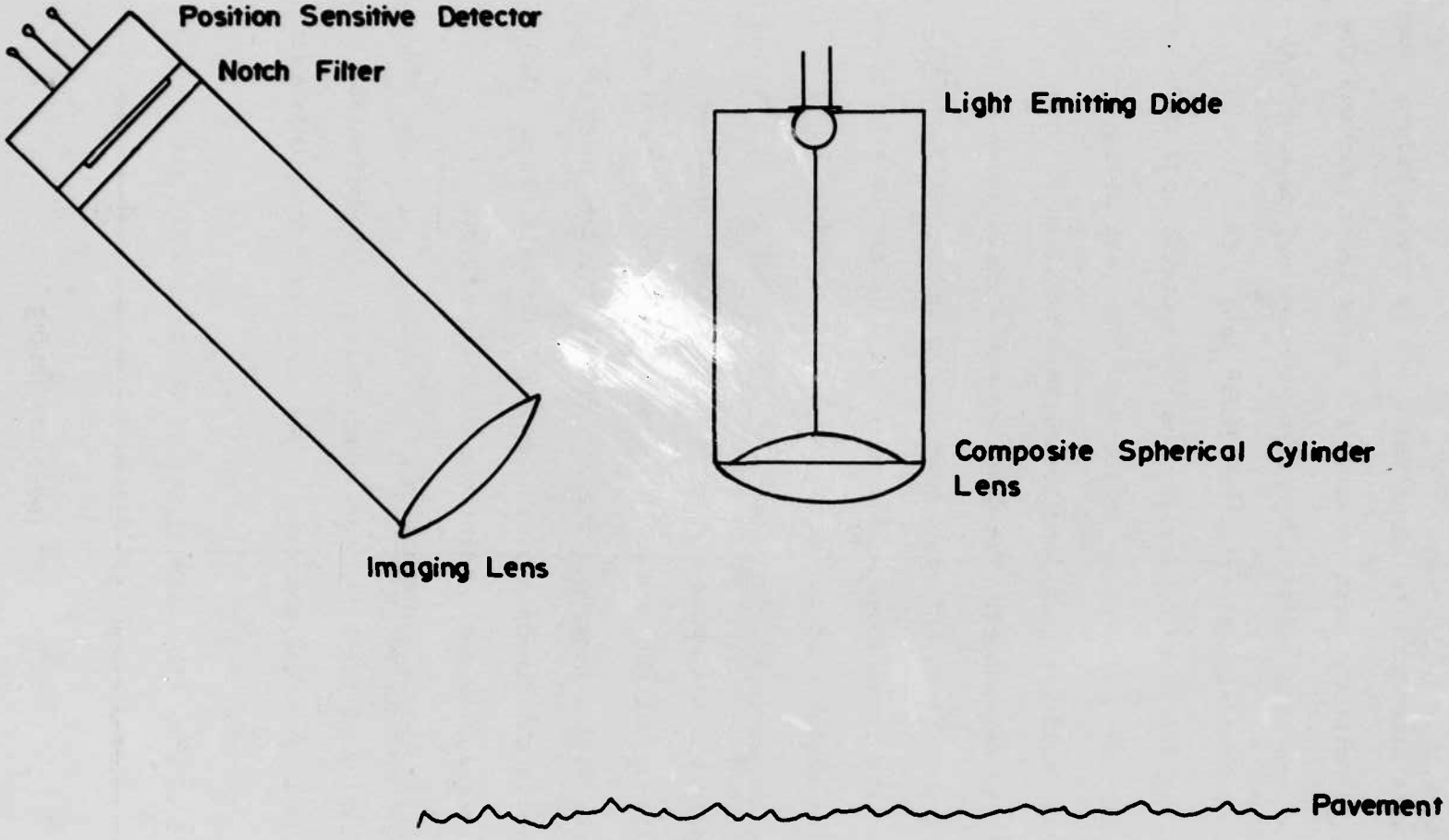



Figure A-7. Light Emitting Diode Triangulation Arrangement

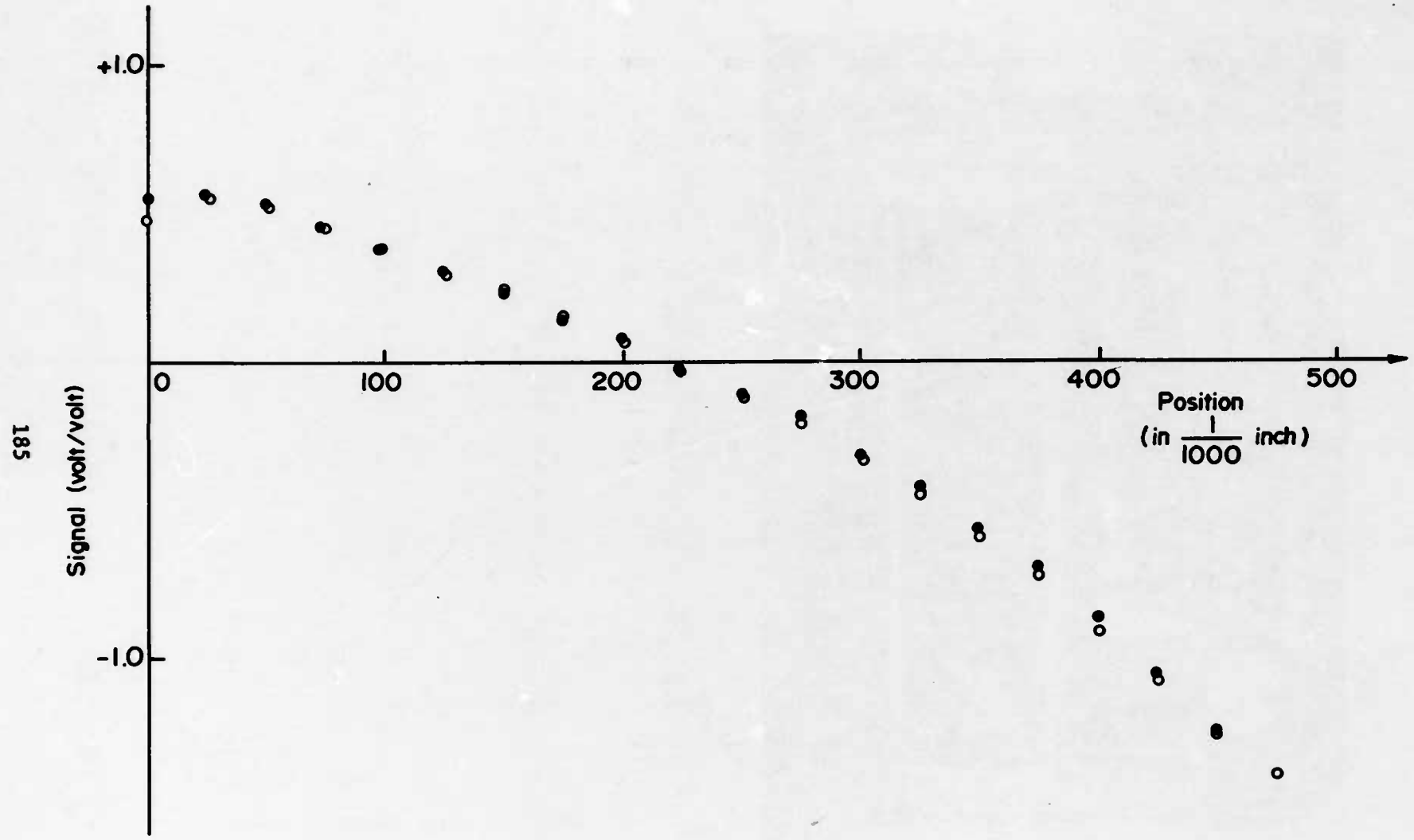



Figure A-8. Light Emitting Diode Displacement Curve

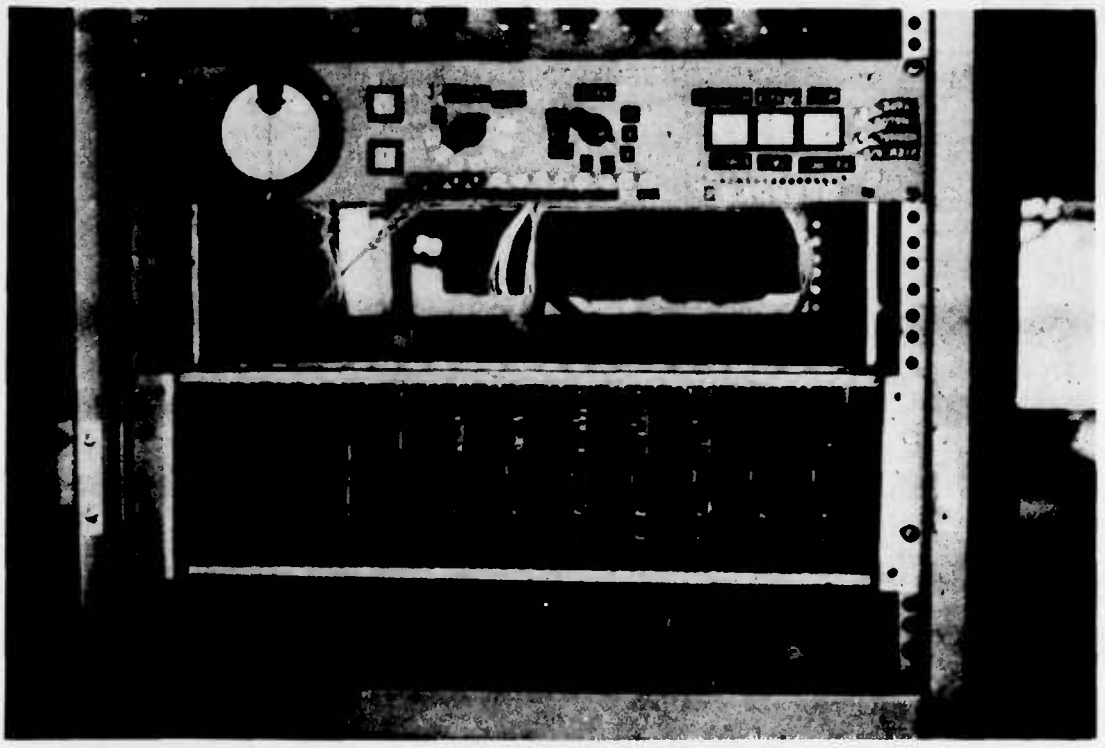


Figure A-9. Repackaged Electronics

electronics.

2. Testing the basic moving beam-moving load concept. Figure A-10 shows the basic test setup.
3. Changing the software to be compatible with the new concept of a moving beam-moving load. Figure A-11 shows a flow chart of the modified software.

c. The LVDT System

The LVDT system was designed and fabricated at Purdue University as part of a study sponsored by the Federal Highway Administration (FHWA). Because an overview of the system has already been presented previously in this repot only the details of the system components are present here.

The use of the system to measure response functions has been discussed previously in this report. For additional details see Baladi (Reference 52). A listing of the basic components of the LVDT system is as follows:

- Light Weight Aluminum I-beam, 80 inches long, 12 inches wide
- Linear Variable Differential Transformers (LVDTs)
- 2 Way Screw Jack
- Pipe (pivot)
- Small Screw Jacks under LVDTs
- 6-Channel Oscillograph Light Beam Recorder
- Kodak-2022-light Sensitive Paper
- Sears Electric Power Generator
- AC-DC Power Converter
- Micrometer-Caliper



Figure A-10. Test Setup Moving Beam - Moving Load Operation: Purdue University

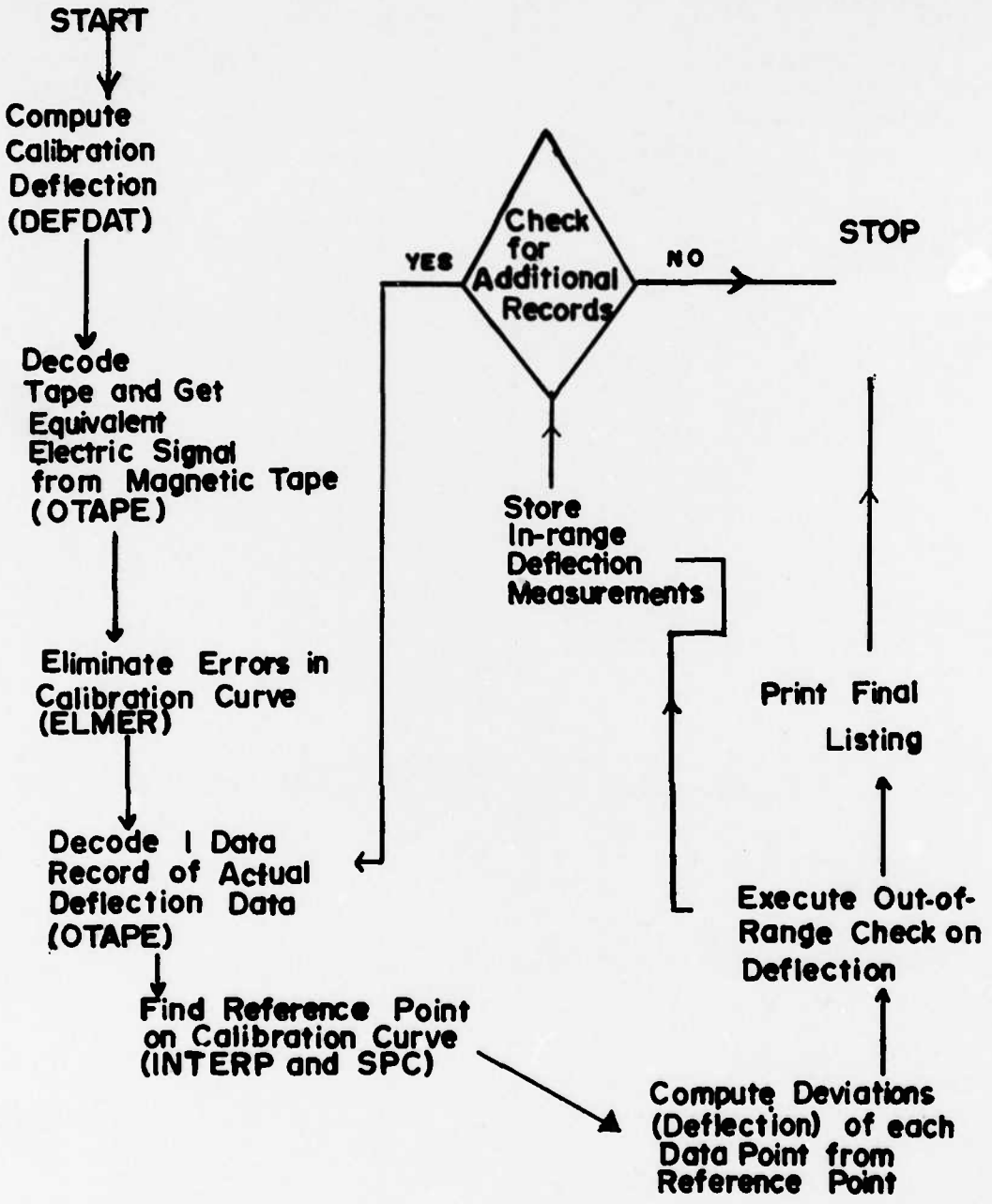



Figure A-11. Summary Flow Chart of LED System Software

- Hydraulic Scales
- Heavy Duty Silver Tape
- Thermometer
- Miscellaneous

## APPENDIX B

## SERIES A: FIELD INVESTIGATIONS

The Series A field investigation program consisted of conducting field tests at Eglin Air Force Base, Florida and Pease Air Force Base in New Hampshire during the period of this study.

### a. Eglin Air Force Base

Two sites were selected at Eglin Air Force Base. The location of the sites is shown in Figures B-1(a) and B-3(a). At each site, LVDT gages were embedded in the pavement. At Site 1, five gages were installed and at site 2, four gages were placed in the pavement. The locations of the gages are shown in Figures B-1(b) and B-3(b).

Details of the boring locations and site profile characteristics are shown in Figures B-2 and B-4.

A summary of the gage installation procedure is shown in the photosequence in Figure B-5. Figure B-6 shows the details of typical installed gage. After installation, the gages were calibrated as discussed in Boyer (Reference 11), and pavement response functions were obtained as discussed previously in this report (see section 5.1).

Grids were laid out as shown in Figures B-1(b) and B-3(b) and response functions were determined using the LVDT beam. The gages were first calibrated using the equipment shown in Figure B-7. Then response functions were obtained at each of the grid locations shown in Figures B-1(b) and B-3(b). Figure B-8 shows a typical pass being made by the P-2 fire truck.

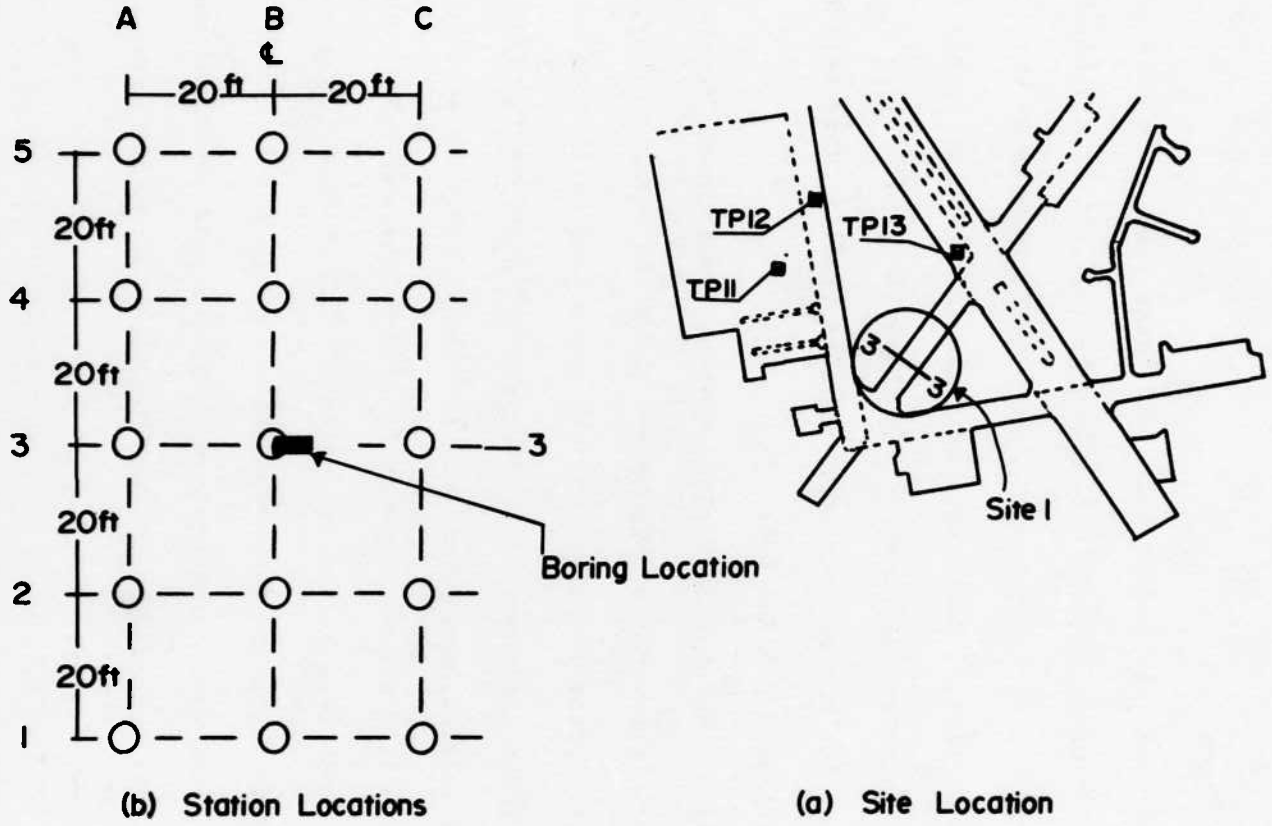
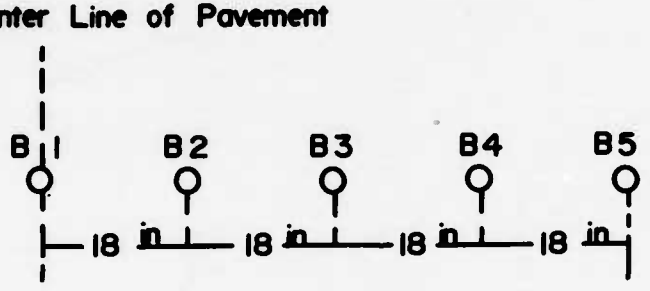



Figure B-1. Eglin Air Force Base: Site 1

| Layer | Boring Number | B 1 | B 2 | B 3 | B 4 | B 5 |
|---|---|---|---|---|---|---|
| A | Layer-A-Asphalt Concrete | 2.25 + | 2.0 | 2.0 | 1.35 | 2.0 |
| B | Layer-B-Sand Asphalt | 7.0 | 7.5 | 7.0 | 7.0 | 7.0 |
| C | Layer-C-Medium Sand | 168 | 168 | 168 | 168 | 168 |

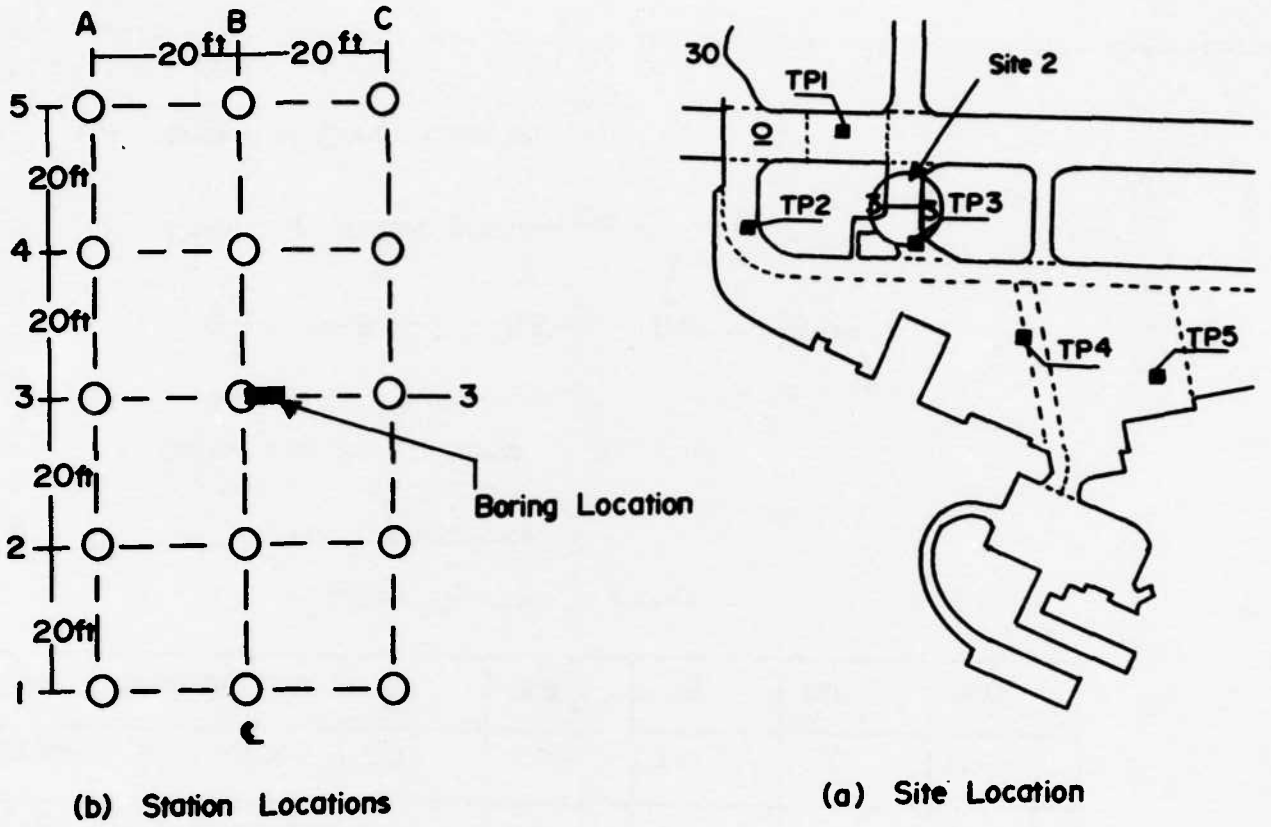
+ Layer Thickness in Inches

(a) Site Profile Characteristics




(b) Details of Boring Location

Figure B-2. Eglin AFB - Site 1: Details of Boring Location and Site Profile Characteristics




(b) Station Locations

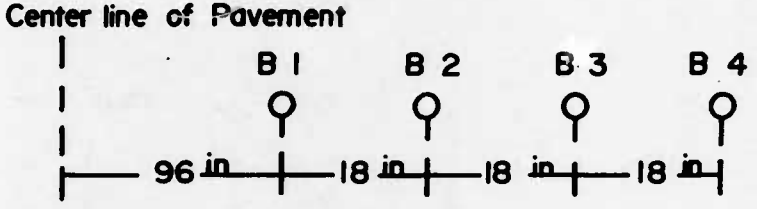
(a) Site Location

Figure B-3. Eglin Air Force Base: Site 2

| Layer | Boring Number | B 1 | B 2 | B 3 | B 4 |
|---|---|---|---|---|---|
| A | Layer A - Asphalt Concrete[1] | 1.25+ | 1.125 | 1.25 | 1.25 |
| B | Layer B - Asphalt Concrete[2] | 3 | 3 | 3 | 3 |
| C | Layer C - Sand Asphalt | 14 | 13.5 | 11.5 | 12.0 |
| D | Layer D - Medium Sand | 132 | 132 | 132 | 132 |
| E | Layer E - Silty Sand | 48 | 48 | 48 | 48 |

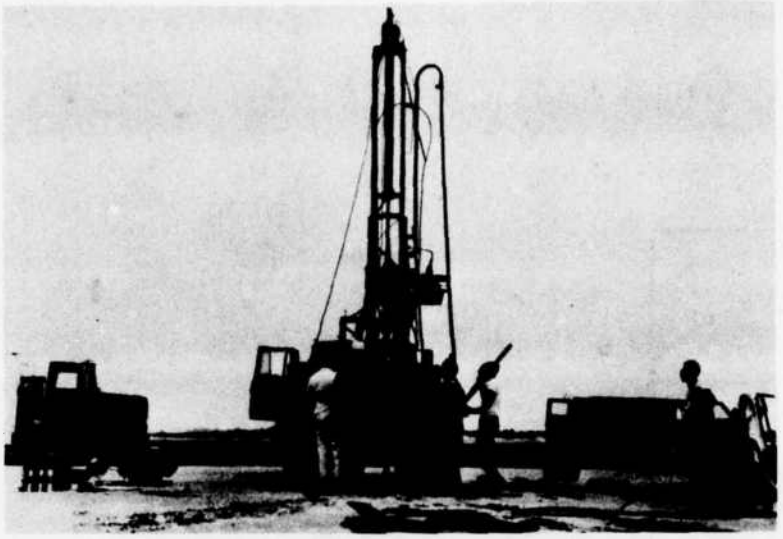
1 Resurfacing
2 Old Surface
+ Layer Thickness in inches

(a) Site Profile Characteristics

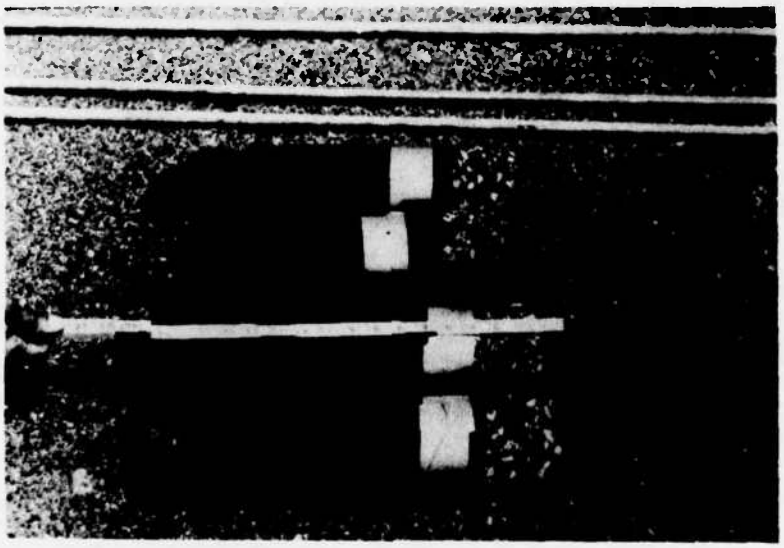



(b) Details of Boring Location

Figure B-4. Eglin - Site 2: Details of Boring Location and Site Profile Characteristics

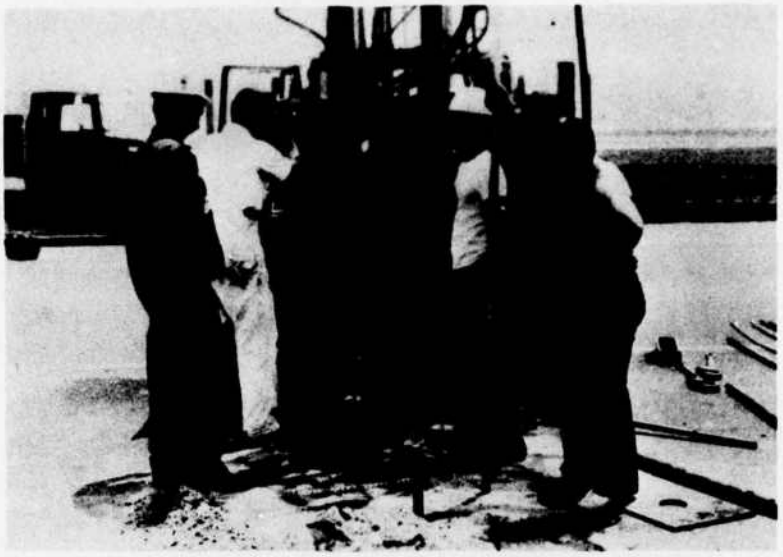


(a) Coring Pavement

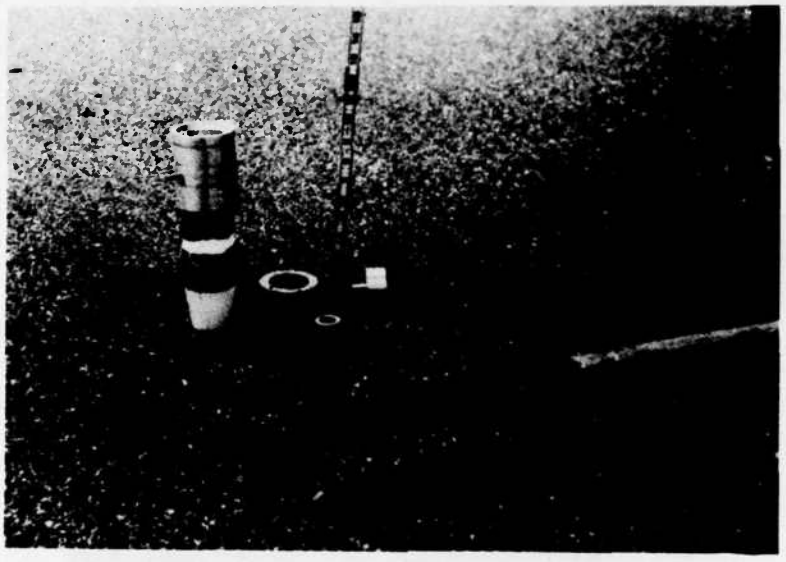


(b) Extract Cores

Figure B-5. Gage Installation Procedure



(c) Drill Hole to about 14 feet



(d) Paraphernalia Ready for Installation in Hole

Figure B-5. (Continued)



(e) Lower Rod, Anchor and Casing into Hole

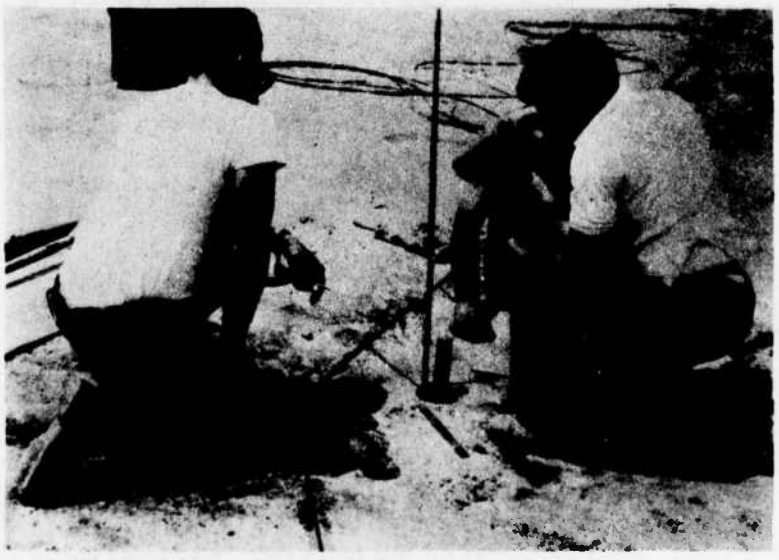


(f) Screw Impact Head to Inner Rod

Figure B-5. (Continued)



(g) Backfill with Sand and Compact

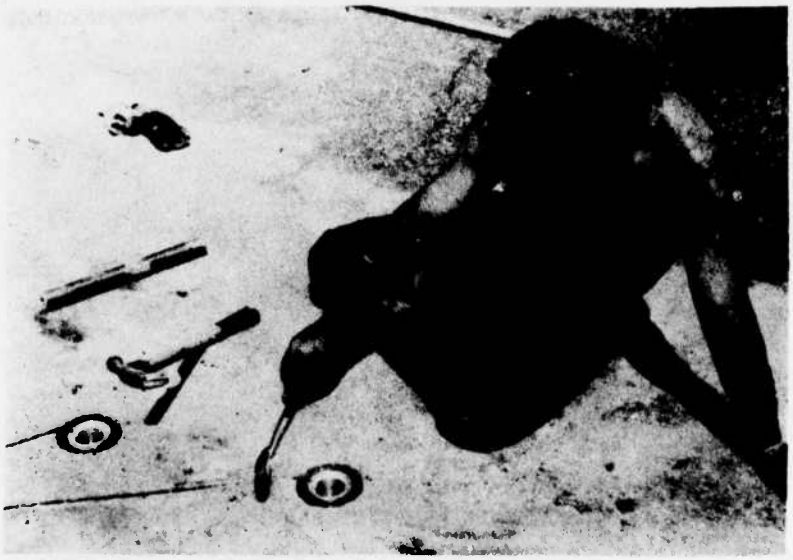


(h) Drive out Anchor Prongs

Figure B-5. (Continued)



(i) Position Upper Paraphernalia

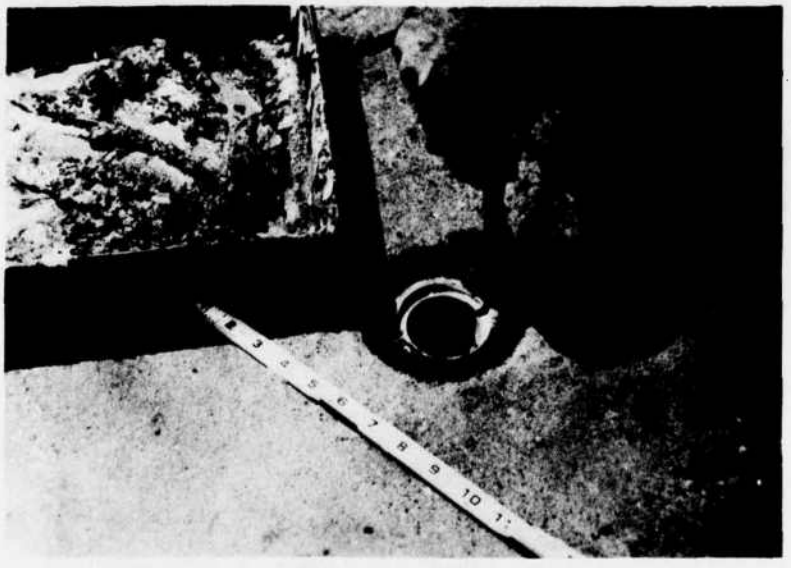


(j) Backfill Around Upper Paraphernalia

Figure B-5. (Continued)



(k) Groove Pavement



(l) Epoxy Upper Paraphernalia to Asphaltic Concrete

Figure B-5. (Continued)



(m) Epoxy Cables for LVDT into Groove



(n) Typical Installation - Partially Epoxied Cables

Figure B-5. (Continued)



(o) Epoxy Cable in Groove to Edge of Pavement



(p) Gages Ready for Element (Sensor) Installation

Figure B-5. (Concluded)

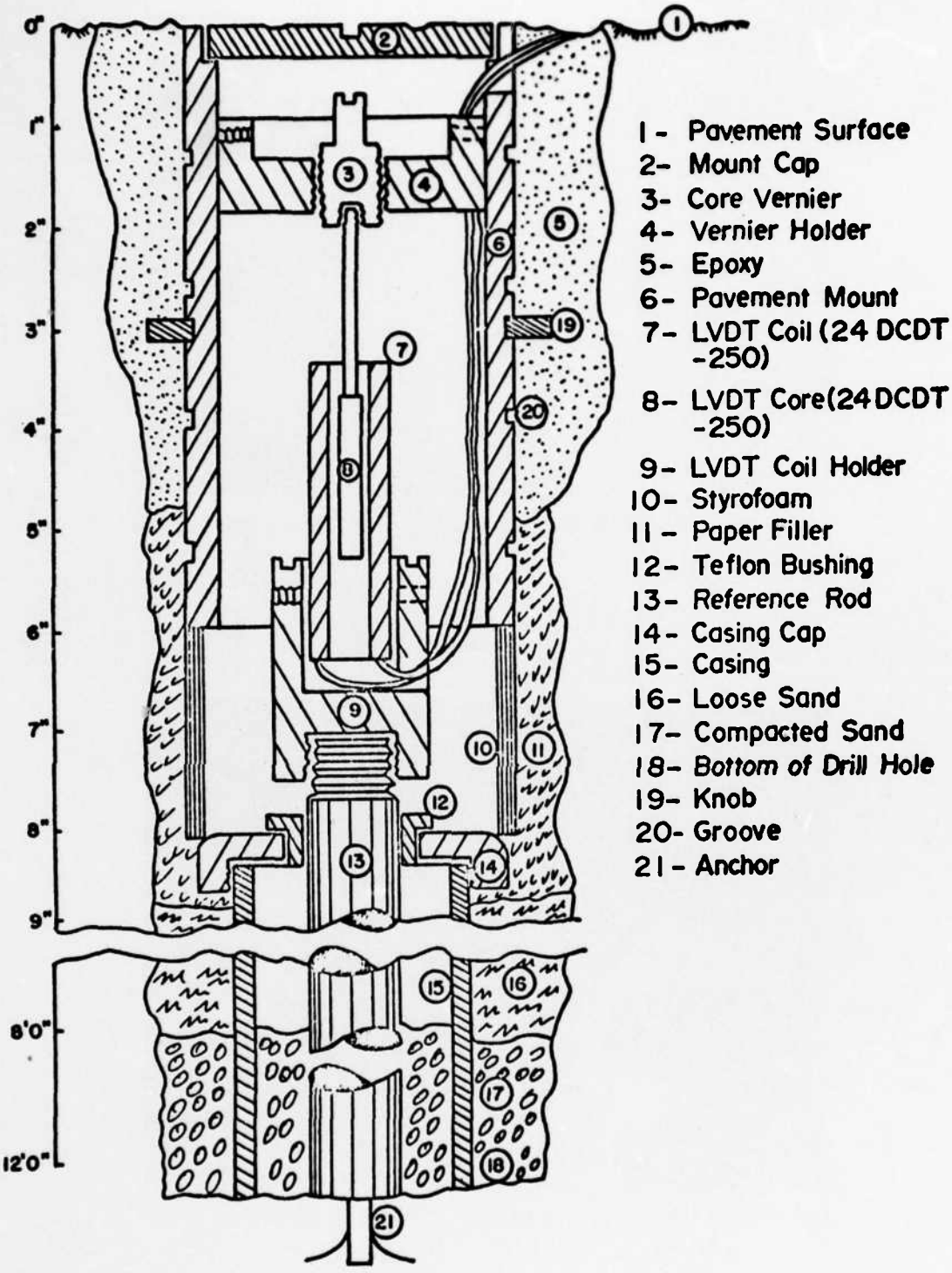



Figure B-6. Gage Installation (after Boyer [Reference 12])

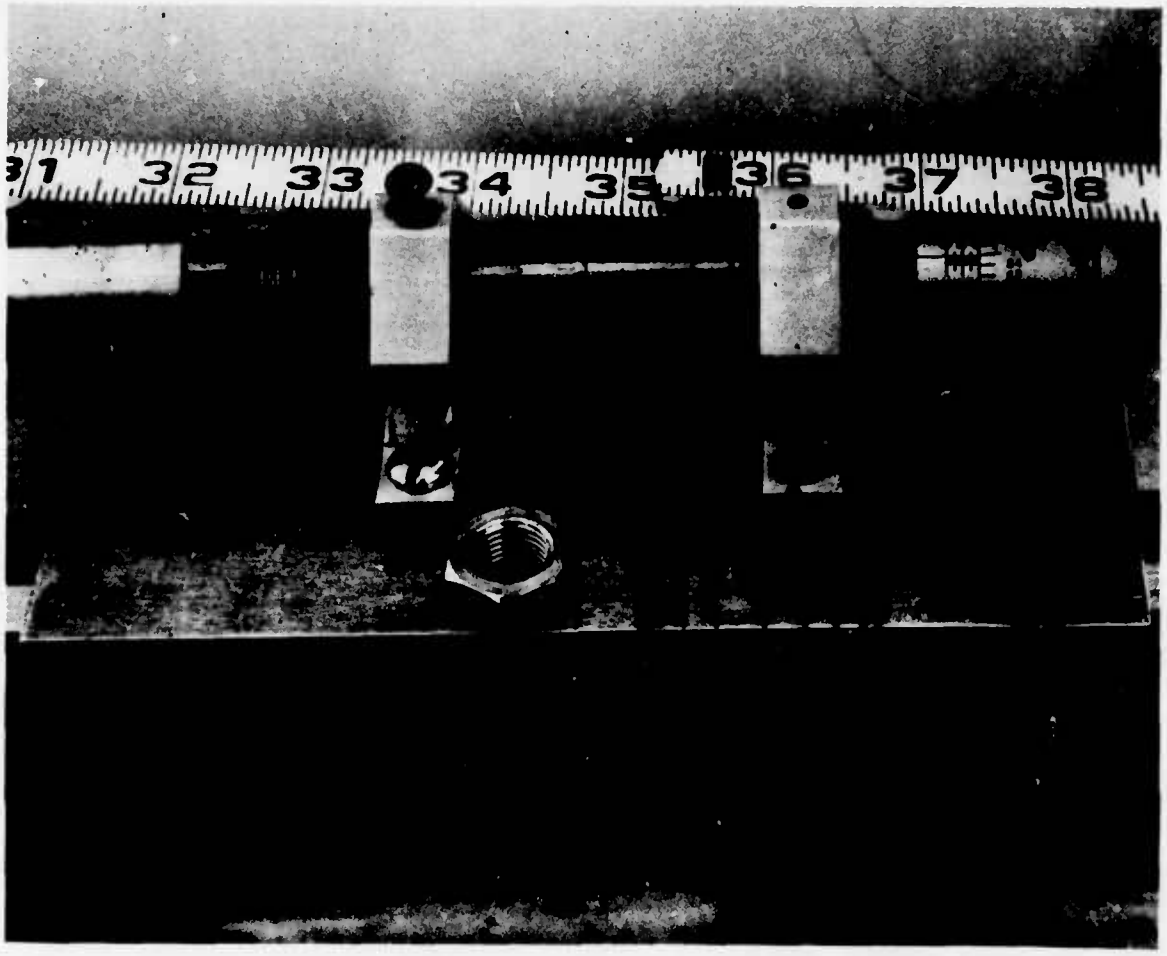



Figure B-7. Calibration Equipment for LVDT Gages

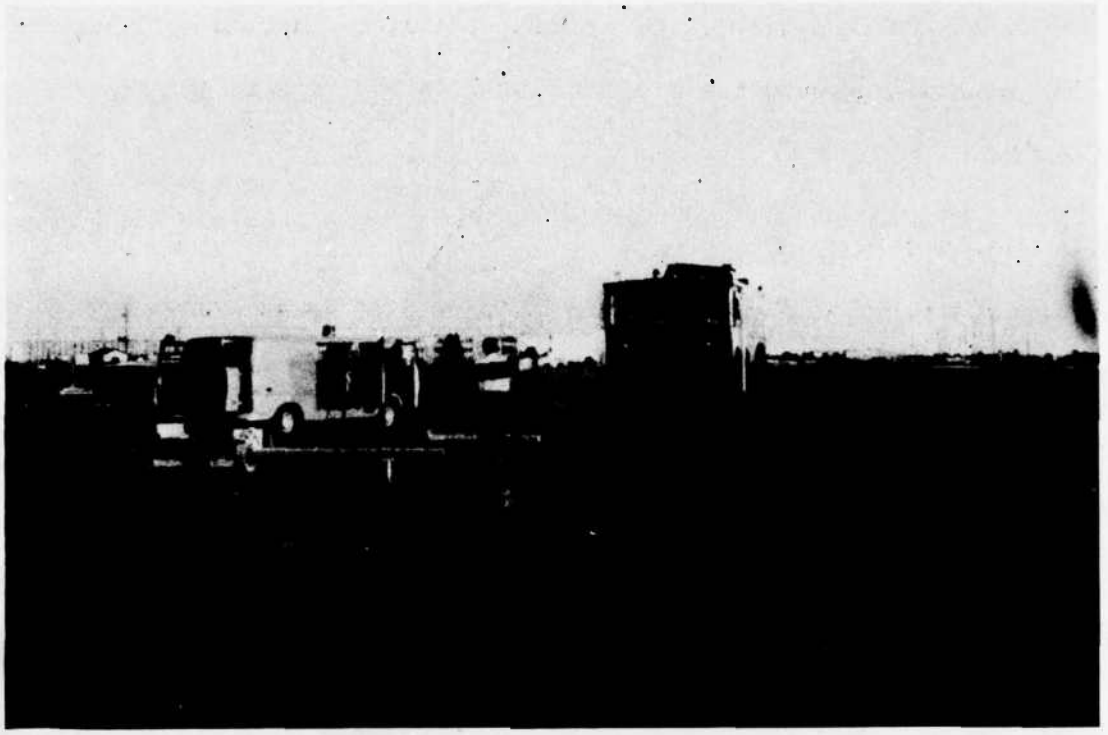


Figure B-8. Photo of P-2 Fire Truck Making a Pass During LVDT Beam Testing

At the locations shown in Figure B-1(b) and B-3(b), attempts were also made to estimate the pavement transfer function by dropping a 60 pound weight onto the pavement close to the gage at the tip of the beam.

b. Pease Air Force Base

One site, on the main runway, was tested at Pease AFB in New Hampshire. At this site only the LVDT beam was used to obtain measurements of pavement response functions in the manner previously described, using the P-2 fire truck and the KC-135A aircraft as prime movers. Typical deflection measurements are presented in Figures B-9 and B-10.

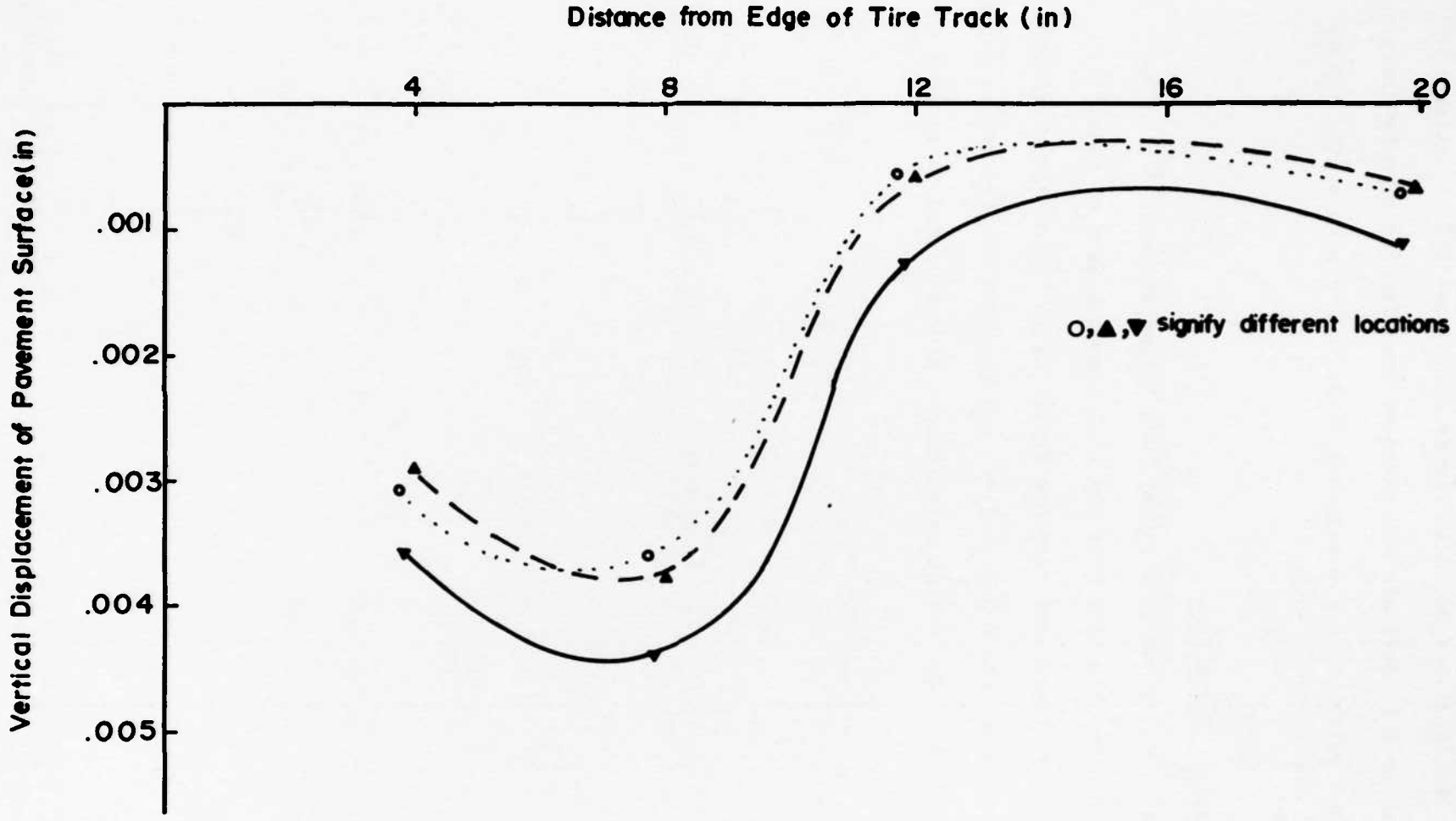



Figure B-9. Variability of Maximum Vertical Displacement of Pavement with Distance from Edge of Track of Tire Closest to Gage : KC-135 A

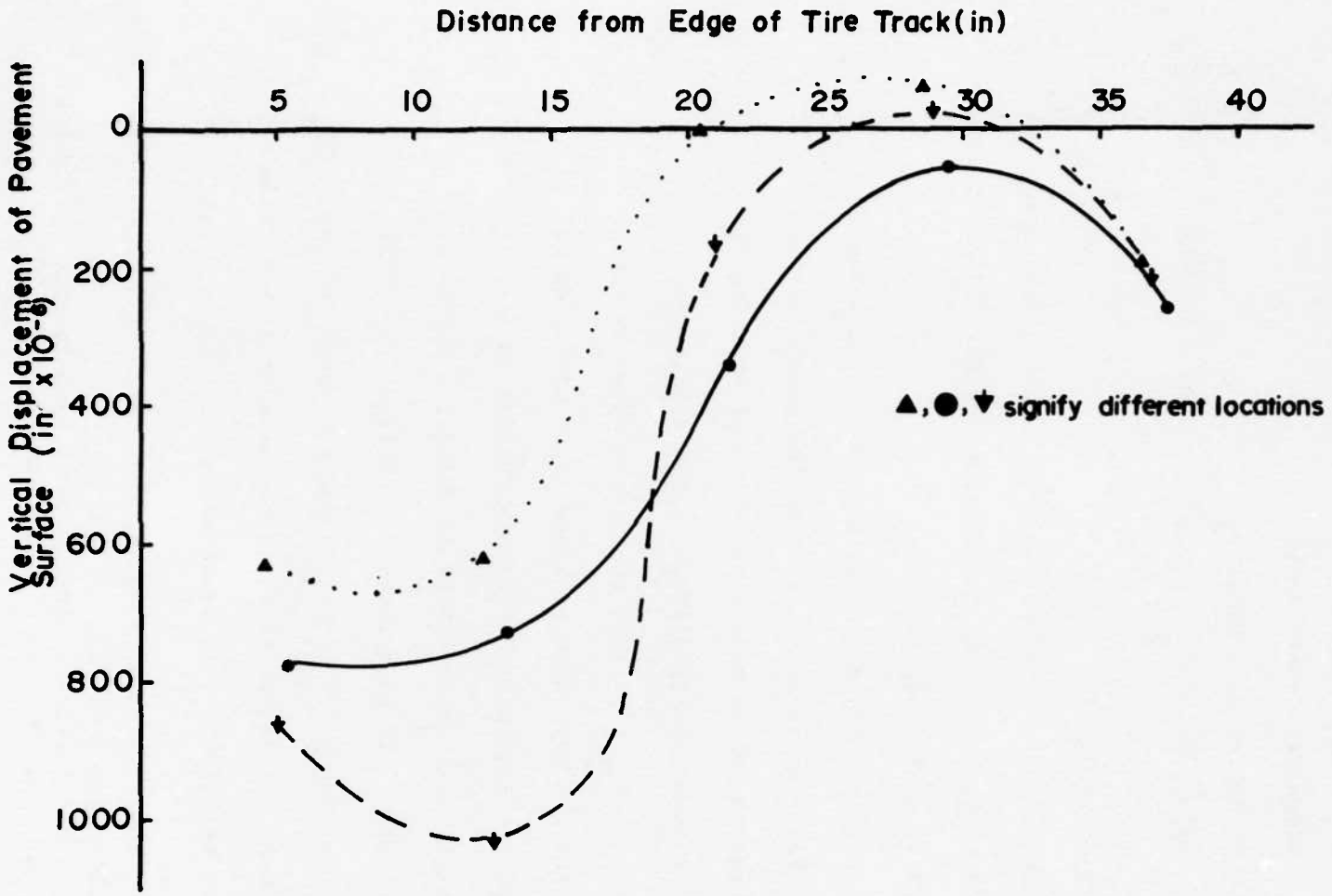



Figure B-10. Variability of Maximum Vertical Displacement of Pavement with Distance from Edge of Track of Tire Closest to Gage: P2 Fire Truck

## APPENDIX C

## COMPUTER PROGRAMS

This Appendix contains the details of the computer program for,

1. Signature determination
2. Parameter determination
3. Prediction

### a. Signature Determination

The signature as defined in the text is calculated using the equations (3) through (10) and the subroutines EXACFIT and SIGNTR. The procedure is as follows:

With reference to Figures C-1 and C-2, a value of $r_{peak}(FXP)$[17] is assumed (0.2) then the left hand side (FLHS) and the right hand side (FRHS) of equation 5a are calculated. Their difference TVAL(1) is then calculated. $r_{peak}(FXP)$ is then incremented by 0.0125 (DFXP) and the left hand side and right hand side of equation 5a, and their difference TVAL(2) is again calculated. The ratio (FDIF) of TVAL(2) and TVAL(1) is calculated. If this ratio is positive, $r_{peak}(FXP)$ is incremented by 0.0125 (DFXP) and the ratio FDIF is again found. This procedure is repeated until the ratio is first negative. This is shown as S in Figure C-2a;

[17] Symbols in capital letters correspond to symbols used in the subroutine EXACFIT which performs the calculations.

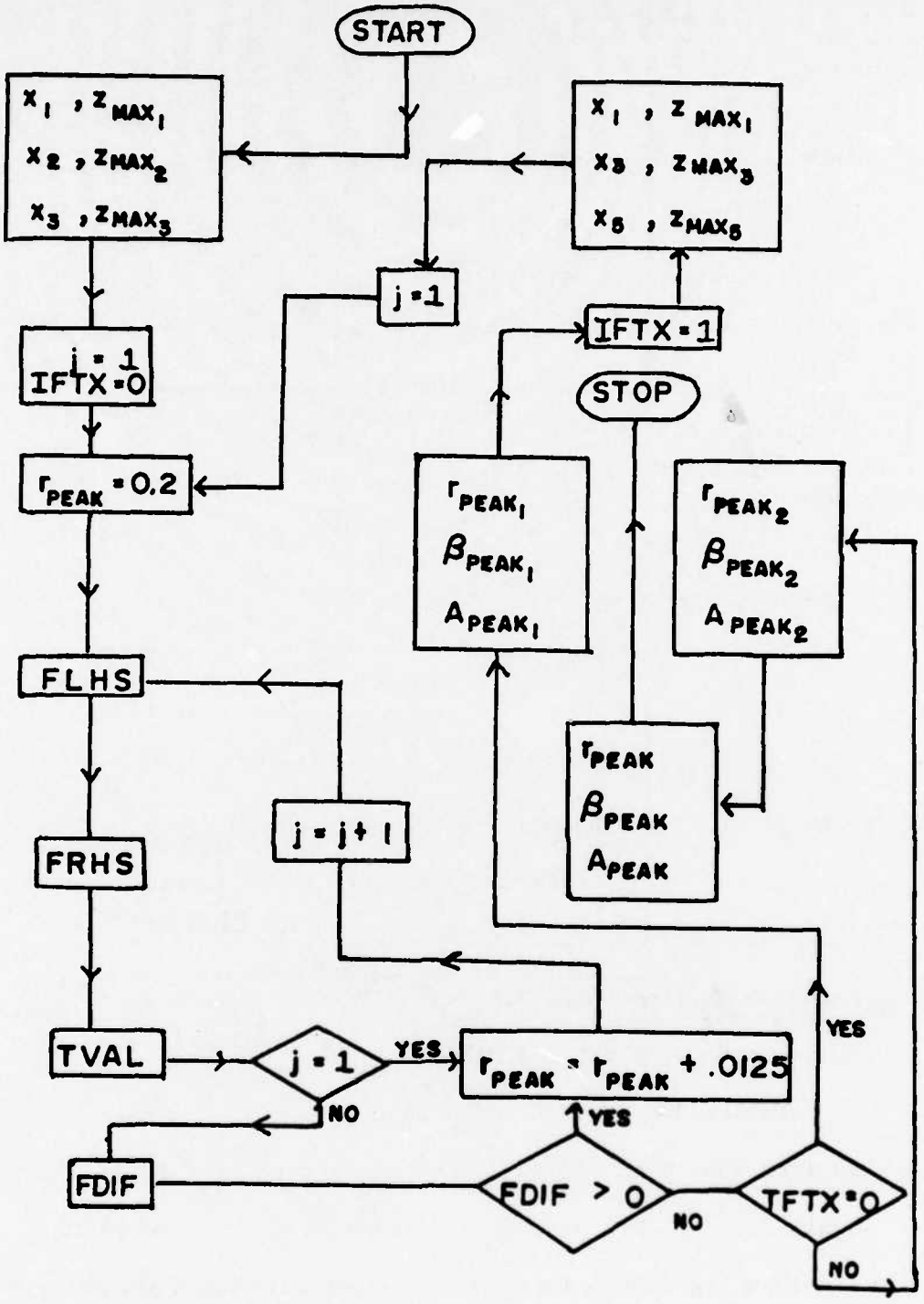



Figure C-1. Summary Flow Chart of Subroutine EXACFIT

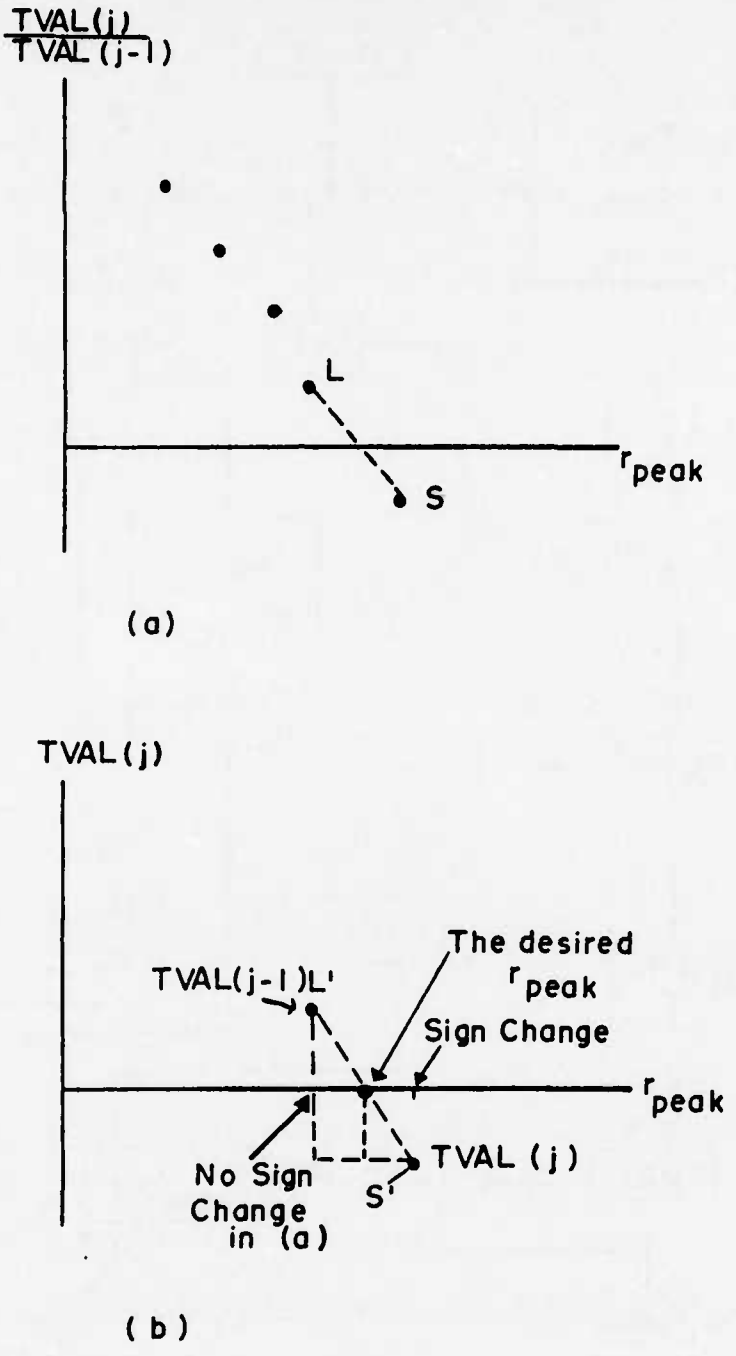



Figure C-2. Details of Interpolation in Subgrade EXACFIT

the point immediately before, at which the ratio is positive is labelled L. In Figure C-2b, the point before the ratio becomes negative is L' and S' is the point at which the ratio is negative. The point where the difference between the left hand side and the right hand side of equation 5a is zero is found by linearly interpolating between L' and S'. With reference to Figure C-2b

$$\text{TFDIF} = |\ \text{TVAL}\ (J-1)\ | + |\ \text{TVAL}\ (J)\ |$$

$$\text{FFXP}_{\text{required}} = \text{FXP}_j - \frac{\text{TVAL}(J)}{\text{TFDIF}} \cdot \text{DFXP} = r'_{peak}$$

$\beta'_{peak}$ is then calculated from equation 5 where

$$\beta'_{peak} = \frac{\ell n\ z_{max_1} - \ell n\ z_{max_3}}{x_1^{r'_{peak}} - x_2^{r'_{peak}}} \qquad (5a)$$

and, $A'_{peak}$ is calculated from equation 3a

$$A'_{peak} = z_{max_1} / [\exp\ (\beta'_{peak}\ x_1^{r_{peak}})] \qquad (3a)$$

This procedure is then repeated using $(x_1, z_1)$, $(x_3, z_3)$ and $(x_5, z_5)$ instead of $(x_1, z_1)$, $(x_2, z_2)$ and $(x_3, z_3)$, and values of $r''_{peak}$, $\beta''_{peak}$ and $A_{peak}$ are calculated.

The desired $r_{peak}$, $\beta_{peak}$ and $A_{peak}$ are found as the average of the values using the equations,

$$r_{peak} = (r'_{peak} + r''_{peak})/2$$

$$\beta_{peak} = (\beta'_{peak} + \beta''_{peak})/2$$

$$A_{peak} = (A'_{peak} + A''_{peak})/2$$

The $A_{peak}$, $r_{peak}$, and $\beta_{peak}$ values thus calculated are the parameters describing the maximum lateral deflection profile.

The signature is then calculated using the $r_{peak}$, and $\beta_{peak}$ parameter and the basic equation, equation 2a but in the form

$$A(t) = z(t)/\exp\ (\beta_{peak}\ x_1^{\ r_{peak}}) \qquad (10)$$

where z(t) refers to the deflection at gate 1 (closest to the wheel), and t is the time. Subroutine SIGNTR performs these computations by direct substitution of z(t), $x_1$, $r_{peak}$ and $\beta_{peak}$ in equation (10).

b. Parameter Determination

The k, c and m parameters as defined by equation (1) in the text are calculated using the methodology, concepts and equations presented in Section III in the paragraph with subheading "Parameter Determination". The subroutines EXACT1, NWCONV, SIGNTR, and EXACFIT are called from the main program FNDPRM in order to perform the necessary computations.

With reference to Figure C-3 and Figure C-4, initially, a value of the spring constant k is assumed where

$$k = EQKA = AA1 \times PMAX/DMAX \qquad (29)$$

where AA1[18] = 0.05

PMAX = 25000, and

DMAX = Maximum value of the signature.

[18] For convenience, the symbols in capitol letters in section (4) are the same symbols used in the computer program FNDPRM.

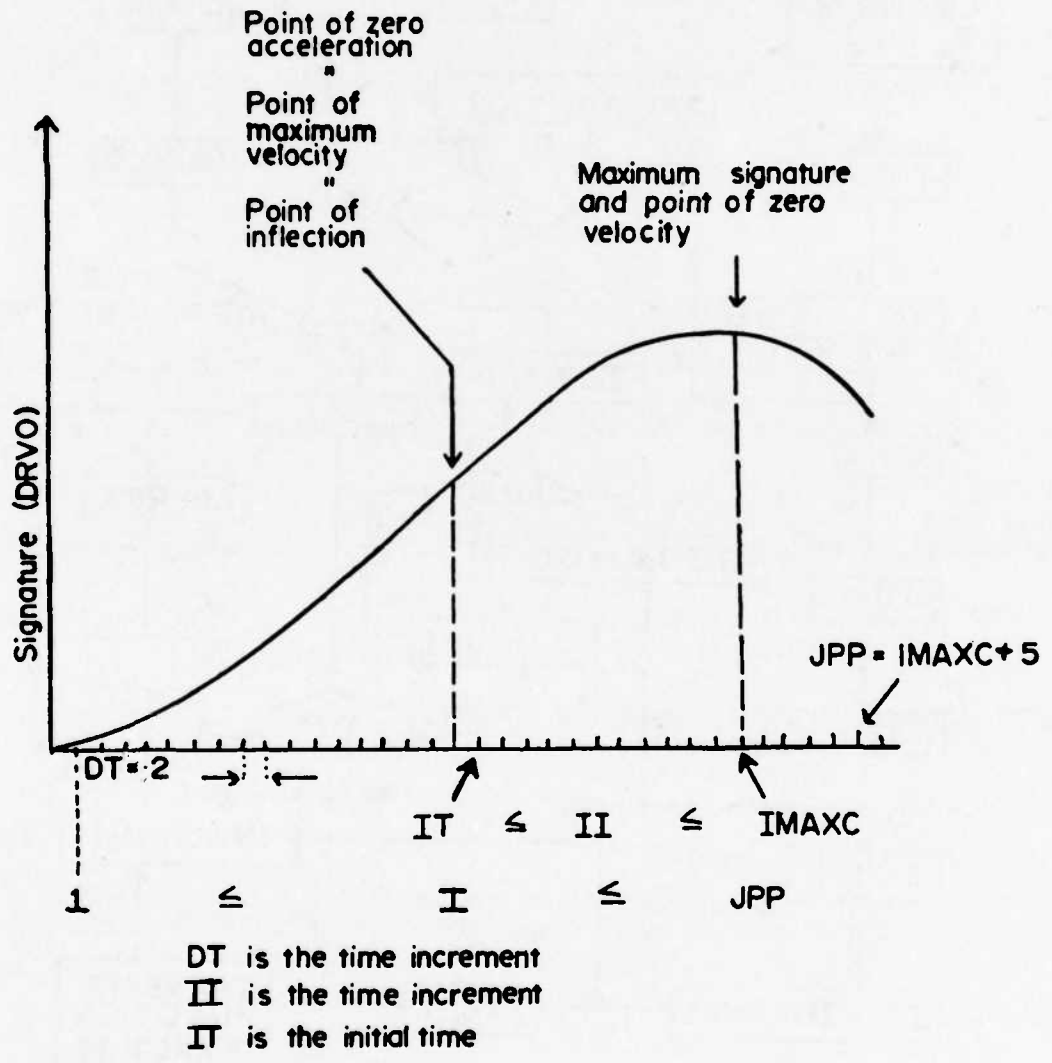



Figure C-3. Definition Sketch for Signature

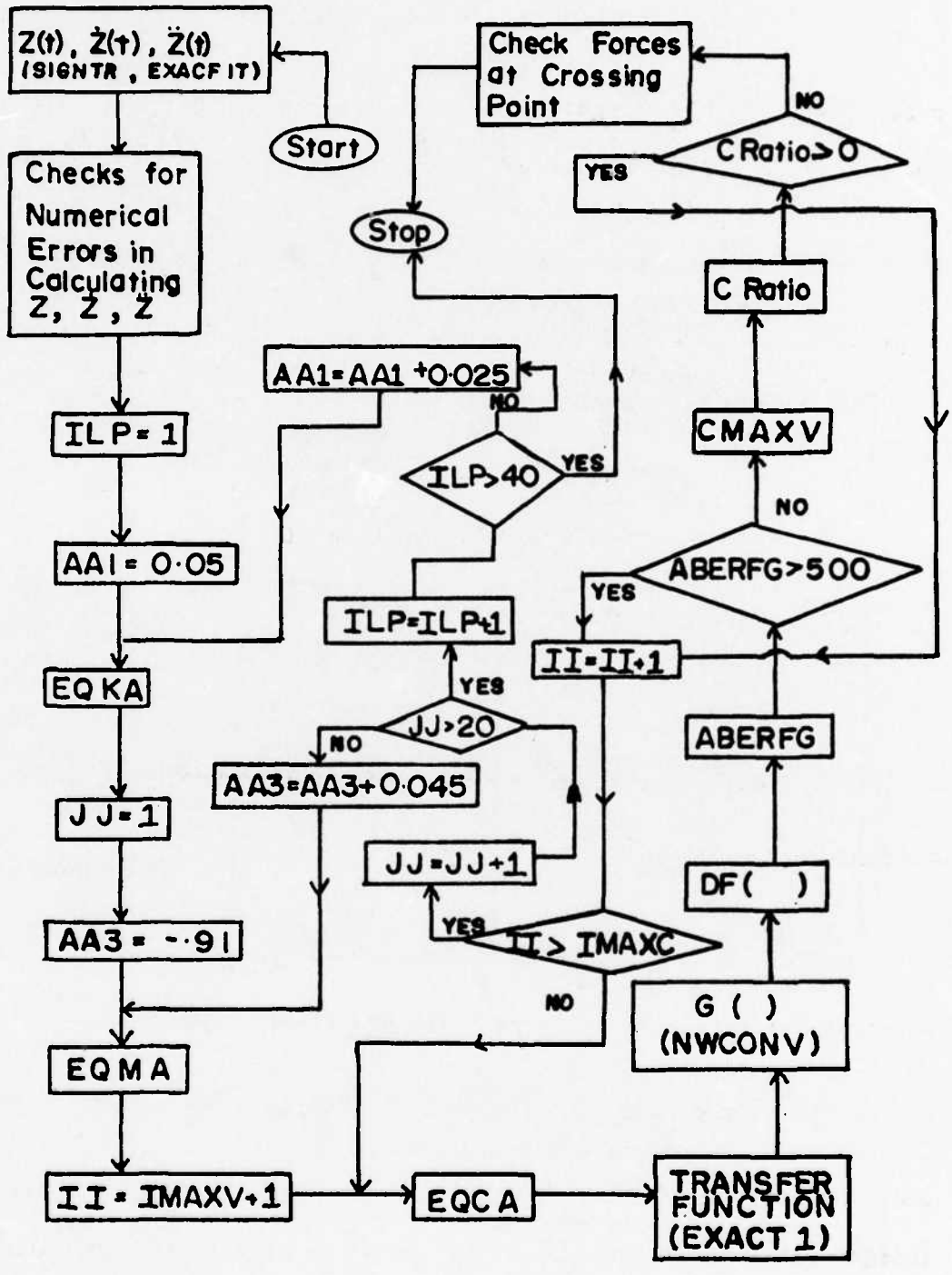



Figure C-4. Summary Flow Chart of Program FNDPRM

Then a value of m is calculated using the equation

$$m = EQMA = AA3 \times PMAX/DRV2\ (IMAXD) \tag{30}$$

where DRV2 (IMAXD) is the acceleration at maximum deflection and AA3 = .91. Equation 30 is derived as follows: Let

$$k = AA1 \times PMAX/DMAX \tag{29}$$

at maximum deflection, i.e., section (3), Figure 7. Using a constant AA2, the equation

$$AA2 \times PMAX = EQMAXDRV2(IMAXD) + EQKA \times DMAX$$
$$= EQMAXDRV2(IMAXD) + AA1 \times PMAX$$

is obtained. Therefore

$$AA2 \times PMAX - AA1 \times PMAX = EQMAXDRV2(IMAXD)$$
$$(AA2 - AA1)PMAX = EQMA \times DRV2(IMAXD) \tag{31}$$

Letting, AA3 = AA2 - AA1 yields

$$m = \frac{AA3 \times PMAX}{DRV\ (IMAXD)} = EQMA$$

Next a value of c is calculated using equation (32) where

$$c = EQCA = EQMA \times DRV2(II)/DRV1(II) \tag{32}$$

where DRV1(II) is the velocity at time increment II (Figure C-3). The initial value of II corresponds to the point of zero acceleration + 1 (Figure C-3). Using the initial value of k, m and c calculated using equation (29), (30) and (32) respectively, the transfer function is

calculated using equation (11a) or (11b) whichever is applicable. Subroutine EXACT1 performs this computation.

Next the value of $\frac{F(t)}{m}$ (equation 33) is calculated using the discrete implicit form of the convolution integral equation (34)

$$O(t) = \int_{o}^{t} I(t-\tau)\cdot G(\tau)\, d\tau \qquad (33)$$

where

$$I(t) = \frac{F(t)}{m}$$

Its implicit form is

$$I(i) = O(i)/\Delta T - \sum_{m=1}^{k=i-1} G(\tilde{m})\cdot I\,(k + 2 - \tilde{m}) \qquad (34)$$

where the initial value of i is 2, and $I(1) = \frac{O(1)}{I(i)\cdot\Delta T}$ (34a)

$G(\tau)$ is the transfer function and $\Delta T$ is the time increment. Subroutine NWCONV performs these calculations.

Next F(t), the equivalent input function, is calculated using the equation

$$F(t) = m \times I(t) = DF(I) \qquad (34a)$$

The maximum value CPMAX of F(t), is then found and compared with 25,000 lbs. If

$$ABERFG = |CPMAX - 25000| > 500 \qquad (35)$$

then II is incremented by 1, and the procedure subsequent to that step is repeated using the DRV2(II) and DRV1(II) values corresponding to

the new II. ILP, JJ and II are counters which have maximum values of 40, 20 and IMAXC (Figure C-3) respectively. These counters ensure that the tested range of values for AA1 is from .05 to 1.05, for AA3 it is from -.91 to -.01, and for II it is from the first point after the point of inflection to the maximum deflection (Figure C-3). If

$$\text{ABERFG} = |\text{CPMAX}-25000| < 500 \qquad (35b)$$

then c is calculated using the equation for section (1), Figure 9, equation 36

$$\text{CMAXV} = (\text{ZVALUF} - \text{EQKA}* \text{ZVALVO})/\text{ZVALU1} \qquad (36)$$

where CMAXV = c

ZVALUF = force at section (1) (Figure 7)

EQKA = k

ZVALVO = the deflection at section (1) (Figure 7)

ZVALU1 = the velocity at section (1) (Figure 7)

The ratio given by equation (37) is next calculated

$$\text{CDIFFR} = (\text{CMAXV} - \text{EQCA})/\text{CMAXV} \qquad (37)$$

where EQCA is the c value computed in equation (32). For the first value of CDIFFR, the procedure increments II by 1 and repeats all the steps from that point. For the second and subsequent values of CDIFFR, the ratio of the current and the preceding value is calculated using the equation

$$\text{CRATIO} = \text{QC(ICC)}/\text{QC(ICC-1)} \qquad (38)$$

where QC(ICC) refers to the current ratio of CDIFFR, AND QC(ICC - 1) refers to the preceding ratio of CDIFFR. If

$$CRATIO > 0$$

then the difference between the c values computed from two independent equations, equation (32) at the crossing point, and equation (36) at the point of inflection, has not passed through zero, so II is incremented and the subsequent steps are repeated. If

$$CRATIO < 0$$

then the difference between the c values calculated by equations (32) and (36) has passed through zero and the c values calculated using these two equations are approximately the same.

It has been found that the two controls, namely,

$$ABERFG < 500, \text{ and,}$$
$$CRATIO < 0$$

ensures that the conditions stated in paragraph 3.2.2, are satisfied.

Finally, the exact solution for the force is calculated by substitution EQCA, EQKA, EQMA, DRV0, DRV1, and DRV2 in the equation,

$$CMPXX(I) = EQKA \times DRV0(I) \times EQMC \times DRV1(I) + EQMA \times DRV2(I) \quad (39)$$

where CPMXX(I) is the force at each time increment I in the record. The force at the crossing point calculated by the convolution and substitution technique are computed. A listing of the program FNDPRM and a typical output is given at the end of this Appendix.

c. Prediction

The subroutines EXACFT, SIGNTR, NWCONV, EXACT 1, ERECT2, and MODPRM are used by the main program PREDCT to predict the signature of a vehicle (Vehicle A) at a site (site I) over which the vehicle has not traversed. It is required to know the signatures of vehicle A at another site (standard site), and a standard vehicle (vehicle B) at both the standard site and site I. Since details of the methodology for determining the parameters of the transfer function, the loading function, and the equivalency function has been detailed previously only a summary flow chart of program PREDCT is given here. Figure C-5 shows the summary flow chart of program PREDCT. A listing of the program and a typical output is given in the following pages of this Appendix.

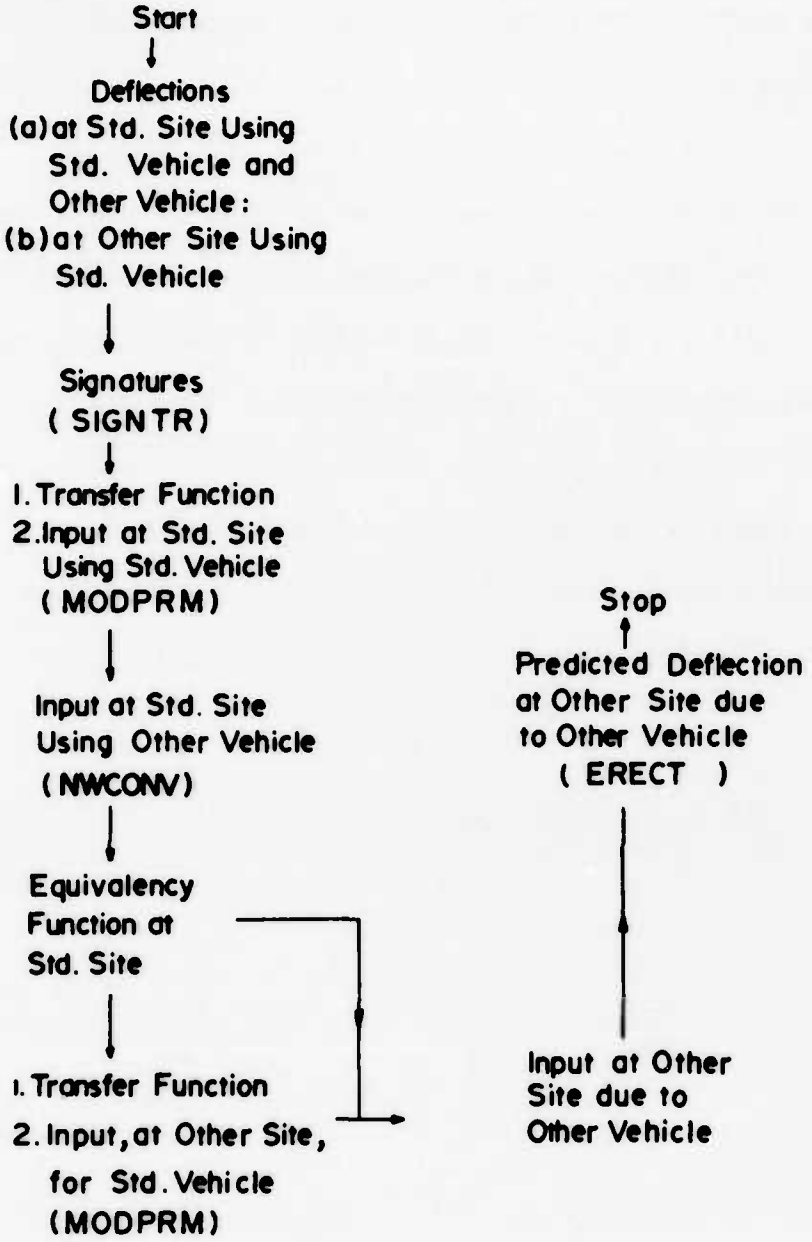



Figure C-5. Summary Flow Chart of Program PREDCT

```
C-------------------------------------------------------
      PROGRAM FNDPRM(INPUT,OUTPUT,TAPE5=INPUT,TAPE6=OUTPUT,PLOT)
C
C             THIS PROGRAM COMPUTES PARAMETERS OF THE
C             REDUCED TRANSFER FUNCTION
C             FROM DEFLECTIONS MEASURED AT 5 POSITIONS
C             PERPENDICULAR TO THE DIRECTION OF TRAVEL
C             OF THE LOAD VEHICLE
C-------------------------------------------------------
C
C             SUBROUTINES REQUIRED
C                           (1)  EXACT1
C                           (2)  NWCONV
C                           (3)  EXACFIT
C                           (4)  SIGNTR
C
C             INPUT-     NR--NUMBER OF RECORDS
C                        JM--NUMBER OF GAGES
C                        AIN--DISTANCE OF GAGE FROM OUTER EDGE OF TIRE PR
C                        NP-NUMBER OF DATA POINTS
C                        PT--TIME INCREMENT IN SECONDS
C                        WMAX--MAXIMUM WHEEL LOAD USED
C                        INITX--DIGITIZED DATA
C                        CALG--CALIBRATION DATA
C
C
C
      DIMENSION FRESP(11,100,5),INITX(11,100,5),CALG(11,5),NP(11),PT(11)
     1,WMAX(11),DRV0(100),GMAX(11,5)
      DIMENSION VIPY(200),VISIG(200)
      DIMENSION AI(5),FI(5)
      DIMENSION AIN(5,11)
      DIMENSION QC(2000)
      DIMENSION APK(100),BT(100),TXPON(100)
      DIMENSION FR(10),DFY(10),FRR(10,6)
      DIMENSION DF(200)
      DIMENSION T(200)
      DIMENSION D(200),GG(200)
      DIMENSION V(200),G(200)
      DIMENSION IVEL(11,5)
      DIMENSION DRV1(200),DRV2(200),CPMXX(50)
C
C
      READ(5,804)NR,JM
      DO 810 K=1,NR
      READ(5,29)(AIN(J,K),J=1,JM)
      READ(5,801)NP(K),PT(K),WMAX(K)
      JP=NP(K)
      DO 800 I=1,JP
      READ(5,802)(INITX(K,I,J),J=1,5)
  800 CONTINUE
      READ(5,803)(CALG(K,J),J=1,5)
  810 CONTINUE
  801 FORMAT(I5,2F10.4)
  802 FORMAT(5(I4,2X))
  803 FORMAT(5F12.10)
  804 FORMAT(2I10)
   29 FORMAT(6F10.5)
C
C**************RECORDS RUN
C***************
C
C   EGLIN     SITE 1    LOC B-4   LD. CT.   3.10.76   3.0  .2   46
C
C***************
C***************
C
C             TOP OF MAIN LOOP THAT OPERATES ON ONE RECORD AT A TIME
C
      DO 811 K=1,NR
C
C
C             CALCULATES DEFLECTION RESPONSE FUNCTION FOR JM GAGES AND
C             THE PEAK FOR EACH GAGE FOR THE K TH RECORD
C
      DO 806 I=1,JM
```

```
32.       FI(J)=AIN(J,K)
33.       RMAX=0.0
34.       JP=NP(K)
35.       DO 807 I=2,JP
36.       FRESP(K,I-1,J)=FLOAT(INITX(K,I,J)-INITX(K,1,J))*CALG(K,J)/12.
37.       VIPY(I-1)=FRESP(K,I-1,2)
38.       IF(FRESP(K,I-1,J).LT.RMAX)GO TO 807
39.       RMAX=FRESP(K,I-1,J)
40.   807 CONTINUE
41.       GMAX(K,J)=RMAX
42.       FI(J)=GMAX(K,J)
43.   806 CONTINUE
      C
      C                    LISTS REDUCED DATA
      C
44.       WRITE(6,833)
45.   833 FORMAT(1H1,40X,*NEW RECORD*//)
46.       WRITE(6,814)
47.   814 FORMAT(//1X,*NUMBER OF DATA POINTS      RECORD NUMBER      MAX. WH
         1EEL LOAD      TIME INCREMENT      NUMBER OF GAGES*/)
48.       WRITE(6,815)NP(K),K,WMAX(K),PT(K),JM
49.   815 FORMAT(10X,I4,19X,I4,18X,F6.0,19X,F4.2,18X,I2/)
50.       WRITE(6,816)
51.   816 FORMAT(//40X,*DEFLECTIONS IN FT*/)
52.       WRITE(6,817)
53.   817 FORMAT(13X,*GAGE 1          GAGE 2          GAGE 3          GAGE 4
        1          GAGE 5*/)
54.       DO 818 I=1,JP
55.       WRITE(6,819)(FRESP(K,I,J),J=1,JM)
56.   818 CONTINUE
57.   819 FORMAT(10X,5(F7.5,10X))
58.       WRITE(6,820)
59.   820 FORMAT(//40X,*PEAK DEFLECTIONS*/)
60.       WRITE(6,819)(GMAX(K,J),J=1,JM)
      C-------------------------------------------------------------
      C             FIT MEASURED PEAK LATERAL DEFLECTION PROFILE TO
      C             EQUATION USING SUBROUTINE EXACFIT
      C-------------------------------------------------------------
      C
61.       CALL EXACFIT(FI,TFXP,TBETAF,FAF,AI)
      C
62.       APK(K)=FAF
63.       BT(K)=TBETAF
64.       TXPUN(K)=TFXP
      C
65.       VBETA=TBETAF
66.       VRVAL=TFXP
67.       VIPX=AIN(2,K)
68.       NV=JP
      C-------------------------------------------------------------
      C             CALCULATE SIGNATURE OF PROTOTYPE USING
      C             SUBROUTINE SIGNTR
      C-------------------------------------------------------------
      C
69.       CALL SIGNTR(VBETA,VRVAL,VIPX,VIPY,VISIG,NV)
      C
      C-------------------------------------------------------------
      C             CALCULATE FIRST AND SECOND DERIVATIVES
      C-------------------------------------------------------------
70.       DO 74 I=1,JP
71.       DRV0(I)=VISIG(I)
72.       TRM1=(VISIG(I)+VISIG(I+1))/2.
73.       IF(I.EQ.1)TRM2=VISIG(I)/2.
74.       TRM2=(VISIG(I)+VISIG(I-1))/2.
75.       DRV1(I)=(TRM1-TRM2)/PT(K)
76.    74 CONTINUE
77.       DO 75 I=1,JP
78.       TRN1=(DRV1(I+1)+DRV1(I))/2.
79.       IF(I.EQ.1)TRN2=DRV1(I)/2.
80.       TRN2=(DRV1(I)+DRV1(I-1))/2.
81.       DRV2(I)=(TRN1-TRN2)/PT(K)
82.    75 CONTINUE
      C-------------------------------------------------------------
      C             IDENTIFY FIRST PEAK BY FINDING POINT WHERE FIRST
      C             DERIVATIVE CHANGES SIGN
```

```
      C-------------------------------------------------------------
   83.       BOTM=0.00000000001
   84.       DO 726 I=1,JP
   85.       HUMP1=DRV0(I+1)-DRV0(I)
   86.       IF(HUMP1.GE.0.0)GO TO 726
   87.       JPP=I+6
   88.       GO TO 727
   89.   726 CONTINUE
   90.   727 CONTINUE
       C-------------------------------------------------------------
       C              REPLACE ZEROES BY AVERAGING BEFORE AND AFTER POINTS
       C-------------------------------------------------------------
   91.       IMAXV=0
   92.       DV1MX=0.0
   93.       DO 315 I=1,JPP
   94.       IF(DRV1(I).EQ.0.0)DRV1(I)=(DRV1(I+1)+DRV1(I-1))/2.
CAUTION - IS FLOATING POINT EQUALITY TO BE EXPECTED       ************************************
   95.       IF(DRV1(I).EQ.0.0)DRV1(I)=(DRV1(I+2)+DRV1(I-2))/2.
CAUTION - IS FLOATING POINT EQUALITY TO BE EXPECTED       ************************************
   96.       IF(ABS(DRV1(I)).LT.BOTM)DRV1(I)=(DRV1(I+1)+DRV1(I-1))/2.
   97.       IF(ABS(DRV2(I)).LT.BOTM)DRV2(I)=(DRV2(I+1)+DRV2(I-1))/2.
   98.       IF(DRV1(I).LT.DV1MX)GO TO 315
   99.       DV1MX=DRV1(I)
  100.       IMAXV=I
  101.   315 CONTINUE
       C-----------------------------------------
       C              FIND MAXIMUM VALUE OF SIGNATURE
       C-----------------------------------------
  102.       DMAX=DRV0(1)
  103.       DO 53 I=2,JPP
  104.       IF(DRV0(I).LT.DMAX)GO TO 53
  105.       DMAX=DRV0(I)
  106.       IMAXD=I
  107.    53 CONTINUE
       C-------------------------------------------------------------
       C              REPLACE   ERRONEOUS ACCELERATIONS BY AVERAGING
       C              BEFORE AND AFTER POINTS
       C-------------------------------------------------------------
  108.       IMAXV1=IMAXV-1
  109.       DO 57 I=2,IMAXV1
  110.       IF(DRV2(I).LE.0.0)DRV2(I)=(DRV2(I-1)+DRV2(I+1))/2.
  111.       IF(DRV2(I).LE.0.0)DRV2(I)=(DRV2(I-2)+DRV2(I+2))/2.
  112.    57 CONTINUE
  113.       IMAXVA=IMAXV+1
  114.       DO 109 I=IMAXVA,JPP
  115.       IF(DRV2(I).GE.0.0)DRV2(I)=(DRV2(I-1)+DRV2(I+1))/2.
  116.       IF(DRV2(I).GE.0.0)DRV2(I)=(DRV2(I-2)+DRV2(I+2))/2.
  117.   109 CONTINUE
  118.       DO 107 I=1,JPP
  119.       IF(DRV1(I+1).EQ.DRV1(I))DRV1(I+1)=(DRV1(I+2)+DRV1(I))/2.
CAUTION - IS FLOATING POINT EQUALITY TO BE EXPECTED       ************************************
  120.       IF(DRV2(I+1).EQ.DRV2(I))DRV2(I+1)=(DRV2(I+2)+DRV2(I))/2.
CAUTION - IS FLOATING POINT EQUALITY TO BE EXPECTED       ************************************
  121.   107 CONTINUE
       C-------------------------------------------------------------
       C              FIND TIME INTERVAL WHERE VELOCITY CHANGES SIGN
       C              AND FRACTION OF VELOCITYTO ZERO BY
       C              LINEAR INTERPOLATION
       C-------------------------------------------------------------
  122.       DO 789 IA=1,JPP
  123.       DEROTS=DRV1(IA+1)/DRV1(IA)
  124.       IF(DEROTS.GT.0.0)GO TO 789
  125.       DZERO=DRV1(IA)-DRV1(IA+1)
  126.       DDTZ=DRV1(IA)/DZERO
  127.       NAFNL=IA
  128.       GO TO 788
  129.   789 CONTINUE
  130.   788 CONTINUE
       C-------------------------------------------------------------
       C              FIND INTERVAL AND TIME WHERE ACCELERATION IS
       C              ZERO AND THE CORRESPONDING DISPLACEMENT
       C              AND VELOCITY
       C-------------------------------------------------------------
  131.       DO 889 IA=1,JPP
  132.       ZEROTS=DRV2(IA+1)/DRV2(IA)_
```

```
133.        IF(ZERO'S.GT.0.0)GO TO 889
134.        TZERO=DRV2(IA)-DRV2(IA+1)
135.        FDTZ=DRV2(IA)/TZERO
136.        IAFNL=IA
137.        DRORNG=DRV0(IA+1)-DRV0(IA)
138.        ZVALU0=DRV0(IA)+FDTZ*DRORNG
139.        DR1RNG=DRV1(IA+1)-DRV1(IA)
140.        ZVALU1=DRV1(IA)+FDTZ*DR1RNG
141.        GO TO 888
142.    889 CONTINUE
143.    888 CONTINUE
      C
      C**********
144.        WRITE(6,99)
145.     99 FORMAT(/37X,*FOR SIGNATURE*/)
146.        WRITE(6,76)
147.     76 FORMAT(//7X,*      INCREMENT   SIGNATURE          VELOCITY      ACCEL
          1ERATION*/)
148.        WRITE(6,77)(I,DRV0(I),DRV1(I),DRV2(I),I=1,JPP)
149.     77 FORMAT(7X,I14,3E15.5)
150.        WRITE(6,1091)
151.   1091 FORMAT(//////////1X,*0*/)
152.        IMAXF=0
153.        PMAX=WMAX(K)
154.        AA1=0.05
155.        ICC=0
      C-----------------------------------------
      C              TOP OF LOOP INCREMENTING AA1
      C-----------------------------------------
156.        DO 104 ILP=1,40
157.        EQKA=AA1*PMAX/DMAX
158.        AA3=-0.91
      C-----------------------------------------
      C              TOP OF LOOP INCREMENTING AA3
      C-----------------------------------------
159.        DO 103 JJ=1,20
160.        IT=IMAXV
161.        EQMA=AA3*PMAX/DRV2(IMAXD)
162.        CPMAX=0.0
163.        AA2=AA1+AA3
164.        IF(AA2.LT.0.0)GO TO 1021
165.        IMAXC=IMAXD
166.        IT=IT+1
      C-------------------------------------------------------------
      C              TOP OF LOOP VARYING TIME BETWEEN ZERO ACCELERATION
      C              AND ZERO VELOCITY AND CALCULATING EQCA
      C              FOR EACH INCREMENT
      C-------------------------------------------------------------
167.        DO 102 II=IT,IMAXC
168.        EQCA=EQMA*DRV2(II)/DRV1(II)
169.        EQCA=-EQCA
      C
      C
170.        EQVK=EQKA
171.        EQMASS=EQMA
172.        EQVC=EQCA
173.        MM=JPP
174.        DT=PT(K)
      C-----------------------------------------------------------
      C              CALCULATING REDUCED TRANSFER FUNCTION USING
      C              SUBROUTINE EXACT1
      C-----------------------------------------------------------
      C
175.        CALL EXACT1(MM,DT,EQVK,EQMASS,T,GG,EQVC)
      C
176.        DO 73 I=1,JPP
177.        D(I)=DRV0(I)
178.        V(I)=GG(I)
179.     73 CONTINUE
180.        N=JPP
      C-----------------------------------------------------
      C              CALCULATE I(T) USING SUBROUTINE NWCONV
      C              BY IMPLICIT CONVOLUTION
      C-----------------------------------------------------
      C
```

```
      CALL NWCONV(N,V,G,D,DT)
C
C-----------------------------------------------------------
C              CALCULATING EQUIVALENT FORCEAS PRODUCT OF
C              I(T) AND EQMASS
C-----------------------------------------------------------
      DO 508 MP=1,JPP
      DF(MP)=G(MP)*EQMASS
  508 CONTINUE
      DO 509 MA=1,JPP
      DF(MA)=(DF(MA)+DF(MA+1))/2.
  509 CONTINUE
C-------------------------------------------------------------
C              AVERAGING AND FINDING MAXIMUM EQUIVALENT FORCE
C-------------------------------------------------------------
      CPMAX=0.
      DO 501 M=1,JPP
      DF(M)=(DF(M)+DF(M+1))/2.
      IF(DF(M).GT.CPMAX)GO TO 20
      GO TO 502
   20 CPMAX=DF(M)
      ICF=M
  502 CONTINUE
  501 CONTINUE
C-------------------------------------------------------------
C              EXECUTING FIRST CHECK TO ENSURE THAT THE
C              ABSOLUTE DIFFERENCE BETWEEN THE MAXIMUM COMPUTED
C              FORCE AND 25 KIPS IS LESS THAN 500 LBS
C-------------------------------------------------------------
      ERFCE=CPMAX-PMAX
      ABERFG=ABS(ERFCE)
      IF(ABERFG.GT.500.0)GO TO 102
C-------------------------------------------------------------------
C              EXECUTING SECOND CHECK TO ENSURE THAT THE DIFFERENCE
C              BETWEEN THE C VALUES COMPUTED AT THE CROSSING POINT
C              AND THE POINT OF INFLECTION GOES THROUGH ZERO
C-------------------------------------------------------------------
      ICC=ICC+1
      DFRNG=DF(IAFNL+1)-DF(IAFNL)
      ZVALUF=DF(IAFNL)+FDTZ*DFRNG
      CMAXV=(ZVALUF-EQKA*ZVALU0)/ZVALU1
      CDIFFR=(CMAXV-EQCA)/CMAXV
      ABCD=CDIFFR
      QC(ICC)=CDIFFR
      IF(ICC.EQ.1)GO TO 102
      CRATIO=QC(ICC)/QC(ICC-1)
      IF(CRATIO.GT.0.0)GO TO 102
C-------------------------------------------------------------
C              CALCULATING FORCE RATIOS COMPONENTS OF FORCE
C              AND TOTAL FORCE AT THE CROSSING POINT
C-------------------------------------------------------------
      FCHK=EQKA*DRV0(II)
      DIFCHK=FCHK-DF(II)
      DFCHKR=DIFCHK/FCHK
      FPFRAC=DF(II)/PMAX
      ICDPT=II
      TRMM=EQMA*DRV2(II)
      TRMC=EQCA*DRV1(II)
      TRMK=EQKA*DRV0(II)
      CPMXX(II)=TRMM+TRMC+TRMK
      WRITE(6,847)
  847 FORMAT(//10X,*GOOD RUN*//)
      GO TO 846
C************
  102 CONTINUE
 1021 CONTINUE
      AA3=AA3+0.045
C**************
  103 CONTINUE
      AA1=AA1+0.025
C********
  104 CONTINUE
 1000 FORMAT(/1X,*000*)
  845 FORMAT(6F15.4,10X,2I5,F10.3)
      WRITE(6,1002)
```

```
231.  1002 FORMAT(/10X,*OUTER LOOP COMPLETED*/)
232.       GO TO 94
233.   846 CONTINUE
234.       WRITE(6,1043)
235.  1043 FORMAT(/////////10X,*INCREMENT*,2X,*M-COMP.*,8X,*C-COMP.*,8X,*K-C
          1OMP.*,8X,*EXACT*,8X,*CONVOLUTION*,8X,*TDT FUNC*,8X,*SIGNATURE*/)
     C-------------------------------------------------------------
     C             CALCULATING COMPONENTS OF FORCE DUE TO INERTIAL
     C             DAMPING AND STIFFNESS
     C-------------------------------------------------------------
236.       JPN=JPP-3
237.       DO 106 I=1,JPN
238.       TMT=EQMA*DRV2(I)
239.       TCT=EQCA*DRV1(I)
240.       TKT=EQKA*DRV0(I)
241.       CPMXX(I)=TCT+TKT+TMT
242.       WRITE(6,1001)I,TMT,TCT,TKT,CPMXX(I),DF(I),GG(I),DRV0(I)
243.   106 CONTINUE
     C-------------------------------------------------------------
     C             CALCULATING FORCE RATIOS AT SECTIONS (1),(2),(3)
     C-------------------------------------------------------------
244.       AFRNG=DF(NAFNL+1)-DF(NAFNL)
245.       DVALUF=DF(NAFNL)+DDTZ*AFRNG
     C******
246.       ZVALUR=ZVALUF/PMAX
     C*******
247.       DVALZD=DVALUF/PMAX
     C******
248.       FDRTIO=ABERFG/PMAX
     C-------------------------------------------------------------
     C             CALCULATING TIME RATIOS AT SECTIONS(1),(2),(3)
     C-------------------------------------------------------------
249.       DENOM=FLOAT(IMAXD)
250.       DENOM1=1.0
251.       TCRSPT=FLOAT(II)/DENOM
252.       TZROA=FLOAT(IAFNL)/DENOM
     C********
253.       WRITE(6,1041)
254.  1041 FORMAT(/////////10X,*EQUIV. MASS*,10X,*EQUIV. STIFFNESS*,9X,*EQUI
          1V. DAMPING*)
255.       WRITE(6,2041)
256.  2041 FORMAT(12X,*SLUGS*,16X,*LBS/FT*,20X,*LBS-SEC/FT*/)
257.       WRITE(6,1042)EQMA,EQKA,EQCA
258.  1042 FORMAT(10X,F10.2,15X,F10.2,12X,F10.1)
259.       WRITE(6,1044)
260.  1044 FORMAT(//20X,*     FORCE RATIOS(FORCE OVER 25000)*/)
261.       WRITE(6,1045)
262.  1045 FORMAT(25X,*SECTION(1) SECTION(2) SECTION(3)*/)
263.       WRITE(6,1046)ZVALUR,FPFRAC,DVALZD
264.  1046 FORMAT(23X,3F10.3)
265.       WRITE(6,1050)
266.  1050 FORMAT(///20X,*      TIME RATIOS(TIME OVER TIME TO MAX. DEF.)*/)
267.       DENOM1=1.
268.       WRITE(6,1045)
269.       WRITE(6,1046)TZROA,TCRSPT,DENOM1
270.       WRITE(6,1060)
271.  1060 FORMAT(///20X,*C-PARAMETER DIFFERENCE RATIO*/)
272.       WRITE(6,1061)CDIFFR
273.  1061 FORMAT(30X,F7.3)
274.       WRITE(6,1070)
275.  1070 FORMAT(///20X,*FORCE DIFFERENCE RATIO AT THE CROSSING POINT*/)
276.       WRITE(6,1061)DFCHKR
277.       WRITE(6,1080)
278.  1080 FORMAT(///20X,*MAXIMUM FORCE DIFFERENCE*/)
279.       WRITE(6,1061)ABERFG
280.  1001 FORMAT(10X,I5,7F15.5)
     C-------------------------------------------------------------
281.   811 CONTINUE
282.    94 CONTINUE
     C
283.       STOP
284.       END
     C
```

```
      C-----------------------------------------------------------------
      SUBROUTINE EXACFIT(FI,TFXP,TBETAF,FAF,AI)
C
C             THIS SUBROUTINE CALCULATES THE PARAMETERS OF THE
C             MAXIMUM LATERAL DEFLECTION PROFILE USING
C             THE DEVELOPED INTERPOLATION-ITERATION PROCEDURE
C-----------------------------------------------------------------
C             INPUT-    FI--MEASURED DEFLECTIONS AT LOCATIONS LATERAL
C                           TO THE TIRE PRINT
C                       AI--LATERAL DISTANCES FROM EDGE OF TIRE PRINT
C                           CORRESPONDING TO FI
C             OUTPUT    TFXP--R PARAMETER
C                       TBETAF--BETA PARAMETER
C                       FAF--A PARAMETER
C
      DIMENSION FI(6),TBETA(3),TVAL(999),AI(5),FA(5),FFXP(5)
C$    TRACE SUBSCRIPTS
C$    TRACE ARITHMETIC
      M=1
      IFTX=0
      I=2
      IG=I+1
      IM=I+2
      ITRID=0
C
C*******************************
C*******************************
C
  710 CONTINUE
      FXP=0.2001
      DFXP=0.0125
      J=0
  771 CONTINUE
      J=J+1
      FXP=FXP+DFXP
      IFCHK=0
  772 CONTINUE
  776 CONTINUE
      CONS1=ALOG(FI(I))-ALOG(FI(IG))
      CONS2=ALOG(FI(I))-ALOG(FI(IM))
      CONF=CONS1/CONS2
      FLHS=CONF*((AI(I)**FXP)-(AI(IM)**FXP))
      FRHS=(AI(I)**FXP)-(AI(IG)**FXP)
      TVAL(J)=FLHS-FRHS
      IF(J.EQ.1)GO TO 771
      FDIF=TVAL(J)/TVAL(J-1)
      ABVAL=ABS(TVAL(J))
      IF(J.EQ.999)GO TO 726
      IF(FDIF.GT.0.0)GO TO 771
      TFDIF=ABS(TVAL(J-1))+ABS(TVAL(J))
      FFXP(M)=FXP-(TVAL(J)/TFDIF)*DFXP
  773 CONTINUE
C
      FBETA1=ALOG(FI(I))-ALOG(FI(IG))
      FBETA2=(AI(I)**FFXP(M))-(AI(IG)**FFXP(M))
      TBETA(M)=FBETA1/FBETA2
      FA1=TBETA(M)*(AI(1)**FFXP(M))
      FA(M)=FI(1)/EXP(FA1)
      GO TO 777
      IF(ITRID.EQ.1)GO TO 727
CAUTION - STATEMENT CANNOT BE EXECUTED - NO STATEMENT NUMBER          **********
      IF(IFTX.EQ.1)GO TO 777
      M=M+1
      IG=IG+1
      IM=IM+2
      IFTX=1
      GO TO 710
  777 FAF=FA(M)
      TBETAF=TBETA(M)
      TFXP=FFXP(M)
      GO TO 728
C*******************************
C**********
  726 CONTINUE
```

```
      ITRID=1
      M=M+1
      IG=IG+1
      IM=IM+2
      IFTX=1
      IF(IM.LE.5)GO TO 730
      WRITE(6,731)
  731 FORMAT(/20X,*DATA DOES NOT FIT--CHECK DATA*/)
      GO TO 720
  730 GO TO 710
  727 CONTINUE
C*****************************
      FAF=FA(2)
      TBETAF=TBETA(2)
      TFXP=FFXP(2)
  728 CONTINUE
      WRITE(6,775)
  775 FORMAT(/20X,*  A PARAMETER      BETA          EXPONENT R*/)
      WRITE(6,778)FAF,TBETAF,TFXP
  778 FORMAT(20X,3E15.5/)
      WRITE(6,750)
  750 FORMAT(/20X,*  CALCULATED Y  *  MEASURED Y      LATERAL DIST.*/)
      DO 701 M=1,5
      YY1=TBETAF*(AI(M)**TFXP)
      YY2=EXP(YY1)
      YY=FAF*YY2
      WRITE(6,20)YY,FI(M),AI(M)
  701 CONTINUE
  720 CONTINUE
   20 FORMAT(20X,3E15.5)
C
      RETURN
      END
C
C
C
C-------------------------------------------------------

      SUBROUTINE SIGNTR(VBETA,VRVAL,VIPX,VIPY,VISIG,NV)
C
C             THIS SUBROUTINE CALCULATES THE SIGNATURE BY
C             DIRECT SUBSTITUTION
C-------------------------------------------------------
C             INPUT-    VBETA--BETA PARAMETER
C                       VIPX--LATERAL DISTANCE OF GAGE FROM OUTER
C                             EDGE OF TIRE PRINT
C                       VIPY--NV VALUES OF MEASURED DEFLECTION
C                             AT VIPX FROM OUTER EDGE OF TIRE PRINT
C                       VRVAL--R PARAMETER
C
C             OUTPUT-   VISIG--NV VALUES OF THE SIGNATURE
C
      DIMENSION VIPY(200),VISIG(200)
      VTOP=VBETA*(VIPX**VRVAL)
      DO 40 I=1,NV
      VISIG(I)=VIPY(I)/EXP(VTOP)
   40 CONTINUE
      RETURN
      END
C
C-------------------------------------------------------

      SUBROUTINE NWCONV(N,V,G,O,DT)
C
C             THIS SUBROUTINE IMPLICITLY CONVOLUTES V(  ) AND O(  )TO
C             YIELD G(  ) AT N POINTS
C-------------------------------------------------------
C
C             INPUT-    V--N VALUES OF INPUT
C                       O--N VALUES OF OUTPUT
C                       DT--TIME INCREMENT
C
C             OUTPUT-   G--N VALUES OF THE IMPLICIT CONVOLUTION RESULT
C
C
```

```
      DIMENSION V(200),G(200),D(200)
      S=0.
      Q=0.0
      G(1)=D(1)/(V(1)*DT)
      DO 984 I=2,N
      K=I-1
      DO 985 M=1,K
      Q=Q+V(K+2-M)*G(M)
  985 CONTINUE
      S=Q
      G(I)=((D(I)/DT)-S)/V(1)
C
C
      Q=0.0
      S=0.0
  984 CONTINUE
      RETURN
      END
C
C
C-----------------------------------------------------------------------

      SUBROUTINE EXACT1(MM,DT,EQVK,EQMASS,T,GG,EQVC)
C
C             THIS SUBROUTINE CALCULATES THE REDUCED TRANSFER FUNCTION
C             BY DIRECT SUBSTITUTION
C-----------------------------------------------------------------------
C
C             INPUT-    EQVK--EQUIVALENT K PARAMETER
C                       EQMASS--EQUIVALENT MASS
C                       EQVC--EQUIVALENT C PARAMETER
C                       DT--TIME INCREMENT
C                       MM--NUMBER OF DATA POINTS
C
C             OUTPUT-   GG--MM VALUES OF THE TIME DEPENDENT TRANSFER FUN
C
      DIMENSION T(200),GG(200)
C$    TRACE ARITHMETIC
C
      DO 630 I=1,MM
      T(I)=FLOAT(I)*DT
      TIME=T(I)
C
C
      BB=SQRT(EQVK/EQMASS)
      AA=EQVC/(2.*EQMASS)
C
      TRI=BB*BB-AA*AA
      IF(TRI.LT.0.0)GO TO 3
C
      GE1=1./SQRT(TRI)
      GE2=1./EXP(AA*T(I))
      G3=SIN(SQRT(TRI)*T(I))
      GG(I)=GE1*GE2*G3
C
C
      GO TO 630
C
    3 CONTINUE
      PP=SQRT(ABS(TRI))
      P1=EXP(PP*T(I))
      P2=1./(EXP(PP*T(I)))
      P3=1./EXP(AA*T(I))
      P5=(P1-P2)/2.
      GG(I)=P3*P5/PP
C
  630 CONTINUE
C
      RETURN
      END
```

NEW RECORD

| NUMBER OF DATA POINTS | RECORD NUMBER | MAX. WHEEL LOAD | TIME INCREMENT | NUMBER OF GAGES |
|---|---|---|---|---|
| 46 | 1 | 25000. | .20 | 5 |

DEFLECTIONS IN FT

| GAGE 1 | GAGE 2 | GAGE 3 | GAGE 4 | GAGE 5 |
|---|---|---|---|---|
| .00001 | 0 | .00001 | .00001 | -.00000 |
| .00003 | .00002 | .00001 | .00001 | 0 |
| .00004 | .00003 | .00003 | .00001 | .00000 |
| .00005 | .00005 | .00004 | .00002 | .00001 |
| .00008 | .00006 | .00005 | .00003 | .00001 |
| .00011 | .00008 | .00007 | .00004 | .00002 |
| .00013 | .00010 | .00009 | .00005 | .00002 |
| .00017 | .00014 | .00011 | .00006 | .00003 |
| .00022 | .00019 | .00014 | .00008 | .00003 |
| .00030 | .00023 | .00018 | .00010 | .00004 |
| .00036 | .00030 | .00023 | .00012 | .00006 |
| .00048 | .00040 | .00028 | .00015 | .00006 |
| .00063 | .00051 | .00037 | .00019 | .00009 |
| .00083 | .00069 | .00048 | .00024 | .00010 |
| .00108 | .00087 | .00060 | .00029 | .00012 |
| .00134 | .00108 | .00072 | .00035 | .00014 |
| .00165 | .00132 | .00086 | .00040 | .00016 |
| .00195 | .00156 | .00097 | .00044 | .00017 |
| .00238 | .00189 | .00112 | .00048 | .00018 |
| .00280 | .00218 | .00124 | .00051 | .00019 |
| .00341 | .00261 | .00140 | .00056 | .00020 |
| .00384 | .00293 | .00150 | .00058 | .00020 |
| .00418 | .00323 | .00161 | .00061 | .00021 |
| .00434 | .00343 | .00166 | .00062 | .00021 |
| .00436 | .00349 | .00166 | .00062 | .00021 |
| .00430 | .00350 | .00168 | .00063 | .00021 |
| .00386 | .00310 | .00153 | .00059 | .00020 |
| .00344 | .00290 | .00145 | .00056 | .00019 |
| .00292 | .00247 | .00123 | .00048 | .00016 |
| .00257 | .00218 | .00111 | .00043 | .00015 |
| .00210 | .00178 | .00090 | .00033 | .00010 |
| .00175 | .00147 | .00073 | .00026 | .00007 |
| .00145 | .00122 | .00059 | .00020 | .00005 |
| .00122 | .00101 | .00047 | .00014 | .00003 |
| .00106 | .00089 | .00038 | .00010 | .00001 |
| .00091 | .00073 | .00030 | .00006 | -.00001 |
| .00082 | .00065 | .00026 | .00004 | -.00001 |
| .00073 | .00057 | .00021 | .00002 | -.00002 |
| .00067 | .00051 | .00018 | .00001 | -.00003 |

| | | | | |
|---|---|---|---|---|
| .00063 | .00049 | .00016 | -.00000 | -.00003 |
| .00062 | .00045 | .00014 | -.00001 | -.00003 |
| .00059 | .00043 | .00013 | -.00001 | -.00003 |
| .00059 | .00043 | .00013 | -.00002 | -.00003 |
| .00058 | .00043 | .00012 | -.00002 | -.00003 |
| .00056 | .00041 | .00011 | -.00002 | -.00003 |
| 0 | 0 | 0 | 0 | 0 |

PEAK DEFLECTIONS

| | | | | |
|---|---|---|---|---|
| .00436 | .00350 | .00168 | .00063 | .00021 |

| A PARAMETER | BETA | EXPONENT R |
|---|---|---|
| 4.79864E-03 | -6.02783E-01 | 1.31790E+00 |

| CALCULATED Y | MEASURED Y | LATERAL DIST. |
|---|---|---|
| 4.35510E-03 | 4.35510E-03 | 2.50000E-01 |
| 3.56827E-03 | 3.49750E-03 | 5.83330E-01 |
| 1.71561E-03 | 1.68158E-03 | 1.50000E+00 |
| 6.38773E-04 | 6.30420E-04 | 2.50000E+00 |
| 2.07310E-04 | 2.12980E-04 | 3.50000E+00 |

FOR SIGNATURE

| INCREMENT | SIGNATURE | VELOCITY | ACCELERATION |
|---|---|---|---|
| 1 | 0 | 7.83911E-05 | 2.93966E-04 |
| 2 | 3.13564E-05 | 1.17587E-04 | 9.79888E-05 |
| 3 | 4.70346E-05 | 7.83911E-05 | 9.79888E-05 |
| 4 | 6.27128E-05 | 7.83911E-05 | 1.46983E-04 |
| 5 | 7.83911E-05 | 1.17587E-04 | 1.95978E-04 |
| 6 | 1.09747E-04 | 1.56782E-04 | 1.95978E-04 |
| 7 | 1.41104E-04 | 1.95978E-04 | 2.93966E-04 |
| 8 | 1.88139E-04 | 2.74369E-04 | 2.93966E-04 |
| 9 | 2.50851E-04 | 3.13564E-04 | 2.93966E-04 |
| 10 | 3.13564E-04 | 3.91955E-04 | 5.87933E-04 |
| 11 | 4.07633E-04 | 5.48737E-04 | 7.83911E-04 |
| 12 | 5.33059E-04 | 7.05520E-04 | 1.07788E-03 |
| 13 | 6.89841E-04 | 9.79888E-04 | 1.27385E-03 |
| 14 | 9.25014E-04 | 1.21506E-03 | 8.81899E-04 |
| 15 | 1.17587E-03 | 1.33265E-03 | 6.85922E-04 |
| 16 | 1.45807E-03 | 1.48943E-03 | 6.85922E-04 |
| 17 | 1.77164E-03 | 1.60702E-03 | 1.07788E-03 |
| 18 | 2.10088E-03 | 1.92058E-03 | 1.17587E-03 |
| 19 | 2.53987E-03 | 2.07736E-03 | 1.27385E-03 |
| 20 | 2.93183E-03 | 2.43012E-03 | 1.07788E-03 |
| 21 | 3.51192E-03 | 2.50851E-03 | -8.81899E-04 |
| 22 | 3.93523E-03 | 2.07736E-03 | -2.05777E-03 |
| 23 | 4.34286E-03 | 1.68541E-03 | -3.03765E-03 |
| 24 | 4.60939E-03 | 8.62302E-04 | -3.62559E-03 |
| 25 | 4.68779E-03 | 2.35173E-04 | -5.38939E-03 |
| 26 | 4.70346E-03 | -1.29345E-03 | -5.58536E-03 |
| 27 | 4.17040E-03 | -1.99897E-03 | -2.05777E-03 |
| 28 | 3.90387E-03 | -2.11656E-03 | -1.07788E-03 |
| 29 | 3.32378E-03 | -2.43012E-03 | -4.89944E-04 |
| 30 | 2.93183E-03 | -2.31254E-03 | 5.38939E-04 |
| 31 | 2.39877E-03 | -2.39093E-03 | 6.85922E-04 |
| 32 | 1.97545E-03 | -1.88139E-03 | 1.00439E-03 |



3000 RUN

| INCREMENT | M-COMP. | C-COMP. | K-COMP. | EXACT | CONVOLUTION | TDT FUNC | SIGNATURE |
|---|---|---|---|---|---|---|---|
| 1 | 72.36842 | 442.25146 | 0 | 514.61988 | 617.71209 | .04052 | 0 |
| 2 | 24.12281 | 663.37719 | 95.83333 | 783.33333 | 675.91968 | .03672 | .00003 |
| 3 | 24.12281 | 442.25146 | 143.75000 | 610.12427 | 618.69802 | .03287 | .00005 |
| 4 | 36.18421 | 442.25146 | 191.66667 | 670.10234 | 788.48276 | .02941 | .00006 |
| 5 | 48.24561 | 663.37719 | 239.58333 | 951.20614 | 1087.28563 | .02632 | .00008 |
| 6 | 48.24561 | 884.50292 | 335.41667 | 1268.16520 | 1409.61497 | .02355 | .00011 |
| 7 | 72.36842 | 1105.62865 | 431.25000 | 1609.24708 | 1875.76839 | .02108 | .00014 |
| 8 | 72.36842 | 1547.88012 | 575.00000 | 2195.24854 | 2377.82005 | .01886 | .00019 |
| 9 | 72.36842 | 1769.00585 | 766.66667 | 2608.04094 | 2916.98704 | .01688 | .00025 |
| 10 | 144.73684 | 2211.25731 | 958.33333 | 3314.32749 | 3850.51099 | .01511 | .00031 |
| 11 | 192.98246 | 3095.76023 | 1245.83333 | 4534.57602 | 5092.77541 | .01352 | .00041 |
| 12 | 265.35088 | 3980.26316 | 1629.16667 | 5874.78070 | 6788.82147 | .01210 | .00053 |
| 13 | 313.59649 | 5528.14327 | 2108.33333 | 7950.07310 | 8855.46687 | .01083 | .00069 |
| 14 | 217.10526 | 6854.89766 | 2827.08333 | 9899.08626 | 10604.18900 | .00969 | .00093 |
| 15 | 168.85965 | 7518.27485 | 3593.75000 | 11280.88450 | 12230.96440 | .00867 | .00118 |
| 16 | 168.85965 | 8402.77778 | 4456.25000 | 13027.88743 | 13946.77641 | .00776 | .00146 |
| 17 | 265.35088 | 9066.15497 | 5414.58333 | 14746.08918 | 16225.51305 | .00694 | .00177 |
| 18 | 289.47368 | 10835.16082 | 6420.83333 | 17545.46784 | 18754.55138 | .00621 | .00210 |
| 19 | 313.59649 | 11719.66374 | 7762.50000 | 19795.76023 | 21549.91447 | .00556 | .00254 |
| 20 | 265.35088 | 13709.79532 | 8960.41667 | 22935.56287 | 24266.73247 | .00498 | .00293 |
| 21 | -217.10526 | 14152.04678 | 10733.33333 | 24668.27485 | 24740.46330 | .00445 | .00351 |
| 22 | -506.57895 | 11719.66374 | 12027.08333 | 23240.16813 | 23698.22351 | .00399 | .00394 |
| 23 | -747.80702 | 9508.40643 | 13272.91667 | 22033.51608 | 21219.97611 | .00357 | .00434 |
| 24 | -892.54386 | 4864.76608 | 14087.50000 | 18059.72222 | 17655.89134 | .00319 | .00461 |
| 25 | -1326.75439 | 1326.75439 | 14327.08333 | 14327.08333 | 11497.90363 | .00286 | .00469 |
| 26 | -1375.00000 | -7297.14912 | 14375.00000 | 5702.85088 | 4443.21485 | .00256 | .00470 |
| 27 | -506.57895 | -11277.41228 | 12745.83333 | 961.84211 | 972.66864 | .00229 | .00417 |
| 28 | -265.35088 | -11940.78947 | 11931.25000 | -274.89035 | -1610.69484 | .00205 | .00390 |
| 29 | -120.61404 | -13709.79532 | 10158.33333 | -3672.07602 | -3627.83553 | .00183 | .00332 |

| EQUIV. MASS SLUGS | EQUIV. STIFFNESS LBS/FT | EQUIV. DAMPING LBS-SEC/FT |
|---|---|---|
| 246179.17 | 3056258.49 | 5641606.1 |

FORCE RATIOS(FORCE OVER 25000)

| SECTION(1) | SECTION(2) | SECTION(3) |
|---|---|---|
| .981 | .460 | .417 |

TIME RATIOS(TIME OVER TIME TO MAX. DEF.)

| SECTION(1) | SECTION(2) | SECTION(3) |
|---|---|---|
| .769 | .962 | 1.000 |



C-PARAMETER DIFFERENCE RATIO

.044

FORCE DIFFERENCE RATIO AT THE CROSSING POINT

.197

MAXIMUM FORCE DIFFERENCE

259.537

```
1.        PROGRAM PREDCT (INPUT,OUTPUT,TAPE5=INPUT,TAPE6=OUTPUT,PLOT)
      C
      C-----------------------------------------------------------------
      C         THIS PROGRAM PREDICTS THE SIGNATURE AT AN UNTESTED SITE
      C        DUE TO VEHICLE A,IF THE SIGNATURE OF A STANDARD VEHICLE
      C        IS KNOWN AT THE UNTESTED SITE, AND THE SIGNATURE OF BOTH
      C        THE STANDARD VEHICLE AND VEHICLE A ARE KNOWN AT A
      C        STANDARD SITE
      C-----------------------------------------------------------------
      C
      C---------------------------------
      C        STANDARD VEHICLE AND SITE
      C        C 131       SITE 1       47      SIGNATURE
      C---------------------------------
      C
      C---------------------------------
      C        C 131      SITE 3    47          BOYER      SIGNATURE
      C        C-135 SITE 1    47  BOYER       SIGNATURE
      C
      C-----------------------------------------------------------------
      C        INCLUDED ONLY FOR PURPOSES OF THIS EXAMPLE-THIS SIGNATURE
      C        IS THE PREDICTED SIGNATURE
      C     C 135   SITE 3       BOYER    SIGNATURE   47
      C-----------------------------------------------------------------
      C-----------------------------------------------------------------
      C        INPUT-          SCR( )      SIGNATURE DUE TO STANDARD VEHICLE
      C                                    AT STANDARD SITE
      C                        X( )        SIGNATURE DUE TO STANDARD VEHICLE
      C                                    AT OTHER SITE
      C                        DFCE( )     SIGNATURE DUE TO OTHER VEHICLE
      C                                    AT STANDARD SITE
      C                        COMPV( )    SIGNATURE DUE TO OTHER VEHICLE
      C                                    AT OTHER SITE(FOR PURPOSES OF
      C                                    THIS EXAMPLE ONLY)
      C                        ALL INPUT SIGNATURES ARE IN INCHES
      C        OUTPUT          DD( )       PREDICTED SIGNATURE IN FT.
      C-----------------------------------------------------------------
      C        SUBROUTINES REQUIRED        (1)  EXACT1(      )
      C                                    (2)  NWCONV(      )
      C                                    (3)  ERECT2(      )
      C                                    (4)  MODPRM(      )
      C-----------------------------------------------------------------
 2.         DIMENSION SOUT1(200),SOUT2(200),VOUT1(200)
 3.         DIMENSION ETINP(200),EQFNC(200)
 4.         DIMENSION ET(200)
 5.         DIMENSION VISIG(200)
 6.         DIMENSION XT(6,200),XF(6,200),DTRK1(200),DF4(200),SFNC(200)
 7.         DIMENSION PP(800),XG(800),DD(800)
 8.         DIMENSION DRV0(100),DRV1(100),DRV2(100)
 9.         DIMENSION DF(200),X(100),DFCE(100),DDEF(100)
10.         DIMENSION SCR(100),T(200),V(200),D(200),G(200),GG(200)
11.         DIMENSION COMPV(200),VOUT2(200)
      C$    TRACE ARITHMETIC
      C
      C
12.      50 FORMAT(//60X,20H----------//)
13.     498 FORMAT(29X,54HEQUIV INPUT IN LBS      TDT FUNCTION      RESPONSE IN
           1FT//)
14.     398 FORMAT(31X,E15.5,5X,E15.5,2X,E15.5)
      C
15.         READ(5,100)(SCR(I),I=1,47)
16.         READ(5,100)(X(I),I=1,47)
17.         READ(5,100)(DFCE(I),I=1,47)
18.         READ(5,100)(COMPV(I),I=1,47)
19.     100 FORMAT(7F10.6)
      C
      C
20.         DO 496 I=1,47
21.         SOUT1(I)=SCR(I)/12.
22.         VOUT1(I)=DFCE(I)/12.
23.         SOUT2(I)=X(I)/12.
24.         VOUT2(I)=COMPV(I)/12.
25.     496 CONTINUE
      C
      C
```

```
      C
26.         JP=47
27.         PMAX =20000.
28.         DT=0.04
29.         MM=47
30.         LL=47
31.         NT=47
      C
32.         DO 74 I=1,NT
33.         VISIG(I)=SOUT1(I)
34.      74 CONTINUE
      C
      C
      C
35.         WRITE(6,497)
36.     497 FORMAT(//2X,23HSITE ONE    STD VEHICLE//)
      C
37.         CALL MODPRM(PMAX,JP,DT,VISIG,EQMASS,DF,GG)
      C
      C
      C
      C           COMPUTE EQUIV.   INPUT FOR VEHICLE 2     SITE 1
38.         DO 721 I=1,MM
39.         T(I)=FLOAT(I)*DT
40.         O(I)=VOUT1(I)
41.         V(I)=GG(I)
42.     721 CONTINUE
      C
43.         N=47
      C
44.         CALL NWCONV(N,V,G,O,DT)
      C
45.         DO 722 I=1,MM
46.         ETINP(I)=G(I)*EQMASS
47.     722 CONTINUE
      C
48.         WRITE(6,50)
49.         WRITE(6,495)
50.     495 FORMAT(//2X,21HSITE ONE    VEHICLE 2//)
51.         WRITE(6,498)
52.         WRITE(6,398)(ETINP(I),GG(I),O(I),I=1,MM)
      C
      C
      C
      C           COMPUTE EQUIVALENCY   FUNCTION
53.         DO 723 I=1,MM
54.         EQFNC(I)=ETINP(I)/DF(I)
55.     723 CONTINUE
      C
      C        COMPUTE TDT FUNCTION ;EQUIV. INPUT FOR NEXTSITE STD. VEHICLE
56.         WRITE(6,397)
57.     397 FORMAT(//2X,23HNEXT SITE   STD VEHICLE//)
      C
      C
58.         DO 724 I=1,MM
59.         VISIG(I)=SOUT2(I)
60.     724 CONTINUE
      C
61.         CALL MODPRM(PMAX,JP,DT,VISIG,EQMASS,DF,GG)
      C
      C
      C        COMPUTE EQUIV. INPUT NEXT SITE    VEHICLE 2
      C
62.         DO 725 I=1,MM
63.         ET(I)=DF(I)*EQFNC(I)
64.     725 CONTINUE
      C
      C        COMPUTE OUTPUT FOR NEXT SITE VEHICLE 2
      C
65.         DO 206 I=1,MM
66.         PP(I)=ET(I)/EQMASS
67.         XG(I)=GG(I)
68.     206 CONTINUE
      C
      C
```

```
      CALL ERECT2(MM,PP,XG,DT,DD)
C
C
      WRITE(6,50)
      WRITE(6,494)
  494 FORMAT(//2X,21HNEXT SITE   VEHICLE 2//)
      WRITE(6,498)
      WRITE(6,398)(ET(I),XG(I),DD(I),I=1,MM)
C
      WRITE(6,50)
      WRITE(6,2000)
 2000 FORMAT(//60X,*PREDICTED*,10X,*MEASURED*//)
      WRITE(6,1000)(DD(I),VOUT2(I),I=1,47)
 1000 FORMAT(52X,2F15.5)
C
      WRITE(6,50)
C
C
C
C
C
C
      STOP
      END
C
C
C

      SUBROUTINE NWCONV(N,V,G,D,DT)
      DIMENSION V(200),G(200),D(200)
      S=0.
      Q=0.0
C
C
      G(1)=D(1)/(V(1)*DT)
      DO 984 I=2,N
      K=I-1
      DO 985 M=1,K
      Q=Q+V(K+2-M)*G(M)
  985 CONTINUE
C
      S=Q
      G(I)=((D(I)/DT)-S)/V(1)
C
C
      Q=0.0
      S=0.0
  984 CONTINUE
      RETURN
      END
C
C
C

      SUBROUTINE ERECT2(MM,PP,XG,DT,DD)
      DIMENSION PP(800),XG(800),DD(800)
C
C
      PS2=0.0
      DO 331 I=2,MM
      K=I-1
      DO 332 M=1,K
      PS2=PP(K+1-M)*XG(M)+PS2
  332 CONTINUE
      DD(I-1)=PS2*DT
      PS2=0.0
  331 CONTINUE
      RETURN
      END
C
C
C

      SUBROUTINE EXACT (MM,DT,EQVK,EQMASS,T,GG,EQVC)
      DIMENSION T(200),GG(200)
```

```
C
C              COMPUTING EXACT TRANSFER FUNCTION
      DO 630 I=1,MM
      T(I)=FLOAT(I)*DT
      TIME=T(I)
C
C
      BB=SQRT(EQVK/EQMASS)
      AA=EQVC/(2.*EQMASS)
C
      TRI=BB*BB-AA*AA
      IF(TRI.LT.0.0)GO TO 3
C
      GE1=1./SQRT(TRI)
      GE2=1./EXP(AA*T(I))
      G3=SIN(SQRT(TRI)*T(I))
      GG(I)=GE1*GE2*G3
C
C
      GO TO 630
C
    3 CONTINUE
      PP=SQRT(ABS(TRI))
      P1=EXP(PP*T(I))
      P2=1./(EXP(PP*T(I)))
      P3=1./EXP(AA*T(I))
      P5=(P1-P2)/2.
      GG(I)=P3*P5/PP
C
  630 CONTINUE
C
C
      RETURN
      END
C

      SUBROUTINE MODPRM(PMAX,JP,DT,VISIG,EQMASS,DF,GG)
      DIMENSION QC(100)
      DIMENSION DF(200)
      DIMENSION T(200)
      DIMENSION D(200),GG(200)
      DIMENSION V(200),G(200)
      DIMENSION IVEL(11,5)
      DIMENSION DRV1(200),DRV2(200),CPMXX(50),VISIG(200),DRV0(200)
C
C
      DO 74 I=1,JP
      DRV0(I)=VISIG(I)
      TRM1=(VISIG(I)+VISIG(I+1))/2.
      IF(I.GT.1)GO TO 744
      TRM2=VISIG(I)/2.
      GO TO 474
  744 CONTINUE
      TRM2=(VISIG(I)+VISIG(I-1))/2.
  474 CONTINUE
      DRV1(I)=(TRM1-TRM2)/DT
   74 CONTINUE
      DO 75 I=1,JP
      TRN1=(DRV1(I+1)+DRV1(I))/2.
      IF(I.GT.1)GO TO 755
      TRN2=DRV1(I)/2.
      GO TO 575
  755 CONTINUE
      TRN2=(DRV1(I)+DRV1(I-1))/2.
  575 CONTINUE
      DRV2(I)=(TRN1-TRN2)/DT
   75 CONTINUE
C
C
      BOTM=0.00000000001
C**************
      DO 726 I=1,JP
      HUMP1=DRV0(I+1)-DRV0(I)
      IF(HUMP1.GE.0.0)GO TO 726
      JPP=I+6
```

```
      GO TO 727
  726 CONTINUE
  727 CONTINUE
C*************
C
      IMAXV=0
      DV1MX=0.0
      DO 315 I=1,JPP
      IF(DRV1(I).EQ.0.0)DRV1(I)=(DRV1(I+1)+DRV1(I-1))/2.
CAUTION - IS FLOATING POINT EQUALITY TO BE EXPECTED       ********************************
      IF(DRV1(I).EQ.0.0)DRV1(I)=(DRV1(I+2)+DRV1(I-2))/2.
CAUTION - IS FLOATING POINT EQUALITY TO BE EXPECTED       ********************************
      IF(ABS(DRV1(I)).LT.BOTM)DRV1(I)=(DRV1(I+1)+DRV1(I-1))/2.
      IF(ABS(DRV2(I)).LT.BOTM)DRV2(I)=(DRV2(I+1)+DRV2(I-1))/2.
      IF(DRV1(I).LT.DV1MX)GO TO 315
      DV1MX=DRV1(I)
      IMAXV=I
  315 CONTINUE
C
C
      DMAX=DRV0(1)
      DO 53 I=2,JPP
      IF(DRV0(I).LT.DMAX)GO TO 53
      DMAX=DRV0(I)
      IMAXD=I
   53 CONTINUE
C
C
      IMAXV1=IMAXV-1
      DO 57 I=2,IMAXV1
      IF(DRV2(I).LE.0.0)DRV2(I)=(DRV2(I-1)+DRV2(I+1))/2.
      IF(DRV2(I).LE.0.0)DRV2(I)=(DRV2(I-2)+DRV2(I+2))/2.
   57 CONTINUE
      IMAXVA=IMAXV+1
      DO 109 I=IMAXVA,JPP
      IF(DRV2(I).GE.0.0)DRV2(I)=(DRV2(I-1)+DRV2(I+1))/2.
      IF(DRV2(I).GE.0.0)DRV2(I)=(DRV2(I-2)+DRV2(I+2))/2.
  109 CONTINUE
      DO 107 I=1,JPP
      IF(DRV1(I+1).EQ.DRV1(I))DRV1(I+1)=(DRV1(I+2)+DRV1(I))/2.
CAUTION - IS FLOATING POINT EQUALITY TO BE EXPECTED       ********************************
      IF(DRV2(I+1).EQ.DRV2(I))DRV2(I+1)=(DRV2(I+2)+DRV2(I))/2.
CAUTION - IS FLOATING POINT EQUALITY TO BE EXPECTED       ********************************
  107 CONTINUE
C********
      DO 789 IA=1,JPP
      DEROTS=DRV1(IA+1)/DRV1(IA)
      IF(DEROTS.GT.0.0)GO TO 789
      DZERO=DRV1(IA)-DRV1(IA+1)
      DDTZ=DRV1(IA)/DZERO
      NAFNL=IA
      GO TO 788
  789 CONTINUE
  788 CONTINUE
C************
      DO 889 IA=1,JPP
      ZEROTS=DRV2(IA+1)/DRV2(IA)
      IF(ZEROTS.GT.0.0)GO TO 889
      TZERO=DRV2(IA)-DRV2(IA+1)
      FDTZ=DRV2(IA)/TZERO
      IAFNL=IA
      DRORNG=DRV0(IA+1)-DRV0(IA)
      ZVALU0=DRV0(IA)+FDTZ*DRORNG
      DR1RNG=DRV1(IA+1)-DRV1(IA)
      ZVALU1=DRV1(IA)+FDTZ*DR1RNG
      GO TO 888
  889 CONTINUE
  888 CONTINUE
C
C*********
C
C
      WRITE(6,99)
   99 FORMAT(/30X,*FOR SIGNATURE*/)
      WRITE(6,76)
```

```
 94.     76 FORMAT(//1X,*      INCREMENT    DEFLECTION          VELOCITY      ACCEL
           1ERATION*/)
 95.        WRITE(6,77)(I,DRV0(I),DRV1(I),DRV2(I),I=1,JPP)
 96.     77 FORMAT(1X,I14,3E15.5)
 97.     78 FORMAT(/15X,2I15/)
     C**********************
     C**********
 98.        IDIFF=IMAXD-IMAXV
 99.        IMAXF=0
100.        AA1=0.05
101.        ICC=0
     C**********
102.        DO 104 ILP=1,40
     C*********
103.        EQKA=AA1*PMAX/DMAX
104.        AA3=-0.91
     C***
105.        DO 103 JJ=1,20
106.        IT=IMAXV
107.        EQMA=AA3*PMAX/DRV2(IMAXD)
108.        CPMAX=0.0
109.        AA2=AA1+AA3
110.        IF(AA2.LT.0.0)GO TO 1021
     C****
111.        IMAXC=IMAXD
112.        IT=IT+1
113.        DO 102 II=IT,IMAXC
114.        EQCA=EQMA*DRV2(II)/DRV1(II)
115.        EQCA=-EQCA
     C
     C
116.        EQVK=EQKA
117.        EQMASS=EQMA
118.        EQVC=EQCA
119.        MM=JPP
120.        CALL EXACT1(MM,DT,EQVK,EQMASS,T,GG,EQVC)
     C
     C
     C
121.        DO 73 I=1,JPP
122.        D(I)=DRV0(I)
123.        V(I)=GG(I)
124.     73 CONTINUE
     C
125.        N=JPP
126.        CALL NWCONV(N,V,G,D,DT)
     C
127.        DO 508 MP=1,JPP
128.        DF(MP)=G(MP)*EQMASS
129.    508 CONTINUE
130.        DO 509 MA=1,JPP
131.        DF(MA)=(DF(MA)+DF(MA+1))/2.
132.    509 CONTINUE
     C
     C
133.        CPMAX=0.
134.        DO 501 M=1,JPP
135.        DF(M)=(DF(M)+DF(M+1))/2.
136.        IF(DF(M).GT.CPMAX)GO TO 20
137.        GO TO 502
138.     20 CPMAX=DF(M)
139.        ICF=M
140.    502 CONTINUE
141.    501 CONTINUE
     C
142.        ERFCE=CPMAX-PMAX
143.        ABERFG=ABS(ERFCE)
144.        IF(ABERFG.GT.500.0)GO TO 102
     C
145.        ICC=ICC+1
     C
146.        DFRNG=DF(IAFNL+1)-DF(IAFNL)
147.        ZVALUF=DF(IAFNL)+FDTZ*DFRNG
148.        CMAXV=(ZVALUF-EQKA*ZVALU0)/ZVALU1
149.        CDIFFR=(CMAXV-EQCA)/CMAXV
```

```
150.        ABCD=CDIFFR
151.        QC(ICC)=CDIFFR
152.        IF(ICC.EQ.1)GO TO 102
153.        CRATIO=QC(ICC)/QC(ICC-1)
154.        IF(CRATIO.GT.0.0)GO TO 102
      C
      C
      C
155.        FCHK=EQKA*DRV0(II)
156.        DIFCHK=FCHK-DF(II)
157.        DFCHKR=DIFCHK/FCHK
158.        FPFRAC=DF(II)/PMAX
159.        ICDPT=II
160.        IBBB=IMAXD-ICDPT
161.        BB1=FLOAT(IBBB/IDIFF)
162.        TRMM=EQMA*DRV2(II)
163.        TRMC=EQCA*DRV1(II)
164.        TRMK=EQKA*DRV0(II)
165.        CPMXX(II)=TRMM+TRMC+TRMK
166.        WRITE(6,847)
167.    847 FORMAT(//10X,*GOOD RUN*//)
168.        GO TO 846
169.    102 CONTINUE
170.   1021 CONTINUE
171.        AA3=AA3+0.045
      C***************
172.    103 CONTINUE
173.        AA1=AA1+0.025
174.    104 CONTINUE
175.   1000 FORMAT(/1X,*000*)
176.    844 FORMAT(1X,7F10.2,3E15.5)
177.    845 FORMAT(6F15.4,10X,2I5,F10.3)
      C******************
      C
178.        WRITE(6,1002)
179.   1002 FORMAT(/10X,*OUTER LOOP COMPLETED*/)
180.        GO TO 94
      C
      C
181.    846 CONTINUE
      C
182.        WRITE(6,1000)
      C*********
183.        AFRNG=DF(NAFNL+1)-DF(NAFNL)
184.        DVALUF=DF(NAFNL)+DDTZ*AFRNG
      C*****
185.        ZVALUR=ZVALUF/PMAX
      C******
186.        DVALZD=DVALUF/PMAX
      C*****
187.        FDRTIO=ABERFG/PMAX
      C*********
188.        DENOM=FLOAT(IMAXD)
189.        DENOM1=1.
190.        TCRSPT=FLOAT(II)/DENOM
191.        TZROA=FLOAT(IAFNL)/DENOM
      C********
192.   1199 FORMAT(/10X,11F11.3/)
193.   1001 FORMAT(10X,I5,7F15.5)
194.        CALL EXACT1(JP,DT,EQKA,EQMA,T,GG,EQCA)
195.        DO 733 I=1,JP
196.        O(I)=DRV0(I)
197.        V(I)=GG(I)
198.    733 CONTINUE
199.        N=JP
200.        CALL NWCONV(N,V,G,O,DT)
201.        DO 518 MP=1,JP
202.        DF(MP)=G(MP)*EQMA
203.    518 CONTINUE
204.
      C
205.     94 CONTINUE
206.        RETURN
207.        END
```

SITE ONE STD VEHICLE

FOR SIGNATURE

| INCREMENT | DEFLECTION | VELOCITY | ACCELERATION |
|---|---|---|---|
| 1 | 1.27667E-04 | 1.92708E-03 | 9.93490E-03 |
| 2 | 1.54167E-04 | 7.94792E-04 | 8.31380E-03 |
| 3 | 1.91250E-04 | 1.03125E-03 | 6.69271E-03 |
| 4 | 2.36667E-04 | 1.33021E-03 | 1.03906E-02 |
| 5 | 2.97667E-04 | 1.86250E-03 | 1.57552E-02 |
| 6 | 3.85667E-04 | 2.59063E-03 | 2.10677E-02 |
| 7 | 5.04917E-04 | 3.54792E-03 | 2.91276E-02 |
| 8 | 6.69500E-04 | 4.92083E-03 | 3.62500E-02 |
| 9 | 8.98583E-04 | 6.44792E-03 | 4.09245E-02 |
| 10 | 1.18533E-03 | 8.19479E-03 | 4.38151E-02 |
| 11 | 1.55417E-03 | 9.95312E-03 | 3.51432E-02 |
| 12 | 1.98158E-03 | 1.10062E-02 | 9.81771E-03 |
| 13 | 2.43467E-03 | 1.07385E-02 | -3.29948E-02 |
| 14 | 2.84067E-03 | 8.36667E-03 | -8.32943E-02 |
| 15 | 3.10400E-03 | 4.07500E-03 | -1.15703E-01 |
| 16 | 3.16667E-03 | -8.89583E-04 | -1.14401E-01 |
| 17 | 3.03283E-03 | -5.07708E-03 | -8.50130E-02 |
| 18 | 2.76050E-03 | -7.69062E-03 | -4.40234E-02 |
| 19 | 2.41758E-03 | -8.59896E-03 | -4.75260E-03 |
| 20 | 2.07258E-03 | -8.07083E-03 | -9.53125E-03 |
| 21 | 1.77192E-03 | -6.89896E-03 | 7.39583E-03 |
| 22 | 1.52067E-03 | -5.80104E-03 | 2.50000E-03 |

GOOD RUN

00

---

SITE ONE VEHICLE 2

| EQUIV INPUT IN LBS | TDT FUNCTION | RESPONSE IN FT |
|---|---|---|
| 7.26622E+03 | 2.30853E-02 | 2.02000E-04 |
| 9.67190E+02 | 2.76124E-02 | 2.68500E-04 |
| 3.38946E+03 | 2.56125E-02 | 3.50500E-04 |
| 6.28019E+03 | 2.17664E-02 | 5.07583E-04 |
| 1.20998E+04 | 1.78084E-02 | 8.30917E-04 |
| 2.26201E+04 | 1.43096E-02 | 1.45967E-03 |
| 3.73522E+04 | 1.13959E-02 | 2.51742E-03 |
| 5.36091E+04 | 9.03463E-03 | 4.03258E-03 |
| 6.66077E+04 | 7.14611E-03 | 5.86650E-03 |
| 5.49146E+04 | 5.64567E-03 | 7.24833E-03 |
| -4.40640E+03 | 4.45756E-03 | 6.66300E-03 |
| -1.88870E+04 | 3.51838E-03 | 5.11650E-03 |
| 1.76576E+04 | 2.77663E-03 | 4.47067E-03 |
| 4.69750E+04 | 2.19108E-03 | 5.00992E-03 |
| 8.37103E+04 | 1.72893E-03 | 6.88358E-03 |
| 6.44724E+04 | 1.36424E-03 | 8.41667E-03 |
| -1.57651E+04 | 1.07645E-03 | 7.41800E-03 |
| -2.57654E+04 | 8.49373E-04 | 5.45308E-03 |
| -5.79904E+03 | 6.70194E-04 | 3.97867E-03 |
| -1.63126E+03 | 5.28813E-04 | 2.96208E-03 |
| 1.61962E+03 | 4.17257E-04 | 2.31008E-03 |
| 4.38986E+03 | 3.29234E-04 | 1.93375E-03 |
| 4.45170E+03 | 2.59780E-04 | 1.69475E-03 |

| | | |
|---|---|---|
| 5.24889E+03 | 2.04977E-04 | 1.55192E-03 |
| 5.77634E+03 | 1.61736E-04 | 1.47250E-03 |
| 4.82121E+03 | 1.27617E-04 | 1.39683E-03 |
| 5.39067E+03 | 1.00695E-04 | 1.34767E-03 |
| 6.05333E+03 | 7.94527E-05 | 1.33158E-03 |
| 4.47763E+03 | 6.26916E-05 | 1.28433E-03 |
| 4.63410E+03 | 4.94664E-05 | 1.23733E-03 |
| 5.15415E+03 | 3.90311E-05 | 1.21075E-03 |
| 5.09242E+03 | 3.07972E-05 | 1.19233E-03 |
| 3.93199E+03 | 2.43003E-05 | 1.14658E-03 |
| 5.04313E+03 | 1.91740E-05 | 1.12867E-03 |
| 5.26145E+03 | 1.51291E-05 | 1.12800E-03 |
| 4.01299E+03 | 1.19375E-05 | 1.09825E-03 |
| 4.74872E+03 | 9.41922E-06 | 1.08333E-03 |
| 6.32678E+03 | 7.43217E-06 | 1.11892E-03 |
| 2.59107E+03 | 5.86430E-06 | 1.06242E-03 |
| 5.12136E+03 | 4.62719E-06 | 1.05375E-03 |
| 5.51294E+03 | 3.65105E-06 | 1.07242E-03 |
| 4.25295E+03 | 2.88083E-06 | 1.06250E-03 |
| 4.31075E+03 | 2.27310E-06 | 1.04625E-03 |
| 5.95350E+03 | 1.79358E-06 | 1.07567E-03 |
| 4.67396E+03 | 1.41521E-06 | 1.08050E-03 |
| 3.94255E+03 | 1.11666E-06 | 1.05650E-03 |
| 4.68328E+03 | 8.81093E-07 | 1.04683E-03 |

NEXT SITE  STD VEHICLE

FOR SIGNATURE

| INCREMENT | DEFLECTION | VELOCITY | ACCELERATION |
|---|---|---|---|
| 1 | 9.95833E-05 | 1.52187E-03 | 7.77344E-03 |
| 2 | 1.21750E-04 | 6.21875E-04 | 6.71224E-03 |
| 3 | 1.49333E-04 | 8.09375E-04 | 5.65104E-03 |
| 4 | 1.86500E-04 | 1.07396E-03 | 6.19792E-03 |
| 5 | 2.35250E-04 | 1.30521E-03 | 5.92448E-03 |
| 6 | 2.90917E-04 | 1.54792E-03 | 7.12240E-03 |
| 7 | 3.59083E-04 | 1.87500E-03 | 8.54167E-03 |
| 8 | 4.40917E-04 | 2.23125E-03 | 9.60937E-03 |
| 9 | 5.37583E-04 | 2.64375E-03 | 1.25000E-02 |
| 10 | 6.52417E-04 | 3.23125E-03 | 1.47917E-02 |
| 11 | 7.96083E-04 | 3.82708E-03 | 1.32161E-02 |
| 12 | 9.58583E-04 | 4.28854E-03 | 7.79948E-03 |
| 13 | 1.13917E-03 | 4.45104E-03 | -6.17187E-03 |
| 14 | 1.31467E-03 | 3.79479E-03 | -2.66797E-02 |
| 15 | 1.44275E-03 | 2.31667E-03 | -4.29948E-02 |
| 16 | 1.50000E-03 | 3.55208E-04 | -4.88021E-02 |
| 17 | 1.47117E-03 | -1.58750E-03 | -3.80990E-02 |
| 18 | 1.37300E-03 | -2.69271E-03 | -1.61849E-02 |
| 19 | 1.25575E-03 | -2.88229E-03 | -1.82292E-03 |
| 20 | 1.14242E-03 | -2.83854E-03 | -5.88542E-03 |
| 21 | 1.02867E-03 | -2.75000E-03 | -7.35677E-04 |
| 22 | 9.22417E-04 | -2.56146E-03 | -7.16146E-04 |

GOOD RUN

00

---

NEXT SITE  VEHICLE 2

| EQUIV INPUT IN LBS | TDT FUNCTION | RESPONSE IN FT |
|---|---|---|
| 2.39378E+04 | 2.79870E-02 | 1.57565E-04 |
| -5.99763E+04 | 4.02600E-02 | -1.68119E-04 |
| 6.45929E+03 | 4.45935E-02 | -2.74326E-04 |
| 1.36858E+04 | 4.49856E-02 | -2.24518E-04 |
| 2.55768E+04 | 4.34868E-02 | -2.40447E-05 |
| 3.73268E+04 | 4.11442E-02 | 3.17975E-04 |
| 5.95647E+04 | 3.84877E-02 | 8.60932E-04 |
| 7.51046E+04 | 3.57813E-02 | 1.58148E-03 |
| 8.03293E+04 | 3.31525E-02 | 2.39395E-03 |
| 6.33737E+04 | 3.06592E-02 | 3.10814E-03 |
| -4.96779E+03 | 2.83238E-02 | 3.29894E-03 |
| -1.96412E+04 | 2.61510E-02 | 3.13688E-03 |
| 1.84098E+04 | 2.41370E-02 | 3.06340E-03 |
| 4.64276E+04 | 2.22741E-02 | 3.21925E-03 |
| 6.79205E+04 | 2.05529E-02 | 3.61990E-03 |
| 3.74124E+04 | 1.89636E-02 | 3.92125E-03 |
| -3.11110E+01 | 1.74966E-02 | 3.91757E-03 |
| 2.12723E+04 | 1.61429E-02 | 3.90907E-03 |
| 5.20213E+03 | 1.48937E-02 | 3.79282E-03 |
| 1.06867E+03 | 1.37411E-02 | 3.60242E-03 |
| -1.67619E+03 | 1.26777E-02 | 3.36579E-03 |
| -3.75658E+03 | 1.16966E-02 | 3.10234E-03 |
| -4.38155E+03 | 1.07913E-02 | 2.83187E-03 |
| -6.42824E+03 | 9.95617E-03 | 2.55472E-03 |
| -9.40418E+03 | 9.18563E-03 | 2.26518E-03 |
| -6.84531E+03 | 8.47472E-03 | 1.99745E-03 |
| -6.04811E+03 | 7.81883E-03 | 1.75536E-03 |
| -7.78484E+03 | 7.21371E-03 | 1.52313E-03 |
| -4.78390E+03 | 6.65541E-03 | 1.32403E-03 |
| -2.34767E+03 | 6.14033E-03 | 1.16421E-03 |
| -3.53550E+03 | 5.66511E-03 | 1.02124E-03 |
| -8.24185E+02 | 5.22666E-03 | 9.09508E-04 |
| 3.66539E+03 | 4.82215E-03 | 8.46376E-04 |
| 5.42162E+03 | 4.44895E-03 | 8.20303E-04 |
| -7.56887E+03 | 4.10463E-03 | 7.27339E-04 |
| 7.55546E+03 | 3.78696E-03 | 7.05572E-04 |
| 1.67329E+03 | 3.49387E-03 | 6.79791E-04 |
| 4.12036E+03 | 3.22347E-03 | 6.69173E-04 |
| 2.13777E+03 | 2.97399E-03 | 6.53120E-04 |
| 1.94469E+03 | 2.74383E-03 | 6.33810E-04 |
| 3.01993E+03 | 2.53147E-03 | 6.20752E-04 |
| 6.73974E+03 | 2.33555E-03 | 6.35642E-04 |
| 2.83888E+03 | 2.15480E-03 | 6.37603E-04 |
| 4.24396E+03 | 1.98803E-03 | 6.42583E-04 |
| 3.23174E+03 | 1.83417E-03 | 6.42152E-04 |
| 6.86666E+03 | 1.69222E-03 | 6.63086E-04 |
| 2.46450E+03 | 1.56125E-03 | 0 |

---

| PREDICTED | MEASURED |
|---|---|
| .00016 | .00018 |
| -.00017 | .00028 |
| -.00027 | .00044 |
| -.00022 | .00068 |
| -.00002 | .00107 |
| .00032 | .00165 |
| .00086 | .00252 |
| .00158 | .00357 |
| .00239 | .00404 |
| .00311 | .00367 |
| .00330 | .00318 |

| | |
|---|---|
| .00314 | .00289 |
| .00306 | .00284 |
| .00322 | .00314 |
| .00362 | .00382 |
| .00392 | .00433 |
| .00392 | .00399 |
| .00391 | .00320 |
| .00379 | .00244 |
| .00360 | .00178 |
| .00337 | .00128 |
| .00310 | .00091 |
| .00283 | .00067 |
| .00255 | .00051 |
| .00227 | .00041 |
| .00200 | .00035 |
| .00176 | .00032 |
| .00152 | .00029 |
| .00132 | .00027 |
| .00116 | .00025 |
| .00102 | .00014 |
| .00091 | .00012 |
| .00085 | .00012 |
| .00082 | .00012 |
| .00073 | .00012 |
| .00071 | .00012 |
| .00068 | .00011 |
| .00067 | .00012 |
| .00065 | .00011 |
| .00063 | .00011 |
| .00062 | .00011 |
| .00064 | .00011 |
| .00064 | .00011 |
| .00064 | .00011 |
| .00064 | .00011 |
| .00066 | .00011 |
| 0 | .00011 |

# APPENDIX D

# DATA DIGITIZED

# FROM LIGHT

# SENSITIVE PAPER

The data listing has the following format

Card 1 - A comment card giving the base name, site number, grid location of measurement point, Load Cart data of test, distance from closest measurement gage to edge of tire track in inches, time increment at which data was digitized and estimated number of cards.

Card 2 - Distance (ft) of measurement point from edge of tire print where Gage 1 is the closest.

Card 3 - Number of cards actually read, time increment used, and weight of load cart (25 kips).

Card 4 to (n-1) - Data digitized and listed (from left to right) as, Gage 1, Gage 2, Gage 3, Gage 4, and Gage 5.

Card n (last card) - Calibration data for Gages 1 to 5 also listed from from left (Gage 1) to right (Gage 5).

```
    LOGIN     SITE 1    LOC A-1   LD. CT.   3.11.76   7.25 .2   48
      .9642      .9375    1.6875    2.6875    3.6875
   48       .200 25000.0
0027   0045   0071   0102   0134
0030   0048   0074   0106   0134
0034   0051   0078   0110   0136
0040   0058   0085   0117   0137
0049   0065   0094   0126   0141
0061   0078   0107   0138   0145
0077   0092   0122   0154   0151
0103   0115   0146   0175   0158
0130   0141   0172   0198   0165
0167   0174   0203   0223   0173
0210   0211   0234   0247   0181
0259   0254   0272   0277   0190
0307   0297   0306   0301   0195
0360   0340   0340   0324   0200
0414   0382   0371   0344   0206
0456   0420   0394   0358   0208
0487   0447   0411   0366   0209
0490   0456   0415   0367   0209
0483   0459   0419   0371   0209
0461   0451   0418   0375   0213
0427   0429   0403   0367   0212
0393   0402   0385   0354   0209
0359   0374   0363   0338   0204
0331   0349   0344   0324   0202
0302   0324   0320   0305   0194
0277   0301   0299   0288   0189
0248   0273   0273   0267   0182
0225   0250   0249   0247   0175
0198   0223   0223   0222   0167
0171   0196   0196   0196   0156
0141   0163   0163   0167   0147
0115   0137   0137   0143   0140
0096   0117   0117   0126   0136
0085   0105   0104   0117   0134
0076   0095   0095   0109   0133
0071   0089   0089   0103   0131
0067   0084   0084   0099   0131
0064   0080   0080   0096   0130
0060   0078   0078   0094   0129
0058   0074   0074   0092   0128
0057   0073   0073   0091   0128
0055   0072   0072   0090   0128
0055   0071   0072   0090   0128
0053   0070   0070   0089   0127
0053   0069   0069   0088   0128
0053   0069   0069   0087   0127
0051   0069   0069   0087   0128
0051   0069   0069   0087   0127
 .00008065   .00006995   .00004052   .00002212   .00002778
```

```
C   EGLIN      SITE 1     LOC A-1   LD. CT.    3.11.76   7.00  .    53
    .58333     .91666    1.83333   2.83333    3.83333
   53       .200  25000.0
0023   0052   0075   0107   0137
0028   0057   0079   0108   0135
0034   0067   0090   0117   0136
0042   0077   0102   0127   0139
0052   0088   0115   0140   0143
0065   0104   0130   0156   0149
0080   0121   0150   0173   0153
0096   0138   0167   0189   0158
0113   0158   0185   0203   0164
0135   0180   0208   0222   0169
0160   0206   0229   0241   0174
0184   0231   0251   0259   0179
0211   0256   0271   0272   0183
0249   0292   0299   0291   0188
0288   0325   0321   0305   0191
0325   0357   0342   0316   0193
0364   0388   0359   0326   0195
0401   0414   0375   0333   0196
0433   0436   0388   0339   0198
0453   0447   0393   0340   0197
0473   0456   0400   0343   0197
0484   0460   0402   0342   0197
0488   0461   0402   0343   0198
0489   0461   0402   0344   0199
0487   0458   0403   0346   0201
0484   0453   0402   0346   0202
0475   0446   0397   0344   0202
0458   0430   0384   0334   0201
0437   0411   0370   0323   0198
0412   0389   0351   0308   0192
0386   0367   0331   0292   0187
0360   0344   0309   0273   0182
0330   0316   0284   0254   0176
0296   0288   0257   0232   0170
0267   0260   0232   0212   0164
0237   0233   0207   0192   0159
0213   0211   0187   0175   0154
0191   0191   0167   0159   0149
0168   0173   0149   0143   0144
0148   0154   0131   0127   0141
0129   0138   0115   0114   0136
0113   0123   0100   0101   0134
0100   0112   0089   0094   0131
0089   0102   0080   0086   0131
0081   0093   0073   0079   0127
0070   0085   0064   0072   0126
0062   0078   0059   0067   0125
0056   0073   0054   0064   0125
0051   0069   0051   0063   0124
0049   0066   0048   0059   0124
0048   0064   0047   0058   0123
0044   0063   0044   0057   0122
0042   0061   0043   0056   0121
 .00008065   .00006995   .00004052   .00002212   .00002778
```

```
C   EGLIN      SITE 1     LOC A-2   LD. CT.    3.11.76    5.50 .2    38
    .45833      .79167    1.70833   2.70833    3.70833
    38        .200 25000.0
0042   0070   0100   0131   0148
0043   0070   0100   0132   0148
0044   0071   0101   0135   0149
0045   0072   0103   0138   0151
0046   0074   0106   0144   0153
0050   0077   0111   0155   0156
0054   0082   0116   0168   0162
0065   0092   0129   0193   0171
0083   0110   0149   0230   0183
0107   0131   0172   0273   0198
0138   0158   0199   0318   0211
0182   0197   0231   0366   0226
0245   0249   0269   0418   0238
0301   0293   0298   0451   0245
0318   0316   0311   0476   0255
0286   0301   0307   0480   0262
0238   0263   0281   0446   0254
0195   0225   0250   0395   0239
0160   0190   0218   0342   0222
0132   0161   0189   0290   0205
0111   0140   0167   0249   0192
0095   0124   0149   0216   0180
0086   0113   0137   0193   0173
0079   0105   0129   0178   0167
0074   0100   0123   0166   0163
0071   0097   0119   0158   0161
0069   0094   0116   0155   0159
0067   0092   0116   0151   0158
0066   0091   0114   0150   0157
0065   0090   0113   0148   0157
0065   0090   0113   0149   0158
0064   0089   0112   0148   0157
0063   0089   0113   0148   0158
0063   0088   0112   0148   0158
0061   0088   0112   0148   0158
0061   0088   0112   0148   0158
0061   0087   0111   0148   0158
0061   0087   0112   0149
 .0001613    .0001399    .00002212    .00002778
```

```
C   EGLIN      SITE 1     LOC A-2   LD. CT.    3.11.76    7.00 .2    45
     .58333     .91666    1.83333   2.83333    3.83333
    45      .200 25000.0
0026   0054   0083   0120   0145
0026   0055   0085   0124   0147
0027   0057   0088   0131   0150
0030   0059   0091   0139   0153
0032   0062   0096   0148   0156
0035   0067   0101   0159   0160
0041   0074   0109   0175   0166
0050   0084   0121   0198   0175
0062   0099   0137   0227   0185
0079   0116   0155   0261   0197
0099   0138   0175   0294   0207
0123   0160   0194   0323   0216
0153   0187   0214   0349   0222
0187   0217   0233   0374   0226
0223   0244   0249   0390   0228
0255   0266   0261   0403   0230
0277   0279   0270   0412   0230
0286   0280   0273   0415   0231
0281   0275   0273   0418   0232
0265   0261   0262   0403   0227
0237   0237   0245   0377   0218
0211   0215   0228   0351   0211
0181   0189   0205   0317   0200
0156   0167   0187   0287   0190
0134   0147   0169   0256   0180
0114   0129   0151   0225   0171
0097   0114   0137   0199   0163
0082   0101   0123   0176   0157
0073   0093   0114   0163   0153
0067   0086   0108   0152   0150
0060   0081   0102   0140   0146
0056   0076   0098   0133   0143
0050   0072   0094   0127   0142
0048   0070   0091   0122   0141
0045   0068   0089   0120   0141
0045   0067   0088   0118   0140
0043   0066   0087   0117   0139
0042   0064   0087   0116   0139
0041   0064   0086   0115   0139
0040   0062   0085   0115   0139
0038   0062   0084   0112   0138
0037   0060   0083   0110   0138
0036   0059   0082   0108   0138
0034   0058   0081   0107   0138
0034   0058   0081   0107   0138
 .0001613    .0001399    .00008104    .00002212    .00002778
```

```
C   EGLIN      SITE 1     LOC A-3   LD. CT.    3.11.76    4.00 .2   37
     .33333     .66666    1.58333   2.583333  3.583333
   37       .200 25000.0
0048   0071   0094   0131   0148
0049   0071   0094   0131   0148
0050   0071   0095   0135   0149
0050   0073   0097   0137   0151
0052   0074   0099   0141   0152
0054   0075   0101   0149   0155
0058   0079   0105   0158   0161
0064   0082   0110   0172   0167
0072   0088   0118   0188   0173
0080   0098   0127   0202   0178
0092   0111   0139   0220   0182
0109   0125   0152   0242   0188
0146   0159   0182   0287   0202
0193   0197   0214   0330   0212
0261   0250   0252   0382   0223
0326   0298   0281   0414   0230
0366   0329   0297   0435   0235
0357   0333   0300   0446   0240
0312   0305   0282   0424   0234
0263   0268   0256   0386   0225
0220   0230   0226   0340   0211
0187   0198   0198   0298   0198
0157   0170   0170   0250   0183
0131   0143   0143   0204   0168
0116   0127   0126   0174   0158
0105   0116   0115   0152   0150
0098   0108   0108   0137   0145
0093   0102   0102   0128   0142
0091   0099   0099   0120   0139
0087   0096   0096   0116   0137
0085   0094   0094   0114   0136
0084   0093   0093   0110   0135
0083   0093   0093   0109   0135
0083   0092   0092   0109   0135
0082   0091   0091   0107   0134
0081   0091   0091   0107   0133
0081   0089   0089   0105   0133
 .0001613    .0001399    .00008104    .00002212    .00002778
```

```
C   EGLIN      SITE 1     LOC A-3   LD. CT.   3.11.76   4.50 .2   45
    .375        .708       1.625     2.625     3.625
   45       .200 25000.0
0030   0049   0081   0100   0140
0029   0049   0081   0102   0140
0030   0049   0081   0103   0140
0030   0051   0083   0106   0142
0031   0052   0085   0111   0143
0034   0055   0088   0117   0145
0037   0058   0092   0126   0149
0040   0064   0098   0137   0152
0047   0070   0105   0151   0157
0054   0078   0114   0168   0163
0064   0089   0125   0188   0169
0079   0105   0140   0212   0176
0097   0123   0157   0242   0186
0120   0144   0176   0270   0193
0149   0170   0194   0293   0198
0186   0203   0215   0320   0204
0232   0239   0238   0349   0211
0278   0271   0255   0367   0214
0322   0298   0268   0378   0215
0345   0308   0272   0378   0214
0349   0308   0272   0378   0215
0334   0295   0265   0368   0211
0303   0269   0248   0339   0203
0270   0242   0227   0312   0196
0234   0211   0200   0271   0185
0203   0184   0176   0234   0174
0173   0159   0154   0199   0165
0153   0141   0138   0175   0159
0136   0126   0126   0153   0150
0124   0116   0115   0138   0147
0113   0108   0108   0126   0143
0105   0099   0101   0113   0139
0098   0094   0093   0102   0134
0092   0089   0088   0093   0131
0088   0086   0085   0086   0129
0083   0083   0082   0079   0126
0080   0080   0080   0074   0124
0079   0079   0079   0073   0124
0077   0077   0077   0070   0124
0075   0075   0075   0066   0121
0073   0073   0073   0063   0121
0072   0072   0072   0060   0119
0072   0072   0072   0060   0119
0070   0070   0070   0058   0118
0068   0069   0069   0056   0117
 .0001613    .0001399    .00008104   .00002212   .00002778
```

```
C   EGLIN      SITE 1     LOC A-4   LD. CT.    3.11.76    5.00 .2    53
    .41667      .75       1.66667   2.66667    3.66667
      53       .200 25000.0
0042   0069   0099   0134   0155
0045   0071   0101   0139   0157
0046   0074   0104   0147   0160
0048   0075   0107   0153   0163
0050   0078   0110   0160   0166
0053   0082   0114   0168   0169
0056   0086   0119   0178   0174
0061   0091   0125   0190   0178
0068   0098   0133   0205   0183
0076   0106   0143   0224   0190
0083   0116   0153   0240   0197
0093   0125   0164   0258   0203
0102   0135   0174   0275   0209
0115   0149   0188   0298   0215
0128   0163   0201   0315   0221
0148   0182   0217   0338   0227
0169   0203   0234   0361   0232
0195   0226   0252   0385   0238
0224   0252   0271   0409   0243
0255   0275   0287   0427   0247
0287   0299   0304   0444   0250
0317   0318   0316   0457   0252
0335   0329   0322   0463   0252
0341   0330   0322   0462   0251
0338   0326   0321   0462   0252
0323   0313   0310   0445   0249
0304   0295   0295   0426   0244
0281   0274   0277   0400   0236
0251   0248   0255   0368   0228
0225   0227   0238   0341   0221
0207   0212   0222   0317   0212
0189   0196   0207   0293   0205
0173   0181   0192   0269   0198
0158   0169   0180   0247   0191
0146   0157   0168   0227   0184
0137   0148   0158   0211   0178
0128   0141   0150   0196   0172
0121   0135   0144   0184   0169
0116   0130   0138   0174   0165
0111   0126   0134   0167   0164
0108   0124   0131   0162   0161
0107   0120   0128   0157   0158
0104   0119   0126   0152   0158
0102   0117   0124   0149   0156
0100   0116   0122   0146   0155
0099   0115   0121   0144   0155
0098   0114   0120   0142   0153
0097   0113   0119   0140   0153
0096   0112   0119   0139   0152
0095   0111   0119   0138   0151
0095   0111   0118   0137   0151
0095   0111   0118   0137   0151
0094   0110   0117   0136   0152
 .0001613    .0001399    .00008104    .00002212    .00002778
```

```
C   EGLIN      SITE 1     LOC A-5   LD. CT.    3:11.76   5.00 .2   43
     .41667      .75       1.66667   2.66667    3.66667
    43       .200 25000.0
0036   0059   0083   0123   0141
0037   0061   0086   0128   0143
0040   0065   0090   0138   0147
0042   0068   0094   0148   0150
0045   0072   0100   0159   0157
0052   0079   0107   0174   0162
0057   0085   0114   0185   0166
0065   0093   0124   0202   0173
0074   0105   0136   0221   0180
0087   0118   0150   0244   0187
0104   0139   0168   0269   0196
0129   0161   0188   0294   0202
0161   0190   0210   0321   0209
0196   0220   0233   0344   0215
0233   0247   0251   0363   0219
0262   0266   0261   0370   0221
0279   0275   0264   0372   0219
0290   0279   0269   0376   0220
0286   0275   0268   0381   0223
0275   0265   0264   0381   0227
0252   0246   0248   0358   0219
0225   0225   0223   0328   0209
0198   0198   0204   0296   0198
0172   0174   0181   0261   0187
0149   0155   0162   0230   0179
0132   0138   0146   0202   0169
0116   0124   0131   0180   0162
0106   0115   0123   0166   0157
0098   0107   0114   0152   0152
0091   0101   0108   0143   0149
0084   0095   0103   0133   0145
0078   0090   0098   0123   0143
0073   0086   0093   0117   0139
0071   0082   0090   0110   0137
0066   0079   0087   0104   0135
0063   0077   0084   0099   0132
0062   0076   0083   0096   0132
0060   0074   0081   0093   0131
0059   0074   0081   0093   0132
0059   0073   0080   0092   0131
0059   0073   0080   0091   0131
0058   0073   0080   0091   0130
0058   0072   0080   0090   0130
 .0001613    .0001399    .00008104   .00002212   .00002778
```

```
C   EGLIN      SITE 1     LOC A-5   LD. CT.    3.11.76    6.00 .2    35
    .5          .83333    1.75        2.75        3.75
   35       .200 25000.0
0070   0082   0094   0122   0140
0071   0084   0096   0126   0142
0073   0086   0099   0132   0144
0075   0088   0101   0138   0147
0078   0092   0106   0148   0152
0084   0097   0112   0159   0156
0091   0104   0120   0176   0163
0104   0115   0132   0197   0171
0122   0132   0150   0227   0181
0142   0149   0167   0251   0188
0175   0179   0195   0293   0200
0209   0208   0217   0320   0208
0257   0250   0250   0359   0219
0294   0277   0266   0372   0218
0313   0296   0276   0380   0222
0305   0298   0279   0387   0226
0273   0275   0261   0365   0221
0238   0247   0240   0337   0213
0201   0214   0212   0298   0203
0176   0188   0188   0265   0191
0152   0165   0165   0226   0180
0135   0147   0147   0197   0169
0122   0132   0132   0171   0161
0113   0122   0122   0154   0154
0106   0114   0116   0142   0150
0103   0110   0110   0132   0147
0099   0109   0105   0125   0144
0096   0105   0102   0120   0142
0096   0103   0100   0116   0139
0094   0103   0100   0115   0140
0093   0102   0099   0113   0139
0092   0101   0098   0111   0138
0092   0100   0097   0111   0138
0091   0100   0096   0109   0137
0090   0099   0097   0110   0137
 .0001613     .0001399     .00008104    .00002212    .00002778
```

```
C   EGLIN      SITE 1     LOC C-1   LD.CT.     3.10.76   7.0  .2   40
    .58333     .91667    1.83333   2.83333    3.83333
   40      .200 25000.0
0018   0037   0054   0067   0102
0019   0037   0055   0069   0103
0020   0038   0056   0071   0103
0021   0040   0059   0075   0103
0024   0043   0060   0080   0103
0026   0045   0063   0085   0104
0029   0048   0068   0095   0103
0033   0053   0073   0104   0104
0039   0058   0079   0117   0105
0047   0065   0087   0132   0107
0059   0074   0096   0150   0111
0075   0085   0109   0170   0117
0097   0098   0123   0194   0124
0121   0113   0137   0216   0129
0149   0128   0153   0240   0153
0184   0145   0167   0258   0142
0222   0165   0183   0279   0145
0249   0183   0194   0289   0146
0263   0194   0201   0294   0146
0260   0196   0202   0295   0147
0250   0194   0202   0296   0148
0227   0183   0195   0287   0150
0202   0169   0183   0271   0147
0171   0149   0164   0242   0139
0144   0132   0148   0215   0131
0117   0113   0128   0182   0122
0096   0099   0113   0157   0116
0079   0083   0097   0128   0110
0064   0070   0083   0104   0105
0054   0060   0073   0085   0104
0046   0054   0065   0071   0104
0042   0048   0060   0061   0104
0038   0044   0055   0053   0104
0035   0042   0052   0047   0103
0035   0040   0050   0043   0103
0034   0039   0050   0042   0103
0034   0039   0050   0040   0103
0034   0039   0049   0040   0103
0034   0039   0049   0039   0103
0034   0038   0048   0038   0103
 .0001613    .0001399    .00008104    .00002212    .00002778
```

```
C   EGLIN      SITE 1     LOC C-1   LD.CT.     3.10.76    7.0  .2   54
    .58333     .91667    1.83333   2.83333    3.83333
   54       .200 25000.0
0036  0055  0076  0095  0120
0037  0056  0077  0098  0120
0038  0057  0080  0101  0120
0039  0059  0081  0104  0121
0042  0061  0084  0108  0123
0044  0064  0087  0116  0124
0046  0067  0091  0121  0126
0049  0070  0095  0127  0127
0052  0075  0099  0134  0129
0057  0080  0105  0143  0132
0062  0084  0109  0150  0133
0070  0091  0115  0160  0136
0076  0098  0123  0170  0138
0087  0106  0131  0183  0142
0098  0114  0140  0195  0145
0112  0126  0150  0210  0149
0129  0137  0161  0226  0153
0148  0150  0170  0239  0155
0171  0164  0183  0255  0161
0196  0178  0193  0267  0162
0225  0191  0204  0284  0167
0251  0200  0211  0293  0170
0277  0211  0219  0304  0174
0291  0216  0222  0310  0177
0299  0217  0224  0314  0179
0299  0215  0226  0323  0184
0291  0207  0222  0319  0186
0276  0195  0213  0308  0185
0256  0181  0201  0293  0183
0235  0171  0191  0277  0181
0213  0159  0179  0258  0176
0191  0147  0168  0238  0171
0170  0134  0154  0215  0164
0152  0123  0141  0195  0157
0138  0113  0132  0179  0151
0127  0106  0122  0163  0146
0119  0098  0115  0148  0140
0112  0094  0108  0138  0137
0108  0090  0104  0128  0132
0104  0086  0099  0120  0130
0100  0083  0097  0114  0127
0097  0080  0093  0107  0125
0095  0079  0091  0102  0123
0093  0077  0088  0094  0121
0092  0075  0086  0092  0119
0090  0074  0085  0087  0118
0089  0073  0084  0084  0117
0089  0071  0083  0083  0116
0087  0071  0082  0081  0115
0087  0070  0081  0079  0114
0086  0070  0080  0077  0114
0085  0070  0080  0077  0113
0085  0069  0079  0074  0114
0084  0069  0078  0074  0113
 .0001613    .0001399    .00008104    .00002212    .00002778
```

```
C   EGLIN      SITE 1     LOC C-2   LD.CT.     3.10.76   4.5  .2   56
    .375        .708       1.625     2.625      3.625
   56       .200 25000.0
0035  0054  0074  0101  0117
0037  0055  0075  0103  0118
0038  0057  0078  0108  0119
0039  0059  0079  0113  0120
0041  0062  0083  0119  0121
0044  0065  0087  0127  0124
0047  0070  0093  0140  0127
0052  0076  0099  0151  0130
0056  0082  0107  0164  0133
0062  0087  0113  0179  0138
0068  0095  0122  0192  0142
0074  0102  0130  0208  0146
0082  0110  0139  0222  0150
0088  0119  0148  0240  0154
0096  0127  0157  0256  0157
0106  0137  0168  0275  0162
0114  0147  0178  0290  0167
0123  0155  0187  0305  0169
0133  0166  0197  0321  0173
0145  0178  0208  0337  0176
0160  0191  0220  0352  0178
0176  0206  0232  0368  0180
0191  0218  0241  0380  0180
0208  0230  0251  0390  0180
0225  0242  0261  0402  0180
0239  0251  0267  0409  0179
0247  0256  0271  0412  0178
0250  0256  0272  0412  0174
0250  0255  0273  0415  0174
0246  0251  0272  0415  0174
0236  0243  0264  0403  0171
0226  0233  0256  0390  0166
0212  0220  0244  0367  0158
0196  0206  0229  0343  0150
0179  0190  0211  0312  0141
0164  0176  0196  0281  0132
0150  0162  0180  0251  0124
0138  0149  0166  0225  0117
0129  0140  0156  0206  0114
0121  0133  0147  0188  0110
0115  0127  0140  0176  0110
0110  0122  0133  0165  0108
0105  0117  0129  0156  0108
0100  0113  0124  0147  0107
0098  0110  0121  0140  0106
0094  0108  0116  0133  0106
0091  0104  0113  0128  0105
0089  0102  0110  0122  0106
0086  0100  0109  0118  0106
0085  0098  0107  0115  0106
0082  0096  0104  0111  0107
0081  0095  0103  0108  0105
0081  0094  0102  0106  0105
0079  0093  0101  0105  0102
0079  0092  0100  0103  0102
0079  0092  0099  0102  0104
 .0001613    .0001399    .00008104    .00002212    .00002778
```

```
C   EGLIN      SITE 1     LOC C-2   LD.CT.     3.10.76    4.5  .2   53
     .375       .708      1.625     2.625      3.625
    53       .200 25000.0
0017   0030   0043   0068   0106
0019   0031   0044   0070   0106
0019   0032   0045   0072   0105
0020   0033   0046   0075   0105
0022   0034   0048   0079   0105
0024   0036   0050   0082   0105
0025   0038   0052   0088   0106
0028   0041   0056   0094   0106
0032   0045   0060   0102   0106
0035   0050   0065   0113   0106
0041   0054   0070   0125   0106
0047   0061   0077   0138   0106
0054   0068   0086   0155   0106
0062   0076   0095   0172   0105
0071   0085   0105   0189   0106
0079   0093   0114   0205   0106
0091   0104   0127   0225   0106
0102   0114   0136   0240   0107
0114   0125   0147   0259   0109
0126   0136   0157   0271   0110
0143   0150   0170   0292   0113
0158   0164   0182   0308   0114
0174   0178   0192   0323   0116
0190   0191   0202   0333   0116
0203   0203   0211   0346   0119
0210   0210   0216   0352   0120
0212   0214   0219   0356   0120
0210   0216   0220   0362   0124
0205   0215   0221   0365   0126
0197   0210   0220   0365   0128
0185   0201   0213   0357   0127
0170   0189   0203   0343   0125
0158   0178   0193   0327   0121
0145   0166   0181   0307   0116
0134   0152   0168   0285   0111
0118   0139   0152   0258   0107
0105   0125   0137   0229   0106
0094   0113   0124   0202   0106
0083   0102   0110   0175   0105
0072   0090   0096   0148   0106
0066   0082   0087   0130   0106
0059   0075   0079   0114   0106
0054   0068   0072   0100   0106
0050   0063   0066   0088   0105
0046   0058   0061   0078   0105
0043   0054   0057   0069   0105
0041   0051   0054   0063   0106
0038   0049   0051   0056   0106
0036   0047   0047   0052   0105
0034   0047   0047   0048   0105
0033   0045   0045   0046   0105
0034   0044   0044   0045   0106
0032   0044   0044   0044   0105
 .0001613    .0001399    .00008104    .00002212    .00002778
```

```
C   EGLIN      SITE 1     LOC C-3   LB.CT.     3.10.76   4.5  .2   60
    .375        .708       1.625     2.625      3.625
     60       .200 25000.0
0037   0060   0084   0118   0131
0038   0061   0086   0121   0133
0039   0062   0089   0127   0136
0041   0065   0091   0134   0139
0043   0067   0094   0140   0140
0044   0068   0097   0145   0144
0046   0071   0100   0153   0148
0049   0074   0104   0163   0151
0052   0078   0109   0177   0158
0055   0082   0113   0186   0162
0058   0086   0120   0198   0167
0063   0091   0126   0212   0172
0069   0099   0135   0230   0180
0075   0106   0143   0245   0186
0084   0115   0154   0268   0194
0094   0126   0167   0295   0204
0103   0136   0178   0317   0213
0113   0147   0190   0340   0222
0124   0158   0203   0362   0230
0136   0170   0217   0386   0238
0148   0182   0229   0407   0245
0161   0197   0242   0428   0252
0174   0210   0255   0450   0258
0189   0224   0268   0472   0265
0203   0235   0277   0485   0268
0218   0248   0288   0501   0274
0234   0259   0295   0513   0276
0245   0265   0299   0520   0279
0247   0264   0300   0521   0280
0242   0259   0298   0521   0279
0232   0248   0289   0503   0273
0217   0237   0278   0482   0264
0203   0222   0264   0454   0254
0189   0209   0251   0426   0242
0176   0196   0237   0399   0231
0164   0183   0222   0370   0218
0154   0173   0209   0343   0206
0142   0163   0197   0315   0195
0134   0153   0186   0295   0185
0125   0145   0175   0271   0176
0118   0138   0167   0252   0167
0111   0130   0158   0233   0159
0106   0126   0153   0221   0153
0101   0121   0147   0208   0148
0098   0118   0142   0198   0145
0094   0114   0138   0190   0142
0091   0111   0134   0181   0138
0088   0108   0131   0175   0136
0086   0107   0128   0171   0134
0085   0105   0126   0166   0133
0083   0103   0124   0163   0131
0082   0102   0124   0159   0131
0081   0100   0121   0157   0130
0079   0099   0121   0154   0129
0078   0099   0120   0153   0129
0078   0098   0119   0152   0129
0078   0098   0118   0151   0129
0077   0097   0119   0150   0129
0077   0097   0118   0150   0128
0077   0097   0118   0149   0128
 .0001613    .0001[illegible]    .00008104   .00002212   .00002778
```

```
C   EGLIN      SITE 1     LOC C-3   LD.CT.     3.10.76   4.0  .2   50
     .33333     .66667    1.58333   2.58333    3.58333
   50      .200 25000.0
0036   0059   0080   0108   0126
0038   0061   0083   0115   0129
0041   0064   0086   0123   0132
0044   0066   0091   0133   0136
0048   0071   0096   0145   0142
0052   0076   0102   0159   0148
0056   0080   0108   0172   0153
0063   0086   0116   0188   0160
0068   0092   0122   0202   0166
0075   0098   0131   0220   0174
0083   0106   0140   0237   0181
0091   0115   0151   0258   0189
0101   0126   0162   0280   0198
0114   0137   0175   0304   0208
0127   0151   0188   0328   0217
0144   0166   0203   0354   0228
0160   0181   0218   0380   0237
0177   0197   0232   0402   0245
0195   0211   0244   0425   0252
0210   0225   0256   0441   0259
0224   0238   0268   0464   0265
0233   0247   0275   0476   0268
0238   0255   0283   0490   0273
0232   0255   0287   0498   0275
0220   0248   0284   0497   0275
0204   0235   0273   0475   0269
0186   0218   0257   0448   0259
0169   0201   0241   0415   0246
0152   0183   0221   0375   0229
0135   0165   0199   0328   0210
0120   0149   0178   0289   0192
0107   0136   0163   0255   0179
0098   0125   0150   0226   0167
0089   0115   0137   0198   0153
0081   0106   0125   0169   0141
0075   0098   0116   0150   0132
0068   0091   0106   0129   0125
0064   0087   0102   0118   0120
0061   0083   0098   0109   0117
0057   0080   0095   0102   0115
0055   0078   0092   0098   0113
0054   0076   0090   0093   0111
0053   0075   0088   0091   0111
0052   0074   0088   0089   0111
0052   0074   0088   0089   0111
0051   0073   0087   0087   0111
0050   0072   0087   0087   0111
0050   0072   0088   0087   0111
0050   0072   0087   0087   0110
0050   0072   0087   0087   0111
 .0001613    .0001399    .00008104   .00002212   .00002778
```

```
C   EGLIN      SITE 1     LOC C-4   LD.CT.     3.10.76    4.0  .2   61
     .33333     .66667    1.58333   2.58333    3.58333
    61       .200 25000.0
0034   0054   0075   0107   0117
0036   0055   0076   0111   0119
0037   0057   0077   0115   0120
0037   0058   0079   0120   0122
0039   0060   0080   0125   0124
0041   0062   0084   0131   0126
0044   0066   0088   0139   0129
0046   0069   0091   0147   0132
0049   0072   0096   0156   0135
0051   0075   0100   0165   0138
0055   0079   0103   0172   0140
0058   0083   0107   0181   0144
0061   0087   0112   0191   0147
0066   0092   0118   0203   0150
0071   0098   0123   0214   0155
0076   0103   0130   0226   0159
0081   0109   0136   0237   0161
0088   0116   0143   0250   0166
0094   0124   0149   0263   0170
0101   0132   0157   0277   0175
0110   0140   0166   0292   0178
0120   0151   0176   0309   0184
0130   0161   0185   0326   0188
0141   0172   0195   0343   0192
0153   0184   0206   0359   0197
0169   0199   0218   0378   0203
0185   0212   0228   0389   0205
0204   0227   0238   0400   0207
0224   0242   0248   0411   0209
0243   0255   0255   0419   0211
0258   0263   0263   0427   0213
0266   0266   0266   0428   0213
0266   0266   0266   0430   0213
0262   0265   0268   0436   0218
0256   0261   0266   0436   0218
0247   0254   0265   0432   0218
0234   0242   0255   0416   0213
0221   0230   0243   0393   0206
0204   0214   0228   0361   0192
0187   0199   0211   0325   0177
0170   0181   0194   0292   0163
0156   0168   0178   0259   0150
0142   0155   0163   0226   0136
0132   0144   0151   0202   0128
0122   0136   0142   0183   0122
0116   0130   0137   0171   0119
0112   0125   0132   0162   0117
0108   0121   0127   0155   0115
0105   0118   0124   0149   0115
0102   0116   0122   0144   0112
0099   0113   0119   0140   0112
0098   0112   0117   0136   0111
0097   0111   0116   0134   0110
0095   0110   0115   0132   0110
0094   0110   0115   0130   0111
0093   0108   0113   0129   0111
0091   0107   0112   0128   0110
0091   0105   0111   0127   0112
0090   0105   0110   0127   0112
0090   0104   0111   0126   0111
0089   0104   0111   0126   0111
 .0001613    .0001399    .00008104    .00002212    .00002778
```

```
C   EGLIN      SITE 1 .  LOC C-4   LD.CT.     3.10.76   4.5  .2   38
    .375        .708      1.625     2.625      3.625
    38       .200 25000.0
0025  0041   0061   0080   0104
0026  0042   0062   0081   0104
0027  0043   0063   0082   0103
0030  0045   0064   0086   0104
0034  0050   0071   0100   0104
0042  0058   0079   0121   0108
0051  0066   0090   0144   0115
0060  0076   0100   0166   0124
0070  0086   0110   0188   0131
0084  0100   0126   0217   0142
0099  0114   0139   0243   0152
0117  0133   0156   0274   0164
0137  0151   0173   0303   0173
0161  0173   0191   0332   0183
0186  0194   0207   0358   0191
0210  0213   0220   0376   0197
0227  0229   0230   0390   0200
0232  0234   0236   0394   0200
0229  0236   0237   0401   0203
0218  0232   0239   0408   0208
0202  0222   0236   0409   0210
0184  0204   0222   0386   0204
0166  0188   0207   0356   0194
0148  0172   0189   0321   0181
0131  0154   0172   0285   0167
0115  0138   0155   0249   0152
0102  0124   0139   0216   0140
0092  0111   0126   0186   0129
0081  0100   0113   0157   0119
0073  0091   0103   0136   0111
0068  0085   0095   0118   0107
0063  0078   0089   0104   0104
0057  0073   0082   0091   0103
0055  0070   0080   0084   0103
0053  0068   0077   0080   0103
0052  0066   0076   0078   0103
0050  0064   0075   0075   0103
0049  0064   0074   0075   0103
 .0001613    .0001399    .00008104    .00002212    .00002778
```

```
C   EGLIN      SITE 1     LOC C-5   LD.CT.     3.10.76   4.5  .2   52
    .375        .708      1.625      2.625      3.625
   52        .200 25000.0
0036   0058   0087   0124   0141
0037   0059   0089   0130   0143
0040   0062   0092   0139   0148
0041   0065   0096   0148   0152
0044   0068   0101   0161   0159
0047   0072   0107   0175   0167
0052   0077   0113   0189   0175
0057   0085   0121   0209   0183
0068   0097   0136   0238   0196
0081   0112   0154   0273   0209
0092   0126   0169   0303   0221
0106   0141   0186   0335   0235
0121   0158   0204   0369   0245
0142   0181   0227   0408   0260
0164   0202   0246   0438   0269
0190   0228   0269   0472   0278
0214   0250   0288   0497   0285
0244   0277   0310   0531   0295
0270   0295   0323   0545   0297
0295   0312   0336   0561   0303
0313   0321   0340   0567   0306
0318   0322   0343   0566   0309
0313   0318   0345   0568   0314
0296   0304   0335   0568   0312
0279   0288   0322   0549   0307
0257   0267   0303   0514   0295
0238   0250   0286   0483   0282
0220   0233   0268   0447   0268
0204   0218   0253   0418   0258
0190   0204   0237   0390   0246
0178   0192   0223   0361   0234
0166   0181   0210   0333   0223
0156   0171   0197   0309   0210
0146   0161   0188   0289   0201
0138   0155   0178   0269   0193
0132   0148   0172   0253   0184
0127   0142   0164   0240   0178
0123   0139   0160   0231   0174
0118   0134   0156   0221   0170
0115   0132   0152   0212   0165
0112   0129   0148   0204   0161
0109   0127   0146   0199   0159
0108   0124   0144   0194   0156
0105   0123   0142   0189   0155
0104   0121   0141   0186   0153
0103   0121   0139   0184   0152
0102   0120   0139   0182   0152
0101   0119   0138   0181   0151
0101   0119   0138   0181   0151
0100   0119   0137   0180   0151
0101   0118   0137   0180   0152
0100   0117   0137   0180   0152
 .0001613    .0001399    .00008104   .00002212   .00002778
```

```
C   EGLIN     SITE 1 .  LOC C-5   LD.CT.    3.10.76   5.0  .2   38
    .41667     .75      1.66667   2.66667   3.66667
   38       .200 25000.0
0033   0041   0056   0072   0160
0034   0044   0057   0075   0163
0036   0044   0059   0080   0165
0037   0046   0062   0088   0168
0040   0049   0065   0095   0172
0045   0054   0071   0108   0178
0049   0059   0077   0121   0183
0055   0065   0085   0138   0192
0065   0074   0095   0158   0201
0074   0084   0107   0181   0211
0088   0096   0122   0210   0223
0102   0110   0137   0241   0233
0122   0130   0156   0276   0246
0148   0153   0178   0313   0261
0175   0179   0202   0352   0275
0206   0206   0225   0386   0285
0238   0233   0245   0415   0294
0266   0256   0262   0436   0299
0282   0271   0273   0449   0302
0283   0279   0279   0461   0306
0272   0276   0282   0466   0309
0250   0263   0274   0458   0309
0226   0240   0254   0425   0300
0201   0217   0232   0388   0285
0175   0190   0207   0336   0265
0153   0168   0180   0284   0243
0128   0141   0151   0224   0220
0110   0120   0127   0181   0200
0098   0107   0112   0151   0185
0089   0098   0101   0125   0173
0081   0090   0092   0106   0164
0077   0085   0087   0094   0159
0075   0082   0084   0087   0156
0072   0080   0081   0083   0154
0071   0078   0079   0079   0152
0070   0077   0077   0077   0151
0069   0076   0076   0075   0149
0068   0075   0076   0073   0149
 .0001613    .0001399    .00008104    .00002212    .00002778
```

```
C   EGLIN      SITE 1     LOC A-4   LD. CT.    3.11.76    5.00 .2    41
    .41667     .75       1.66667    2.66667    3.66667
    41       .200 25000.0
0108  0126  0139  0159  0175
0110  0127  0139  0159  0175
0110  0128  0140  0162  0177
0111  0128  0142  0165  0178
0112  0129  0143  0169  0180
0113  0130  0146  0173  0182
0116  0133  0148  0179  0185
0117  0134  0150  0185  0187
0121  0137  0154  0194  0191
0124  0141  0159  0202  0195
0128  0144  0163  0212  0198
0132  0148  0168  0222  0202
0139  0154  0175  0234  0207
0146  0161  0182  0247  0211
0155  0169  0191  0263  0216
0166  0180  0202  0279  0221
0181  0193  0216  0302  0227
0200  0210  0232  0328  0235
0230  0235  0253  0355  0242
0267  0267  0278  0387  0249
0302  0295  0302  0414  0254
0338  0322  0323  0439  0260
0374  0354  0343  0463  0265
0391  0371  0354  0474  0267
0387  0375  0358  0480  0271
0363  0361  0349  0471  0268
0327  0333  0327  0439  0260
0290  0300  0300  0400  0249
0254  0267  0267  0349  0234
0222  0236  0236  0298  0215
0196  0210  0208  0244  0196
0178  0185  0190  0206  0182
0164  0171  0176  0176  0171
0157  0165  0168  0159  0166
0147  0157  0150  0141  0158
0145  0155  0147  0137  0158
0143  0154  0147  0136  0158
0142  0153  0146  0134  0157
0142  0152  0146  0134  0158
0142  0152  0145  0134  0158
0141  0150  0145  0135  0158
 .0001613    .0001399    .00008104    .00002212    .00002778
```

```
C   EGLIN      SITE 2     LOC A-1   LD.CT.     3.11.76   3.0  .2   70
    .25         .58333    1.5         2.5         3.5
     70       .200 25000.0
0023   0055   0079   0104   0125
0027   0060   0082   0108   0129
0032   0067   0087   0115   0135
0038   0073   0092   0120   0140
0044   0079   0096   0125   0144
0051   0086   0100   0131   0150
0057   0094   0106   0136   0154
0065   0101   0111   0144   0160
0072   0111   0117   0150   0166
0082   0120   0123   0157   0173
0092   0130   0129   0165   0178
0102   0141   0136   0172   0185
0113   0152   0143   0179   0191
0125   0163   0150   0186   0196
0138   0175   0157   0194   0204
0151   0187   0164   0201   0209
0163   0198   0170   0208   0215
0176   0209   0176   0214   0220
0191   0221   0183   0221   0227
0202   0230   0188   0226   0230
0212   0239   0193   0230   0234
0220   0245   0198   0235   0238
0225   0251   0201   0237   0241
0227   0253   0202   0239   0244
0228   0254   0204   0241   0246
0229   0256   0205   0244   0248
0228   0255   0206   0246   0252
0227   0254   0208   0250   0260
0226   0253   0208   0252   0264
0225   0252   0202   0239   0244
0224   0251   0208   0253   0267
0220   0246   0205   0251   0268
0213   0240   0202   0248   0266
0206   0233   0198   0244   0264
0200   0228   0195   0241   0263
0193   0220   0190   0236   0259
0187   0214   0187   0232   0256
0181   0208   0183   0228   0253
0175   0203   0179   0224   0250
0170   0197   0175   0220   0246
0165   0192   0172   0217   0246
0160   0187   0169   0213   0243
0154   0181   0165   0208   0237
0146   0173   0160   0202   0231
0140   0167   0155   0196   0227
0133   0159   0150   0189   0220
0126   0153   0145   0184   0215
0119   0146   0140   0177   0209
0114   0140   0136   0173   0204
0108   0135   0131   0166   0197
0102   0129   0127   0161   0191
0098   0123   0123   0157   0184
0093   0119   0119   0152   0180
0090   0116   0116   0149   0177
0086   0114   0112   0144   0173
0083   0112   0111   0142   0171
0080   0109   0107   0140   0167
0079   0102   0108   0136   0162
0076   0102   0106   0134   0160
0075   0098   0104   0131   0156
0073   0097   0103   0131   0155
0071   0096   0102   0130   0154
0070   0095   0101   0127   0153
0069   0094   0100   0127   0152
0068   0092   0098   0125   0149
0066   0090   0097   0123   0147
0066   0089   0096   0122   0145
0065   0088   0095   0120   0142
0065   0086   0095   0119   0141
0064   0085   0094   0118   0141
 .000040325  .000034965  .00004052   .00002212   .00001111
```

```
^       N      SITE 2     LOC A-2   LD.CT.     3.11.76   4.5  .2   72
        .675       .708       1.625     2.625      3.625
     66        .200 25000.0
 (  )  0154   0165   0190   0207
0141   0155   0166   0192   0208
0142   0155   0166   0193   0209
0144   0157   0167   0194   0211
0146   0158   0168   0195   0213
0146   0159   0169   0196   0215
0147   0160   0170   0197   0216
0150   0163   0172   0201   0219
0153   0165   0174   0203   0224
0155   0168   0176   0206   0227
0159   0172   0179   0210   0232
0163   0175   0182   0215   0237
0167   0180   0186   0219   0243
0174   0187   0190   0227   0252
0180   0193   0195   0233   0260
0189   0201   0201   0241   0271
0198   0211   0209   0250   0280
0209   0221   0217   0260   0292
0221   0232   0224   0269   0303
0235   0246   0234   0282   0315
0252   0261   0245   0294   0327
0269   0276   0255   0307   0340
0290   0295   0268   0321   0354
0310   0314   0280   0334   0367
0335   0336   0293   0348   0382
0357   0356   0305   0361   0392
0382   0377   0319   0373   0405
0399   0393   0328   0382   0412
0409   0406   0337   0391   0419
0416   0415   0342   0397   0425
0421   0416   0345   0401   0430
0425   0415   0350   0408   0438
0424   0412   0351   0412   0444
0412   0397   0348   0409   0444
0396   0376   0335   0398   0435
0376   0355   0323   0385   0424
0355   0331   0308   0367   0407
0334   0312   0295   0351   0390
0313   0291   0281   0333   0371
0295   0274   0268   0316   0351
0277   0259   0255   0299   0331
0261   0244   0244   0284   0313
0248   0232   0232   0269   0295
0236   0224   0222   0258   0279
0226   0217   0213   0247   0266
0218   0211   0206   0239   0256
0211   0205   0202   0232   0247
0205   0195   0201   0227   0241
0201   0191   0198   0222   0234
0197   0189   0196   0217   0229
0192   0186   0192   0214   0226
0189   0182   0190   0213   0223
0188   0180   0188   0210   0220
0187   0179   0187   0209   0219
0185   0177   0186   0208   0218
0183   0175   0185   0207   0217
0184   0181   0173   0206   0216
```

```
0184   0181   0173   0204   0214
0184   0180   0173   0204   0214
0183   0180   0171   0204   0214
0182   0179   0170   0204   0214
0182   0178   0170   0202   0213
0181   0178   0170   0203   0212
0182   0178   0169   0202   0212
0181   0177   0168   0202   0211
0180   0176   0167   0202   0212
0180   0176   0165   0202   0211
0180   0175   0164   0201   0211
 .000040325  .000034965  .00004052   .00002212   .00001111
```

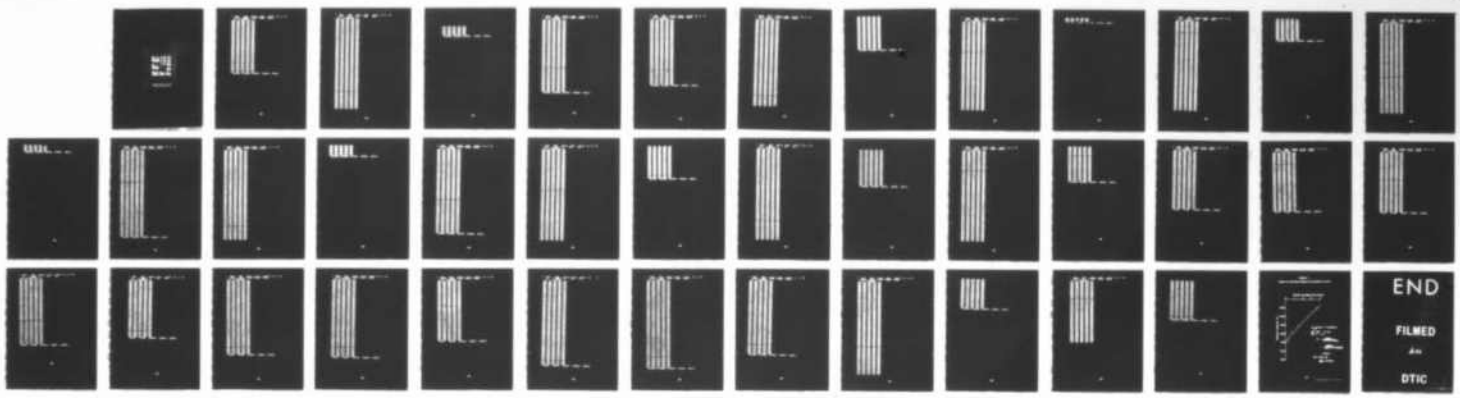
```
C   EGLIN      SITE-2     LOC C-1   LD.CT.     3.11.76   4.5  .2   70
    .375       .708       1.625     2.625      3.625
   70      .200 25000.0
0041   0057   0117   0141   0192
0041   0058   0117   0142   0194
0042   0059   0118   0142   0194
0043   0060   0118   0142   0194
0044   0060   0119   0144   0195
0045   0062   0119   0145   0197
0047   0062   0120   0146   0197
0049   0065   0121   0149   0200
0052   0067   0123   0150   0202
0054   0069   0125   0152   0204
0056   0072   0127   0156   0207
0060   0074   0130   0159   0210
0063   0079   0132   0162   0213
0067   0082   0134   0166   0217
0072   0087   0138   0169   0220
0078   0093   0142   0175   0225
0085   0099   0146   0179   0229
0092   0106   0151   0186   0235
0101   0113   0155   0190   0239
0111   0121   0162   0197   0244
0122   0131   0169   0203   0249
0136   0145   0177   0212   0257
0152   0159   0186   0220   0263
0171   0176   0196   0230   0271
0193   0195   0208   0239   0278
0220   0218   0220   0251   0286
0250   0243   0236   0261   0293
0284   0271   0251   0271   0299
0315   0295   0263   0278   0305
0348   0320   0277   0284   0306
0376   0341   0285   0288   0308
0402   0362   0294   0293   0308
0419   0378   0301   0296   0308
0427   0390   0307   0299   0311
0426   0398   0312   0304   0315
0418   0400   0313   0309   0320
0401   0391   0311   0309   0325
0368   0365   0297   0298   0320
0327   0330   0280   0284   0313
0297   0305   0267   0273   0306
0268   0279   0252   0260   0298
0242   0255   0238   0247   0289
0215   0229   0223   0234   0277
0193   0207   0210   0222   0268
0173   0189   0199   0210   0259
0159   0173   0188   0201   0249
0145   0159   0179   0191   0242
0134   0147   0171   0183   0234
0125   0137   0164   0175   0227
0115   0127   0157   0168   0220
0110   0120   0152   0163   0215
0103   0114   0147   0157   0210
0099   0108   0143   0153   0206
0095   0104   0139   0150   0204
0092   0101   0138   0148   0202
0088   0098   0135   0146   0200
0087   0096   0134   0145   0199
0085   0095   0134   0144   0199
0083   0093   0132   0143   0198
0083   0092   0132   0143   0198
0082   0091   0132   0142   0198
0080   0089   0132   0142   0198
0080   0089   0131   0142   0198
0079   0089   0130   0142   0198
0079   0087   0130   0141   0197
0079   0087   0130   0141   0197
0079   0087   0130   0141   0198
0077   0087   0130   0141   0197
0077   0087   0130   0142   0197
0076   0087   0130   0142   0198
 .000040325  .000034965  .00004052   .00002212   .00001111
```

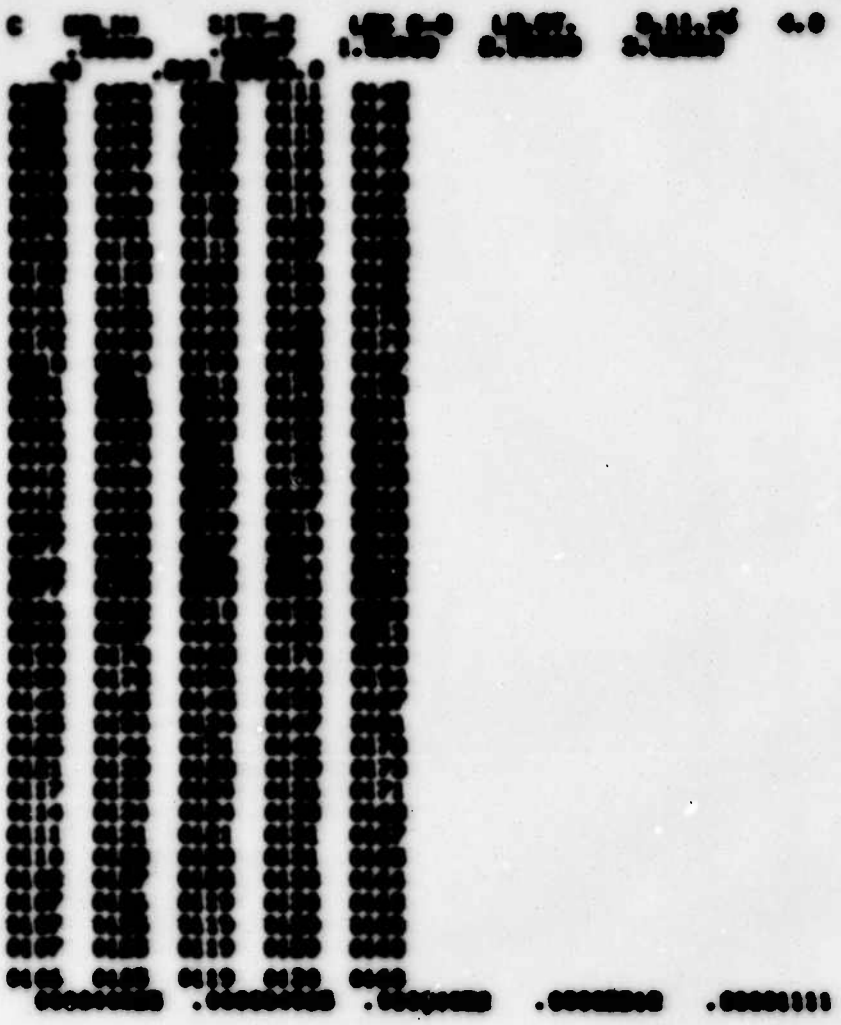
```
C   EGLIN      SITE-2     LOC C-2   LD.CT.     3.11.76   4.0  .2   60
     .33333     .66667    1.58333   2.58333    3.58333
   60      .200 25000.0
0071   0087   0105   0130   0157
0073   0088   0106   0132   0160
0076   0090   0107   0132   0162
0077   0092   0109   0134   0163
0079   0094   0110   0136   0165
0081   0097   0112   0139   0168
0085   0100   0114   0141   0171
0089   0103   0117   0143   0173
0094   0109   0121   0148   0178
0100   0114   0124   0152   0181
0109   0122   0130   0158   0187
0117   0130   0136   0163   0192
0129   0142   0142   0170   0198
0140   0154   0152   0177   0205
0158   0169   0163   0187   0214
0174   0183   0172   0192   0218
0195   0203   0184   0202   0226
0216   0222   0197   0208   0232
0242   0247   0211   0218   0239
0269   0269   0225   0224   0244
0301   0297   0241   0232   0250
0330   0320   0253   0235   0251
0364   0345   0266   0240   0254
0390   0364   0276   0242   0256
0415   0384   0287   0246   0259
0429   0398   0292   0248   0262
0435   0407   0297   0251   0263
0428   0409   0299   0255   0268
0409   0400   0294   0257   0271
0382   0382   0283   0255   0270
0352   0357   0270   0251   0267
0320   0330   0253   0243   0260
0290   0301   0236   0235   0253
0264   0278   0219   0226   0246
0239   0250   0203   0216   0237
0212   0226   0186   0205   0228
0188   0199   0167   0193   0216
0168   0179   0154   0183   0208
0155   0167   0146   0175   0199
0148   0157   0140   0169   0194
0142   0151   0137   0163   0188
0137   0145   0133   0160   0184
0133   0142   0130   0157   0181
0131   0139   0129   0154   0178
0128   0136   0128   0152   0176
0126   0133   0126   0150   0174
0126   0133   0125   0150   0172
0125   0132   0125   0150   0172
0124   0130   0124   0148   0170
0124   0129   0123   0148   0169
0122   0129   0122   0146   0169
0121   0127   0121   0146   0168
0121   0127   0121   0145   0168
0121   0126   0120   0145   0167
0119   0126   0121   0145   0167
0118   0125   0121   0145   0167
0118   0125   0121   0145   0166
0117   0124   0121   0145   0166
0117   0125   0121   0144   0167
0117   0124   0121   0144   0166
 .000040325  .000034965  .00004052   .00002212   .00001111
```

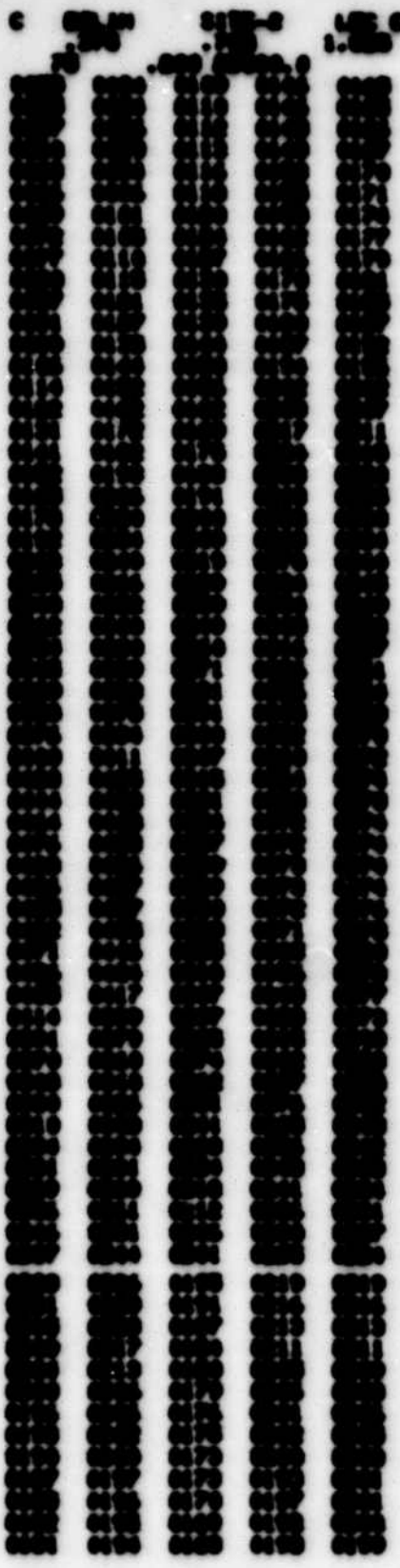
AD-A047 161 NONCONTACT NONDESTRUCTIVE DETERMINATION OF PAVEMENT DEFLECTION UNDER MOVING LOADS(U) PURDUE RESEARCH FOUNDATION LAFAYETTE IN M E HARR ET AL AUG 77

4/4

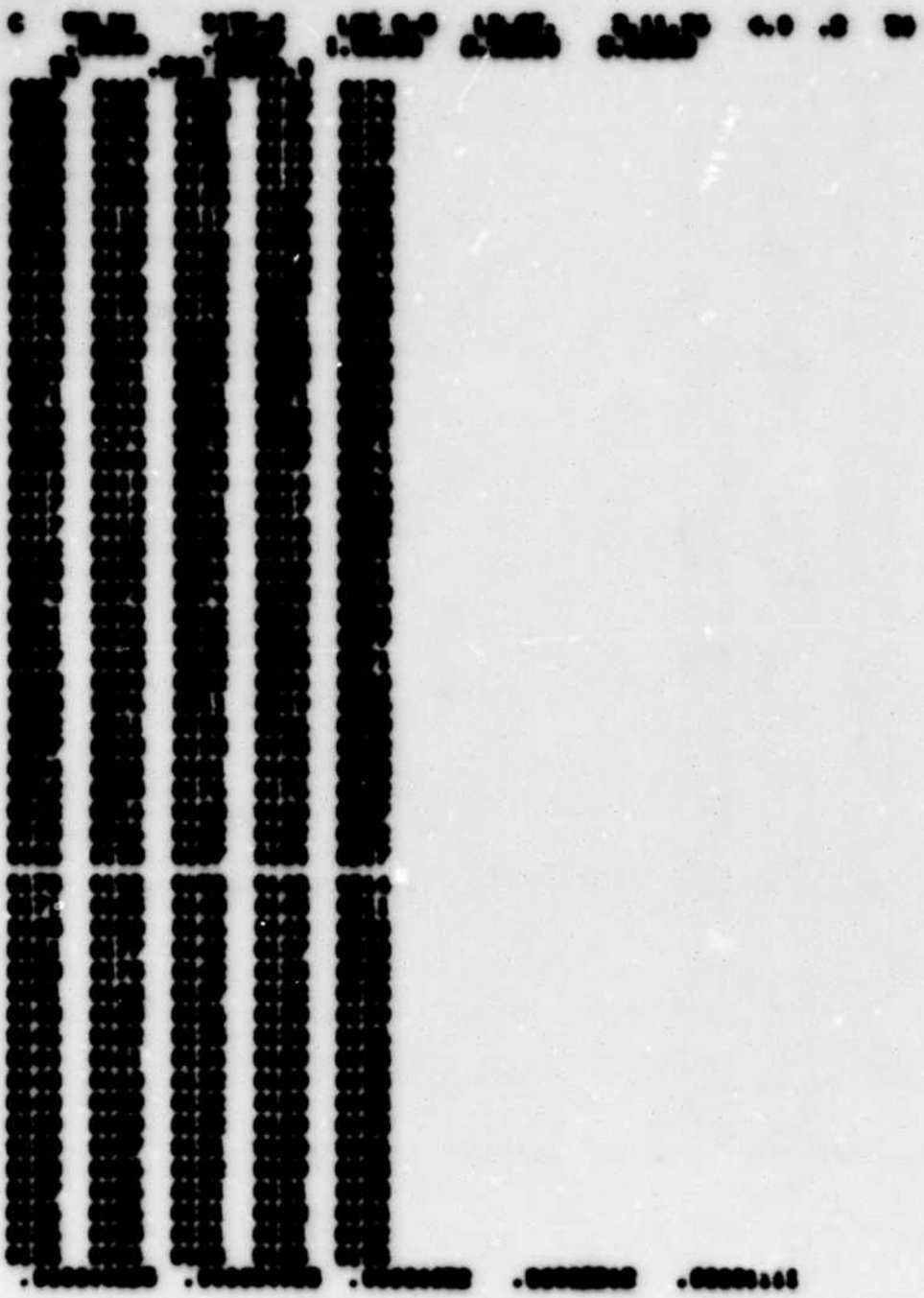
UNCLASSIFIED FAA-RD-77-127 DOT-FA73WAI-361 F/G 13/2 NL

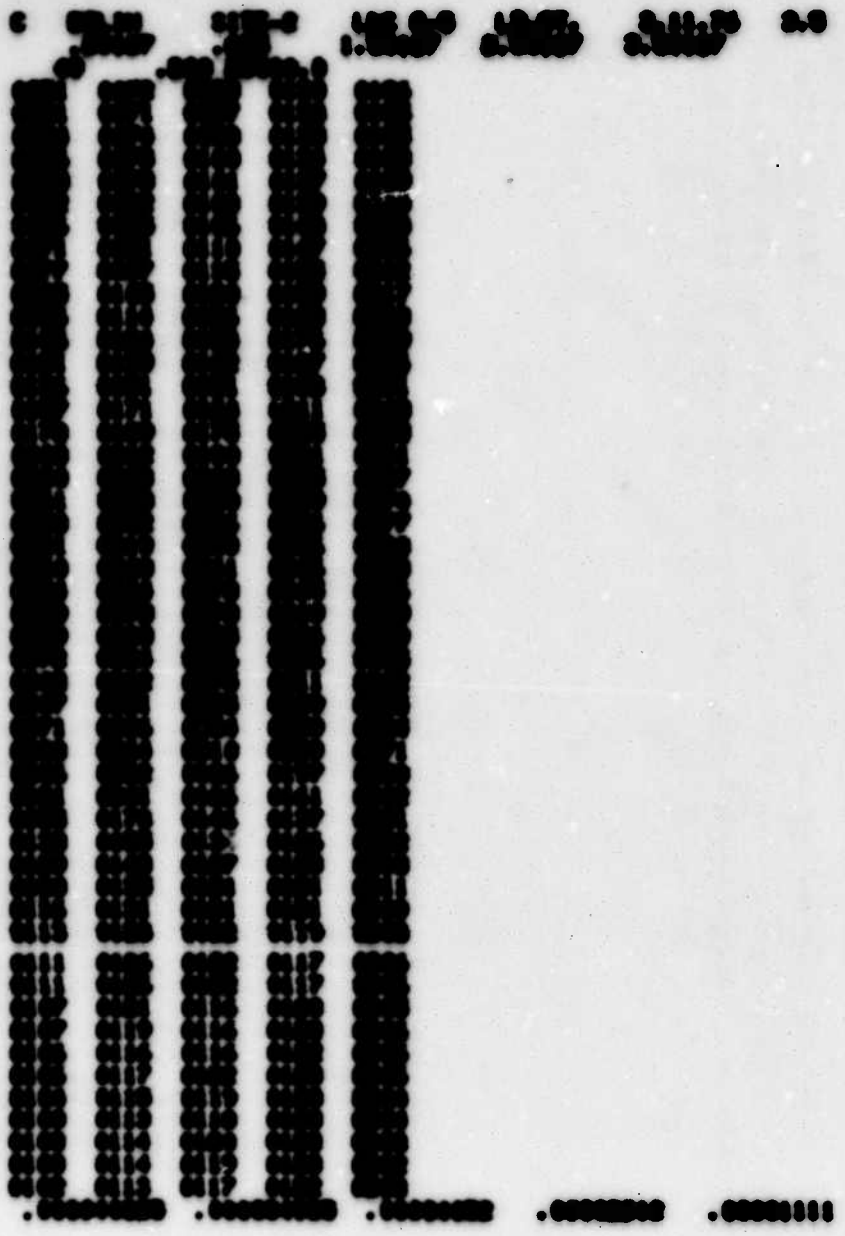




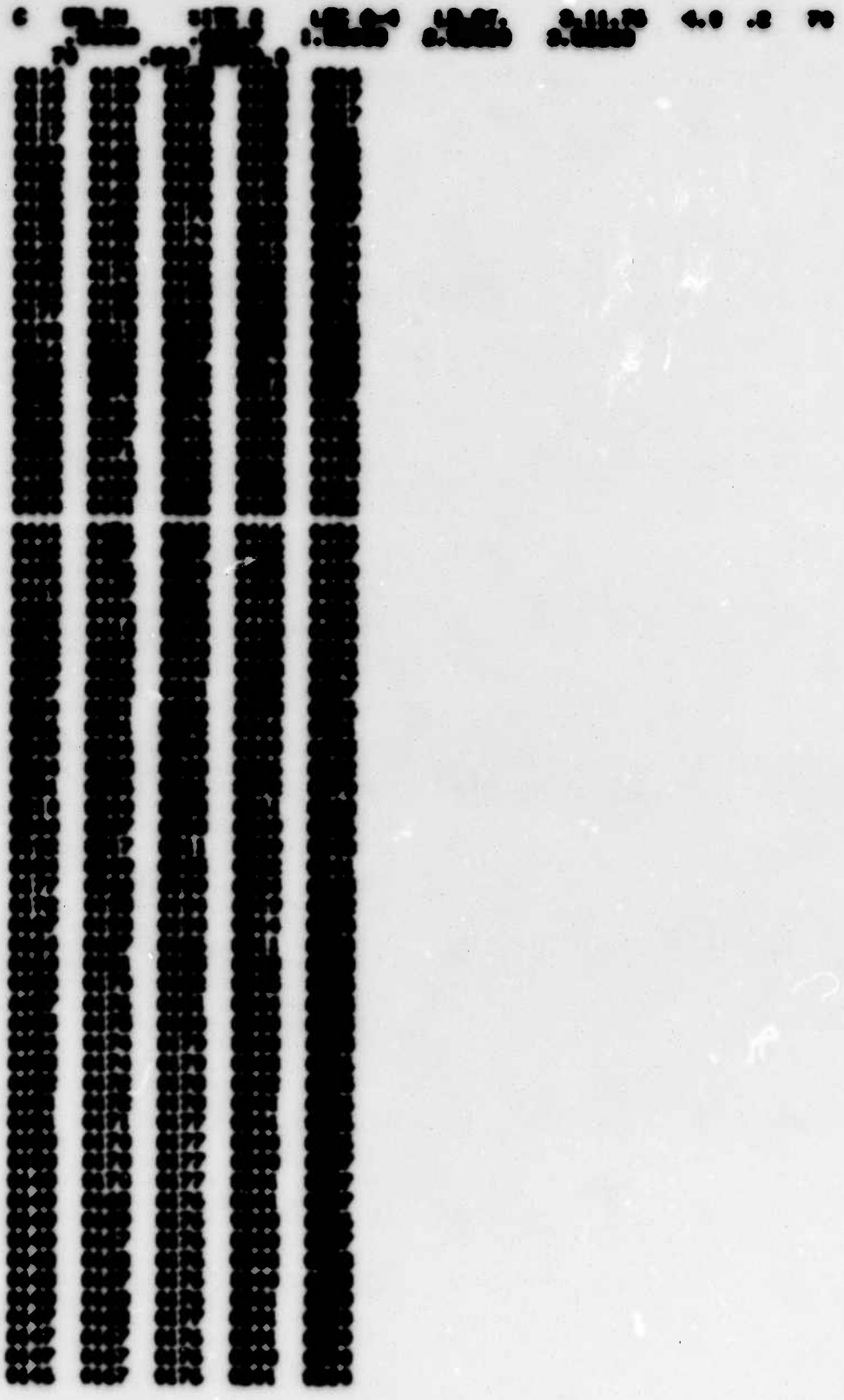


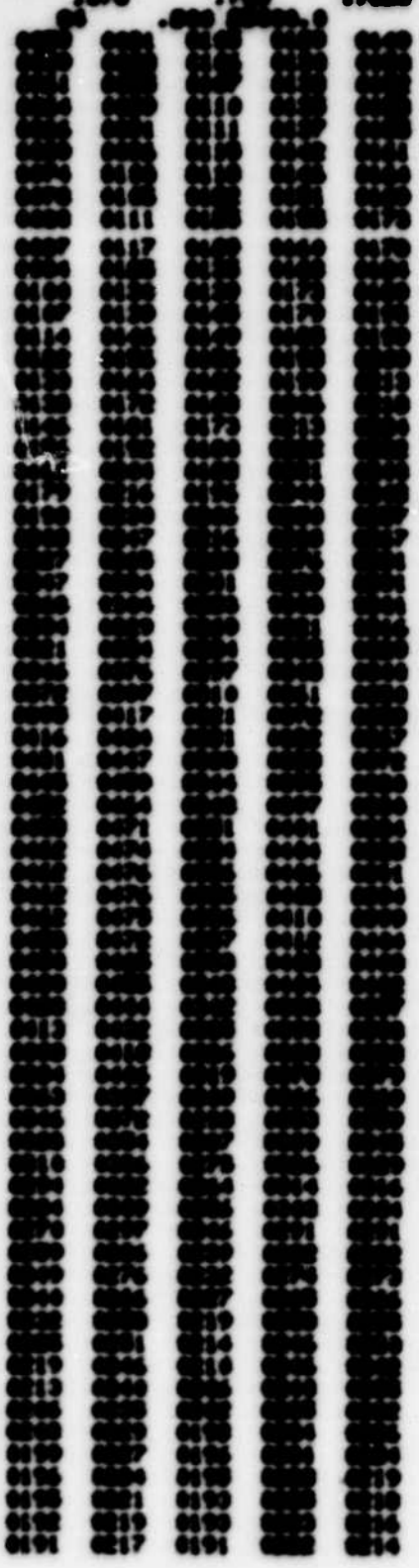


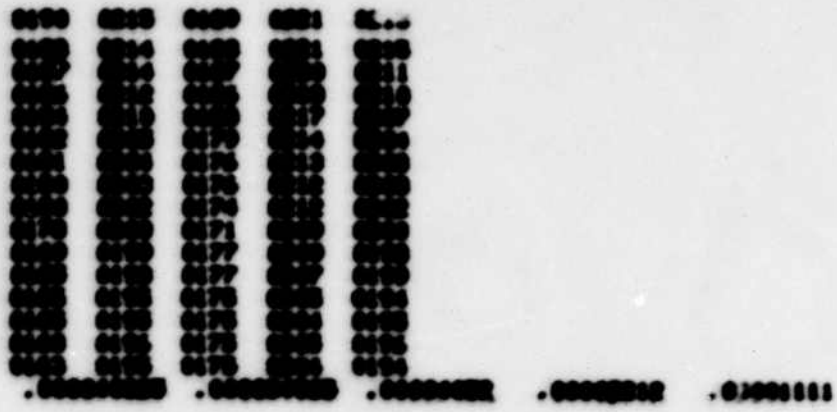


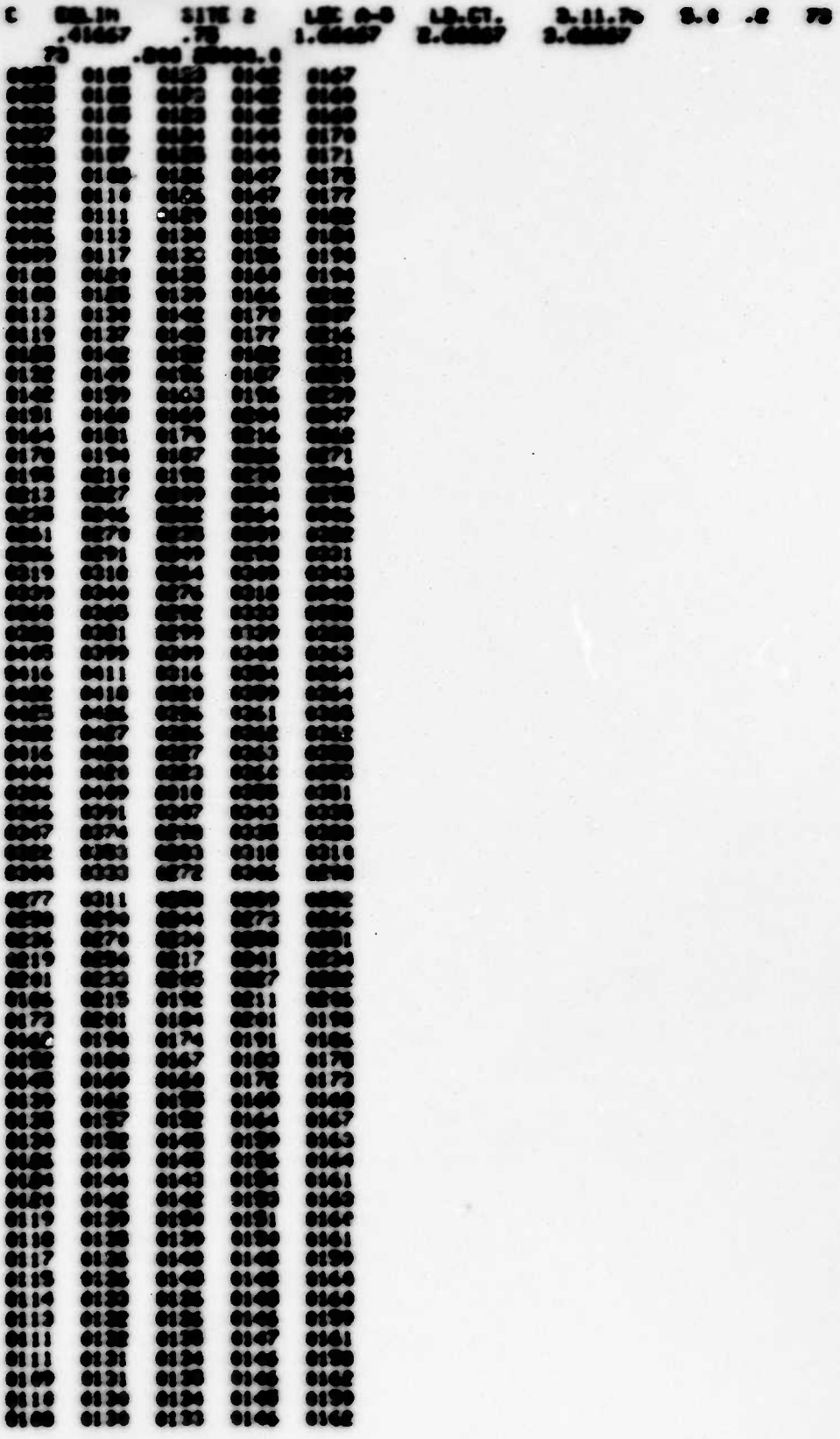




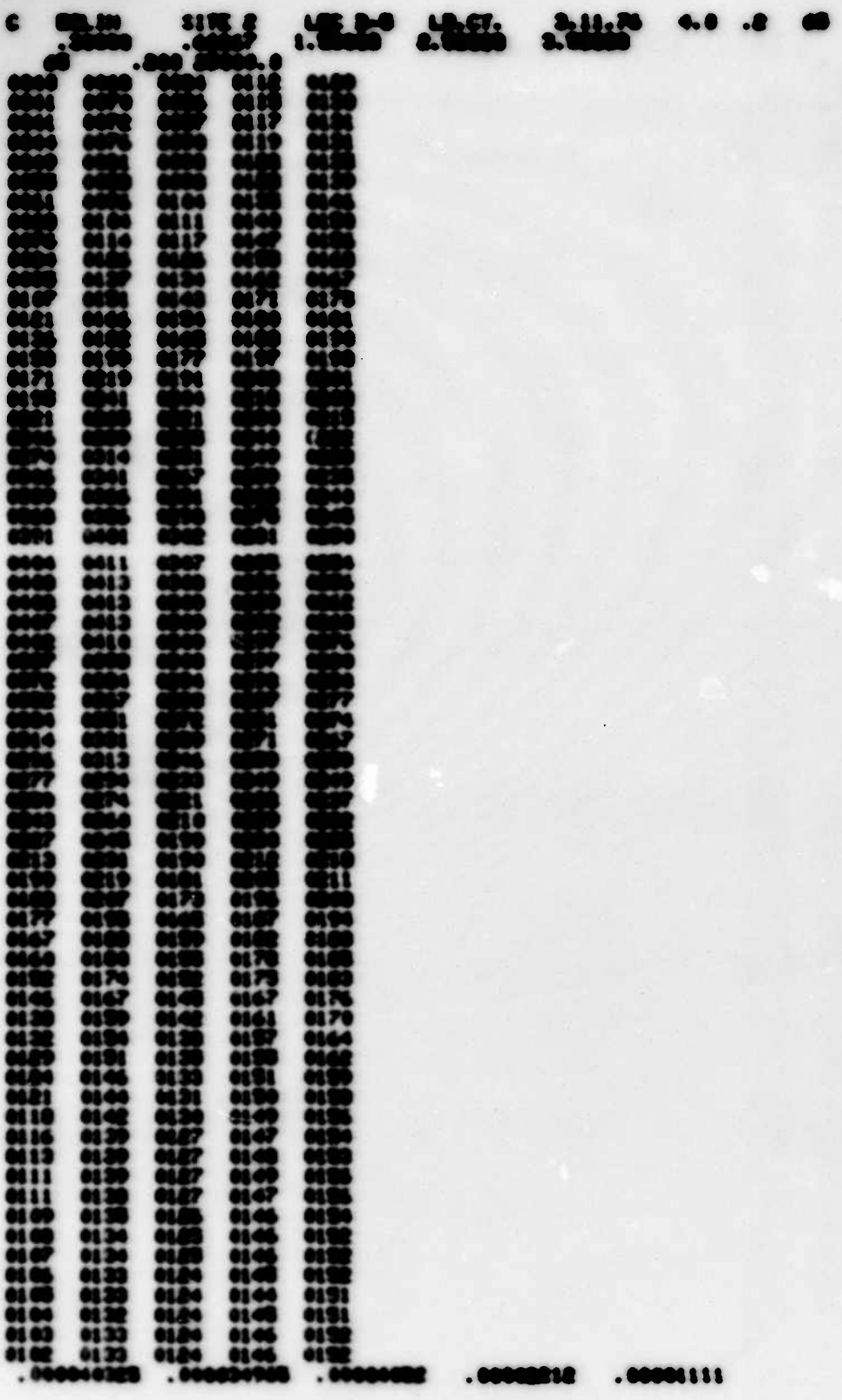


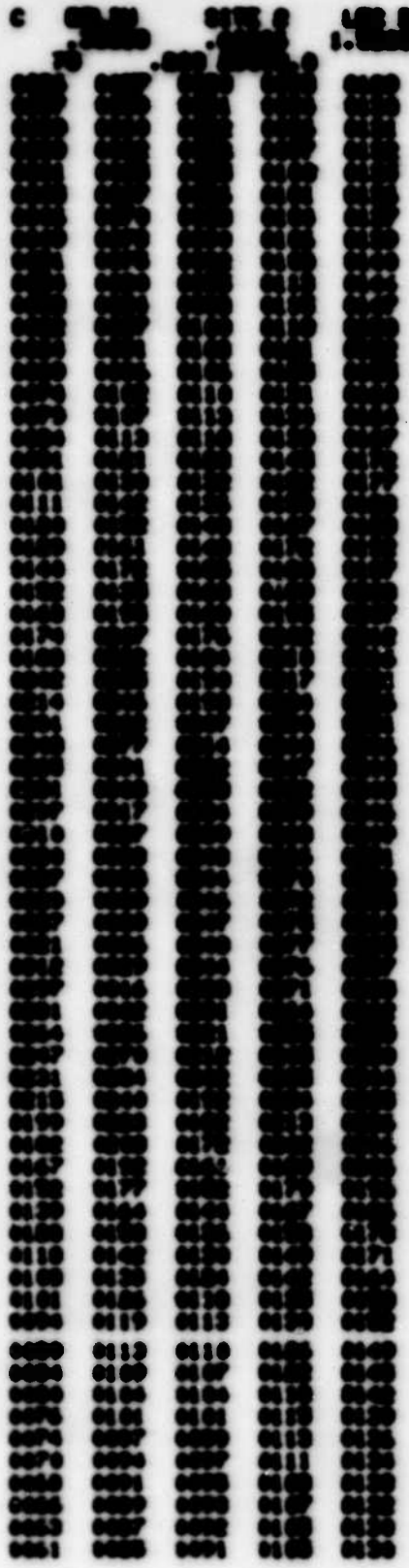


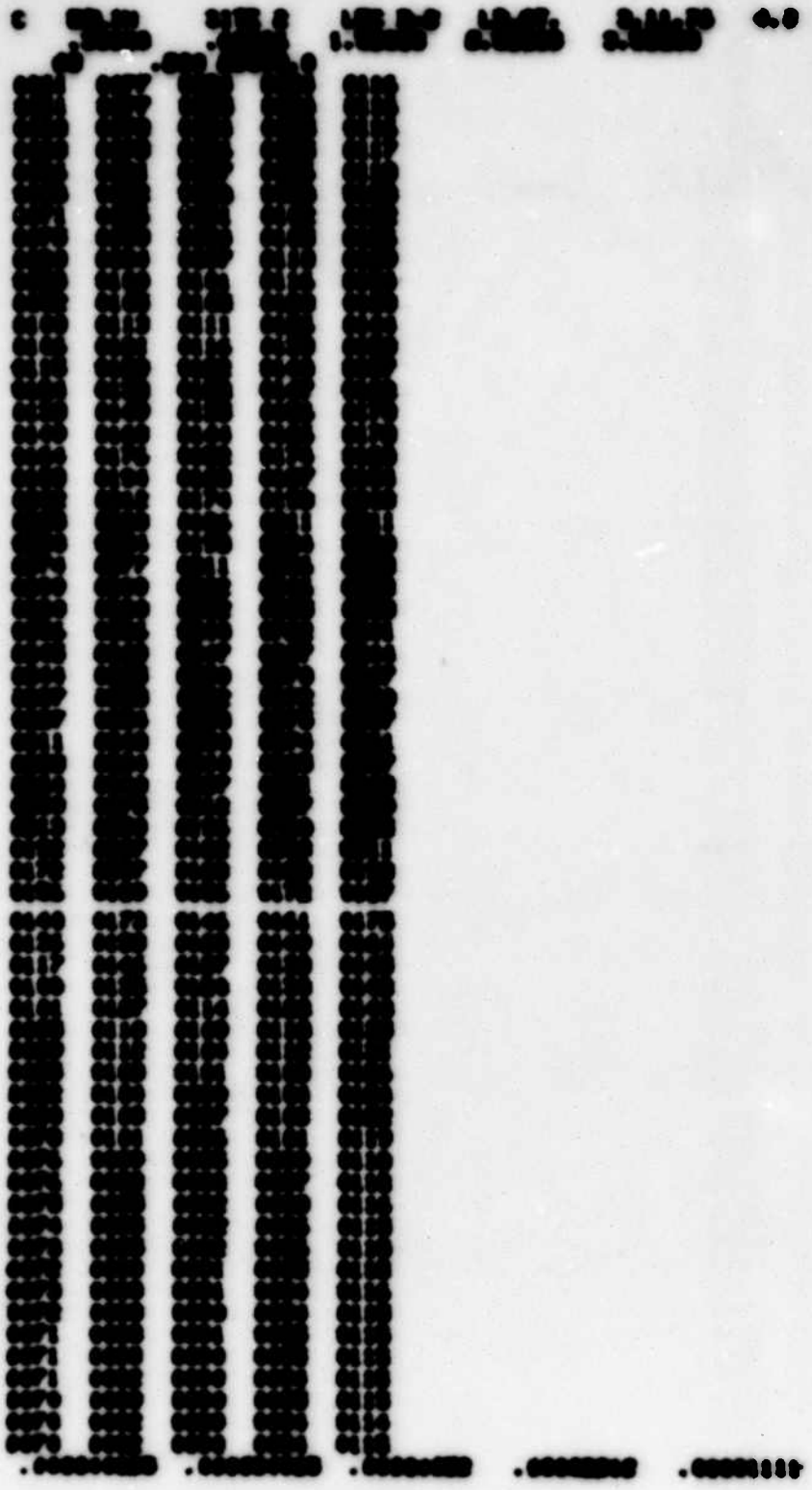


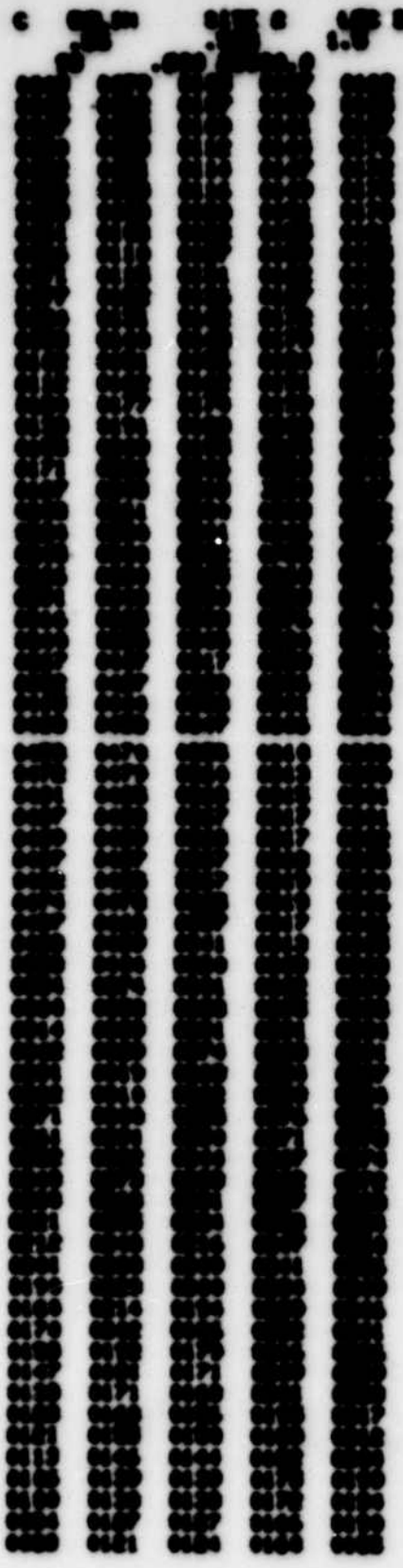




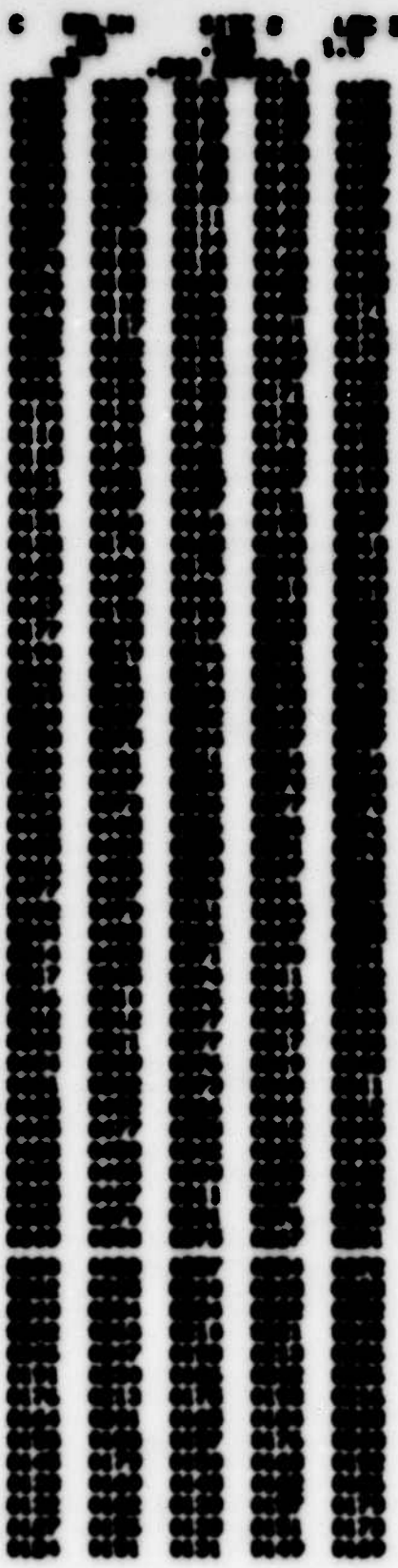


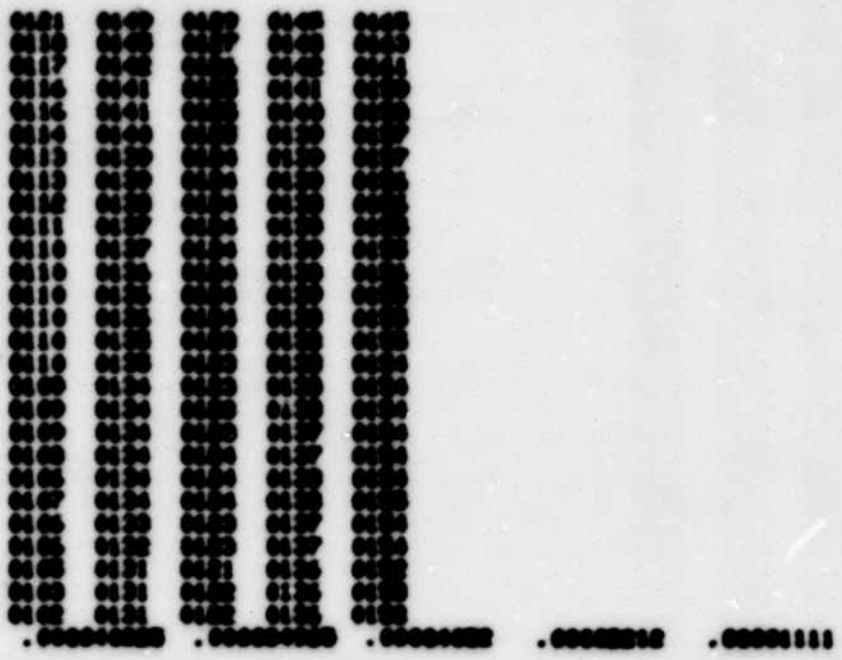


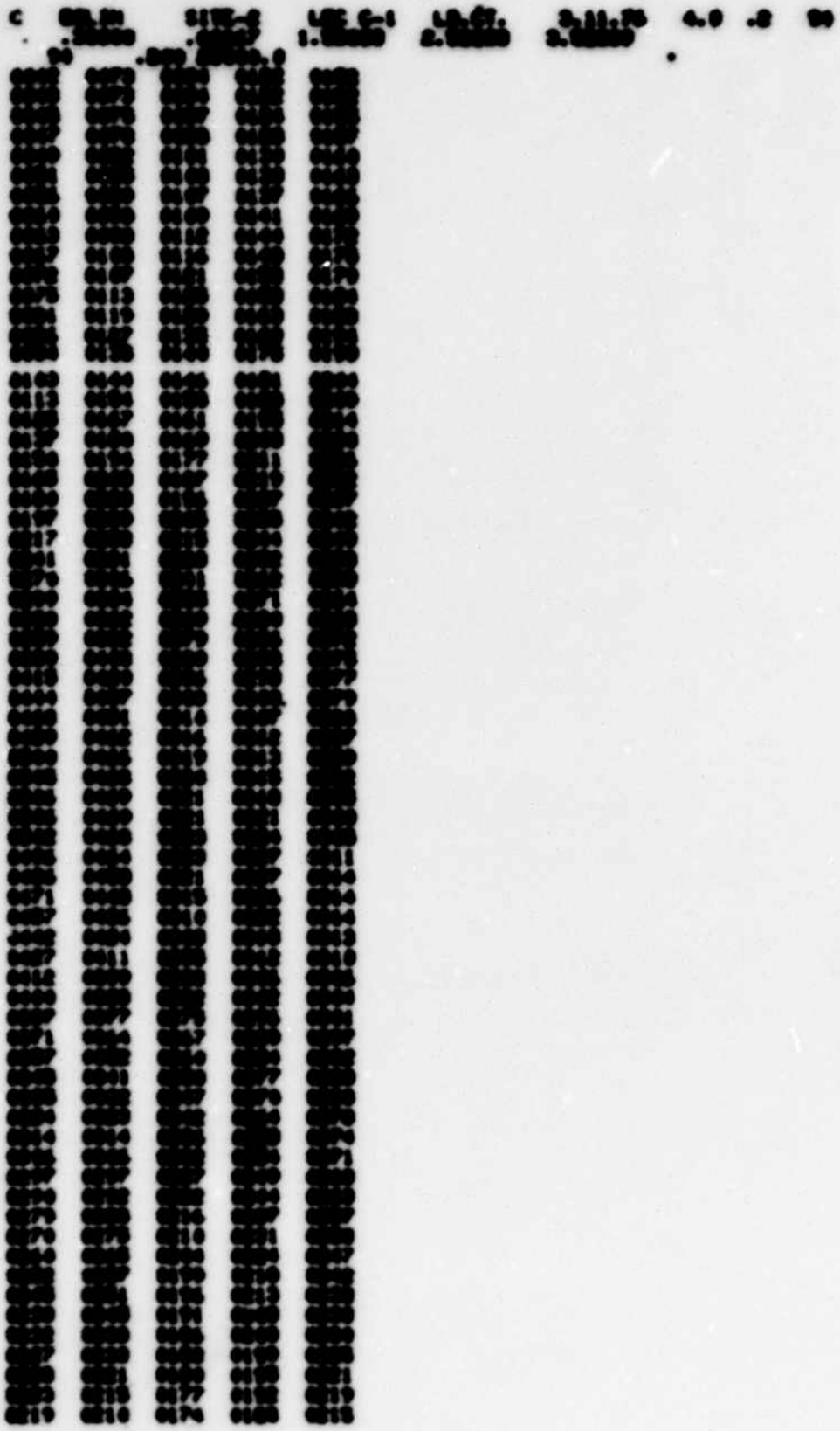


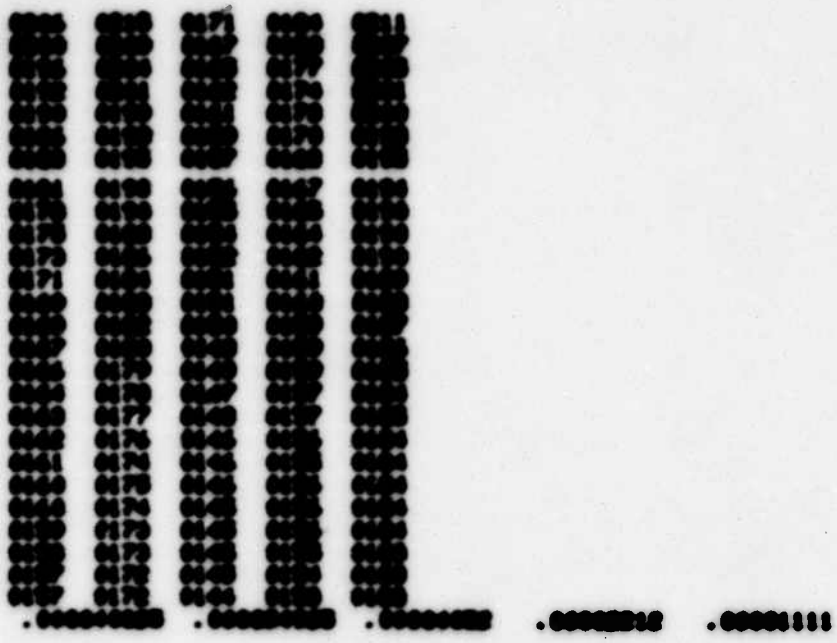


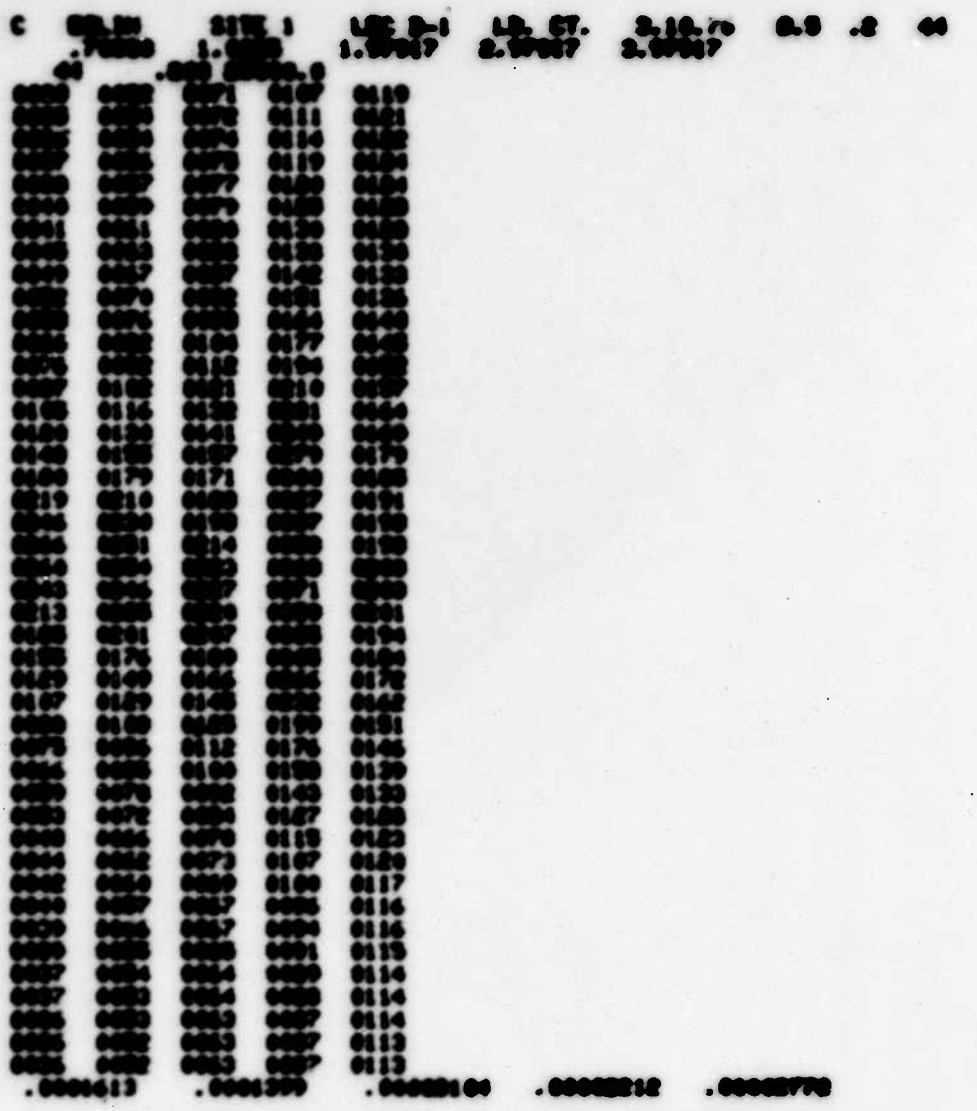


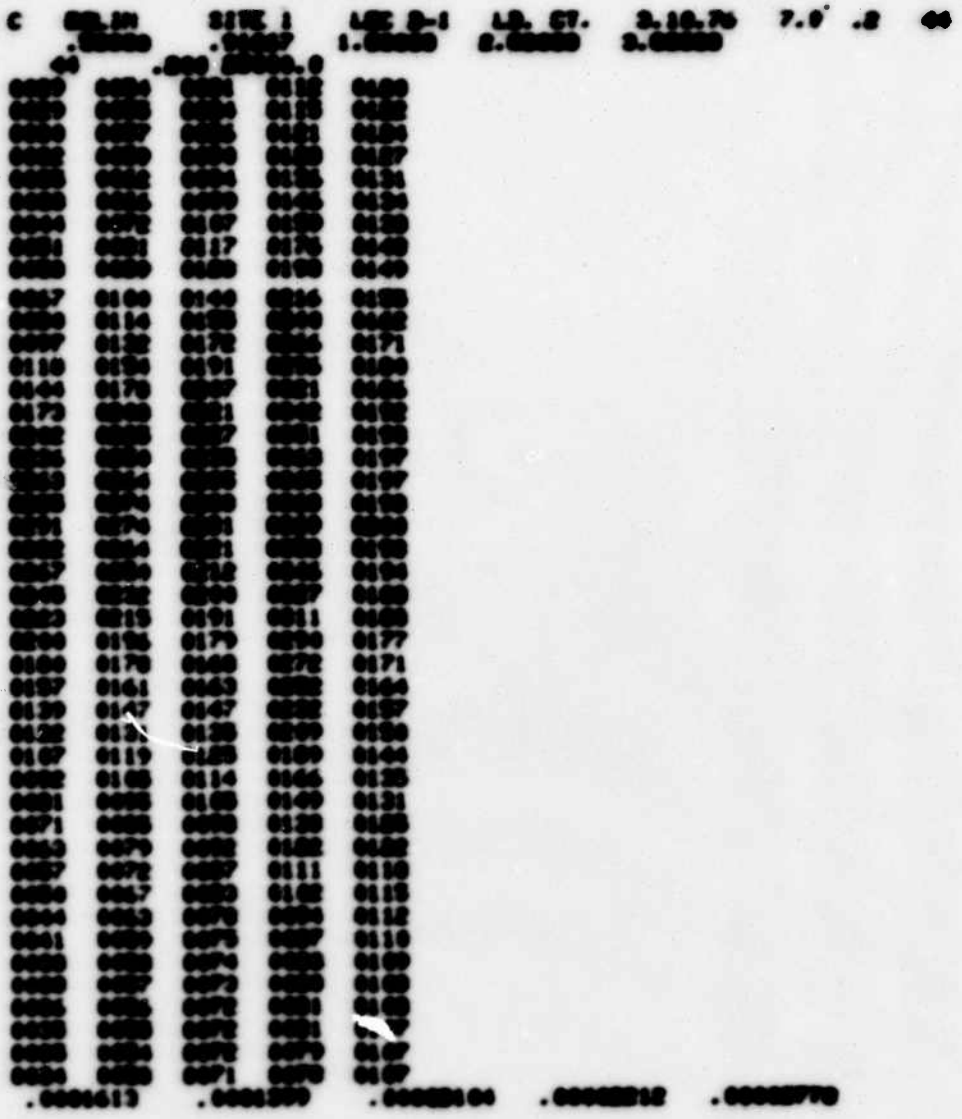


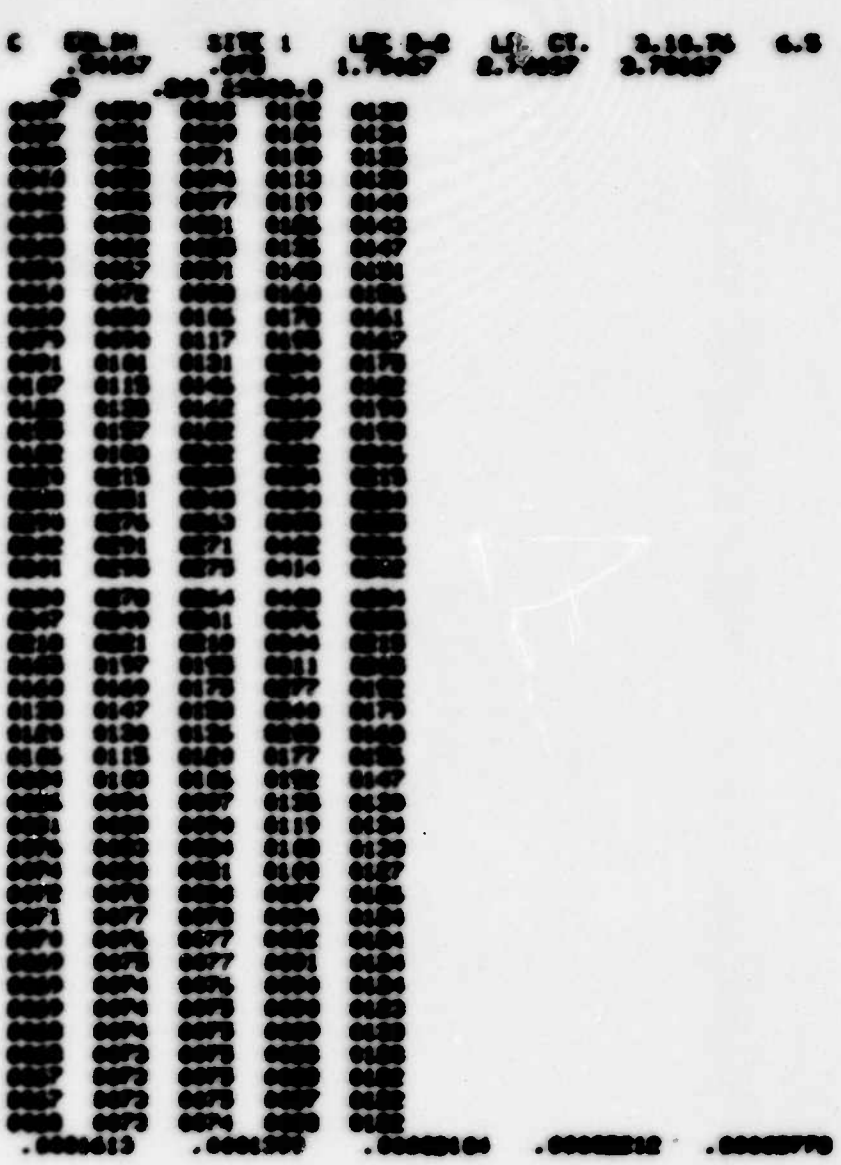


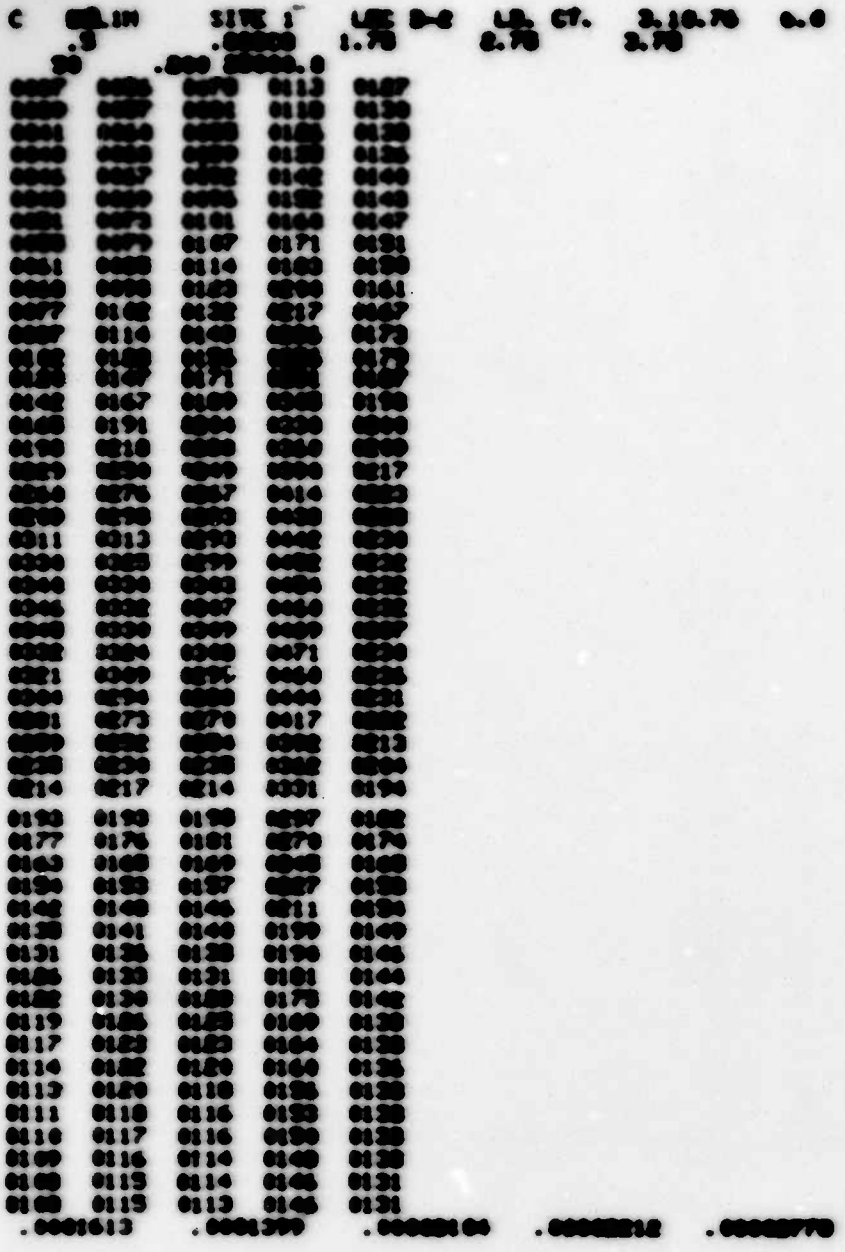


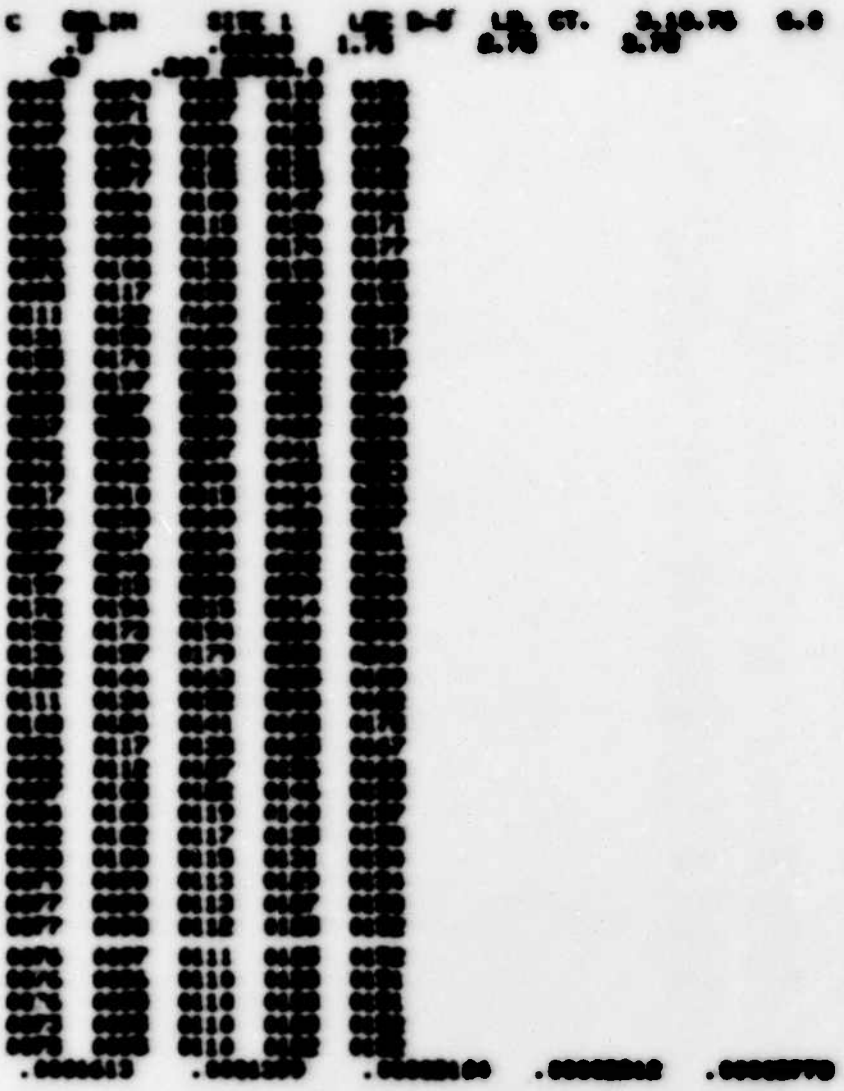


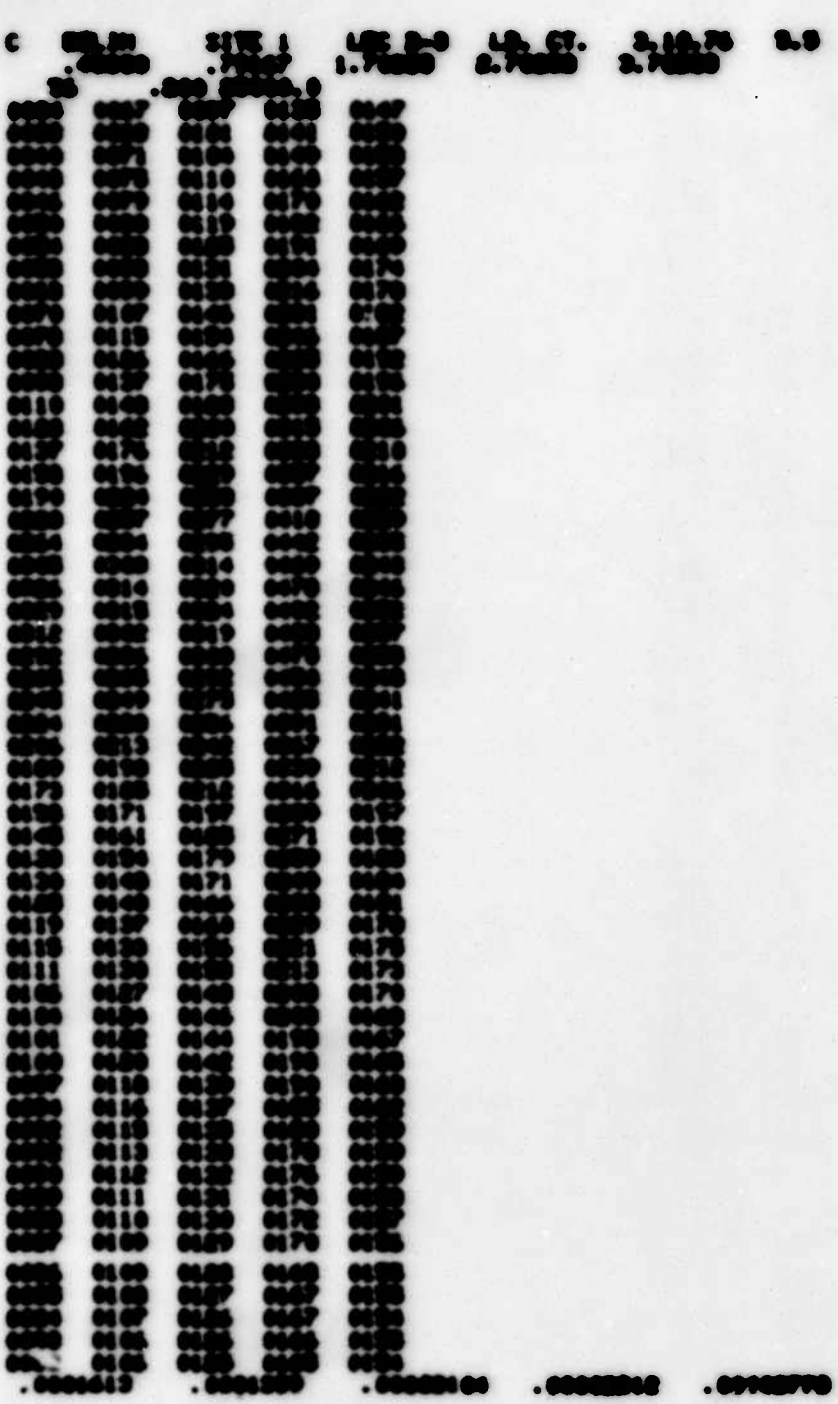


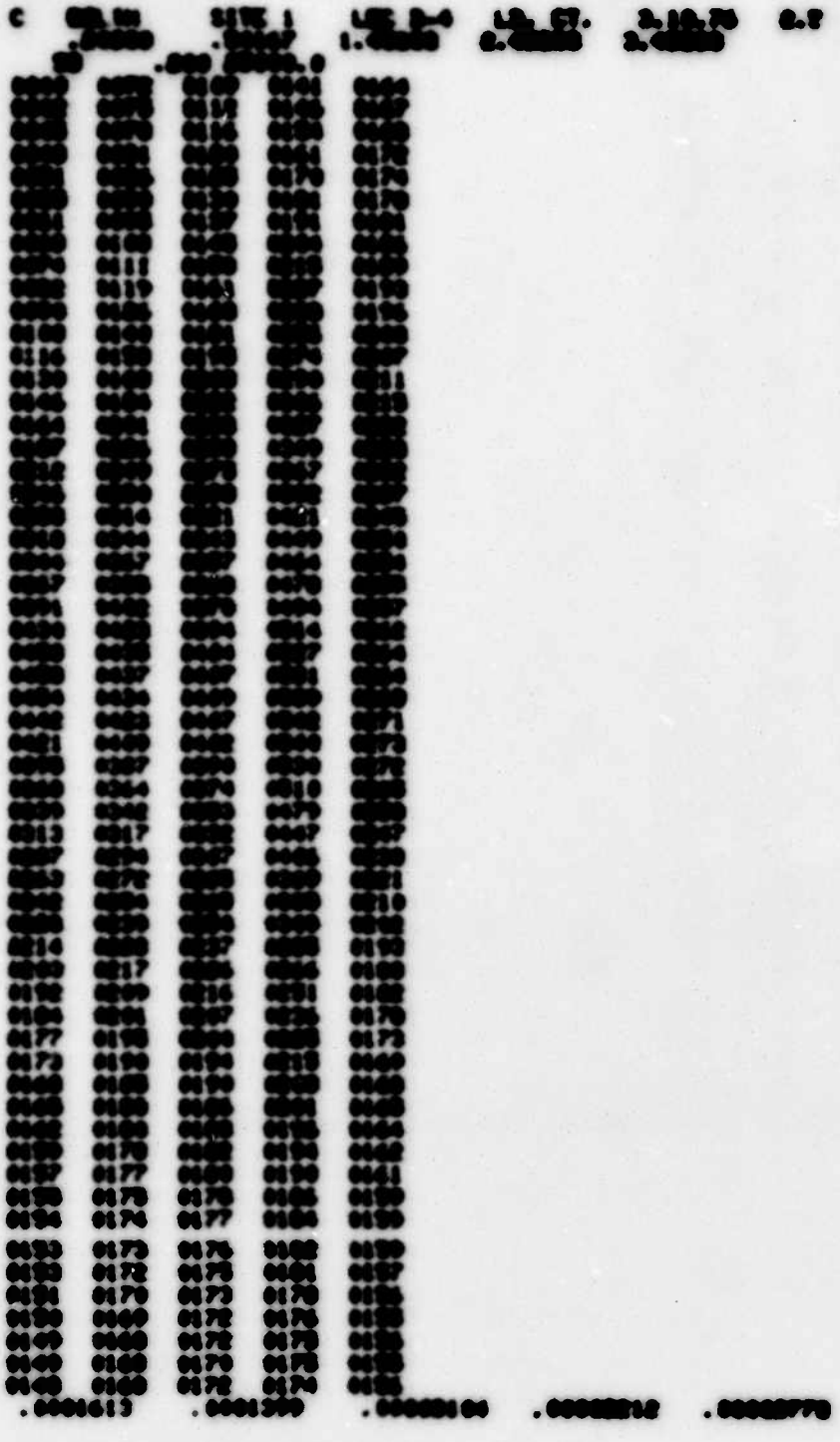


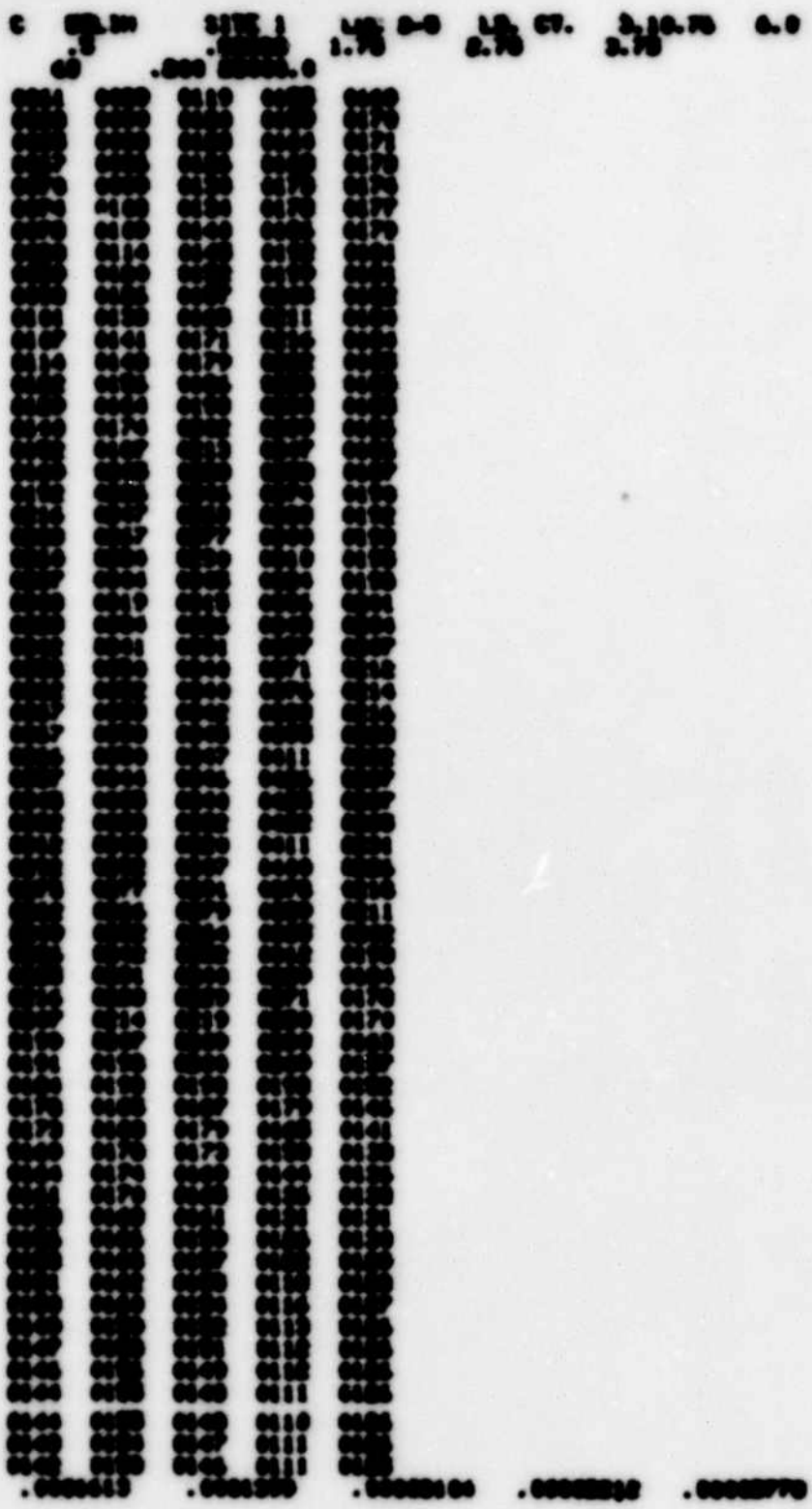


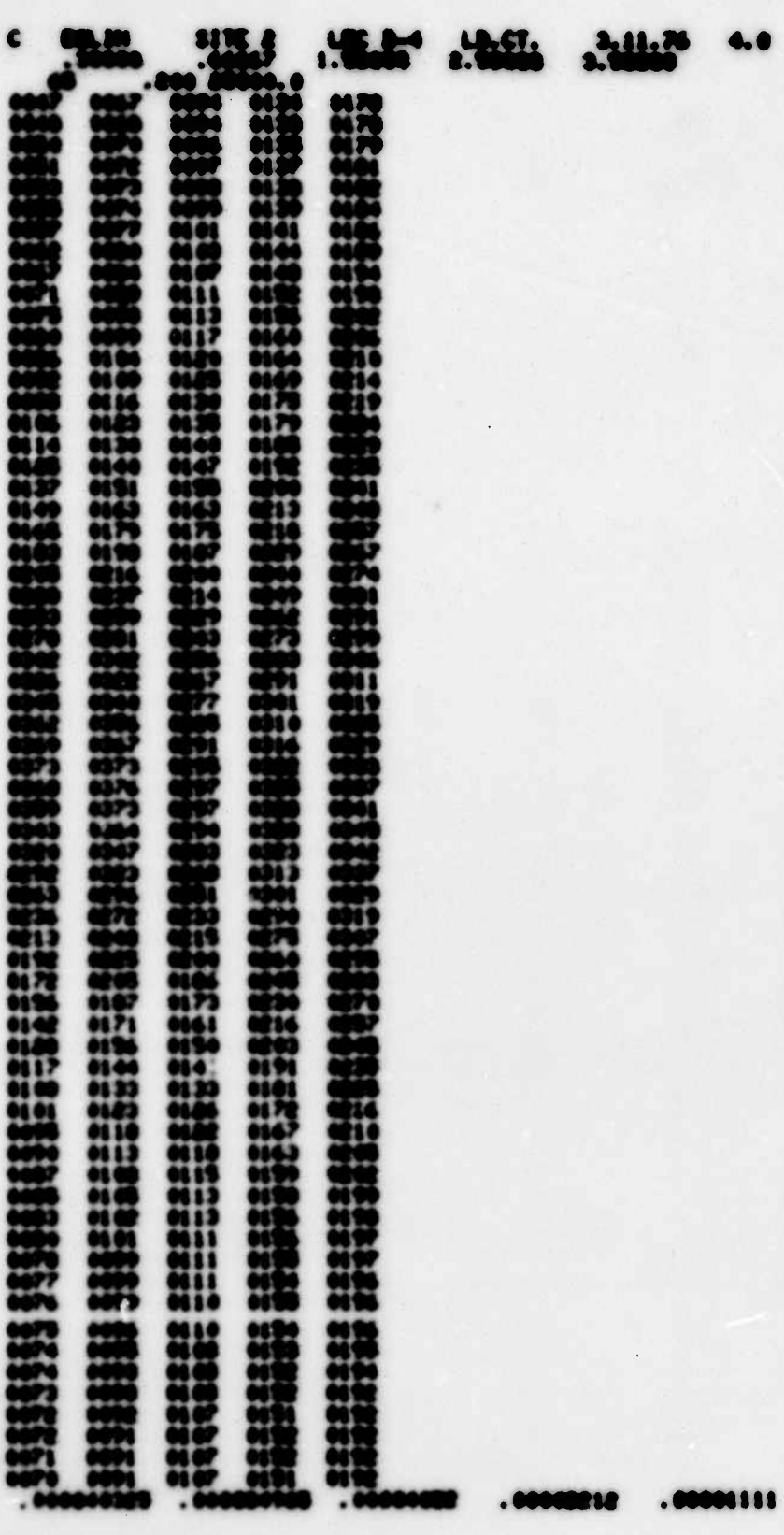


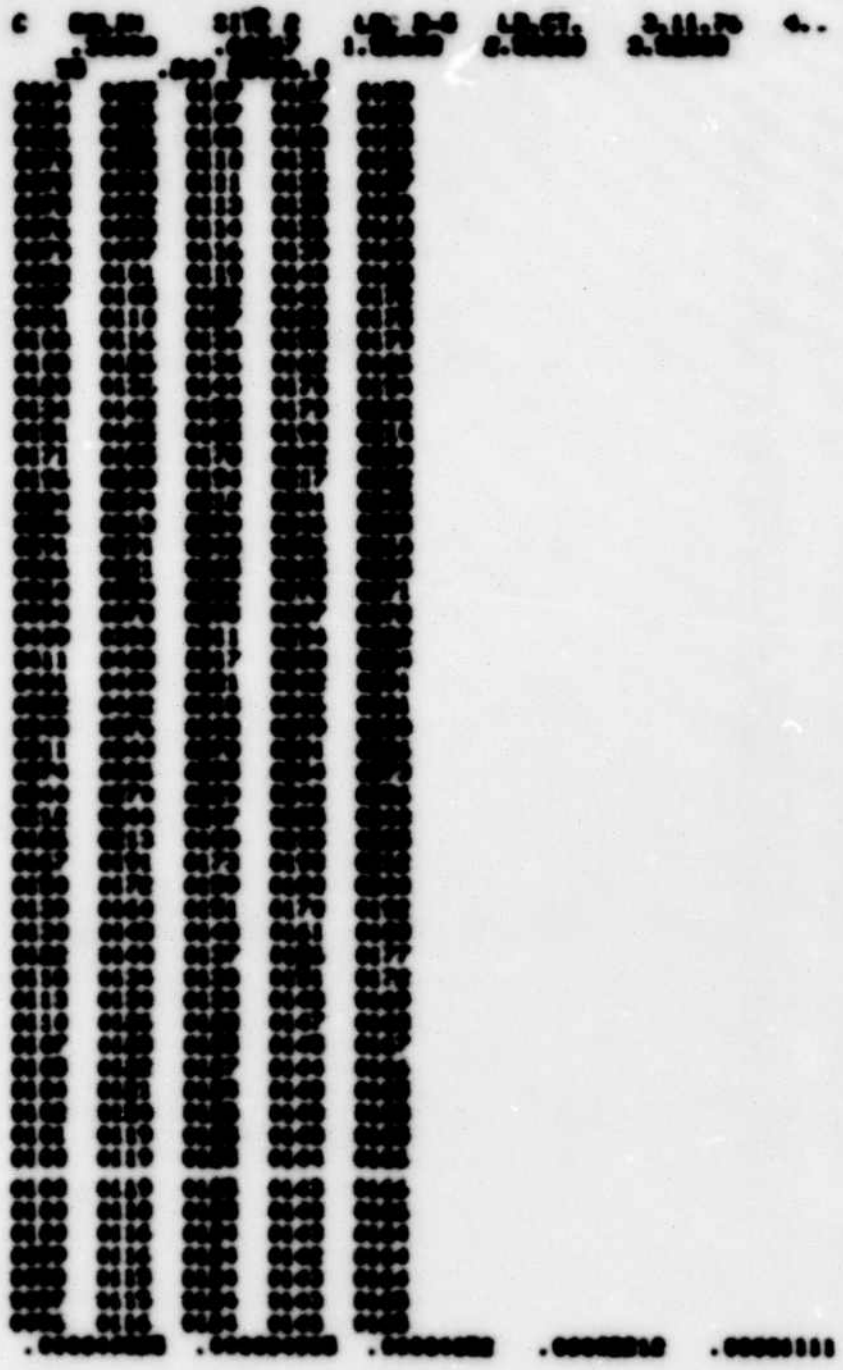


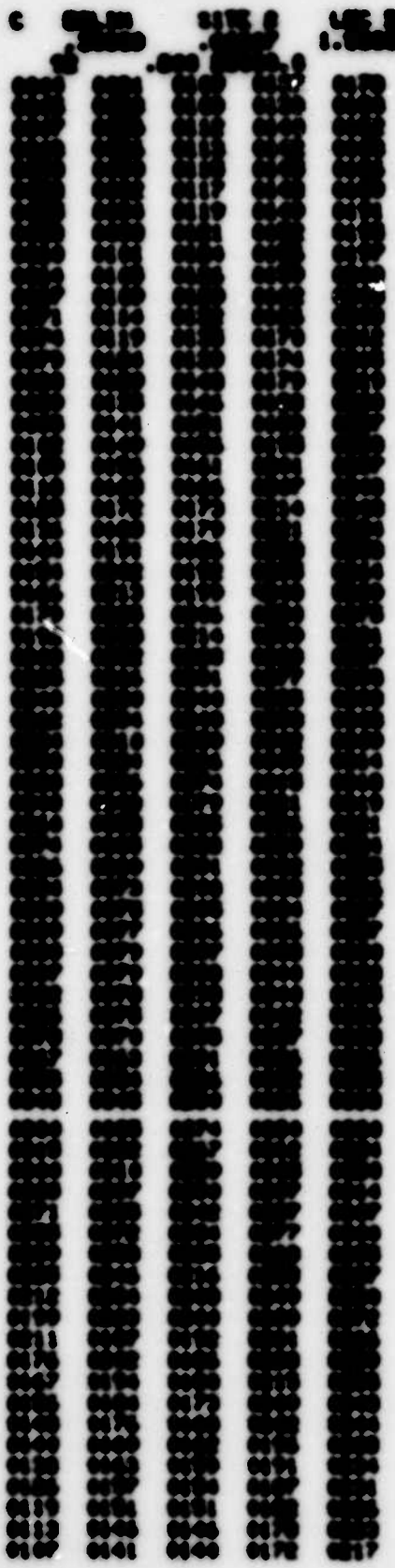




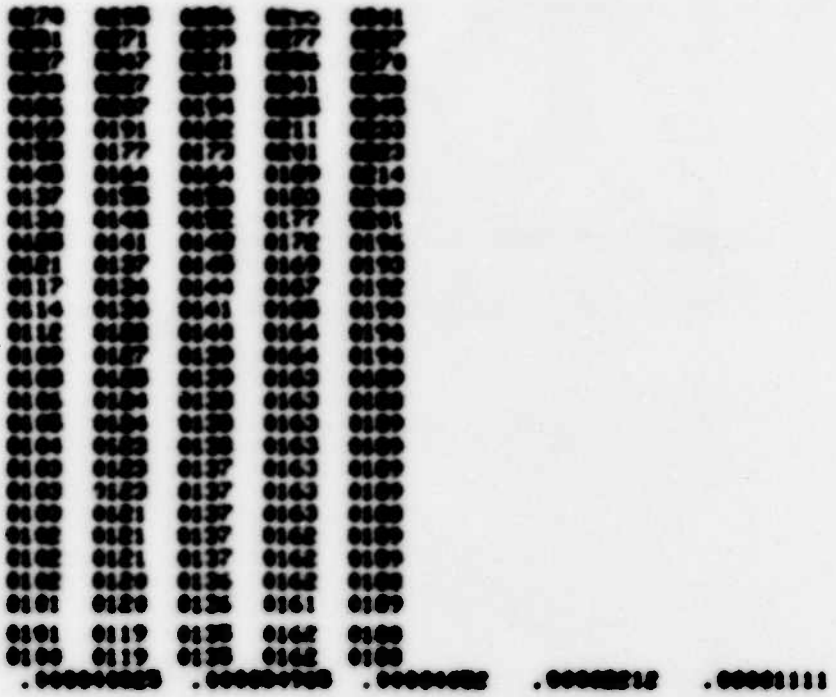




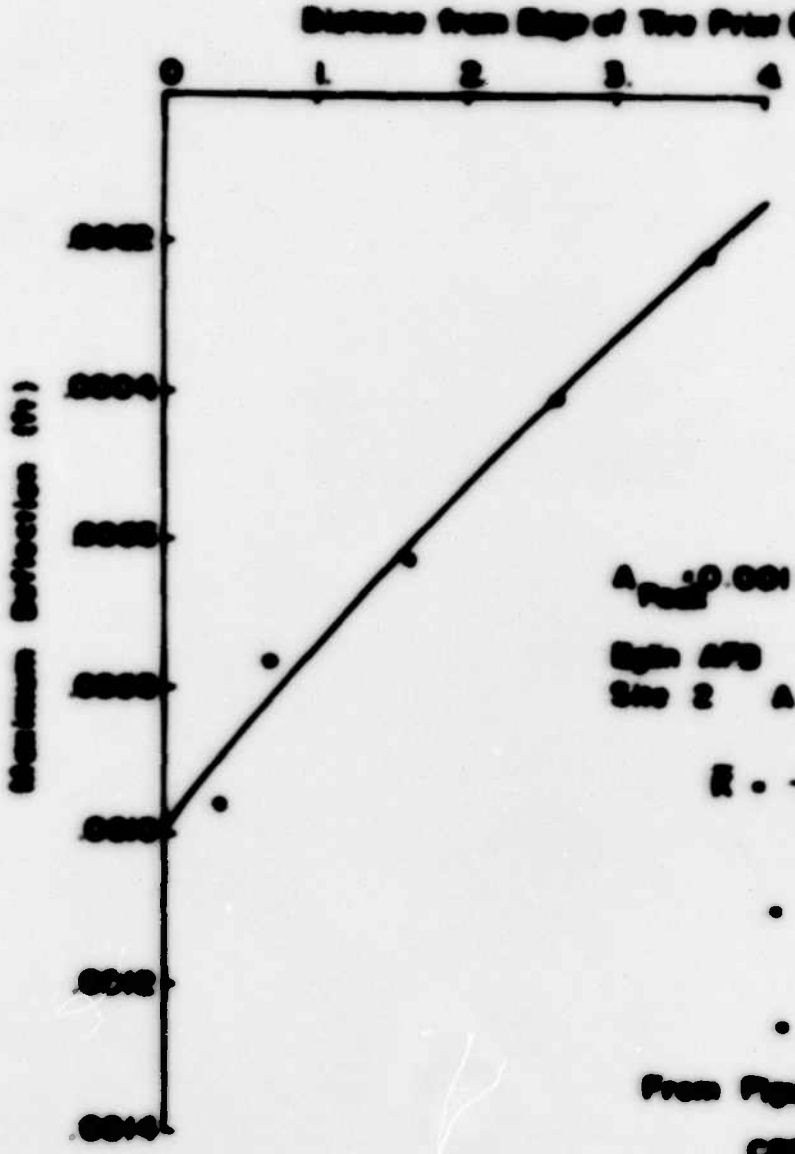








[redacted]




[redacted]

END

FILMED

3-86

DTIC